Immune responses to AAV gene therapy in the ocular compartment

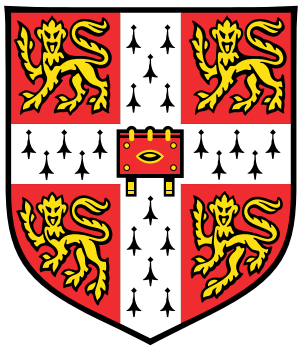

Michael James Robert Whitehead

Department of Clinical Neuroscience, University of Cambridge

Supervisors: Dr. Patrick Yu Wai Man, Professor Keith Martin

This dissertation is submitted for the degree of

Doctor of Philosophy

Queens' College 2021

I would like to dedicate this thesis to my late grandfather, Luc Matthews.

Declaration

I hereby declare that except where specific reference is made to the work of others, the contents of this dissertation are original and have not been submitted in whole or in part for consideration for any other degree or qualification in this, or any other University. This dissertation is the result of my own work and does not include work done in collaboration, except where specifically indicated in the text. This dissertation does not exceed the word limit specified by the School of Clinical Medicine Degree Committee. This work was supported by tthe Novo Nordisk Research Foundation UK (G103197), Addenbrookes Charitable Trust (G104080 & G109216), and the National Eye Research Council (G104353). The funders had no role in study design, data collection and analysis, decision to publish, or preparation of the dissertation.

The following publications were part of my PhD training and were published before submitting this dissertation:

Whitehead M, Osborne A, Yu-Wai-Man P, Martin K. Humoral immune responses to AAV gene therapy in the ocular compartment. Biological Reviews of the Cambridge Philosophical Society. 2021 Apr. DOI: 10.1111/brv.12718.

Michael James Robert Whitehead
2021

Acknowledgements

Firstly, I would like to acknowledge my supervisors, Dr. Patrick Yu Wai Man and Professor Keith Martin, for their support and guidance throughout my doctoral studies. I would also like to thank Dr. Andy Osborne for all his technical training and assistance, especially during the early years of my PhD. I am grateful to my two assessors, Dr. Caroline Gray-Williams and Dr. Dominik Fischer, for giving up their time to review my thesis and conduct the viva voce examination. A big thanks to Dr. Katie Hall at the Van Geest Building for keeping everything shipshape in the lab! I would also like to acknowledge my parents, Belinda Whitehead and Rob Whitehead, for their ongoing support and encouragement throughout my PhD. A big thank you to my brother Chris Whitehead, whose comparatively stratospheric trajectory in life has proven a worthwhile source of personal motivation. You may have a house, but at least I have a motorbike. I would like to acknowledge the University of Cambridge Official Rick and Morty Fan Club TM (Russell, Popescu, Albrow-Owen et. al.) whose memes and general good sense of humour have proven a welcome intermission from the more monotonous aspects of life as a PhD student. A big thank you also to the Cam Boys (Russell, MacIver, Camp, Smyth and Gallagher). We have had a lot of fun over the last few years and I look forward to our next 0% ABV themed excursion should the COVID-19 crisis allow it. I would like to acknowledge two South African chaps, Doug Van Niekerk and Josh Subel, for being absolutely solid mates, and of course for their introduction to some of the lesser known Queens' traditions. I would also like to thank my grandparents, Roger Whitehead and Jenny Whitehead, for providing me frequent safe refuge on Sunday afternoons to enjoy a spot of afternoon tea and biscuits. A big thank you to Elaine Matthews whose inspirational Zoom capabilities really made me chuckle on several occasions. I would like to acknowledge Chester (the cat) for being a lovable fluffball when I most needed it. And lastly I would like to thank Taylor Gorske for putting up with me through thick and thin. I'm so proud of you and can't wait to see what the future has in store for us.

Abstract

Adeno-associated virus (AAV) is a viral vector that can be used to deliver therapeutic genes to diseased cells in the eye. Whilst some consider the eye to be an immuneprivileged organ, recent reports have begun to suggest that injection of AAV may elicit local and systemic immune activation. The objective of this thesis was to further our understanding of the nature of the immune response to intraocularly-delivered AAV vectors, and to develop strategies to achieve repeated gene transfer (i.e. successful follow-on injections) to the inner retina.

A literature review was conducted into the role that pre-existing and induced neutralising antibody responses may play in the context of ocular gene therapy. This concluded that a multifaceted/comprehensive approach may be required to circumvent anti-capsid humoral immunity and enable repeated gene transfer in humans. As such, two possible components of this strategy were tested in this thesis.

First, a capsid mutagenesis strategy was tested in which certain capsid residues, termed phosphodegrons, were mutated to attenuate cytosolic degradation of AAV. This was to enable robust transduction of the murine retina at low vector dose and thereby circumvent the generation of neutralising antibodies that is associated with injection of high doses of AAV. In fact, it was found that phosphodegron mutant AAV serotype 2 (AAV2) resulted in higher levels of immune activation across all tested parameters vs. wild-type AAV2, including neutralising and total AAV binding antibody levels, microglia activation, Muller glia activation, CD4+ and CD8+ T-cell infiltration into the retina, splenic germinal center B-cell activation and class-switching, and activation of conventional dendritic cells. Mechanistically, it was shown that the capsids demonstrated reduced binding affinity to the AAV2 primary receptor, heparan sulphate proteoglycan, and as such it was suggested that reduced sequestration of virions in the heparan-rich inner limiting membrane may increase cellular infection levels in the retina, thereby increasing overall immune activation. The phosphodegron mutant capsids also demonstrated that a slight escape from anti-AAV2 neutralising serum, suggesting they may be more refractory to pre-existing neutralising antibodies in seropositive patients.

Second, an assessment was made as to whether perioperative administration of immunosuppressive glucocorticoid steroids would circumvent immune responses to AAV. It was found that prednisolone was effective at reducing anti-AAV neutralising and total AAV binding anti-

body titres. This effect may have occurred via the inhibition of splenic germinal center B-cell reactions and class-switching of immunoglobulin antibody isotypes, and reducing follicular helper T-cell levels. Despite the reduction in NAb and TAb titres, it was found that perioperative prednisolone administration was insufficient to enable repeated gene transfer following a second eye injection of AAV2. Interestingly, repeated bilateral AAV2 injections may have resulted in a slight reduction in electrophysiological activity in the retina compared to mice who received two control PBS injections.

In conclusion, this thesis highlighted novel aspects of phosphodegron mutant AAV2 immunobiology and identified a possible utility for the administration of prednisolone as a tool for enabling repeated gene transfer of AAV gene therapy vectors.

Contents

List of Figures

List of Tables

List of abbreviations

AAV Adeno-associated virus
AAV-R AAV receptor
AAVR BD AAV receptor binding domains
AAP Assembly-activating protein
ACAID Anterior chamber-associated immune deviation
ADCC Antibody-dependent cellular cytotoxicity
AID Activation-induced cytidine deaminase
ANOVA Analysis of variance
APC Antigen presenting cell
ASM Acid sphingomyelinase
ASR Ancestral sequence reconstruction
AQP4 Aquaporin-4
AUC Area-under-the-curve
BBB Blood-brain barrier
BCVA Best-corrected visual acuity
BSA Bovine serum albumin
CCR5 Chemokine receptor 5
cDC1 Conventional DCs subset 1
cDC2 Conventional DCs subset 2
CM Cerebromedullary
CNS Central nervous system
CRIM Cross-reactive immunologic material
CSF Cerebrospinal fluid
CSR Class-switch recombination
DC Dendritic cell
DMD Duchenne's Muscular Dystrophy
DMEM Dulbecco's Modified Eagles Medium
EAU Experimental autoimmune uveitis

EGFR-TK Epidermal growth factor receptor tyrosine kinase
ERG Electroretinography
ETDRS Early Treatment Diabetic Retinopathy Study
FBS Fetal bovine serum
FGF-R Fibroblast growth factor receptor
FSC Forward scatter
GAA Acid α-glucosidase
GC Genome copies
GR Glucocorticosteroid receptor
HBDs Heparan binding domains
HCC Hepatocellular carcinoma
HGF-R Hepatocyte growth factor receptor
HRP Horse raddish peroxidase
HS Heparan sulphate
HSPG Heparan sulphate proteoglycan
IFNγ Interferon-γ
IL2 Interleukin-2
ILM Inner limiting membrane
IRF Interferon regulatory factor
INL Inner nuclear layer
ITR Inverted terminal repeats
IVT Intravitreal injection
IVIg Pooled human immunoglobulin G
LCA2 Leber's Congenital Amaurosis type 2
LHON Leber's Hereditary Optic Neuropathy
LPS Lipopolysaccharride
MERTK MER proto-oncogene tyrosine kinase
MHC Major histocompatibility complex
MOI Multiplicity-of-infection
MyD88 Myeloid differentiating factor 88
NAbs Neutralising antibodies
NADH Nicotinamide adenine dinucleotide dehydrogenase
ND4 NADH subunit 4
nAMD Neovascular age-related macular degeneration
NFχB Nuclear factor χB
NGS Normal goat serum

NLS Nuclear localisation sequence
NPC Nuclear pore complex
OCT Optical coherence tomography
OIS Ocular inflammation score
ONL Outer nuclear layer
OTC Ornithine transcarbamylase
rAAV Recombinant adeno-associated virus
PAMPs Pathogen-associated molecular patterns
PBS Phosphate buffered saline
PCs Plasma cells
PD1 Programmed cell death protein-1
pDCs Plasmacytoid dendritic cells
PEG Polyethylene glycol
PFA Paraformaldehyde
PRRs Pattern recognition receptors
P/S Penicillin/streptomycin
pSTR Positive scotopic threshold response
RFUs Relative fluorescence units
RGC Retinal ganglion cell
RWMs Retinal wholemounts
RIVEM Radial Interpretation of Viral Electron Density Map
RPE Retinal pigment epithelium
RLUs Relative luminescence units
RMSD Root mean squared deviation
ROIs Regions-of-interest
SEM Standard error of the mean
SHM Somatic hypermutation
SSC Side scatter
SMA Spinal muscular atrophy
SRT Subretinal injection
TAb Total binding antibody
TBS Tris-buffered saline
Tfh Follicular helper T-cells
TLR2 Toll-like receptor 2
TMB 3,3',5,5'-tetramethylbenzidine
TNFα Tumour necrosis factor-α

VEGF Vascular endothelial growth factor
WT Wild type

Chapter 1

Humoral immune responses to AAV gene therapy in the ocular compartment

1.1 Declaration

Whitehead M, Osborne A, Yu-Wai-Man P, Martin K. Humoral immune responses to AAV gene therapy in the ocular compartment. Biological Reviews of the Cambridge Philosophical Society. 2021 Apr. DOI: 10.1111/brv.12718.

This literature review was written in collaboration with the above authors. The contribution of each author is the following: MW performed the literature review and wrote the manuscript. AO, PYWM and KM provided feedback on the manuscript.

1.2 Abstract

Viral vectors can be utilised to deliver therapeutic genes to diseased cells. Adeno-associated virus (AAV) is a commonly used viral vector that is favoured for its ability to infect a wide range of tissues whilst displaying limited toxicity and immunogenicity. Most humans harbour anti-AAV neutralising antibodies (NAbs) due to subclinical infections by wild-type virus during infancy and these pre-existing NAbs can limit the efficiency of gene transfer depending on the target cell type, route of administration and choice of serotype. Vector administration can also result in *de novo* NAb synthesis that could limit the opportunity for repeated gene transfer to diseased sites. A number of strategies have been described in preclinical models that could circumvent NAb responses in humans, however, the successful translation of these innovations into the clinical arena has been limited. Here, a comprehensive review of the humoral immune response to AAV gene therapy in the ocular compartment is provided. Basic AAV biology and clinical application, the role of pre-existing and induced NAbs, and possible approaches to overcoming antibody responses is covered. To conclude, a framework for a comprehensive strategy for circumventing humoral immune responses to AAV is proposed.

1.3 General introduction to AAV gene therapy

Adeno-associated virus (AAV) is a non-enveloped Parvovirus that was originally identified as a contaminant in adenoviral cultures [1]. The virus exhibits a T=1 icosahedral shape with a 25nm diameter [2]. AAV capsid proteins contain a ssDNA genome [3] flanked by inverted terminal repeats (ITRs) [4]. Transcription mapping of the genome of AAV2 reveals three overlapping mRNA molecules that are produced from three promoters, namely, p5, p19 and p40 [5]. The p5 and p19 promoters are known to mediate expression of *rep* genes required for AAV DNA replication and packaging of genetic cargo into AAV particles [6], whereas the p40 promoter drives transcription of *cap* gene mRNA, which is alternatively spliced to yield three distinct protein products, VP1, VP2 and VP3 in a 1:1:10 ratio respectively [7]. p40 also mediates expression of assembly-activating protein (AAP) in a different open reading frame (ORF) [8]. AAP is not present in mature AAV capsids, but it is known to play a key role in enabling production of high titre AAV preps for certain serotypes [9].

To produce recombinant AAV (rAAV) for gene therapy, the rep/cap genes are removed and replaced with a therapeutic gene and a promoter sequence to drive expression. The maximum size of a genetic sequence that can be packaged into AAV is around 4.4kbp, which limits the application of the vector to diseases requiring the delivery of large gene expression cassettes exceeding this capacity [10]. When rAAV genomes enter the cell nuclei, second-strand syn-

thesis occurs that converts a linear ssDNA molecule into a dsDNA episome, thus enabling the synthesis of therapeutic constructs [11]. Achieving nuclear transfer of AAV genetic cargo is a complex multistep process, however. First, the virus must bind to a cell and undergo endocytosis by utilising a number of primary receptors and co-receptors, many of which have not yet been identified [12]. AAV then 'escapes' from the endosome as it acidifies and it is thought to be trafficked to the nucleus via a nuclear localisation sequence (NLS) on the VP1 and VP2 capsid monomers [13]. Recent studies have shown that nuclear import of rAAV is mediated by nuclear pore complexes (NPCs) and this process is dependent upon interactions with importin-α [14]. After nuclear import, rAAV capsids uncoat, thereby releasing their genetic cargo into the target cell [15].

1.4 Successes in AAV clinical trials

A number of successful clinical trials have now demonstrated the potential of using AAV as a gene transfer device for therapeutic purposes. AAV is an attractive vector for human gene therapy beneffitting from several advantages. First, it is largely non-integrating, thereby reducing the risk of insertional mutagenesis via the disruption of tumour suppressor genes, which is a major concern for lentiviral gene therapies, for example [16]. Second, AAV can be used to target a very broad range of cell types as a number of different serotypes exist, each with a unique tissue tropism [17]. Whilst the packaging capacity of AAV is relatively limited, it is thought to induce long-term transgene expression in both dividing and non-dividing cells [18]. Finally, although there is an emerging body of evidence implicating a negative impact of humoral and cellular immune responses on AAV-mediated gene transfer, AAV is largely considered a safe vector for human gene therapy, especially when delivered locally close to the site of pathology, such as the vitreous cavity of the eye [19].

Here a number of examples of the application of AAV for human gene therapy will be highlighted. SB-FIX (NCT02695160; phase I trial) is a zinc finger nuclease therapeutic delivered by systemic injection of AAV2/6 (AAV6 capsid with AAV2 ITR-containing gene expression cassette) that aims to edit the factor IX gene in patients with haemophilia B [20]. DTX301 (NCT03636438; phase I/II trial) is an AAV8-based gene therapy to treat ornithine transcarbamylase (OTC) deficiency via systemic delivery, and it has shown an acceptable safety profile and some indication of therapeutic efficacy in the nine patients that have been treated to date [21]. FLT190 (NCT04040049; phase I/II trial) is an AAV8-based gene therapy delivered by intravenous infusion for the treatment of Fabry disease, which is a lysosomal storage disease caused by deficiency of the enzyme alpha-galactosidase A. FLT190 has shown long-term therapeutic efficacy in animals models and patients are currently being recruited for the clinical

trial [22]. AAV2/8-hCARp-hCNGB3 is a retinal gene therapy to treat achromatopsia, a rare and inherited form of congenital colour blindness (NCT03001310; phase I/II trial) [23].

The above examples highlight the broad utility of AAV as a gene transfer device. To date, the application of gene therapy has focussed on the treatment of rare and inherited genetic diseases. More recently, this technology has been extended to complex diseases and the eye has been at the forefront of these therapeutic innovations. There are now several reports of gene therapy being used to deliver anti-VEGF (vascular endothelial growth factor) agents to treat exudative (wet) age-related macular degeneration, and in many instances, mutagenised capsids are used to enhance the delivery of their genetic cargo [24]. Whilst these developments are still in the nascent stages of clinical development (phases I/II), they provide an interesting proof-of-concept for the broader application of AAV gene therapy therapy to late-onset neurodegenerative disorders that affect an increasingly large number of individuals in rapidly ageing populations in the developed world [25].

In addition to the number of AAV gene therapies currently in early-stage clinical trials, three programmes have demonstrated efficacy in phase III studies. Zolgensma (onasemnogene abeparvovec-xioi) was approved by the USA FDA in 2019 for the treatment of spinal muscular atrophy (SMA) in patients harbouring biallelic mutations in the *smn1* gene. The therapy utilises the AAV9 serotype, which is unique in its ability to cross the blood-brain barrier (BBB), to deliver cDNA encoding the *smn1* gene under control of the CAG promoter [26]. In one study, participants demonstrated remarkable improvements in motor function and quality-of-life, with 11/12 patients achieving full head control and two patients even walking independently [27, 28]. Luxturna (voretigene neparvovec) is an AAV2-based gene therapy for biallelic (homozygous or compound heterozygous) mutations in the *rpe65* gene, such as Leber's Congenital Amaurosis type 2 (LCA2). RPE56 encodes a critical enzyme essential for phototransduction (process that converts energy contained in a photon of light to biochemical signals) to that mediates the transition of all-trans-retinyl esters to 11-cis-retinol [29]. In an open-label, randomised phase III study, no therapy-related serious adverse events or unacceptable immune responses occurred, whilst 65% of treated patients demonstrated improvements in visual function [30]. Further assessment has corroborated the safety of the approach, demonstrating that Luxturna can deliver benefits to patients up to four years after administration [31]. In summary, the successful gene therapy programme for LCA2 illustrates the merits of AAV-mediated gene delivery to the outer retina by subretinal injection, providing the impetus for other programs targeting disorders affecting photoreceptors and retinal pigment epithelium (RPE). Programs targeting the inner retina, and specifically the retinal ganglion cell (RGC) layer, have also demonstrated promising results for the amelioration of genetic disease. Lenadogene (GS010) is an AAV2-based treatment for Leber's Hereditary Optic Neu-

ropathy (LHON), which is is the most common cause of mitochondrial blindness, affecting at least 1 in 35,000 of the population. The majority of patients carry one of three point mitochondrial DNA (mtDNA) mutations (m3460A>G in MTDN1, m.11778G>A in MTND4, and m.14484T>C in MTND6), which all affect genes encoding subunits of the mitochondrial respiratory chain complex I [32]. In a phase III study, Lenadogene treatment resulted in improvements in best-corrected visual acuity (BCVA) with an increase of 26 Early Treatment Diabetic Retinopathy Study (ETDRS) letters were seen in the treated eyes at 96 weeks following intravitreal injection, which is more than what would be expected from the natural history of LHON [33]. Further, a secondary analysis of a phase I/II trial of patients receiving Lenadogene showed the treatment was safe and well-tolerated, with mostly mild and transient intraocular inflammation in the anterior chamber and vitreous [34]. Overall the Lenadogene trials demonstrate the potential of AAV-mediated gene transfer to the inner retina. However, the unexpected observation that the unilateral intravitreal injections given to patients resulted in improvements in visual acuity in the contralateral (untreated) eye is something that warrants further investigation [33].

1.5 Immune responses to AAV - key considerations

1.5.1 How are immune responses initiated?

An organism mounts an immune response to protect themselves against foreign protein structures, termed antigens, that they deem to be detrimental to their survival. Immune responses can be classified as innate or adaptive. In an innate immune response, pathogen-associated molecular patterns (PAMPs) are recognised by pattern recognition receptors (PRRs). This drives a rapid and non-specific response that does not induce any immunological memory [35]. During a wild-type AAV infection, PRRs can recognise viral nucleic acids and membrane glycoproteins, which leads to nuclear factor κB (NFκB) and interferon regulatory factor (IRF) activation and synthesis of proinflammatory cytokines and type I interferons respectively [36]. Adaptive immunity arises after the innate immune response and results in the development of 'immunological memory', which allows the organism to mount a faster and more efficient immune response when encountering the antigen for the second time. Adaptive immunity begins with the presentation of a particular antigen by an antigen presenting cell (APC) to T and B lymphocytes. These cells are then activated, and undergo clonal expansion (this refers to the proliferation of T and B cells that are specific to the particular antigen that has been recognised). This is followed by T and B cell differentiation into effector cells (CD4+ or CD8+ T-cells, or plasma cells (PCs)) which act to eliminate the antigen via the de-

struction of virally-infected cells or de novo antibody synthesis [37–39]. Finally, a population of memory T and B cells are able to quickly recognise the antigen if the organism encounters it a second time [40].

1.5.2 Is AAV non-pathogenic and non-immunogenic?

Until recently, wild-type AAV was not generally considered to be associated with any known human pathology. This is considered a key factor given that up to 90% of people are thought to be asymptomatically infected with AAV throughout their lifetimes [41]. However, recent evidence has arisen that has suggested a role for wild-type AAV2 in the development of hepatocellular carcinoma (HCC). The authors observed AAV2 genome integration in 11/194 HCC samples tested, and concluded that wild-type AAV2 may have been a causative factor via oncogenic insertional mutagenesis [42]. It should be emphasised however, that their findings related to wild-type AAV2 and in later publications, the authors sought to insist that their findings should not be confounded with the use of rAAV gene therapies in the clinic [43]. Given the inherent similarities between wild-type AAV2 and rAAV2 however, more research into the possibility of oncogenic genome insertion is needed.

As mentioned, a key factor underpinning the progress of AAV-based gene therapy into the clinic is the safety profile of the vector. Depending on the route of administration, choice of serotype and dosage used, rAAV exhibits a relatively tolerable safety profile when compared to other gene transfer devices like adenovirus and lentivirus [44]. A number of theories have been suggested to explain why wild-type and rAAV appears to be relatively non-immunogenic. First, most AAV serotypes may be poor transducers of professional APCs, such as dendritic cells, and may only result in minimal upregulation of major histocompatibility complex (MHC; key molecular player in the presentation of antigens to the immune system) proteins in target cell types. This has been demonstrated in a number of publications investigating immune-competent sites like the liver and muscle [45, 46], however, there is little literature to support this claim in sites generally considered more immuneprivileged, like the eye and central nervous system (CNS). A second theory suggests that a lack of viral DNA in rAAV vectors reduces recognition by PRRs. Whilst the removal of cap genes from rAAV particles obviates the *in vivo* proliferation of the virus, thereby avoiding amplification of capsid antigens, this theory does not explain why rAAV is less immunogenic than adenoviral vectors, for example, which also have the genes required for capsid replication removed [47].

1.5.3 Innate immune responses to AAV

Innate immune responses against AAV have recently been implicated as a possible cause for the toxicities that have been observed in gene therapy clinical trials. Innate immunity can be driven by anti-capsid and anti-nucleic acid pathways. It is now recognised that anti-capsid responses are likely derived via toll-like receptor 2 (TLR2) signalling, which is expressed on the cell surface [48]. TLR9 signalling is responsible for the recognition of viral DNA sequences, and endosomal TLR9 has been implicated in the sensing of unmethylated CpG motifs in dendritic cell types [49]. Further, upregulation of TLR9 has been correlated with improved antigen presentation to the naiive CD8+ T-cells with MHC class I molecules, and signalling of this receptor with myeloid differentiating factor 88 (MyD88) has been implicated as a key pathway instigating immune responses against transgenes in the liver and muscle [50, 51].

It has been established that the inhibition of key molecular players in the pathways mediating activation of the innate immune response can prevent anti-AAV CD8+ cytotoxic T-cell responses. Here, inhibition of TLR9 and type I interferon signalling has been shown to attenuate anti-AAV2 CD8+ T-cell induction [49], and blockage of type I interferons with monoclonal antibody therapy has demonstrated reduced cross-priming of anti-AAV8 CD8+ T-cells by plasmacytoid dendritic cells (pDCs) [52]. Innate immunity against dsRNA molecules was also recently identified by Shao et. al. in 2018. Their findings implicated AAV ITR-driven dsRNA synthesis as a cause of type I interferon expression in transduced hepatocytes and also demonstrated that inhibition of MDA5 (a cytoplasmic RNA sensor) improved transgene expression in these cells [53]. This study in particular highlights the evolving understanding of innate immunity against AAV vectors but also provides a tangible example of how clarifying the molecular mechanisms underpinning AAV immunity can improve efficacy in preclinical and clinical studies.

1.5.4 Cellular immune responses to AAV

The innate immune response is clearly linked to the development of cellular immunity against AAV vectors. Cellular immunity can be pre-existing (arises before administration of therapy; likely via asymptomatic infections by wild-type AAV) or arise de novo from the administration of an AAV gene therapy.

1.5.4.1 Pre-existing cellular immunity to AAV

Pre-existing cellular immunity to AAV is thought to arise during infancy following a wild-type AAV infection, which was recently evidenced by flow cytometry analysis demon-

strating a memory T-cell phenotype (i.e. expression of differentiation markers) in subjects' lymphocyte populations. These memory T-cells expressed interferon-γ (IFNγ), interleukin-2 (IL2) and tumour necrosis factor-α (TNFα) and exhibit a cytotoxic phenotype (induce apoptosis of AAV infected cells) as demonstrated by expression of granzyme B and CD107a [54].

Whilst anti-AAV T-cells exhibit high cross-reactivity and demonstrate responses to a variety of AAV serotypes [55, 56], the exact role of pre-existing cellular immunity is not well-understood, and it is noted that the patterns of T-cell reactivity to AAV in gene therapy trials differ from those seen during a typical viral infection. As Verdera et. al. suggest, this observation may reflect the fact that the mode of administration of AAV gene therapies is the injection of a large number of non-replicating recombinant vectors into the body, which does not match that of an ongoing viral infection with replicating virions [54]. More research is required here to further understanding of this aspect of cellular immunity against AAV which may be useful to inform inclusion and exclusion criteria in clinical trials, for example.

1.5.4.2 Induction of anti-AAV cellular immune responses

As discussed previously, a cellular immune response is mounted against AAV antigens following administration when APCs present immunogenic capsid proteins to cytotoxic CD8+ T-cells via MHC class I. These capsid-specific T-cells are now directed against AAV infected cells and can induce their apoptosis via cell-mediated cytotoxicity. This effectively clears AAV-transduced cells and thereby decreases expression of a particular transgene product [57, 58]. Presentation of viral capsid proteins on MHC class II can also occur which results in the activation of CD4+ T-cells, which are known to mediate both cellular and humoral immunity in response to AAV gene therapy [59]. One of the first examples of cellular immunity against AAV2 in the clinic was seen during haemophilia B gene therapy trials. After an initial intravenous infusion of 2E12 gc (genome copies)/kg AAV2 carrying a functional copy of the factor IX (FIX) gene, transgene expression reached levels around 10% of that seen in healthy controls. After four weeks however, FIX levels decreased to baseline levels in tandem with an increase in liver transaminase levels in which an anti-AAV2 capsid T-cell response was implicated [60]. Later studies confirmed this CD8+ T-cell response using ELISPOT assays and flow cytometry in response to transduction of the liver, and showed that the T-cell response was directed against the AAV2 capsid protein [58]. In clinical trials investigating intramuscular delivery however, anti-AAV cellular immune responses have been observed, yet these have not apparently attenuated transgene expression as has been seen in liver gene transfer studies [61, 62]. A number of factors may underpin these differences, including the serotype used (AAV1 was used in the muscle gene transfer studies cited above), the route of administration used, the number of viral particles administered, and the immune status of the enrolled pa-

tients at baseline (i.e. when initially recruited to the study). One interesting study did identify the infiltration of regulatory T-cells into the transduced foci and the development of the "exhausted" T-cell phenotype - one that is usually associated with tolerance of viral antigens and chronic viral infections - in which signalling via the programmed cell death protein-1 (PD1) and it's cognate ligand PDL-1 was implicated [63].

Anti-capsid cellular immune responses can clearly have a detrimental impact on the efficacy of AAV gene therapy. Anti-transgene cellular responses have also been noted involving both CD4+ and CD8+ T-cells. As with anti-capsid CD8+ responses, anti-transgene cellular immunity can decrease transgene expression of AAV transduced cells via cell-mediated cytotoxicity mechanisms [64]. A number of factors have been implicated as key mediators of anti-transgene cellular immunity, including the route of administration, choice of promoter, frequency of CpG-rich sequences, and secretion of the transgene product [54]. In the clinic however, anti-transgene cellular immune responses have only been observed in rare cases, usually in trials utilising the intramuscular delivery route, such as anti-Dystrophin T-cells in Duchenne's Muscular Dystrophy (DMD) trials, for example [65]. More recently, however, this effect has also been observed in organs considered to be more immuneprivileged. In a clinical study investigating mucopolysaccharidosis type IIIB, anti-transgene T-cells were documented following intracranial delivery of AAV5 [66].

1.6 Humoral immune responses to AAV

There is a clear role for the innate and cellular arms of the immune system in limiting the efficacy of AAV-based gene transfer strategies. It is now well-established that the generation of antibodies against various viral components also represents a significant barrier for AAV gene therapy. This section will review the role of the humoral immune response in terms of pre-existing humoral immunity and the induction of anti-vector antibody responses. Understanding the fundamental biological concepts underpinning the production of antibodies and the mechanisms of neutralising antibodies is key to deriving counterstrategies.

1.6.1 How are antibodies produced?

Antibodies are glycosylated proteins that can be presented on the surface of B-cells (and act as antigen receptors (B-cell receptors)) or secreted by B-cells so they can bind to and neutralise target proteins. Antibodies are composed of two "light" and two "heavy" chains which are linked by disulphide bonds. At the N-terminus on an antibody are the hypervariable regions which determine antigen specificity. Five classes of antibodies have been described

(IgM, IgD, IgG, IgA, IgE), each varying according to their respective C-terminal domains, termed Fc regions. Fc regions mediate the effector functions of antibodies, for instance, when facilitating antibody-dependent cell-mediated cytotoxicity by recruiting CD8+ T-cells [67].

Immature B-cells originate from the bone marrow in adult humans. They derive from haematopoeitic stem cells into pro-B-cells, then pre-B-cells and immature B-cells. This development follows rearrangement of immunoglobulin heavy and light chains on the cell surface, resulting in expression of an antigen-specific IgM B-cell receptor [68]. Mature B-cells migrate to the spleen where they are activated by an antigen-presenting dendritic cell (DC) via interactions with the B-cell receptor and helper signals from a specialised CD4+ T-cell subset called follicular helper T-cells (Thf). Antigen binding to B-cell receptors activates gene expression changes and internalisation of the antigen into an endosome. Antigen proteins are subsequently degraded and presented on the B-cell surface by MHC class II molecules, which facilitates interactions with Tfh helper CD4+ T-cells [69]. Some activated B-cells develop into plasmablasts without entering the B-cell follicles within the spleen. Others return to the follicles where they undergo affinity maturation of antigen-binding sites (via somatic hypermutation (SHM)) and immunoglobulin class switching (via class-switch recombination (CSR)) to generate high affinity antibody producing plasma cells and memory B-cells with a diverse set of effector functions. Here, SHM induces point mutations in antigen-binding regions to enable selection of high affinity clones whilst CSR replaces DNA sequences that dictate isotype. The latter permits the generation of antibodies with various effector functions without altering their antigenic specificity. These plasma cells home to the bone marrow and produce antibodies independently of further antigen exposure [70–72].

1.6.2 How do antibodies neutralise AAV?

Despite the relevance of pre-existing and induced humoral immunity against AAV, the precise mechanisms by which antibodies neutralise AAV have yet to be elucidated. Here the main mechanisms that antibodies utilise to neutralise viral infections will be summarised.

Antibodies can have a neutralising or binding (non-neutralising) function. A neutralising antibody is defined as one that is capable of inhibiting the infectivity or pathogenesis of a virus. Binding, or non-neutralising antibodies, are thought to lack neutralising activity but may be involved in the recruitment of immune cells and the induction of antibody-dependent cellular cytotoxicity (ADCC) [73].

Some NAbs can impede a virus by inhibiting its function prior to its binding to a cell. IgA and IgM antibodies can induce aggregation of certain types of bacteria, and some IgG antibodies have exhibited this function in the context of polio virus infections, for example [74]. Other antibodies appear to induce loss-of-function conformational changes in their targets that

destabilises their capsid structures. This has been demonstrated with NAb against Sinbis virus [75] and human immunodeficiency virus-1 (HIV-1) [76].

NAbs can also interfere with the attachment of viruses to cells. For example, NAbs can bind to HIV-1 gp120 and thereby prevent the binding of the virus to its cognate receptor, CD4 [77]. This mechanism, thought to occur due to steric interference between virus cell-binding ligands and cell surface receptors, has also been shown to apply to flavivirus [78], parvovirus [79] and rotavirus [80].

Other NAbs may interfere with enveloped viruses like HIV-1 post-attachment by preventing fusion of viral and endosomal membranes once the virus enter its target cell [81]. Non-enveloped viruses enter cells via endocytosis and must 'escape' from endosomes in order to prevent their degradation in lysosomes. Antibodies against polio virus have been shown to destabilise capsid proteins so that the virus cannot escape from the endosome [82].

NAbs may also interfere with other essential viral intracellular processes. For instance, some NAbs against human papilloma virus have been shown to prevent trafficking of viral DNA to the nucleus [83]. Recently, a novel mechanism of intracellular virus neutralisation was described in which a cytosolic antibody receptor, called Trim21, binds to antibody-coated adenoviruses and facilitates its proteasomal degradation [84].

Clearly, NAbs can utilise a number of mechanisms to neutralise virus infections. However, an understanding of how NAbs interact with AAV is very limited, and only a few studies have investigated this aspect of gene therapy. A correlation between the levels of NAbs and IgG titres has been established [41], and it appears that IgG1, IgG2, and IgM are the main subtypes that are correlated with anti-AAV NAbs [85]. However, it has not yet been characterised which subtype is primarily responsible for neutralising activity against AAV as opposed to binding activity against AAV. One paper has shown that NAbs are associated with the accumulation of AAV in the lymphoid organs, whilst binding antibodies have been shown to increase transduction of the liver, highlighting the possibility that certain subclasses of antibody may be capable of partially redirecting vector tropism [86]. Further, interactions between humoral immune responses and complement pathways have also been identified. In an *in vivo* study, mouse models deficient in complement receptor 1/2 and complement component 3 demonstrated a delayed antibody response to AAV2 vectors and significantly lower terminal NAb titres compared to wild-type controls [87]. Interactions between Ig subtypes and the cellular immune system have also been observed, with one study highlighting a possible correlation between IgG3 antibody levels and the development of T-cell reactivity against AAV capsid proteins [88].

1.6.3 Pre-existing humoral immunity to AAV

The prevalence of patients' seropositivity (the harbouring of antibodies against an antigen) varies substantially depending upon the particular serotype in question and the geography in which the study was conducted [89, 90]. In studies examining people from four continents, the prevalence of NAbs against AAV1/2 ranged from 30-60%, which was greater than the 15-30% ranges observed for AAV7/8/9, and the 2% seropositivity seen for AAV4 [90]. These disparities may reflect the possibility of wild-type infections by a particular serotype, given that pre-existing humoral immunity, much like pre-existing cellular immunity described above, is thought to arise from asymptomatic wild-type AAV infections throughout a patient's lifetime. Anti-AAV NAbs are also known to be highly cross-reactive, and patients are often observed to harbour NAbs against most, if not all, AAV serotypes; a finding that may reflect the conservation of epitope binding regions across different AAV serotypes [91].

In most liver gene transfer studies, AAV serotypes 2 and 8 have been utilised, however, in a recent clinical trial investigating haemophilia B, AAV5 was used. Of the ten participants included in the trial, none were deemed to have pre-existing NAbs against AAV5, and although some did demonstrate anti-AAV5 IgG and IgM, this had no detectable impact on the efficiency of gene transfer [92]. These findings have been corroborated by reports from Drygalski et. al. who used a highly sensitive Luciferase-based NAb assay to identify low anti-AAV5 NAb titres in haemophilia B patients undergoing gene therapy-based FIX replacement. They also showed that these low levels of NAbs had no observable effect on the outcome of gene transfer in these patients. In this way, they were able to identify a new opportunity to include anti-AAV5 NAb seropositive patients in the clinical trial who were previously ineligible [93].

An alternative route of administration for gene therapy-based treatment of haemophilia B involves the injection of AAV vectors into the muscle. In 2003, rAAV vectors were used to deliver a functional copy of the FIX gene into male participants with severe haemophilia B. No evidence of local or systemic toxicity to the vector were observed up to 40 months post-injection, and the presence of antibodies directed against FIX protein were also not detected. In contrast to liver gene transfer studies that would be conducted in the proceeding years, the presence of anti-AAV NAbs in these patients did not have an apparent impact on the efficiency of gene transfer to the muscle [94].

Further, another study investigated the possibility of utilising intrathecal injections as a treatment for mucopolysaccharidosis type III. The prevalence of NAbs against AAV2 and AAV9 was assessed in the sera and cerebrospinal fluid (CSF) of healthy volunteers and enrolled patients. In the sera, anti-AAV2 NAbs were detected at a higher level than anti-AAV9 NAbs, and overall levels of both anti-AAV2 and -AAV9 NAbs were higher in the sera than CSF. Upon vector administration via intrathecal delivery (which involves injection of a vector-

containing solution into the spinal canal such that it reaches the CSF), the presence of these pre-existing NAbs did impact the efficiency of gene transfer, but did not completely block transduction [95]. In a non-human primate study, the detection of pre-existing NAbs at a 1:128 titre did not have any apparent effect on the efficacy of gene transfer when an AAV9.GFP gene therapy was used [96]. Taken together, these findings highlight the immuneprivileged status of the CNS and demonstrate a role for the blood-brain-barrier in limiting the transfer of NAbs from the systemic circulation into the CSF.

Studies utilising non-human primate models have demonstrated that pre-existing NAbs against AAV may limit the efficiency of transgene expression following an intravitreal injection (IVT). Pre-existing sera NAb titres of 1:10 or greater were found to reduce transgene expression, although some animals with 1:25-1:100 NAb levels still exhibited some degree of retinal transduction [97]. Data emerging from clinical trials, however, has suggested that pre-existing sera NAb titres may not represent a significant barrier to effective transduction of the retina via IVT. In one study, 2/5 patients demonstrated improvements in visual acuity following administration of an AAV-based treatment for LHON, in spite of the fact they harbored sera NAb titres of 1:5,120 and 1:20,480 at baseline [98]. Further, in a follow-up study to this trial, the same investigators showed that, of the 14 patients enrolled in the clinical study, the four that demonstrated the greatest increases in visual acuity also had the highest (1:20,480) NAb titres at baseline [99]. By contrast, a clinical trial investigating AAV2.sFLT1 (soluble FMS-like tyrosine kinase-1, an anti-VEGF agent) IVT gene therapy for neovascular age-related macular degeneration (nAMD) showed that pre-existing NAb titres of 1:400 appeared sufficient to preclude effective vector administration and transduction of the retina. sFLT1 protein expression was also blocked in patients with 1:3,200 NAb titres but no evidence of vector neutralisation was seen in the patient with a baseline titre of 1:100 [100].

1.6.4 Induction of anti-AAV humoral immune responses

Pre-existing antibodies to AAV represent a key barrier to successful gene transfer in seropositive individuals. A related issue is whether the administration of AAV induces a robust NAb response that precludes re-administration of a gene therapy. The importance of repeated gene transfer varies according to the route of administration and target organ, however, the ability to re-administer a gene therapy is a clinically relevant consideration for most, if not all, *in vivo* gene therapy programmes. Administration to young adults suffering from haemophilia, for example, is faced with the problem that the liver is a dividing tissue, leading to dilution of transgene expression over time. Further, as discussed above, CD8+ T-cell responses may clear transduced cells from target organs, especially after systemic or intramuscular delivery, again leading to reduced transgene expression over time. In addition, whilst many gene therapy

programs are targeting monogenic recessive disorders, there is an increasing interest in developing AAV constructs for diseases exhibiting complex aetiologies. In these diseases, multiple pathogenic pathways are involved which may require sequential administration of different gene therapies. There is also the possibility that an initial gene therapy injection is sufficient to induce a robust NAb response but insufficient to rescue a clinical phenotype. Lastly, it is possible that methylation of viral promoter sequences may occur years after AAV administration, which may lead to transgenic silencing. In these scenarios, a repeat injection of AAV could be used to circumvent reduced therapeutic transgene expression and maximise clinical benefit. Therefore, a discussion of the possibility of NAb induction and possible strategies to circumvent these responses is warranted. In this section, NAb responses following administration of AAV to the liver, skeletal muscle and CNS will be summarised. A detailed analysis of NAb induction observed in ocular gene therapy trials is then provided.

1.6.4.1 Gene therapy trials targeting the liver and skeletal muscle

A number of clinical studies have reported increased anti-AAV NAb levels after vector administration to target the liver and skeletal muscle. In summary, these reports suggest that these two routes of administration lead to elevated NAb titres, which, in some cases, were observed up to 52 weeks after vector infusion. Further, the utilisation of immunosuppression in two of the trials discussed below did not appear to be sufficient to abrogate anti-capsid NAb responses. Given the role that pre-existing NAbs may play in limiting the effectiveness of gene transfer, the induction of NAbs in these trials may represent a possible barrier to vector re-administration in these individuals, which may limit the clinical utility of gene therapy. A summary of humoral immune responses in clinical trials targeting the liver and skeletal muscle for human gene therapy is provided in the table below.

Table 1.1: Summary of humoral immune responses in clinical trials targeting the liver and skeletal muscle for human gene therapy

Reference	**Disease**	**Therapy**	**Delivery**	**IS**	**Patients with increased Nabs**
[60]	Haemophilia B	AAV2.FIX	Intravenous	None	7/7
[101]	Haemophilia B	scAAV2/8.FIX	Intravenous	None	6/6
[94]	Haemophilia B	AAV2.FIX	Intramuscular	None	8/8
[62]	AAT deficiency	AAV2.AAT	Intramuscular	n/a	12/12
[61]	AAT deficiency	AAV2.AAT	Intramuscular	n/a	12/12
[102]	AAT deficiency	AAV1.AAT	Intramuscular	n/a	9/9
[103]	LPL deficiency	AAV1.AAT	Intramuscular	None	8/8
[104]	LPL deficiency	AAV2.LPL(S447X)	Intramuscular	CyA, MMF	14/14
[105]	LPL deficiency	AAV2.LPL(S447X)	Intramuscular	CyA, MMF, Pred	5/5

AAV = adeno-associated virus; scAAV, self-complemetary AAV; FIX = factor 9; AAT = α1-antitrypsin; LPL (S447X) = low density lipoprotein variant harbouring single point mutation; IS = immunosuppression; CyA = cyclosporin A (T-cell inhibitor); MMF = mycophenolate mofetil (T- and B-cell inhibitor); Pred = prednisolone (steroid immunosuppressant); NAb, neutralising antibody.

1.6.4.2 Gene therapy trials targeting the central nervous system

Gene delivery to the CNS can be achieved via systemic vector delivery provided an appropriate AAV serotype [106] (or mutated AAV capsid [107, 108]) is used. As outlined potential of gene transfer for treating diseases affecting the CNS has been demonstrated in the context of SMA, and an FDA-approved therapy (Zolgensma) now exists for the condition which uses AAV9 expressing survival motor neuron-1 (SMN-1).

The earliest clinical trials investigating SMA gene therapy via systemic delivery did not report the induction of antibodies against either the AAV9 capsid protein or the SMN-1 transgene [27, 109, 110]. Similarly, a study conducted in non-human primates and piglets did not report the development of humoral immune responses against capsid proteins or transgene products, in spite of the observation of severe toxicity following high-dose intravenous administration of an AAV9 variant, AAVhu68, carrying the SMN-1 transgene [111].

An alternative route of delivery to the CNS is intrathecal delivery. A study investigating intrathecal delivery of AAV9 as a possible treatment for mucopolysaccharidosis type III showed that vector administration induced a robust systemic humoral immune response against AAV9 capsids, despite all dogs demonstrating undetectable levels of anti-AAV9 NAbs at baseline. Eight days after vector administration, NAb titres were greater than 1:1,000. Interesting correlations between systemic and corresponding CSF NAb titres were also observed and appeared to be dependent upon the presence of inflammation in the CSF. In the absence of inflammation, CSF samples were negative or had NAb titres of <1:10, however, in dogs exhibiting signs of inflammation in the CNS, NAb titres of 1:100-1:1,000 were seen, suggesting that the presence of inflammation may compromise the integrity of the BBB [95].

Injections can also be performed directly into the brain in order to transfer genes to the CNS. One non-human primate study examined injections of AAV9 expressing acid sphingomyelinase (ASM) into the cerebromedullary (CM) space of a Niemann-Pick disease type A model (a lysosomal storage disease). Slight increases in anti-AAV9 NAb levels were seen in both the sera (1:400-1:800) and CSF (1:100-1:200) at one and three month timepoints respectively in response to vector administration [112].

Overall, the results of non-human primate studies and clinical trials investigating the induction of NAbs following delivery to the CNS indicate possible differences to other modes of administration. Principally, that pre-existing sera NAb titres appear to have less of an impact in neutralising vector administration, likely due to the impermeability of the BBB.

1.6.4.3 Gene therapy trials targeting the eye

The eye has been at the forefront of gene therapy research for a number of reasons. First, its compartmentalised nature and tightly-regulated transport of molecules across the blood-retinal-barrier (BRB) reduces the risk of vector leaking into the systemic circulation, thereby mitigating a significant regulatory/safety concern [113]. Second, the eye is relatively accessible for vector administration, and several well-characterised routes of delivery, such as IVTs and subretinal injections (SRTs) are available for ophthalmologists. Third, a number of non-invasive tools can be used to assess clinical endpoints for a particular therapy, such as electroretinography (ERG) and optical coherence tomography (OCT). Anatomically, the eye is also smaller than other organs, such as the brain, which obviates the need for high vector doses to achieve robust transduction of target cell types. Lastly, the eye is generally considered to have an 'immuneprivileged' status and generally exhibits lower immune responses than other organs. As mentioned, this is in part is due to the impermeability of the BRB to humoral and cellular arms of the immune system which has been shown to limit access of circulating anti-capsid antibodies into the eye [114]. The phenomenon may also be accounted for by a process called anterior chamber-associated immune deviation (ACAID). During ACAID, immunogenic antigens induce a tolerogenic immune response that involves regulatory T-cell and anti-inflammatory M2 macrophage induction, and increases synthesis of anti-inflammatory cytokines [115–118]. An overview of the clinical studies reporting NAb titres for SRT and IVT gene therapies is in the table below.

Table 1.2: Summary of humoral immune responses in clinical trials utilising SRT and IVT for human gene therapy

Reference	**Disease**	**Therapy**	**Delivery**	**IS**	**Patients with increased NAbs**
[119]	LCA2	AAV2.hRPE65	SRT	Oral pred	0/3
[120]	LCA2	AAV2.hRPE65	SRT	Oral pred	6/12
[121]	LCA2	AAV2.hRPE65	SRT	n/a	1/3
[122]	LCA2	AAV2.hRPE65	SRT	Topical pred	6/14
[123]	LCA2	AAV2.hRPE65v2	SRT	Oral pred	1/3
[124]	LCA2	AAV2.hRPE65v2	SRT	Oral pred	2/12
[125]	LCA2	AAV2.hRPE65v2	SRT*	Oral pred	0/3
[126]	LCA2	AAV4.RPE65	SRT	Oral pred	2/9
[127]	RP	AAV2.hMERTK	SRT	None	2/6
[128]	nAMD	AAV2.sFLT1	SRT	Topical pred	2/9
[129]	nAMD	AAV2.sFLT1	SRT	Topical pred	3/21**
[130]	LHON	AAV2.ND4	IVT	Oral pred	0/9
[98]	LHON	AAV2.P1ND4v2	IVT	None	1/5
[99]	LHON	AAV2.P1ND4v2	IVT	None	2/14
[34]	LHON	AAV2.ND4	IVT	None	14/15
[100]	nAMD	AAV2.sFLT1	IVT	None	7/19

AAV, adeno-associated virus; LCA2 = Leber's congenital amaurosis type II; RP = retinitis pigmentosa; nAMD = neovascular age-related macular degeneration; LHON = Leberâs hereditary optic neuropathy; RPE65 = retinal pigment epithelium-65; RPE65v2 = retinal pigment epithelium-65 with enhanced Kozak sequence; MERTK = c-Mer protooncogene tyrosine kinase; sFLT1 = soluble FMS-like tyrosine kinase; ND4 = NADH dehydrogenase subunit 4; P1ND4v2 = NADH dehydrogenase subunit 4 containing mitochondrial targeting sequence; SRT = subretinal injection; IVT = intravitreal injection; IS = immunosuppression; NAb, neutralising antibody. * Participants received an SRT of AAV2 into the contralateral eye. **In this study, 3/9 patients seroconverted after receiving IVT of AAV2 (for the remaining 12 patients, NAb titres were not reported).

1.6.4.3.1 Gene delivery to the outer retina by subretinal injection A gene therapy for *rpe65* mutations was approved by the FDA in 2018. Efforts to develop an AAV-based gene therapy for LCA2 have helped to improve our understanding of AAV vector immunobiology when delivered into the subretinal space. These studies showed that the immuneprivileged status of the eye, and the relatively non-immunogenic properties of AAV as a vector did not necessarily circumvent immune responses to vector administration.

Initial testing of humoral immune responses in C57BL/6 mouse models showed that a significant systemic antibody response against AAV capsid proteins could be induced by SRT. It was also found however, that the induction of systemic humoral immunity did not preclude vector readministration into the ipsilateral eye [131]. The authors later characterised a deviant immune response upon SRT of AAV two years later, and highlighted similarities to ACAID. Here, the generation of a population of immunosuppressive Th2-type T-cells were reported post-SRT and were identified as potential mediators of the immune deviation mechanism observed [132]. These data would contrast with later reports which demonstrated SRT of AAV2 did not result in a detectable increase in NAb levels. This may reflect the discrepancy in AAV serotypes used by the two investigators, however [133].

In 2008, the first report of AAV2.hRPE65.hRPE65 (used an RPE65 promoter) gene delivery to the subretinal space as therapy for LCA2 were published by researchers from University College London, however, only three patients were included in this study. None of the enrolled patients developed humoral immunity against AAV2 following vector administration, and sera NAb titres were either undetectable or <1:7 at baseline throughout the 12 month follow-up period [119].

Later reports examined the long-term safety of AAV2.hRPE65.hRPE65 gene therapy for LCA2, and provided evidence that intraocular inflammation and immune responses occurred when higher doses of vector were used. The study also highlighted a potential humoral immune response against AAV2. In 3/4 of patients receiving low dose AAV2, circulating NAb titres increased from 1:1-1:4 to 1:2-1:16 throughout the three year follow-up period. In the remaining patient in the low dose group, NAb titres increased from 1:512 to 1:1,024 between baseline and 4 months. In the high dose group, four patients showed no changes in NAb levels throughout the study period. In two patients, however, vector administration apparently induced a humoral immune response. In one patient, NAb levels increased from 1:2 to 1:1,024 between baseline and four months follow-up, and in the other, an increase from 1:4 at baseline to 1:125 after four weeks was observed. In both of these patients, an asymptomatic episode of posterior intraocular inflammation was correlative with NAb titre increases. Throughout the study however, no anti-RPE65 transgene NAbs were detected. Crucially, this clinical trial demonstrated that humoral immune responses could be induced against AAV2 capsids even

when a prophylactic oral glucocorticoid immunosuppressive drug regimen was given to patients before and after vector administration [120].

Other studies investigating SRT delivery of AAV2.CB.hRPE65 (chicken β-actin promoter) for LCA2 gene therapy have reported similar results. In a phase I trial conducted by researchers from the University of Pennsylvania, humoral immune responses were measured at baseline, and days 14 & 90. Whilst 2/3 patients did not demonstrate an anti-vector NAb response, one patient exhibited a 7.5-fold increase in their 90-day antibody titre compared to baseline levels, however, this did not correlate with AAV2 capsid-specific reactivity of peripheral lymphocytes in which no changes were observed in any patients between baseline and days 14 or 90. In this study, anti-transgene NAb induction was not reported [121].

In a long-term assessment of the safety and efficacy of AAV2.CB.hRPE65, humoral immune responses were measured throughout a three-year follow-up period. 8/14 patients enrolled in the study actually demonstrated a decline in anti-AAV2 NAb titres throughout the study, whilst 6/14 demonstrated increases in NAb titres vs. baseline. 5/6 of these patients showed modest changes of around 1.2 to 2.0-fold increases. In the remaining patient however, a nine-fold increase was seen, but this did not apparently correlate with their NAb titre observed at baseline. Indeed, across all cohorts tested, no apparent correlation between AAV2 dosages and anti-AAV2 antibody titres was evident [122]. Interestingly, in the University of Pennsylvania studies [121, 122], no patients were given prophylactic glucocorticoid immunosuppressants, and this did not have an apparent effect on the induction of humoral immunity when compared to patients enrolled in the University College London trials [119, 120].

In a phase I trial published in 2008 (sponsored by Spark Therapeutics), AAV2.CB.hRPE65v2 (voretigene neparvovec (Luxturna)) SRT administration was found to induce an anti-AAV2 NAb response in 1/3 patients enrolled in the study. The levels of this patient's NAbs were elevated after 14 days, and did decrease by 30 days post-SRT but remained high compared to baseline. No evidence of anti-RPE65 NAbs were observed in this study [123].

The safety and efficacy of AAV2.CB.hRPE65v2 was then further investigated in a phase I dose escalation trial which introduced middle and high dose cohorts. In the middle dose cohorts, 4/6 patients did not exhibit signs for an anti-AAV2 humoral immune response. In 2/6 patients however, significant increases in NAb levels were evident vs. baseline values. In one patient, NAb levels rose from 1:100 at baseline to 1:1,000 at day 14, then decreased to 1:316 after one year. In another patient, NAb levels were 1:350 at baseline and day 14, but then increased to 1:3,160 after 90 days. Perhaps unexpectedly, in the high dose cohort, no evidence of a humoral immune response was detected in any of the three patients. It should be noted however, that the two patients from the middle dose cohort who exhibited the greatest increases in NAb levels also had the highest NAb levels at baseline. Therefore, it is possible

that these patients had some pre-existing immunity to AAV2 that was sufficient to induce a humoral immune response upon vector administration but not sufficient to be excluded from the trial [124].

The investigators then tested whether readministration of AAV2.CB.hRPE65v2 resulted in increased sera NAb levels. Of the three patients included in this follow-on trial, baseline NAb levels were 1:1 to 1:3.16 and remained at these low levels in spite of vector administration into the contralateral eye [125]. Notably, in all studies examining AAV2.CB.hRPE65v2, systemic corticosteroid immunosuppressive treatment was given to patients to mitigate the occurrence and severity of vector-mediated immune responses.

The majority of studies investigating gene therapy for LCA2 have utilised AAV2 for the delivery of therapeutic transgenes. One study from the University of Nantes has utilised the AAV4 serotype, however. Of the nine patients enrolled in this study, six did not exhibit any detectable anti-AAV4 IgG at baseline or after vector administration. In two patients, a significant increase in anti-AAV4 IgG and NAb levels were seen. Here, NAb titres as high as 1:500 and 1:1,000 were seen as early as 14 days after the SRT of AAV4. In one patient, a NAb titre of 1:50 was seen at baseline, but remained unchanged at 1:50 until 180 days follow-up, indicating that a humoral immune response was not induced by AAV4 SRT in this patient. In these studies, prednisolone glucocorticoids were administered daily one week before and after the SRT fo AAV4 to prophylactically inhibit immune reactions to the vector [126].

Outside of LCA2, SRT of AAV vectors has been investigated for possible therapeutic effects in other genetic eye disorders like retinitis pigmentosa. More recently, the platform has also been applied to diseases with complex etiologies like nAMD.

Mutations in MER proto-oncogene tyrosine kinase (MERTK) cause retinitis pigmentosa. MERTK aberrations disrupt phagocytic activity of RPE cells, which in turn causes degeneration of rod and cone photoreceptors. AAV2 has been used to deliver functional MERTK genes into RPE cells via SRT. In a phase I study, 3/6 patients demonstrated improvements in visual acuity and all patients exhibited acceptable safety profiles. In 2/6 patients, anti-AAV2 humoral immune responses were also recorded. In one patient, a 26-fold increase in NAb titre was observed vs. baseline levels after ten days, which declined to a 16-fold increase after one year post-SRT. In a second patient, an eight-fold increase in circulating NAbs was seen after ten days, however, no data was reported for this patients NAb titres after one year of follow-up [127].

The first reports of SRT gene therapy being used to treat nAMD in patients were published in 2015. In this phase I study, nine patients were enrolled and administered rAAV2.sFLT1 via SRT. The therapy was shown to reduce the requirement for 'rescue' injections of intravitreal anti-VEGF agents (Ranibizumab), whilst no drug-related adverse events were reported. Total

anti-AAV2 and neutralising AAV2 antibodies were reported between baseline and one year follow-up in six of the patients enrolled. In 4/6 patients, NAb titres remained unchanged at <1:20 throughout the study. Patient 2's NAb levels also remained unchanged at 1:20-1:100 at baseline and throughout the study, possibly indicating that, although they harboured some pre-existing immunity to AAV2, this did not lead to a significant humoral immune response upon vector administration. In patient 6, a robust humoral immune response was evident, however. This subject's NAb titres were <1:20 at baseline and increased to 1:20-1:100 at three weeks, and persisted at this level until 52 weeks [128].

Further testing of this gene therapy in a phase IIa study corroborated previous findings. Of the 21 patients studied, nine displayed no anti-AAV2 NAbs at baseline, whilst 12 had titres between 1:20-1:100. In 3/9 patients with no detectable NAbs at baseline, anti-AAV2 NAbs were observed at completion of the study. In this publication however, the data on NAb levels were not included, rendering analysis in this review challenging [129].

1.6.4.3.2 Gene delivery to the inner retina by intravitreal injection IVT is a simpler route of delivery for AAV-based gene therapies. IVTs can be performed in an ophthalmologist's office in a matter of minutes, and only requires topical analgesics for the injection. IVTs are also necessary to target inner retinal cells, principally RGCs. Recently, evidence has emerged suggesting that specific AAV serotypes can target the outer retina/photoreceptor layer via IVT. This has increased the interest in this delivery route for treating common blinding disorders like nAMD and diabetic retinopathy [134, 135]. A number of preclinical and clinical studies utilising IVTs of AAV gene therapies have now been completed. These have highlighted similarities and differences between IVT and SRT in terms of the induction of humoral immunity against AAV capsid proteins.

One of the earliest reports contrasting the induction of NAbs following SRT and IVT of AAV2 was published in 2008 [133]. In a rodent model, it was shown that unilateral SRT did not trigger a humoral immune response against AAV2 capsid proteins. As a result, subsequent administration of AAV2 into the contralateral eye was permissible when delivered by SRT and IVT, a finding that supported clinical studies investigating SRTs and contralateral eye administration [125]. When an initial injection of AAV2 was delivered via IVT however, the induction of humoral immunity was evident. The authors reported up to ten-fold increases in total anti-AAV2 antibodies following IVT, a finding that correlated with the levels of NAbs against AAV2 capsids. Upon readministration of AAV2 to the contralateral eye, the authors found that SRT delivery resulted in robust transduction of the outer retina, however, they observed diminished expression if the IVT delivery route was used for vector readministration [133]. Their findings therefore highlighted possible differences between the immune deviation

mechanisms employed by the vitreous cavity vs. the subretinal space, however, it should be noted that their observation that SRT does not result in a humoral immune response is in partial disagreement with some clinical [120–122] and preclinical studies [131, 132].

In non-human primate studies, further evidence has arisen that IVT may induce stronger NAb responses than SRT. In 2015, Kotterman et. al. published data relating to the induction of anti-AAV NAb following IVT of multiple serotypes and mutagenised capsid protein AAV variants, and their analysis showed that IVT of all AAV variants caused a NAb response. They tested AAV2, AAV5, AAV9, AAV7m8 (peptide insert mutant AAV) and AAV2 (Y-F tyrosine mutant AAV2), all of which were found to elevate NAb levels from 1:1-1:100 at baseline to 1:100-10,000 after the injection. In some of the non-human primates, NAb levels were assessed over a period of seven months. All injected animals demonstrated consistent NAb levels in the first three months proceeding IVT, but some showed a 2-5-fold decline after three months. In general however, the persistence of elevated NAb titres for long periods after gene therapy administration was observed. The authors also reported cross-reactivity of NAbs generated against multiple AAV serotypes. Here, injection of AAV5 and AAV9 was found to increase anti-AAV2 NAb levels, and IVTs of AAV2, AAV7m8 and AAV2(Y-F) induced anti-AAV5, -AAV8 or -AAV9 humoral immune responses. The authors also noted an interesting but non-significant trend in which higher pre-injection NAb titres correlated with a lesser fold-change between pre- and post-injection titres. It was postulated that this may be due to higher rates of vector neutralisation which attenuated retinal transduction and antigen presentation to the immune system [97].

In a comparable non-human primate study, IVT and SRT of AAV capsid mutant variants AAV7m8 and AAV8BP2 (9mer peptide insert into AAV8 capsid) were found to induce humoral immune responses. Following IVT, AAV8BP2 increased sera NAb titres in 4/4 non-human primates from <1:3.16 to 1:10-100, and AAV7m8 IVT also elevated sera NAb levels from <1:3.16-1:10 to 1:10 to 1:1,000. These increases therefore appeared to be slightly lower than that observed by Kotterman et. al. [97], however, this discrepancy may be explained by a multitude of confounding variables, such the different timepoints used in the study, difficulties in accurately titering AAV preps (rendering comparison between studies challenging) and of course the use of different AAV serotypes/mutant capsids. This study also compared sera NAb titres to vitreous NAb titres. After IVT of AAV8BP2, post-injection vitreous NAb titres remained unchanged at <1:3.16 in all animals. Following AAV7m8 IVT however, vitreous NAb levels rose from <1:3.16 to 1:100 in 2/6 non-human primates Interestingly, this study also reported increases in NAb levels following SRT in some animals (1/3 after AAV8BP2 SRT and 4/4 after AAV7m8 SRT), a finding that reflects certain preclinical and clinical studies [120–122, 131, 132]but disagrees with the results of investigations utilising mouse models

[133].

Reports detailing the induction of humoral immunity in clinical trials following IVT of AAV-based gene therapies arose sometime after those utilising the SRT route of administration. In 2016, one study described the use of AAV2 expressing mitochondrial reduced nicotinamide adenine dinucleotide (NADH) dehydrogenase subunit 4 (ND4) as a possible treatment for LHON. Patients enrolled in this clinical trial were given oral prednisolone for one week prior to and eight weeks after the administration of the therapy. At baseline and six months post-IVT, NAb titres in all patients remained unchanged and at levels below 1:20, however, it should be noted that no improvements in visual acuity were observed in this study [130].

In the same year, the data from another clinical trial investigating LHON gene therapy were published. In this study however, a self-complimentary AAV2 (scAAV2; contains ds-DNA genome) harbouring tyrosine to phenylalanine substitutions and an ND4 gene expression cassette (AAV2.CBA.P1ND4v2) was utilised, and no immunosuppressants were given to the five patients enrolled in the study. Only one patient experienced an increase in NAb levels from 1:5 at baseline to 1:20 after seven days, which then decreased back to baseline levels after 90 days follow-up. It should be noted however, that the other four patients enrolled exhibited very high (1:5,120-1:20,480) NAb levels at baseline, but this did not appear to inhibit transduction efficiency/therapeutic efficacy in patients 4 a"Gene therapy for leber hereditary optic neuropathy initial resultsnd 5 who had a baseline NAb titres of 1:5,120 and 1:20,480 respectively [98]. In the follow-up to these initial results, similar data were reported that corroborated previous findings [99]. In accordance with other studies investigating SRT of AAV gene therapies [120–122], there was no obvious correlation between baseline NAb titres and the induction of a humoral antibody response. For instance, patient 6 (received a 'medium' dose IVT) showed an increase in NAb titre from 1:80 at baseline to 1:20,480 after seven days which persisted throughout the one-year follow-up period. By contrast, patient 4, who had a baseline NAb titre of 1:5,120 and also received a 'medium' dose IVT of AAV2(Y-F), did not demonstrate an increase in NAb levels, and in fact exhibited a titre of 1:1,280 at the one-year timepoint. Further, whilst patient 3 had a baseline NAb titre of 1:5 and received a 'low' dose of AAV2, their titres increased to 1:20 after seven days then decreased to baseline levels after 90 days, patient 8 did not demonstrate a humoral immune response against AAV2 despite receiving a 'medium' dose IVT and having a baseline NAb titre of 1:5. Another comparison between this study and the data reported by the SRT investigations is that the observation of a significant humoral immune response (patient 6) correlated with an episode of anterior uveitis, a finding similar to that reported by Bainbridge et. al. [99, 120].

This induction of humoral immune responses in a subset of patients administered with AAV2 gene therapies in the absence of prophylactic immunosuppressants has also been shown

in a phase I/II study investigating the use of AAV2.ND4 in LHON patients. In this trial, 13/15 patients presented with episodes of anterior uveitis and vitritis, two of which were administered immunosuppressants to counteract this ocular inflammation. The authors also concluded that there was no observable correlation between the ocular inflammation score (OIS) and the vector dose administered. They also reported no apparent association between the humoral immune response and vector dose, nor the humoral immune response and OISs. Most patients did demonstrate an increase in their NAb titres after the AAV2 IVT, however. 3/3 patients receiving the lowest dose (9E9 vector genomes/eye) had elevated NAb titres shortly after vector administration which persisted throughout the 52-week follow-up period. 3/3 patients receiving 3E10 vector genomes/eye also showed increases in NAb titre levels between baseline which largely persisted throughout the 96-week follow-up period. In patients who received 9E10 viral genomes/eye, however, the results were less clear, and whilst a transient increase in NAb titres was observed in 5/6 patients, these resolved back to baseline levels in two cases, but persisted until week 96 in the remaining three cases. Finally, in patients who received 1.8E11 viral genomes/eye, 3/3 showed elevated NAb titres shortly after receiving an IVT of AAV2.ND4, however, these decreased back to baseline levels in one patient. Overall, this study provided evidence that AAV2 IVTs may induce NAb responses, however, it should be emphasised that these patients did not receive prophylactic immunosuppressant therapy [34]. Here, more research is required to understand whether glucocorticoid therapy is able to circumvent the induction of humoral immunity in patients receiving IVTs of AAV2 and what the importance of this finding may be, for instance, in enabling readministration of the vector to the ipsilateral or contralateral eye.

Whilst clinical studies utilising AAV2 IVT have mostly targeted genetic diseases, the approach has also been used to target nAMD. AAV2.sFLT1 (delivered by IVT) was studied in 19 patients, and 6/19 demonstrated substantial reductions in retinal oedema and improvements in vision. There was some evidence of the induction of humoral immunity against AAV2, however, this was not associated with the vector dose administered. 6/6 patients in the low dose groups (2E8-2E9 vector genomes/eye) showed no detectable increase in NAb levels. In patients who received 6E9 vector genomes/eye, 2/3 demonstrated anti-AAV2 NAb responses. For patients in the first 2E10 cohort, one patient had a 1:3,200 baseline titre which rose to 1:25,000 after 12 weeks and then decreased to 1:12,800 after one year. In the other two patients, no NAbs were observed at baseline, but rose to 1:800 in one patient and 1:100-1:200 in another throughout the one-year follow-up period. In the other cohort of patients receiving the highest dose of AAV2.sFLT1 (2E10 vector genomes/eye) 2/7 demonstrated increases in NAb titres, with one patient's levels increasing from zero at baseline to 1:200-1:400 throughout the follow-up period, and another's increasing from 1:100 to 1:800-1:1,600 through the

duration of the study. The utilisation of prophylactic immunosuppressants was not reported in this study, however, topical steroids were used to treat episodes of pyrexia and intraocular inflammation in two patients in the high-dose cohort [100].

1.6.4.3.3 Is the eye immuneprivileged to AAV gene therapies? Despite the assumption that the eye is a relatively immuneprivileged environment and therefore favourable for testing gene therapies, the above discussion highlights a number of key findings suggesting that humoral immunity to AAV, either pre-existing via wild-type infection or induced by vector administration, may represent a significant hurdle for successful gene transfer to the inner and outer retina. The number of patients enrolled in the clinical trials described above is limited, reflecting the small patient populations for their respective indications. However, a number of trends may be evident in the data. These patterns highlight unanswered questions in the field and identify possible research questions for the future.

1. Only a subset of patients demonstrate increases in anti-AAV NAb levels after vector administration via SRT [120, 129] or IVT [34, 100]. Some of these patients exhibit very low/undetectable NAb titres at baseline, others had high NAb titres, yet evidence of the induction of humoral immunity to AAV was occasionally observed in both cases post-injection. One possible explanation here is that patients that are seronegative at baseline may harbour AAV reactive T-cells [58, 136] which facilitate a strong humoral immune response upon vector administration.

2. One trend that is evident is that the significant increases in NAb levels observed in some patients appear to correlate with episodes of intraocular inflammation. A number of studies investigating SRT [120] and IVT [34, 99, 100] have shown that the onset of events such as vitritis and anterior uveitis was seen in patients who exhibited the greatest changes in their NAb titres between baseline and the weeks/months proceeding vector administration. It should also be noted that some of the patients who developed intraocular inflammation had very low/undetectable NAbs at baseline. More research is required here to understand why this subset of patients developed much stronger NAb responses compared to other enrolled participants. Further, patients who developed high NAb titres and intraocular inflammation may be at increased risk of CD8+ T-cell infiltration into the retina and the clearance of transduced cells overtime, which may eventually lead to the loss of therapeutic efficacy. This suggests patients who did develop intraocular inflammation should be closely monitored for signs of diminished transgene expression. In this regard, considering the apparent failure of AAV reactive T-cells to recirculate in peripheral blood [36] (rendering their ex vivo analysis via blood

sampling/ELISPOT assay challenging) episodes of intraocular inflammation could serve as a surrogate biomarker for those patients most at risk of deleterious CD8+ T-cell infiltration into the retina.

3. There is no apparent correlation between baseline NAb titres and the magnitude of increase in NAb titre observed after vector administration. Of the patients that did exhibit significant increases in NAb levels after SRT [120, 128, 129] and IVT [34, 99, 100], high and low/undetectable baseline NAb titres were observed. This evidence may discount a possible theory that high baseline NAb levels leads to rapid neutralisation of vectors upon injection, which in turn precludes the presentation of their capsid proteins to the immune system [97]. It also suggests that a 'primed' immune system (i.e. one harbouring NAbs/B-cell epitopes against AAV) may not necessarily lead to stronger NAb responses compared to a patient who has no detectable NAbs at baseline.

4. It is unclear whether AAV administration via SRT or IVT induces NAb responses in a dose-dependent manner, which may simply reflect the small sample sizes used in these studies. However, it is notable that two studies [124, 125] investigating SRT of AAV2 found no evidence of a dose-response effect. Further, in studies using IVT for vector delivery, one reported higher frequencies of elevated NAb titres in the low dose group than the medium dose group [99], and another detected NAb responses in both low and high dose groups [34]. In the largest study reported in the literature, no NAb response was reported in the low dose group, but equitable increases in NAb levels were seen in the medium and high dose groups [100]. One possible explanation here is that delivery of AAV above a certain threshold is sufficient to induce NAb production, but this might not be further enhanced by administration of additional capsid antigens.

5. The administration of perioperative steroids may not be sufficient to attenuate production of anti-AAV NAbs. Of the 16 clinical studies highlighted in this review, seven reported the use of oral prednisolone glucocorticoid steroids to prophylactically treat the immunological complications of AAV gene transfer. Of these seven however, four reported increased NAb levels in some of the patients enrolled, suggesting that steroid therapy may not have been sufficient in circumventing humoral immunity in these individuals [120, 123, 124, 126].

6. Further research is required to understand how the induction of anti-AAV NAbs may affect vector readministration in ocular gene therapy trials, especially for the IVT route of delivery. Some of the studies discussed showed that high NAb titres can persist years after delivery of AAV via SRT and IVT in a subset of patients [34, 100, 120, 122],

and whilst most studies suggest high pre-existing sera NAb levels limit the efficiency of gene transfer to the retina [97, 100], others showed that patients with high NAb titres at baseline actually demonstrated the greatest therapeutic response to the gene therapy [99]. In this regard, one possible line of investigation could be to determine the effect that IVT or SRT AAV administration has on vector readministration via other routes, e.g. intravenous infusion for liver indications. In the future, this may be pertinent to patients who exhibit multiple morbidities affecting different organs and require several gene therapy treatments.

Figure 1.1: The humoral immune response in relation to ocular gene therapy

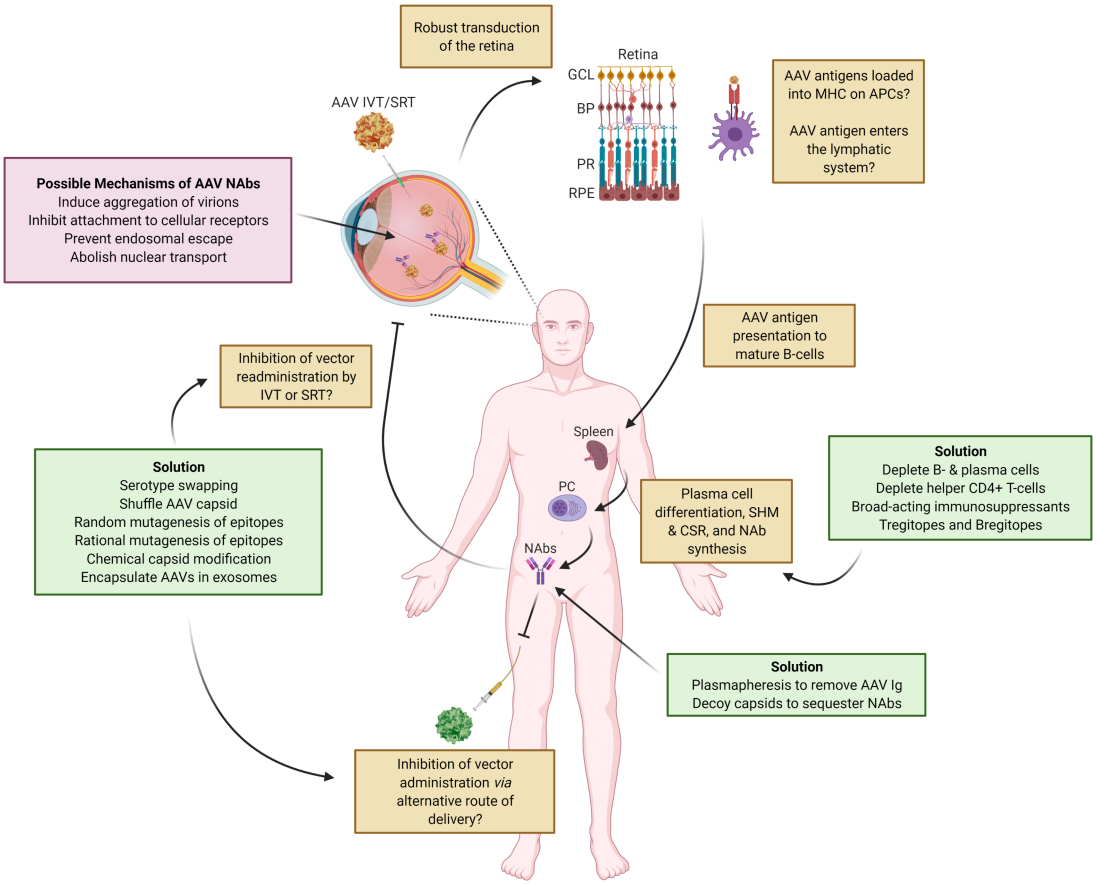

The humoral immune response in relation to ocular gene therapy. This review suggests that a subset of patients develop anti-AAV NAbs after SRT or IVT of AAV, however, it is not clear whether this can be circumvented via administration of perioperative systemic steroids. Further studies are needed to determine whether the induction of anti-AAV NAbs affects re-administration into the eye by IVT/SRT or into other organs. In addition, the precise mechanisms utilised by AAV NAbs remain unknown, and more research is needed to elucidate the basis of their neutralising activity. AAV, adeno-associated virus; APC, antigen presenting cell; BP, bipolar cell; CSR, class switch recombination; GCL, ganglion cell layer; IVT, intravitreal injection; MHC, major histocompatibility complex; NAb, neutralising antibody; PC, plasma cell; PR, photoreceptor; RPE, retinal pigment epithelium; SHM, somatic hypermutation; SRT, subretinal injection.

1.7 Possible strategies to circumvent humoral immunity to AAV

As discussed, an increasing body of evidence implicates a deleterious role for pre-existing and induced NAbs in the context of retinal gene therapy. Further, it is unclear whether oral prednisolone is effective at inhibiting NAb responses in patients enrolled in clinical trials. This suggests that the development of strategies to circumvent humoral immunity to AAV will likely be helpful in improving the outcomes of gene therapy trials. Here a number of possible strategies that may be applicable to this problem will be described.

1.7.1 Overcoming pre-existing AAV NAbs

As outlined above, pre-existing NAbs against AAV represent a major hurdle to the successful application of gene transfer technologies, and may even have a detrimental effect in immuneprivileged sites like the CNS and retina. To overcome this problem, a number of approaches have been reported, including modifications to the vectors and the utilisation of clinical procedures.

Table 1.3: Summary of possible strategies to circumvent pre-existing immunity to AAV

Strategy	**Advantages**	**Disadvantages**	**Translational barriers**
Alter the route of administration	Clinically translatable approach	May alter the pattern of transduction, reducing gene delivery to target cell type or tissue. Limited number of routes of administration depending on the target tissue	Low: Possible to draw on examples from other clinical trials demonstrating safe vector delivery for a given route for some serotypes/organs
Use alternative AAV vectors	Increasing number of novel AAV vectors identified which may be effective at NAb evasion. Increasing understanding of AAV epitopes is enabling rational mutation of antigenic regions could be applied to any vector. *In vitro* and *in vivo* screens available to identify resistant vectors	Engineering novel AAVs can expensive and technically-challenging, especially when applying multiple rounds of *in vivo* selection. Novel AAVs may be able to circumvent NAbs but may have unwanted and unintended properties such as high toxicity	High: Extensive safety and efficacy testing likely required by regulators to demonstrate benefits of novel capsid in preclinical models and patients. High economic cost associated with regulated clinical trials
Chemical modification of AAV	Non-genetic modifications require relatively simple chemistries amenable to scalable manufacturing	Data suggests limited resistance of PEGylated AAV to NAbs. Limited number of examples of other biological polymers applied to AAV to date	High: Safety of biological polymers may be established, but extensive safety testing would be required for novel formulated vectors

Strategy	Advantages	Disadvantages	Translational barriers
Use decoy capsids	Clinically translatable if 'known' serotype (e.g. AAV2) decoy capsids are used. Possible to use higher/lower ratio of decoy:full capsids depending on pre-existing NAb titre	Inclusion of additional decoy capsids may increase immune responses, possibly resulting in (i) CD8+ T-cell activation and destruction of transduced cells and (ii) stronger induction of NAb responses. Would require production of more AAV capsids which could create a manufacturing bottleneck	Medium: AAV vectors (e.g. AAV2 or 8) used for decoys have established safety profiles in humans, but some additional safety/toxicity studies may be required as higher overall capsid titres will be used
Plasma-pheresis	Effective at reducing pre-existing NAb levels if multiple rounds are used. Relatively non-invasive and safe procedure; routinely used in other applications to deplete antibody levels	May not be effective if pre-existing titres are very high. 'Rebound' phenomenon may limit effectiveness and possibility of repeated use	Low: Routinely used for treatment of autoimmune conditions. Relatively safe and non-invasive procedure

Strategy	**Advantages**	**Disadvantages**	**Translational barriers**
Use broad-acting immuno-suppres-sants	Possible to utilise FDA-approved drugs to suppress immune responses; highly translatable. Well-characterised safety and efficacy profiles and mechanisms-of-action	May be ineffective at completely depleting memory B-cells in the bone marrow, which may be required to overcome humoral immunity. Little evidence the approach may enable vector administration in spite of reducing NAb levels in pre-immunised models	Low: Many immunosuppressants are FDA-approved and are routinely used in patients. Many immunosuppressants have favourable safety/toxicity profiles

AAV, adeno-associated virus; NAb, neutralising antibody; PEG, polyethylene glycol; IdeS, an immunoglobulin-cleaving enzyme.

1.7.1.1 Altering the route of administration

This strategy may be applied to certain gene therapies targeting certain organs/tissues. For instance, it has been discussed how intramuscular [94] and intravenous [92] injections of AAV can be used to treat haemophilia B. Data from one study would suggest that injections into the muscle are less susceptible to the presence of pre-existing NAbs than intravenous infusions however, highlighting a possible strategy to administer AAV to haemophilia B patients who would normally be excluded from clinical trials [94]. Similarly, intrathecal delivery of AAV to the CSF has been shown to partially circumvent pre-existing anti-AAV9 NAbs [95], suggesting this mode of administration may be preferable to systemic administration of AAV9 for delivering genes to the CNS [137]. However, it should be noted that altering the route of administration may attenuate effective transduction and therapeutic efficacy in a target organ.

1.7.1.2 Use of alternative AAV vectors

In spite of the high rates of cross-reactivity exhibited by anti-AAV NAbs [89], alternative AAV vectors with differing epitopes might be able to evade pre-existing or induced humoral immunity. This may involve the utilisation of naturally-occurring AAV isolates or the engineering of novel AAV vectors.

Approximately 100 naturally-occurring AAVs have now been identified in humans and non-human primates, each of which harbours a distinct tissue tropism, immunogenicity and susceptibility to NAbs. AAVrh32.33, for example, was isolated from Rhesus macaque monkeys, and can transduce a variety of human cell types [138, 139], yet only 2% of humans are thought to harbour pre-existing NAbs against the virus [90]. Whilst this may prove helpful in circumventing humoral immunity, it should be noted that AAVrh32.33 may be highly immunogenic when injected intramuscularly, possibly limiting its application as a gene therapy vector [139]. Another natural AAV isolate is AAVrh10, which has been shown to be largely safe and effective at delivering genes to the central nervous system, lung, liver and heart in animal models. One study reported that 21% of humans are seropositive for AAVrh10, and harbour pre-existing NAbs against this virus, which is lower than that reported for AAV2 (20-90% humans are seropositive), for example, suggesting AAVrh10 may be an effective means of transferring genes to patients refractory to AAV2-based gene therapies [140].

Ancestral sequence reconstruction (ASR) via phylogenetic analysis of AAV capsid sequences has also been proposed as a tool for identifying ancestral AAVs with favourable vector immunobiology properties. Anc80L65 is one such vector that is an ancestor of AAVs 1, 2, 8 and 9, and can deliver genes to the retina, liver, and muscle. Analysis of the structure and sequence alignment of Anc80L65 with extant AAVs demonstrated that Anc80L65 was

structurally distinct from AAV2, 8 and rh10, exhibiting 12.2%, 9.1% and 8.6% cap sequence divergence respectively. As a result, it was found that the vector was significantly more resistant to neutralisation by cross-reactive anti-AAV2 and anti-AAV8 sera than AAV2 and AAV8 vectors. Overall, Anc80L65 is a promising candidate vector for circumventing humoral immunity [141].

Other means of engineering the AAV capsid to overcome neutralistation by NAbs involves the modification of antigenic epitope regions on the capsid surface, using molecular biology techniques like error-prone PCR and DNA shuffling, to generate diverse capsid libraries which can subsequently be screened for capsids resistant to neutralisation by anti-AAV NAbs [142].

An early demonstration of the potential of this approach was reported in 2008, when an adapted DNA family shuffling technology was used to create hybrid AAV capsid proteins. Two round of selection were used. The first used *in vitro* hepatocyte cultures to identify AAVs effective at transducing target cells. Pooled human immunoglobulin G (IVIg) was then used to isolate an AAV2/8/9 chimera, termed AAV-DJ, that was found to be more resistant to NAbs than AAV2 in IVIg-immunised mice [143].

This approach was explored further to identify AAV capsids that were resistant to neutralisation. A number of AAV capsid libraries were utilised, including a randomly mutagenised AAV2 library, an AAV2 library with specific residues subject to saturation mutagenesis, a 'shuffled' AAV cap library (generated from AAVs 1, 2, 4, 5, 6, 8, & 9), and an AAV library in which surface hypervariable loops had been swapped between serotypes. Two rounds of selection were then used to identify AAV capsids resistant to neutralisation by NAbs by IVIg and sera samples from patients excluded from haemophilia B clinical trials harbouring high-titre AAV NAbs. The authors conclude that the novel AAV capsids generated may be used to treat patients with high titre pre-existing NAbs and repeated gene transfer (i.e. readministration of a gene therapy) in patients who have developed NAbs against AAV [144].

Asides from directed evolution, AAVs can also be rationally designed via the mutagenesis of epitope regions. This first requires the identification of regions important for binding/neutralisation by antibodies. One method utilises peptide scanning, in which short linear epitopes are used in ELISA screens to identify capsid proteins that bind to anti-AAV antibodies. Peptide insertion into AAV capsids can also be used to disrupt NAb epitopes and thereby identify antibody binding regions on the vector [145]. *In silico* modelling and systematic mutagenesis of IgG2a antibodies to AAV2 has also been used to identify residues important for antibody binding [146]. These discoveries have aided the development of NAb-resistant AAVs using a structure-guided approach that does not require the use of IVIg or high NAb titre patient sera to exert selective pressures on large capsid libraries for identifying resistant clones. In one report, synthetic AAVs were evolved via rational mutation of AAV1 antigenic epitopes,

which were found to evade polyclonal anti-AAV1 neutralising sera without impacting the tissue tropism or transduction efficiency of the vectors in mouse models and non-human primates [147].

Whilst most modifications to AAV to improve NAb resistance have focussed on modification of cap gene/capsid protein sequences, recent reports have shown that the encapsulation of AAVs in exosomes can also reduce their susceptibility to humoral immune responses. Termed exosome-associated AAV (exoAAV), these novel vectors have demonstrated improved transduction of across a range of cell types and tissues, in addition to enhanced resistance to NAbs in IVIg-immunised mice. This reduced sensitivity to NAbs has been shown for exoAAV8 in the liver [148] and exoAAV9 in the CNS [149].

1.7.1.3 Chemical modification of AAV

The engineering of AAV to avoid neutralisation by NAbs has resulted in the development of exciting novel vectors capable of circumventing humoral immune responses via the disruption of antigenic epitopes. An alternative approach to preventing NAb-AAV binding/neutralisation is to shield epitopes via chemical modification of AAVs.

Polyethylene glycol (PEG) can be chemically conjugated to AAVs to mask them from NAbs, for example. Whilst PEG-coated AAVs have been shown to exhibit greater resistance to NAb-mediated neutralisation, it should be noted that only partial protection was inferred via this chemical modification. It was also noted by the authors that the addition of PEG above a certain threshold attenuated the AAVs transduction potential, likely via steric hindrance between cell surface receptors and cognate AAV capsid proteins [150].

Alternative approaches have sought to encapsulate AAVs in a polymer gels like poly-lactic glycolic acid and alginate that gradually degrade *in vivo*. This approach has been applied to adenoviruses [151, 152] and has shown to increase the resistance of these vectors to NAbs, suggesting the approach may also be effective for AAV vectors. However, the development of anti-polymer antibody responses may pose a significant challenge to this particular technology [153].

1.7.1.4 Use decoy capsids

The use of decoy capsids to circumvent anti-AAV NAbs involves the administration of empty capsid AAVs or infection-deficient AAVs to sequester NAbs prior to or at the same time as therapeutic vector administration. In non-human primates, this approach has been shown to competitively block circulating NAbs in a dose-dependent manner and concomitantly restore transduction efficiency [154], however, other studies have shown that the approach is not al-

ways effective at circumventing humoral immune responses [155]. The authors also showed that the presence of empty capsids in their AAV8 vector preps did not prevent neutralisation of FIX.R338L delivery in their models via a so-called 'decoy capsid' action [154, 155]. In contrast to previous reports, which utilised IVIg [154], the authors opted for a passive transfer strategy involving the generation of anti-AAV8 NAbs in one group of mice which was then collected and transferred to a different group of mice receiving the FIX.R338L gene therapy. The authors reported that 1:2 or 1:16 NAb titres were sufficient to attenuate transfer of FIX.R338L, but this effect was not rescued by the inclusion of empty capsids in the AAV8 preparation. This was in opposition to previous findings suggesting that "decoy capsids" may be an effective means of circumventing anti-AAV NAbs [154]. Several key differences between these studies are evident, however. First, the source of NAbs (use of hIVIg [154] vs. passive transfer of mouse sera [155]) is a key disparity. Further, in Mingozzi et. al.'s study, a higher ratio of decoy vector to full vector was used, both of which may explain the discrepancy in outcomes.

The use of capsid decoys may represent a possible strategy for overcoming NAb responses, however, the approach may have certain drawbacks. The inclusion of empty capsids in vector formulations has been shown to reduce transduction efficiency and increase vector-related immunotoxicity in one study investigating liver gene transfer with AAV8 [156], however, in a non-human primate study investigating AAV2-mediated gene delivery to the retina, the removal of empty capsids had no detectable impact on the generation of anti-AAV lymphocyte or NAb responses [157].

1.7.1.5 Plasmapheresis

Plasmapheresis is a clinical procedure that involves *ex vivo* removal of NAbs from an individual's blood by using filtration- or centrifugation-based techniques, before the blood transferred back [158]. The approach can be used to reduce the build-up of antibodies in conditions like haemorrhagic lupus pneumonitis [159] and Guillain-Barre syndrome [160], both of which involve elevated levels of pathologic antibodies. It is also used in patients with visual loss from atypical optic neuropathies mediated by antibodies against aquaporin-4 (AQP4) and myelin oligodendrocyte glycoprotein (MOG) [161]. In terms of gene therapy, plasmapheresis provides a possible means of achieving a transient drop in NAb titres below a certain threshold to enable vector administration. It could, therefore be applied to an individual with high pre-existing NAb levels or one who develops high NAb titres after receiving a gene therapy. This approach was tested in a non-human primate model, and found to be effective with six rounds of plasmapheresis over a two-day period effectively reducing NAb levels in seropositive animals. Following vector administration, animals that had undergone plasmapheresis

exhibited the same transduction levels as seronegative animals following intravenous injection of a microDystrophin-expressing AAV construct [162]. Plasmapheresis is usually well tolerated from a safety perspective [163]. However, one possible limitation to using plasmapheresis however, is a phenomenon known as 'rebound', in which IgG levels quickly return to the same or even higher levels following treatment. In a clinical trial, it was shown that multiple rounds of plasmapheresis were required to reduce NAb levels for gene therapy, which could be partly explained by this 'rebound' effect. Whilst reductions to <1:5 NAb titres were achieved in some individuals across multiple serotypes (AAV1, 2, 6 & 8), it should be noted that such an outcome required five rounds of plasmapheresis in some instances. Furthermore, in those individuals exhibiting very high pre-existing NAb titres, for example, 1:12,800 anti-AAV2 in one particular case, successive rounds of plasmapheresis did not reduce the titre below 1:200. This suggested that the process may be ineffective in enabling efficient gene transfer in all patients with pre-existing NAbs [164].

Recently, a novel plasmapheresis protocol was described, in which the specific depletion of anti-AAV IgG from plasma without depleting total IgG levels was achieved. Using this approach, high titre human IgG pools and plasma samples were tested, and near complete removal of anti-AAV IgG was achieved using an N-hydroxysuccinimidyl sepharose column onto which AAV8 particles were grafted. The process was able to reduce anti-AAV8 IgG to levels that enabled efficient gene transfer in mouse models. This study highlighted the possible advantages to specific depletion of AAV IgG using plasmapheresis, which has distinct safety advantages, mitigating the risks of leaving an individual vulnerable to opportunistic pathogens following pan-IgG depletion [165].

1.7.1.6 Use of pharmacological immunosuppressants

The use of immunosuppressant drugs, which may impact both the innate and adaptive arms of immune system, appears to be largely effective in managing anti-AAV T-cell responses when administered prophylactically or once a rise in liver transaminases is detected. Completely circumventing pre-existing anti-AAV humoral immunity with broad-acting immunosuppressants is more challenging however, likely due to the inability of these compounds to effectively deplete memory B-cells in the bone marrow [36]. One report utilising a mouse model of AAV immunity has shown that pharmacological intervention can be used to reduce pre-existing NAb levels, however. Pre-existing immunity was generated by an intravenous injection of AAV9 vectors. A combination of rapamycin and prednisolone administered daily for eight weeks reduced anti-AAV9 NAb levels by 85-93%, and in addition, decreased levels of B-cells and plasma cells were observed. This combination was found to selectively inhibit helper T-cell-mediated B-cell activation in the spleen, leading to effective anti-AAV9 NAb

depletion. Although such an approach could prove an attractive strategy for circumventing humoral immune responses to AAV, this study did not confirm whether vector readministration was possible in their model after treatment with rapamycin and prednisolone [166].

1.7.2 Preventing the induction of AAV NAbs

Pre-existing NAbs represent a significant barrier to the success of gene therapies in the clinic. As outlined above, the delivery of AAV into most, if not all, sites in the body appears to result in the development of humoral immunity against the capsid, which may limit the possibility of vector readministration. This is an important aspect of AAV gene therapy for several reasons. First, gene therapy constructs may display reduced efficacy overtime as cells epigenetically downregulate 'foreign' gene expression cassettes via CpG island hypermethylation [167]. Second, in dividing tissues such as the liver, transduced cells are lost overtime, thereby reducing therapeutic efficacy [54]. In a number of non-dividing tissues, such as the inner retina/RGC layer, many pathologies exhibit a degenerative phenotype which may lead to the loss of transduced cells overtime [168]. For many diseases, titrating the vector dose may prove a useful strategy towards 'tailoring' a gene therapy to a particular patient due to disparities in age and/or stage of disease progression, for example. In all of these scenarios, efficient vector readministration is required, in which preventing the development of anti-AAV NAbs is key. Here a number of possible strategies that could be used to achieve this goal in clinical trials and preclinical studies will be discussed.

Table 1.5: Summary of possible strategies to prevent induction of anti-AAV NAbs

Strategy	**Advantages**	**Disadvantages**	**Translational barriers**
Inhibit T-cell activation	Several pathways can be targeted to prevent anti-AAV NAb responses using FDA-approved drugs, such as Cedelizumab. Tregitopes may be used to induce tolerance of AAV antigens	T-cell inhibition may leave patient vulnerable to infection and cancer development. Fewer FDA-approved modalities than small molecule-based approaches to immunosuppression	Medium: Some FDA-approved anti-CD4 mAbs are available for creating immunosuppression in patients. Little clinical data supporting safety of approach in humans
Inhibit B-cell activation	Inhibiting B-cell function may prevent NAb formation whilst retaining cytotoxic T-cell function, against tumourigenic cells for example. FDA-approved drugs are available for this application. Preclinical evidence suggests generation of tolerogenic B-cells is possible	B-cell levels may take 6-12 months to recover, leaving patients vulnerable to opportunistic pathogens and tumourigenesis. Fewer FDA-approved modalities than small molecule-based approaches to immunosuppression	Medium: Some FDA-approved anti-CD20 mAbs are available for creating immunosuppression in patients. Little clinical data supporting safety of approach in humans
Use broad-acting immuno-suppres-sants	Possible to utilise FDA-approved drugs to suppress immune responses; highly translatable. Well-characterised safety and efficacy profiles and mechanisms-of-action	Preclinical evidence suggests this approach may not be sufficient to prevent NAb formation or enable vector readministration. Outcomes of clinical trials (see above) investigating gene delivery to the retina also suggest this approach may not be effective in all patients	Low: Many immunosuppressants are FDA-approved and are routinely used in patients. Many immunosuppressants have favourable safety/toxicity profiles

1.7.2.1 Inhibition of T-cell activation

CD4+ 'helper' T-cells can indirectly affect the humoral immune response by regulating the function of B-cells and their antibody-producing progeny plasma cells. Downregulating CD4+ T-cell function can therefore be utilised as a means of reducing anti-AAV NAb levels. For instance, anti-CD4 antibodies have been used to deplete (via induction of apoptosis in target cells) CD4+ T-cell levels and abolish anti-AAV NAb levels following a tail vein injection of AAV in a mouse model. This study also demonstrated however, that delivery of the vector directly into the portal circulation produced a humoral immune response that was only partially T-cell-dependent, thereby reducing the effectiveness of the anti-CD4 depletion strategy. Overall the study demonstrated that CD4 depletion may be an effective means of circumventing NAb responses for certain routes of delivery [169].

Alternative approaches have described the use of non-depleting anti-CD4 antibodies to prevent NAb responses. Here, intravenous administration of an anti-CD4 monoclonal antibody (mAb) prior to delivery of an AAV2/9 vector demonstrated reductions in anti-vector and anti-transgene (acid α-glucosidase (GAA)) NAbs in a mouse model of Pompe disease. The authors concluded that the mAb prevented co-receptor (CD4) stimulation of T-cells, in turn rendering them ineffective as B-cell activators [170]. T-cell-dependent activation of B-cells can also be inhibited by blocking other signalling pathways. Antibodies and fusion proteins against CD40-CD40L and CD28-CD80/86 receptors have been shown to reduce NAb levels against AAV proteins and thereby enable readministration to the lung in a rabbit model [171]. One study sought to combine a non-depleting anti-CD4 mAb therapy with the T-cell immunosuppressive drug, CyA, and showed that a 20-fold reduction in NAb levels was possible using this approach [172]. Other studies have utilised 'Tregitopes' [173] (IgG-derived MHC epitopes) to activate regulatory T-cell (Treg) responses in order to inhibit NAb production. In a mouse model, Tregitopes were fused to AAV capsid peptides, and subsequently used to induce proliferation of Treg cells that suppressed CD8+ T-cell cytotoxic function against AAV-expressing cells [174]. This demonstrated an interesting proof-of-concept and suggests Tregitopes could be applied to reducing NAb levels after vector administration.

1.7.2.2 Inhibition of B-cell activation

The inhibition of T-cell activation can prevent anti-AAV antibody production by B-cells/plasma cells. Efforts to inhibit activation and/or induce apoptosis of B-cell/plasma cells have also shown promise as tools for overcoming humoral immunity to AAV. The activation of B-cells and their maturation into antibody-producing plasma cells is a complex process. With AAV gene therapy, APCs are thought to display AAV capsid peptides to mature B-cells

which initiate downstream signalling pathways resulting in the endocytosis of AAV antigens [175, 176]. The B-cell then presents the antigen on its surface with MHC class II molecules, which can be recognised by CD4+ helper T-cells, causing it to proliferate and migrate to the germinal centres, where somatic hypermutation and isotype switching occur. Most activated B-cells will become plasma cells and produce NAbs against AAV, whilst others develop into memory B-cells [177].

Understanding the process by which B-cells are activated therefore helps to inform strategies to prevent NAb responses. Bortezomib, an FDA-approved therapy for multiple myeloma (plasma cell tumour), is a proteasome inhibitor that attenuates antigen processing and presentation of epitopes on the surface of B-cells. Administration of Bortezomib has been shown to reduce NAb titres by 8-10-fold by depleting AAV2/8-specific IgG-producing plasma cells in the lymphoid organs and bone marrow. However, this reduction was not sufficient to allow vector readministration, which the authors attribute to residual anti-AAV8 NAbs due to the inability of Bortezomib to completely eradicate anti-AAV8 plasma and memory B-cells [178].

Depletion of activated B-cells can also be utilised as a means of reducing NAb levels. Rituximab, an anti-CD20 antibody, can induce B-cell apoptosis by (i) recruiting cytotoxic natural killer and macrophage cells to antibody-bound B-cells or (ii) activating the cytotoxic complement cascade via C1q binding to induce B-cell lysis [179]. In a clinical trial, Rituximab treatment was shown to reduce circulating NAb levels up to 24 weeks after two intravenous infusions, however the authors of this study noted that these reductions were only observed in a subset of patients with titres of <1:1,000, and only a minority of subjects' titres were reduced to <1:5 [180]. This finding was corroborated by reports that a combination of rituximab and rapamycin in a 45-month old patient with Pompe disease was an effective strategy to mitigate anti-AAV immune responses. The authors conclude that the strategy allows for the possibility of vector readministration in the future, but no data is presented in relation to this, and it should also be noted that this was a single subject clinical trial [181]. In a non-human primate study, CyA (calcineurin inhibitor, inhibits T- and B-cells) was trialed in combination with Rituximab. The study showed that anti-transgene (FIX for haemophilia B) NAb levels could be significantly reduced with this strategy. Further, in one animal, anti-AAV6 NAb titres dropped to undetectable levels, which was subsequently shown to be permissive of vector readministration. In the other animal however, the dual immunosuppression strategy did not appear to be effective and readministration appear to be blocked by anti-AAV6 NAbs [182].

Clearly, B-cell depletion strategies may be an effective means of overcoming humoral immunity to AAV, however, the approach is not without its drawbacks. For instance, following Rituximab treatment, patients are immunocompromised for a period of around 6-12

months as their B-cell levels return to normal, which can lead them vulnerable to opportunistic pathogens. In two severe cases, activation of dormant human polyomavirus was associated with the onset of progressive multifocal leukoencephalopathy following administration of Rituximab [183]. Further, it should be noted that anti-CD20 antibodies will not deplete plasma cells, which are the antibody-producing cells of the immune system, possibly limiting the ability of the strategy to reduce NAb levels whilst still posing a significant safety concern [184].

As an alternative to B-cell depletion, the induction of B-cell tolerance can be utilised to prevent the generation of anti-AAV NAbs and thereby allow for vector readministration. For instance, antigen-specific immunotherapy can be used to inhibit B-cell activation by inducing Treg cells for a particular antigen. In one study, an immunogenic protein was fused to an immunoglobulin heavy chain, and transferred into activated B-cells *in vitro* using a retroviral vector. The generation of tolerogenic B-cells was observed which were found to attenuate immune responses against multiple epitopes of the cloned protein. Mechanistically, this effect was linked to the stimulation of Treg cells by the transduced B-cells [185]. Whilst this approach has not yet been applied to AAV gene therapy, the results from this study suggest it might be effective at limiting humoral immune responses.

Another means of preventing B-cell activation is to target inhibitory co-receptors present on the surface of B-cells. CD22 and SIGLEC-G are two sialic acid-binding co-receptors known to play a role in mediating the induction of tolerance of self-antigens. Recent data has shown that high-affinity ligands for these co-receptors can induce antigen-specific B-cell tolerance, highlighting a possible strategy for treating autoimmune diseases which may be applied to preventing anti-AAV humoral immune responses in the future [186]. For instance, immunisation of mice with nanoparticles conjugated to human factor VIII and CD22 has been shown to induce tolerance to and antibody production against factor VIII [187], suggesting a similar approach could be applied to AAV capsid proteins.

1.7.2.3 Use of pharmacological immunosuppressants

In addition to targeting specific arms of the immune system with anti-CD4 or anti-CD20 antibody-based depletion strategies, the use of broad-acting small molecule immunosuppressants has been trialed, either alone or in combination. Many of these are FDA-approved and routinely used in patients, making this approach highly clinically translatable.

In a mini-pig model of advanced heart failure, AAV1 encoding sarcoplasmic reticulum calcium ATPase gene (SERCA2a) was delivered by intravenous administration. A combination of immunosuppressive drugs was tested to see whether this could circumvent NAb responses. Here, oral MMF and rapamycin were administered daily from two weeks before

to three months after vector infusion, and methylprednisolone sodium succinate was administered daily by intramuscular injection up to three months after AAV1 delivery. In spite of the utilisation of this aggressive immunosuppressive regimen, the induction of AAV1 NAbs were still observed in both the immunosuppressed and non-immunosuppressed groups, and comparison of these groups revealed no apparent effect immunosuppression of the development of NAbs [188].

Studies examining immunosuppression in non-human primates have suggested the approach may not be effective for liver gene therapy with AAV5. Here, animals were injected intravenously with AAV5 to generate an immune response. Over the next 12-week period, anti-thymocyte IgG, methylprednisolone, tacrolimus and rituximab were given in combination. These were found to attenuate anti-AAV5 NAbs during the 12 weeks, but NAb levels rose significantly once this treatment stopped. The authors then demonstrated that this 'rebound' in NAb levels completely inhibited repeated vector readministration of AAV5 [189].

These results were corroborated by another study in non-human primates investigating microDystrophin delivery to the muscle. Animals receiving (i) prednisolone alone, (ii) a prednisolone, tacrolimus and mycophenolate mofetil combination, and (iii) no immunosuppressants were compared. No differences in transgene expression were observed in seropositive animals between these three groups, indicating that the immunosuppressants given may have been ineffective at reducing anti-AAV NAb levels. This was in spite of the fact that the immunosuppressants were shown to downregulate lymphocyte proliferation, a finding which may highlight the challenge in attenuating pre-existing humoral immunity to AAV [162].

The complexity of overcoming the induction of NAbs against AAV following delivery to the CNS has been demonstrated in clinical studies. One study tested an AAV2 vector expressing aspartoacylase and delivered by intracranial injection in patients with Canavan disease. In this study, only 3/10 patients developed low to moderate sera NAb titres vs. baseline, in spite of the fact that no patients were given perioperative immunosuppressants [190].

In another trial, an AAVrh10 vector encoding arylsulphatase A was delivered by intracerebral injection in patients with metachromatic leukodystrophy. Steroids were administered one day prior and ten days after the surgery, however, in all patients enrolled in the study, the development of anti-AAV antibodies were observed in the sera and CSF. This suggestion that steroids may not be effective in preventing anti-AAV NAb responses has been supported by recent data investigating AAV9 gene therapy. Here, AAV9 vectors were used to transfer gigaxonin into the CNS of cross-reactive immunologic material (CRIM)-negative giant axonal neuropathy patients, and a combination of methylprednisolone, prednisone, tacrolimus and rapamycin was used. Anti-AAV9 NAbs were still observed in the sera and CSF, however, after vector infusion, in spite of the fact that the combination of immunosuppressants was ef-

fective at preventing inflammation (pleocytosis; elevated CSF lymphocyte counts) [54]. This is possibly in accordance with clinical studies investigating AAV gene transfer to the retina reviewed above in which some patients developed NAb responses in the absence of intraocular inflammation.

Recently, small molecule immunosuppressants have been modified to improve their properties *in vivo*. In a study utilising non-human primate and mouse models, rapamycin was encapsulated in polylactic acid nanoparticles, termed SVP rapamycin (rapa). SVPrapa was found to prevent anti-AAV cellular and humoral immune response induction, thereby permitting readministration of the vector, when co-administered with the initial injection of AAV. The drug mitigated antigen-specific activation of T-cells and B-cells, prevented CD8+ T-cell infiltration into the liver, and inhibited memory T-cell responses. Interestingly, the authors showed that the adoptive transfer of splenocytes from treated to naiive mice transferred the immunomodulatory properties of SVPrapa. They then demonstrated that anti-CD25 antibody depletion partially rescued SVPrapa's effect on anti-AAV8 IgG levels, suggesting that Treg cells may be involves in the mechanism-of-action [191].

1.7.3 Overcoming humoral immune responses to AAV - the need for a comprehensive approach

The studies discussed above highlight the possible challenges of circumventing humoral immune responses to AAV. It is clear that some approaches have shown promise in preclinical models and human patients. However, effective strategies to overcome pre-existing NAbs and prevent the induction of humoral immunity against AAV gene therapies are still under development. Here a comprehensive strategy that could be used to circumvent both pre-existing and induced humoral immunity to AAV is outlined. This aims to provide a framework for future investigations in the field so that robust and repeatable vector administration to previously untreatable patients is possible.

To completely eliminate pre-existing humoral immunity against AAV, especially if a patient presents with a high NAb titre, may require a combinatorial approach. AAV-specific plasmapheresis may initially be used to reduce NAb titres, followed by a vector infusion incorporating a novel vector with either (i) mutated capsid epitopes (via a random or computational approach) or (ii) NAb-resistant chemical modifications or (iii) a combination of both. The inclusion of decoy capsids may also be utilised to sequester any NAbs that were not cleared by plasmapheresis. In conjunction, a combination of broad-acting small molecule immunosuppressants may be administered perioperatively, along with a T- or B-cell targeted peptide immunotherapy approach to induce antigen-specific tolerance to an AAV antigen and prevent

the induction of anti-AAV NAbs that may arise to certain gene therapies.

This example, whilst hypothetical, demonstrates the range of possible solutions currently under investigation and highlights the need for a range of approaches to ensure efficient and repeatable vector administration to target organs. However, there is a need for more research into what combination of possible solutions provides maximal benefit depending on the target organ and route of administration. Further studies are also needed to establish safety and efficacy profiles of novel vectors in particular, which will require regulatory approval before routine clinical use is feasible. In the future, a library of FDA-approved, antigenically-distinct engineered AAVs with highly specific tissue tropisms would likely be beneficial, which may enable repeated 'swapping' of vector capsids for a particular therapeutic construct to overcome pre-existing and/or induced humoral immunity whilst ensuring robust and tissue/cell-specific transduction. Here, high-throughput NAb assays could enable selection of an AAV variant from a library that is resistant to neutralisation by a particular patient's sera. A peptide scanning based-approach [192] could even be used to subsequently identify epitopes on the selected capsid, allow rational mutagenesis of these regions and ensure maximal resistance of the engineered virion to neutralisation and facilitate 'individualised' gene delivery to a particular patient based on a thorough characterisation of their NAbs.

Figure 1.2: Possible approaches to enable repeated gene transfer

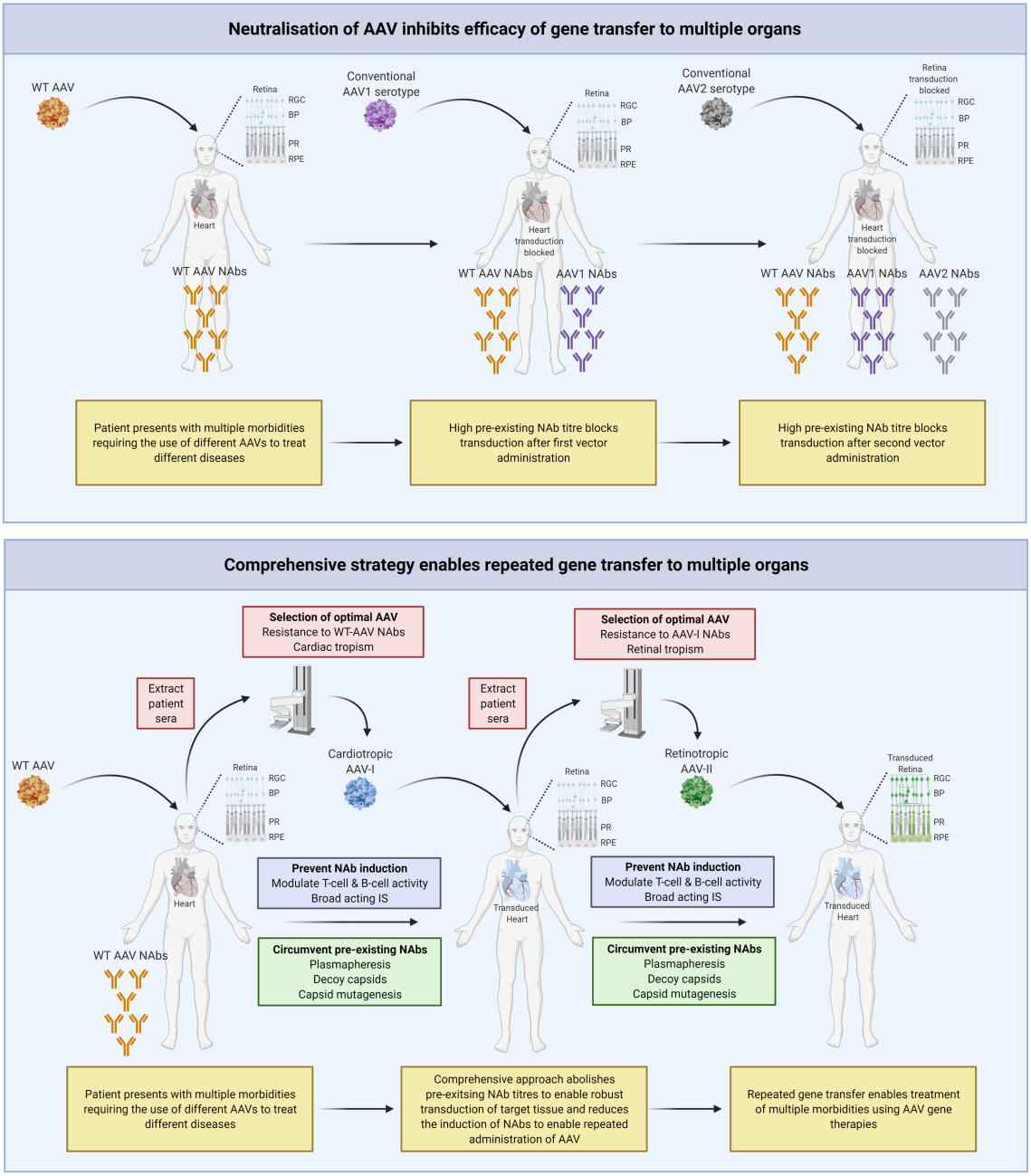

Top panel: an individual with a high pre-existing NAb titre that results in neutralisation of conventional AAV serotypes in the absence of immunomodulation. Bottom panel: Pre-existing NAbs are depleted and immunomodulation is used to reduce induction of anti-AAV NAbs post-administration. Patient sera is extracted and used to screen an AAV library for NAb-resistant and target tissue-tropic clones. This enables repeated gene delivery to multiple organs in a patient presenting with multiple morbidities. AAV, adeno-associated virus; BP, bipolar cell; IS, immunosuppression; PR, photoreceptor; RGC, retinal ganglion cell; RPE, retinal pigment epithelium; NAb, neutralising antibody.

1.8 Conclusions

1. AAV is a promising vector for delivering therapeutic genes to diseased cells. Although a number of clinical trials have shown that AAV is a safe and effective vehicle for gene therapy, the deleterious role of NAbs remains a significant barrier in a proportion of treated individuals.

2. Pre-existing NAbs limit the efficiency of gene transfer to the cells being targeted with a potential negative impact on treatment efficacy. This is an especially important consideration for strategies that involve intravenous AAV infusions into the circulation where very low or even undetectable NAb titres may completely abolish transduction of the target tissues. Injections of AAV into skeletal muscle and the CNS, including the retina, also appear to be partially limited by pre-existing NAbs.

3. After vector administration, an increase in AAV NAbs have been documented in some individuals recruited into clinical trials investigating muscular, hepatic and neurological disorders. In the ocular compartment, the increased NAb titres observed after IVT or SRT does not appear to be clearly correlated with the vector dose or baseline NAb titre. Interestingly, intraocular inflammation appears to be more common in those individuals who do exhibit significant increases in NAb titres. More research is, therefore, needed here to understand why this particular subgroup exhibit greater NAb responses with early evidence pointing towards AAV reactive T-cells playing a role in these seronegative individuals. The longevity of the therapeutic effect of AAV vectors in individuals with intraocular inflammation could be monitored with long-term follow-up, as this group may be most at risk of CD8+ T-cell clearance of transduced cells and eventual loss of efficacy.

4. Circumventing AAV NAbs to enable repeated dosing to multiple organs will require a comprehensive strategy capable of overcoming both pre-existing and induced humoral immune responses. More research is also required to understand whether prophylactic steroid administration prevents NAb induction, and the application of other T-cell and B-cell immunomodulators to block this critical step could also prove beneficial. To overcome pre-existing high titre of NAbs, the potential application of plasmapheresis and decoy capsids require further evaluation. Utilising patient sera to select NAb resistant clones from a capsid library, followed by rational mutation of capsid epitopes could prove a useful strategy in the future, enabling targeted gene delivery to a particular individual.

Chapter 2

Aims and objectives

The analysis undertaken in Chapter 1 provided a detailed review of the role of pre-existing and induced NAbs in response to intraocular delivery of AAV2 gene therapy vectors, with a focus on the outcomes of clinical studies. The conclusion of this assessment was that a comprehensive, multifaceted strategy may be required to circumvent anti-AAV2 antibody responses, that could be used to enable repeated gene transfer to the eye. This latter point may be useful in a number of scenarios. For instance, (i) to deliver several different therapeutic constructs to the eye to tackle a disease with a complex molecular pathophysiology, (ii) to increase the therapeutic effect if the benefits of the first gene therapy injection decline over time, (iii) to ensure safe and effective readministration to the contralateral eye, or (iv) to enable titration of vector dosages to a patient via sequential administration of AAV until a therapeutic effect (or unwanted side effects) are observed. Considering the need to develop a comprehensive strategy to overcome AAV NAbs, this thesis sought to test several possible approaches that could be used to circumvent humoral immune activation in murine models.

2.1 Can capsid mutagenesis reduce anti-AAV2 NAb titres?

First, mutation of AAV2 at key residues termed phosphodegrons was assessed as a possible means of reducing anti-AAV2 NAb synthesis following injection to the vitreous cavity by enabling robust transduction at a lower vector dose. The key research questions addressed in this chapter were:

1. How is transduction of the retina altered via incorporation of phosphodegron mutations?
2. What changes in NAb and TAb levels are observed after IVT of phosphodegron mutant AAV2 vs. wild-type capsids?
3. Is there a change in the levels of T-cell infiltration after injection of mutant and wild-type vectors?
4. Does the incorporation of phosphodegron mutations affect splenic lymphocyte populations?
5. Is microglia, Muller glia and astrocyte activation affected by the injection of phosphodegron mutant AAV2 vs. wild-type capsids?
6. Do the selected mutant residues lay proximal or distal to the primary receptor attachment sites of AAV2, and how might this affect binding affinity to the primary receptor and anti-AAV2 NAbs?
7. Is the injection of phosphodegron mutant AAV2 capsids via IVT associated with electrophysiological perturbations or structural damage in the retina?

2.2 Is perioperative administration of glucocorticoid immunosuppressants sufficient to circumvent generation of anti-AAV2 NAbs and enable repeated gene transfer?

Next, the effect of a small molecule glucocorticoid immunosuppressant drug, prednisolone, was assessed in the context of reducing immune activation in response to repeated bilateral IVTs of AAV2. The key research questions addressed in this chapter were:

1. How does administration of prednisolone affect generation of NAbs and TAbs in response to AAV2 IVTs?
2. What is the underlying cellular mechanism by which prednisolone attenuates antibody responses in terms of modulating splenic lymphocyte populations?
3. Does prednisolone impact the infiltration of CD4 and CD8 T-cells into the retina, or the activation of microglia cells?
4. Is prednisolone monotherapy sufficient to lift the blocking effect imposed by anti-AAV2 NAbs and enable repeated gene transfer?
5. Is the repeated bilateral IVT of AAV2 associated with elecrophysiological changes in the retina, and is this changed by prednisolone treatment?

Chapter 3

Materials and methods

3.1 Vector production

To create AAV2 capsids with phosphodegron mutations, pRep2/Cap2 was mutagenised by Vector Biolabs (293 Great Valley Pkwy, Malvern, PA 19355, United States). Mutant plasmids were maxiprepped, then sequenced by Sanger sequening (Department of Biochemistry, University of Cambridge) to ensure the correct mutations had been incorporated. AAV2 and capsid mutant AAV2 vectors were manufactured at ViGene Biosciences (9430 Key West Avenue, Suite 105, Rockville, MD 20850, USA). For AAV2 manufacturing, a standard triple plasmid transfection protocol was used (pAAV-sCAG-GFP, pHelper, pRep2/Cap2). Vectors were extracted from HEK293T cells via repeated freeze-thawing, purified using iodixanol gradient ultracentrifugation and suspended in phosphate-buffered saline (PBS).

3.2 Cell culture and viral transductions

HEK-293T cells were cultured on poly-L-lysine (10μg/mL; Sigma Aldrich) coated plates. Cells were incubated in Dulbecco's Modified Eagles Medium (DMEM) supplemented with 10% fetal bovine serum (FBS) and 1% penicillin/streptomycin (P/S) until 80% confluent. For transduction with vectors, cells were washed with PBS, then incubated with vectors diluted to stated concentrations in serum-free DMEM. Cells were passaged in T75 flasks in a 37C 5% CO_2 incubator Media was replaced every two days and cells were split 1:10-1:20 when they had reached 80-90% confluency. Cells were counted using haemocytometry with trypan blue live dead staining, and cultures were only used for experiments if viability exceeded 90%. To determine the efficiency of cellular transduction, HEK239T cells were detached with TrypLE (Thermo Fisher, Cat Number: 12604013) for 5min in the incubator. The TrypLE was deactivated by addition of DMEM +10% FBS +1% P/S, and cells were centrifuged at 300RCF for 5min. The supernatant was aspirated and the remaining pellet was fixed in 150 μL 4% paraformaldehyde (PFA). To assess the number of transduced GFP+ cells, an Acurri C6 flow cytometer was used. Forward (FSC) and side scatter (SSC) gating was used to identify an approriate population for analysis (no large clumps of cells or cellular debris). An FSC/FITC-A gate was used to identify GFP+ cells, and the population with a FITC-A fluorescent intensity of >10^4 RFUs was deemd to be expressing GFP. These settings were applied with assistance from a senior technician from the Addenbrookes Phenotyping Hub. Analysis of the percentage of GFP+ cells was undertaken using BDFacs software. To determine the neutralisation of wild-type and mutant AAV2 capsids in the presence of heparan sulphate (HS), 4,000 AAV2 GC/ng HS was mixed and incubated at room temperature for 1h before addition to HEK293T cell cultures. This stoichiometry was used to account for the fact that some of the AAV2 mu-

tant capsids yielded higher transduction rates, therefore, equitably lower concentrations of HS and AAV2 (or capsid mutant) were used as appropriate. This is important as the linear range of detection (MOI : % GFP+ cells) of cellular transduction with viruses is 1-20%, meaning that, if a mutant capsid was used that exceeded these values, determination of remaining infectivity would not be accurate. The importance of ensuring viral transduction experiments remained within the linear range of detection was highlighted by Dr. Will McEwan (Department of Clinical Neurosciences, University of Cambridge). To study the neutralisation of wild-type and mutant AAV2 capsids by anti-AAV2 NAbs, a similar experimental design was employed. Wild-type, Y444F/K556E/S662V, and triple mutant (TM) AAV2 were incubated with anti-AAV2 NAb containing sera (samples from mice previously injected with AAV2 intravitreally) for 1h before addition to HEK293T cell cultures, and equitable dilutions of vector and sera were made to ensure the level of transduction remained within the linear range of detection. To assess differences between groups, the remining infectivity (I/I_0) was calculated by normalising the values for neutralised wild-type and mutant AAV2 to no-sera or no-HS control groups.

3.3 Neutralising antibody assays

HEK-293T cells were seeded at 10,000 cells per well in white-walled, clear-bottomed 96-well plates (Sigma Aldrich) and used in the neutralising antibody (NAb) assay when 80% confluent. Blood sera samples were collected via saphenous vein bleeds or cardiac puncture into red capped tubes, allowed to clot overnight at 4C, then centrifuged at 300RCF. The resulting supernatant was designated sera and stored at -20 until further use. Two- or three-fold serial dilutions of serum samples were prepared in DMEM in a 96-well plate. AAV2.CMV.Luciferase was added to a final concentration of 1E9 GC (genome copies)/mL, and incubated for 1h to allow the anti-AAV NAbs to bind to the vectors. Sera-AAV mixtures (100μL) were then transfered to the HEK-293T cultures and incubated for 24h. Luminescent signal was detected by aspiring the media and adding 25μL of ProMega BrightGlo assay substrate (Cat Num: E2610), covering the plates with foil and incubating for 5min. Luminescence was recorded using a FLUOstar Omega plate reader with gain adjustment set to 5%. In these assays, each plate had a eight no sera controls (positive control) and eight no AAV2.CMV.Luciferase control (negative control). An average background was subtracted from the negative control groups and used for blank-correction. Each value was then normalised to the average positive control value for a given plate, which allowed calculation of remaining infectivity (I/I_0)[193].For data analysis, IC50 (dilution of sera that yielded a 50% reduction in the luminescent signal) was calculated using variable-slope non-linear regression functions. Recommended GraphPad set-

tings were used. To ensure goodness of fit, R^2 values were also recorded and all these were >0.98. Area-under-the-curve (AUC) was also calculated to corroborate IC50 analyses.

To validate the NAb assay, a serial dilution of AAV2.CMV.Luciferase was performed between 5E9 GC/mL and 7.81E7 GC/mL (multiplicity-of-infection (MOI; GC/cell) from 50,000 to 78). The assay demonstrated a very low background to noise ratio (8:98,743 relative luminescence units (RLUs).

Figure 3.1: Validation of AAV2.CMV.Luciferase-based NAb asssay

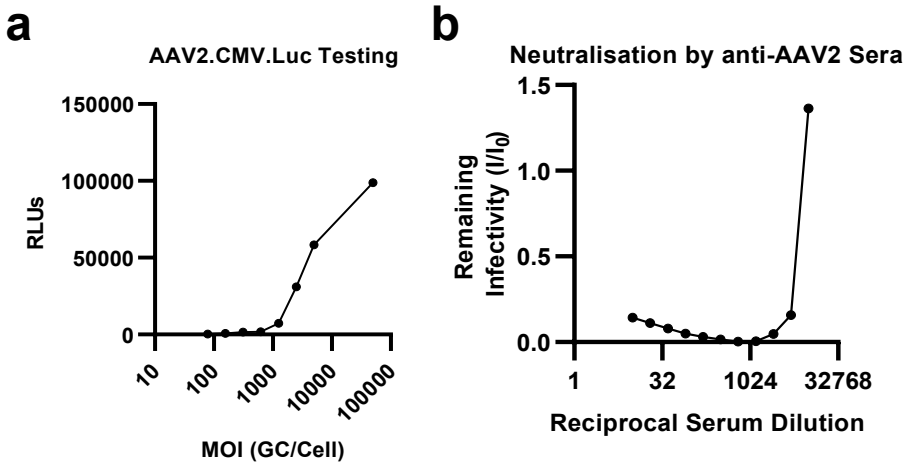

Validation of AAV2.CMV.Luciferase-based NAb assay. Graphs show an average of duplicate datapoints.

(a) Serial dilutions of AAV2.CMV.Luciferase (not background corrected) demonstrate low background to signal ratio.

(b) Addition of anti-AAV2 NAb-containing sera reduces remaining infectivity in the assay, measured as a reduction in the luminescent signal.

3.4 Total binding antibody assays

To assess total binding antibody (TAb) levels, an enzyme-linked immunosorbent assay (ELISA) was used. 96-well plates were coated with 50μL 1E10 GC/mL AAV2.CAG.GFP for 2h at room temperature. AAV was aspirated and plates were blocked with a 5% milk powder 0.2% tween-20 solution for 2h at room temperature. Serum samples were diluted 1:2,000 (optimal dilution calculated below) in the blocking solution and added to the wells in a 100μL volume. Plates were incubated overnight at 4C, followed by one wash in blocking solution and two washes with tris-buffered saline (TBS). Horse raddish peroxidase (HRP)-conjugated secondary antibodies (a kind gift from Dr. Andrew Sage; University of Cambridge Department of Surgery) were diluted to a final concentration of 1:50,000 in TBS, added to the wells at a 100μL volume, and incubated for 2h at room temperature. Plates were washed three times with TBS, followed by addition of 50μL 3,3',5,5'-tetramethylbenzidine (TMB) substrate, and a 30min incubation at room temperature. Signal detection was performed on a FLUOstar Omega plate reader, measuring absorbance at 650nm. All values were background-subtracted from negative control wells (wells containing no sera). To reduce intra-plate variation, all samples were run in duplicate. The coefficient of variation between replicates was 18.5% in Chapter 4 and 9.5% in Chapter 5. In this thesis, one isotype was assessed per plate to reduce the impact of inter-plate variability, however, additional controls could have been included to further increase the reliability of the assay.

Figure 3.2: Validation of TAb assays

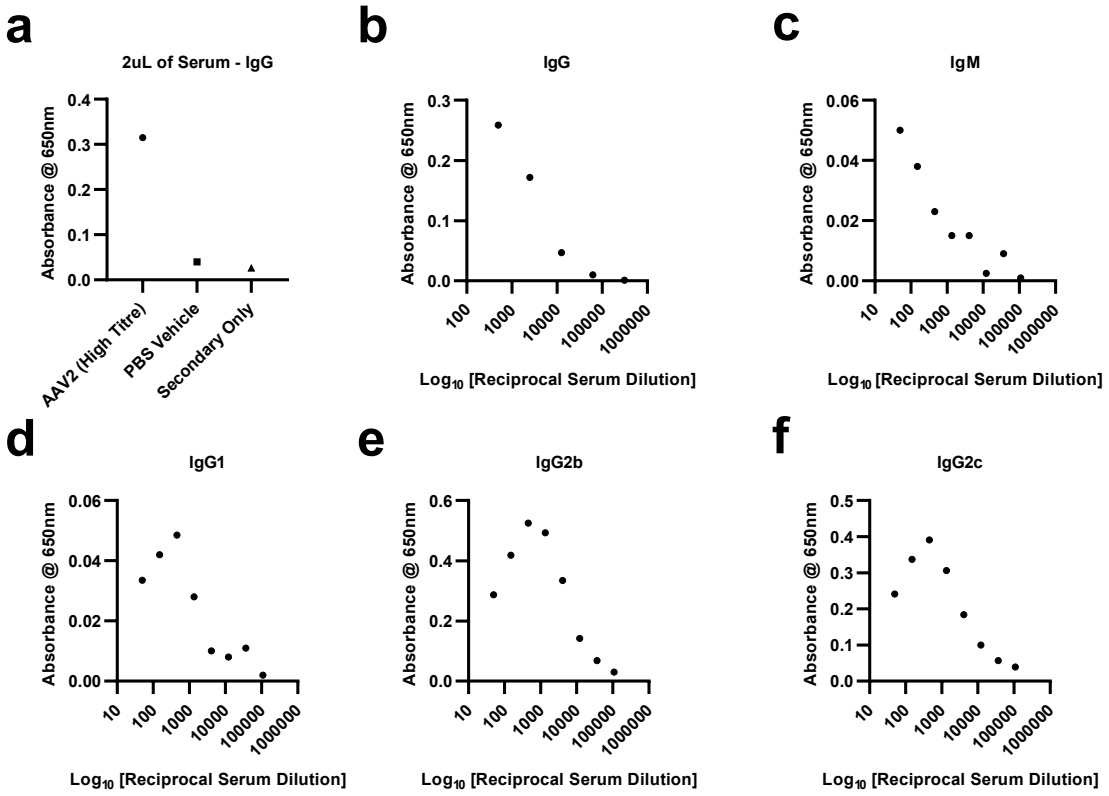

Validation of TAb assays. These experiments highlighted a 1:2,000 dilution as appropriate for these assays. Anti-AAV TAb-containing sera is a sample derived from an animal who received a high titre injection of AAV2 intravitreally.

(a) Addition of anti-AAV TAb-containing sera induces higher signal than sera from PBS injected animal. Background signal from secondary antibody only controls was also low.

(b) Dose response for IgG in the presence of serially diluted anti-AAV TAb containing sera.

(c) Dose response for IgM in the presence of serially diluted anti-AAV TAb containing sera.

(d) Dose response for IgG1 in the presence of serially diluted anti-AAV TAb containing sera.

(e) Dose response for IgG2b in the presence of serially diluted anti-AAV TAb containing sera.

(f) Dose response for IgG2c in the presence of serially diluted anti-AAV TAb containing sera.

3.5 *In silico* modelling of AAV capsids and mutagenenised residues

Throughout this thesis, AAV2 VP1 numbering is used to refer to specific residues. To visualise VP3 AAV2 capsid monomer and oligomers *in silico*, 6ih9, a 2.8Å resultion cyro-electron microscopy-derived structure, was downloaded from the Protein Data Bank. Both monomeric and oligomeric forms of 6ih9 were visualised using PyMol software. To depict the mutated capsid residues used in this thesis, PyMol's internal mutagenesis wizard was used. The residue and the appropriate substitute residue was selected, then the correct rotameric conformation of the mutated amino acid was chosen in accordance with PyMol's suggestion. Here, PyMol chooses the most appropriate rotamer based upon predicted interactions with surrounding VP3 residues derived from the crystal structure/coordinate files, for instance, by ensuring that two hydrophillic portions of adjacent amino acids are not in close proximity. Mutated residues were coloured Y444F, red; K556E, green; S662V, yellow. Heparan binding domains (HBDs; R484, R487, K532, R585, and R588) were coloured in blue. AAV receptor binding domains (AAVR BDs; R471, D528, Q589, T592, S262, Q263, G265, A266, S267, N268, H271, N382 and Q385) were highlighted in orange. To visualise AAV-DJ, 7kfr, a 1.56Å cryoelectron microscopy-derived structure, was downloaded from the Protein Data Bank. To analyse structural changes in variable region I (VR-I) between wild-type AAV2 and AAV-DJ, VR-I sequences were selected and the root mean squared deviation (RMSD) was calculated as follows. RMSD units are in angstroms (Å) and give a quantitaive indication of the degree of structural similarity between two proteins or protein sequences, Where δ is the distance between a particular i atom and the mean position of the corresponding n atoms from the other protein structure:

$$RMSD = \sqrt{\frac{1}{n}\sum_{i=1}^{n}\delta\binom{2}{i}}$$

To complement the visualisation of capsid residues in PyMol, a Radial Interpretation of Viral Electron Density Map (RIVEM) was also produced. This was undertaken by Dr. Suzanne Scott at the University of Sydney. This programme reads atomic coordinates from Protein Data Bank files, and converts the protein chosen residues onto a stereographic projection, that is, a normally spherical 3D shape into a flat 2D shape.

In this thesis, an attempt was also made to use open source software to predict how our mutagenesis strategy may affect the structure of AAV2 capsids. SWISS-MODEL was initially used but produced low Q-mean values (a score indicating how well the software thinks

it has been able to determine the structure of a protein). Transform restrained (tr) Rosetta (https://yanglab.nankai.edu.cn/trRosetta/) was then used which gave itself TM-scores (measure of confidence in reliability of the structure) ranging from "high" to "very high". trRosetta uses a deep residual neural network to predict inter-residue distance and orientations, which are converted into smooth restrains, allowing trRosetta to build 3D protein structures using a direct energy minimisation method.

3.6 Use of animals

All procedures performed on animals were approved by the UK Home Office in accordance with the UK Animals (Scientific Procedures) Act, and undertaken in accordance with the Association for Research in Vision and Ophthalmology's (ARVO) Statement for the Use of Animals in Ophthalmic and Visual Research. To collect tissues, mice were sacrificed using the Schedule 1 method of cervical dislocation, or asfixiation in a CO2 chamber if cardiac puncture was performed.

3.7 Intravitreal (IVT) vector injection

Adult, male C57BL/6 mice were procured from Charles Rivers Laboratories. For anaesthesia, 50mg/kg ketamine and 10mg/kg xylazine were delivered through intraperitoneal (IP) injection. An eyedrop of 1% tetracaine solution (Bausch & Lomb) was also used as a local anaesthetic. Pupils were dilated with an eyedrop of 1% tropicamide to visualise correct placement of the needle in the vitreous. To visualise the IVT procedure, a 40x objective microscope was used, and a strong light source. Vectors were thawed and diluted in sterile PBS to obtain the desired vector concentration in 2μL solution. 2.5μL was pipetted onto the bottom on a petri dish to make sure that exactly 2μL could be drawn into the Hamilton syringe. Colibri forceps were used to position the mouse eye so that the sclera could be seen clearly. A 5L Hamilton Syringe (#65RN; Needle: 33G, 8 mm, point style 2, Hamilton Company) was used to puncture the sclera approximately 1mm posterior to the superior-temporal limbus and inject the vector solution into the vitreous. Solution was injected slowly over a 30 second period to prevent sudden increases in intraocular pressure. The cornea was then punctured with a 30G needle to limit reflux of the injection solution from the site of injection. Animals were recovered in a warm cabinet and monitored every 15 minutes until fully recovered, using lacrilube to ensure the eyes did not dry out. Eyes would be excluded from analysis if (i) the injection score was graded 'poor' e.g. due to significant reflux of injected solution, or (ii) a cataract developed.

3.8 Retinal wholemounts

Eyes were enucleated, taking care to avoid punturing the eye, and removing all fat and muscle from the sclera. The cornea was punctured with a 25g needle to allow more fixative to enter the eye cup. Samples were immersed in ice-cold 4% PFA for 24h. Under a dissecting microscope, the cornea was pinched with microforceps, and microdissecting scissors were used to remove tthe cornea by cutting carefully along the limbus. The lens was removed and the retina was carefully dissociated from the eye cup using forceps. Four incisions were then made from the peripheral retina to within 0.5mm of the optic nerve head to allow the retina to flatten. To stain retinas, samples were washed three times in PBS, then blocked/permeabilised in 10% normal goat serum (NGS) 0.5% Triton X100 for 1h at room temperature. Primary antibodies were diluted to the concentrations stated below in 5% NGS 0.5% Triton X100 and incubated with retinas overnight at 4C on a slow rocker. When staining for IBA1 however, primary antibodies were incubated for 48h at 4C to allow the antibodies to permeate deeper into the retinal layers. Samples were washed three times in PBS for 10min (1h for IBA1 staining), then goat secondary antibodies were diluted to a 1:1,000 concentration in 5% NGS 0.5% Triton X100 and incubated with samples for 2h at room temperatre. Retinas were washed three times in PBS, then mounted onto Superfrost Plus slides (VWR; Cat Number: 631-0108) using a nitrocellulose membrane (Merck Millipore; Cat Number: AABG01300) with RGCs facing upwards. Any remaining PBS on the slide was removed using filter paper, and Fluosave mounting media (VWR; Cat Number: 345789-20) was added around the samples. A glass coverslip was carefully placed on top to avoid generating airbubbles. To obtain tilescan images of the whole flatmounted retina, a Leica DMi8 microscope was used and set to a 20x objective. An SPE confocal microscope equipped with a 20x magnification (Leica Microsystems) was used to obtain high magnification images. For quantification, eight images per retina were taken, four from the peripheral retina and four from the middle/central retina from each quadrant of the sample. To obtain representative images, an SPE confocal was used at 40x objective, however when obtaining representative images of GFAP, a Zeiss Airyscan superresolution confocal was used. Acquisition settings such as frame averaging, resolution, section thickness etc, were chosen as appropriate for quantification and representative images.

3.9 Retinal cryosections

Following enucleation, the cornea was punctured with a 25g needle to allow more fixative to enter the eye cup. Eyes were immersed in 4% PFA for 24h at 4C, dehydrated in 30% sucrose for 24h at 4C, and embedded in optimal cutting temperature compound (OCT; Sakura Finetek

Cat Number: 4583). 13μm tissue sections (through the dorsal-ventral/superior-inferior axis of the retina) were prepared using a Bright OTF 5000 cryostat (Bright Instruments) and Superfrost Plus slides (see above), and stored at -20C until further use. Samples were thawed at room temperature for 2h to prevent loss of tissue from the slides. Sections were washed three times in PBS for 5min to remove the OCT. For some staining procedures (see table below), citrate buffer-mediated antigen retreival was used. A 100x stock of citrate buffer (AbCam; Cat Number: ab93678) was diluted in PBS and heated to 90C in a waterbath. Slides were placed into the buffer in glass coplin jars for 30min, removed from the buffer and allowed to cool at room temperature for 5min, then washed twice in PBS to dilute residual citrate buffer before proceeding with the staining protocol. PBS was carefully removed from the slides with filter paper to allow application of the ImmuneEDGE (Vector Labs; Cat Number: H-4000) wax pen around the edge of the slides (three times to maximise retention of buffers on the slide). Tissue sections were blocked and permeabilised with 10% NGS, 0.5% Triton X-100 and 0.5% bovine serum albumin (BSA) diluted in PBS for 1h at room temperature. Primary antibodies were diluted to the concentrations stated below in 5% NGS, 0.5% Triton X-100 and 0.5% BSA, and incubated with sections overnight at 4C, without agitation to reduce loss of buffer/solutions from the slide. Samples were washed three times with PBS for 10 mins, then incubated with goat secondary antibodies at a 1:1,000 concentration, and DAPI diluted at 1:5,000, for 2h at room temperature. Slides were washed three times in PBS for 10 mins, and filter paper was used to remove any remaining PBS. Fluosave mounting media was applied, and glass coverslips placed gently on top, taking care to avoid creating airbubbles. For imaging, a Leica DM6000 epifluorescent microscope set to a 20x objective was used to obtain eight images per sample for quantification of fluorescence intensity. A 40x objective was used to obtain representative images.

3.10 List of antibodies used for immunohistochemical analysis

Table 3.1: List of antibodies used for immunohistochemical analysis

Target	Species	Supplier	Catalogue Number	Dilution	Antigen Retrieval
RBPMS	Guinea pig	PhosphoSolutions	1832-RBPMS	1:500	No
CD4	Rabbit	AbCam	ab183685	1:300	Yes
CD8	Rabbit	AbCam	ab217344	1:500	Yes
IBA1	Guinea pig	Synaptic Systems	234 003	1:500	No
GFAP	Rabbit	Dako Omnis	Z0334	1:500	No
MHC c. II	Rat	Thermo Fisher	14-5321-82	1:200	No
GFP	Rabbit	AbCam	ab290	1:1,000	No
mCherry	Mouse	AbCam	ab167453	1:500	No

3.11 Quantification of immunohistochemisty data

3.11.1 GFP+ RBPMS+ cells in retinal wholemounts

This assessment was undertaken in Volocity software. First, RBPMS+ regions-of-interest (ROIs) were identified using 'threshold' and 'identify objects' functions. Size and circularity parameters were adjusted until the software could accurately recognise RBPMS+ ROIs. A 'watershed' function was also applied to divide closely spaced RBPMS+ ROIs (for example, splitting a single ROI into three distinct RBPMS+ retinal ganglion cells). The mean GFP fluorescence intensity within each RBPMS+ ROI was then calculated. An RBPMS+ ROI with a GFP mean fluorescence intensity of greater than 5 relative fluorescence units (RFUs) was deemed GFP+. This analysis enabled quantitation of the number of GFP+ RBPMS+ ROIs/field-of-view (FOV) and the mean GFP fluorescence level in each RBPMS+ ROI.

3.11.2 GFP, IBA1, RBPMS levels in cryosections

Quantification of these markers in images of retinal cryosections was performed in ImageJ. A threshold was applied to convert the 8-bit files into binary images. If applicable (for instance, with high a background signal in the outer segments of the photoreceptor cell layer) the freehand tool was used to select the area in which the fluorescence intensity would be calculated. Integrated density was measured to determine the fluorescent signal. When appropriate (datasets with no background signal in the photoreceptor outer segments) a Macro script was written to expedite the analysis process. An example script is given below. The threshold settings would be adjusted for different datasets/stains.

run("Threshold..."); setThreshold(80, 255); setOption("BlackBackground", true); run("Convert to Mask"); run("Measure");

3.11.3 CD4 and CD8 levels in retinal cryosections

To assess the infiltration of CD4 and CD8 cells into the retina, images were thresholded and the number of CD4 or CD8 ROIs/FOV was determined using the 'Analyse Particles' function. Size and circulatory parameters were optimised for a particular dataset until the software could accurately identify individual cells. A Macro script was used to expedite the data acquisition process, an example of which is given below. Note that the 'theshold' settings were different for CD4 and CD8 analyses given the differences in background staining between these datasets.

run("Threshold..."); setThreshold(60, 255); setOption("BlackBackground", true); run("Convert to Mask"); run("Analyze Particles...", "size=20-250 circularity=0.30-1.00 display clear summarize");

3.11.4 GFAP+ Muller Glia in retinal cryosections

To quantify GFAP+ Muller glia immunofluorescence in retinal cryosections, an ImageJ plugin, Simple Neurite Tracer (SNT) was used. This was to ensure that this assessment was selective for GFAP+ Muller glia and that the presence of GFAP+ astrocytes in the retinal ganglion cell layer did not affect interpretation of the results (for instance, by quantifying all GFAP immunoreactivity in a given FOV). SNT was used to trace all visilble GFAP+ fibril in a particular image. This process was done manually due to the lack of a soma region which some programmes can use to automatically trace dendritic processes. SNT calculated the length of each GFAP+ fibril and the fluorescence intensity of each fribil.

3.11.5 GFAP+ astrocytes in retinal wholemounts

To assess changes in the morphology of GFAP+ astrocytes, images were thresholded and skeletonised in ImageJ. The properties of the skeleton were analysed using the 'Summarize Skeleton' function which calculates multiple parameters, including the number of junctions (where two lines in the skeleton meet) and the number of quadruple points (where four lines intersect at a single node). To expedite this analysis, a Macro script was used:

run("Threshold..."); setThreshold(70, 255); setOption("BlackBackground", true); run("Convert to Mask"); run("Close"); run("Remove Outliers...", "radius=2 threshold=50 which=Bright"); run("Skeletonize (2D/3D)"); run("Summarize Skeleton");

3.12 Electroretinography

Electroretinography (ERG) was peformed using a Diagnosys ColorDome LabCradle machine. Mice were dark adapted in a closed cabinet for 18-24h before the ERG procedure. All ERG was done in a dark room with all light sources covered and head torches with red lights (covered with tape to reduce light intensity) to ensure maximum dark adaptation. For anaesthesia, 50mg/kg ketamine and 10mg/kg xylazine were delivered through IP injection. An eyedrop of 1% tetracaine solution was used as a local anaesthetic to stop the mice blinking during administration of dilating agents. Pupils were dilated with an eyedrop of 1% tropicamide and 2.5% phenylephrine hydrochloride. Mice were placed back into the dark cabinet

during this time to reduce exposure to ambient light. Before placement of electrodes, eyes were checked for cataracts or red reflux, which would result in exclusion of that particular eye. The presence of dilating drops on the eye after this step was also checked to ensure maximum dilation of the pupils. Eyes that did not have a drop after this step (for instance, if the mouse had blinked) had the drops reapplied and were placed back into the dark cabinet for an additional five minutes. Prior to placement of electrodes, eyes were thoroughly dried with a cotton wool swab (moisture on the eyes can cause interference with the ERG). A grounding electrode was placed into the tail, and the reference electrodes were placed around the eyes. Here, care was taken to ensure the head of the mouse was completely level, as imbalances affect the ERG signal. The recording electrodes were then placed very gently onto the apex of the cornea (indentations will affect the ERG signal). A small drop of lacrilube was then applied to the cornea using a 1mL syringe/30g needle to couple to the recording electrodes to the eye. After a 30 second period, a test flash was used to assess whether the coupling of the electrodes had been successful. Electrodes would be removed and placed back onto the eyes if there had been an issue. Each mouse would receive three test flashes to ensure equal dark adaptation between groups/samples. Before running the ERG protocol, a 4.5min pause in the procedure was applied to ensure maximum dark adaptation. The protocol used had 17 steps, including 7 positive scotopic threshold responses (pSTRs; measure of retinal ganglion cell function), 4 B-waves (rod bipolar cell function) and 4 A-waves (rod photoreceptor function). For data analysis, representative pSTR (7th pSTR), B-wave (4th B-wave) and A-wave (4th A-wave) waveforms are shown, across an entire recording period (400ms). Peak voltage (μV) was also measured across all light intensities tested, which was defined as the maximum (pSTR and B-wave) or minimum (A-wave) voltage values across a recording.

3.13 Flow cytometry

All flow cytometry (including tissue extraction, processing, staining, cytometry, and data analysis) of splenic samples was performed by Dr. Andrew Sage (Department of Surgery, University of Cambridge). Spleens were processed into a single cell suspension by passing through a 70μm cell sieve using a syringe plunger. Red blood cells were first lysed with ammonium chloride RBC lysis buffer, and then 1-2x10^6 cells were stained with a cocktail of fluorescently-tagged antibodies and a live-dead stain (Zombie aqua, Biolegend). After washing, cells were fixed with formaldehyde solution (BD Cellfix) and filtered through a 30μm filter before analysis on a LSRII Fortessa flow cytometer (BD). Prior to antibody gating, live single cells are gated based on FSC, SSC and negative live-dead staining. A list of the antibodies used for these analyses is given below. Spleen cells stained with single antibodies

were used to set PMT voltages and create a compensation matrix in FACSDiva software before acquisition of main samples. Example flow plots for key cell populations are provided in Appendix Figure A1.

Table 3.2: List of antibodies used for flow cytometry

Target	**Fluorophore**	**Clone**	**Supplier**
CD19	BV650	6D5	Biolegend
IgM	APC	II/41	Thermo Fisher
IgD	PerCPVio700		Miltenyi
CD95	PE-Cy7	Jo2	BD Biosciences
GL7	eF450	Ly-77	Biolegend
MHC c. II	APCVio770		Miltenyi
CD3	AF488	145-2C11	Biolegend
CD4	AF700	RM4-5	Biolegend
CD8	PerCP	53-6.7	Biolegend
CXCR5	PE	L138D7	Biolegend
PD-1	PE-Cy7	4B12	Biolegend
CD44	BV605	1M7	Biolegend
CD62L	PacBlue	MEL-14	Biolegend
CD25	APC	PC61	Biolegend
CD11c	PE-Cy7	N418	Biolegend
CD8a	PerCP	53-6.7	Biolegend
CD11b	AF488	M1/70	Biolegend
XCR1	APC	MPC-11	Biolegend
SiglecH	PE		Miltenyi

3.14 Statistical analyses

To confirm that the correct statistical tests had been chosen, the author of this thesis contacted the Statistical Laboratory, Centre for Mathematical Sciences, University of Cambridge, who confirmed that proper statistical analyses had been applied to the datasets. First, the normality of distribution was assessed with a Shapiro Wilk test. If the data did not meet this assumption, non-parametric Kruskal-Wallis and Dunn's posthoc tests to assess more that two groups, or a Mann-Whitney test to compare two groups. The homogeneity of variance was also assessed, and for data that was normally distributed but exhibited heteroskedasticity, a Brown-Forsythe ANOVA and Dunnett's T3 posthoc test was used to compare more than two groups, and a Welch's t-test to compare two groups. If datasets were normally distributed and exhibited homogeneity of variance, ordinary one-way ANOVA and Tukey or Dunnett's posthoc tests (more than two groups) or a Student t-test (two groups; two-tailed, unpaired) was used.

Chapter 4

Immunology of a rationally-designed AAV capsid mutant in the ocular compartment

4.1 Declaration

The material in this chapter has not yet been published, however, a manuscript is being prepared for submission. This work was funded by the National Eye Research Centre Seed Funding Award (G104353; £9,750), and Addenbrookes Charitable Trust Small Grant Award (G104080; £7,500), both of which were written by the author of this thesis, with feedback from Dr. Patrick Yu Wai Man and Professor Keith Martin.

The scientific hypotheses tested in this chapter were those of the author of this thesis with input from Dr. Patrick Yu Wai Man and Professor Keith Martin. All of the data presented was the work of the author, with the exception of the flow cytometry (performed by Dr. Andrew Sage, see Chapter 2), and the RIVEM plot (Dr. Suzanne Scott, see Chapter 2).

4.2 Chapter synopsis

The injection of AAV into the eye via the intravitreal (IVT) route is known to elicit an immune response that may limit therapeutic efficacy and pose safety concerns for patients. In this chapter, AAV2 was mutated at certain residues termed phosphodegrons, which have been posited to limit cytosolic degradation of virions, and reduce capsid antigen presentation via major histocompatibility complex class I (MHC c. I). These mutations have demonstrated two effects: (i) an increase in transduction of infected cells; and (ii) reduced CD8 T-cell-mediated killing of transduced hepatocytes in a $rag^{-/-}$ mouse. The objective of this chapter was to assess whether the incorporation of phosphodegron mutations into AAV2 could be used to circumvent anti-capsid immune responses by enabling robust transduction at a low vector dose. In fact, increased activation of the cellular and humoral arms of the adaptive immune response, in addition to innate immune activation was observed with the mutant capsids vs. wild-type AAV2. A slight attenuation of binding affinity to AAV2's primary attachment receptor, heparan sulphate proteoglycan (HSPG), was also observed. Mechanistically, it was suggested that, in accordance with similar publications in the literature, reduced sequestration of capsids in HSPG-rich extracellular matrices may increase cellular infection levels, particularly of microglia cells, which may be linked to increased anti-viral immune responses. In summary, this chapter identified novel aspects of immune activation arising from IVT of phosphodegron mutant AAV2 capsids, but suggests that these may not be a suitable approach to circumvent anti-AAV2 immune responses in the eye, and enable repeated gene transfer to the inner retina.

4.3 Introduction

AAV2 has achieved a number of successes in the clinic, most notably with the FDA granting approval to Luxturna (AAV2 targeting *RPE65* mutations) and Zolgensma (AAV9 targeting *SMA1* mutations) [24]. Compared to animal models, however, achieving robust transduction whilst limiting activation of the immune response in humans is more challenging. For instance, after systemic administration of AAV2 expressing FIX, a robust CD8 T-cell response was seen that cleared the transduced cells in haemophilia B patients [36]. To develop a possible solution to this problem, phosphodegron mutant AAV2 capsids have been described that may limit presentation of vector antigen to cross-primed CD8 T-cells in transduced hepatocytes [194]. Here, a brief description of the pathway to transduction of a cell by an AAV vector is given. AAV begins a cellular infection by binding to its primary receptor, heparan sulphate proteoglycan (HSPG) on the cell surface. Through an unknown mechanism, this is thought to facilitate interactions with proteinaceous receptors, such as the AAV receptor (AAV-R), hepatocyte growth factor receptor (HGF-R), and fibroblast growth factor receptor (FGF-R), although additional receptors will likely be identified in the future [12, 195, 196]. This facilitates the internalisation of viral particles via clathrin-mediated endocytosis. To transfer their genome into the host cell's, AAV must first 'escape' from an endosome into the cytosol to avoid degradation in a lysosome. Cytosolic AAV is trafficked to the nucleus, where it enters via a nuclear pore, and the capsid protein uncoats (possibly due to a slight increase in acidity in the nucleus). Thus, the AAV genome (containing the therapeutic gene of interest) is released and exists as an episomal plasmid capable of expressing functional mRNA transcripts [15].

Figure 4.1: Mechanism of AAV2 cellular entry

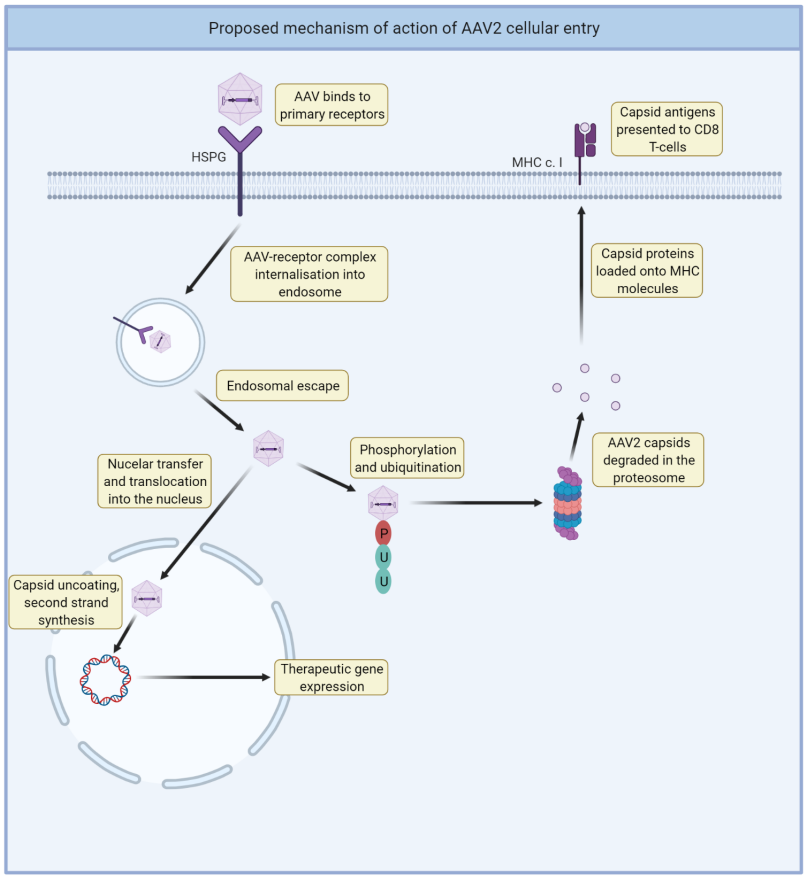

Outline of AAV2 mechanism of cellular entry and nuclear transfer and proposed mechanism-of-action for phosphodegron mutant AAV2. AAV2 binds to its primary receptor HSPG which induces clathrin-mediated endocytosis. AAV2 escapes from the endosome, possibly using a region in its VP1u monomers [197]. Some AAV2 capsids are trafficked to the nucleus and enter via nuclear pore complexes. The capsid then uncoats, possibly in a pH dependent manner, releasing its ssDNA genetic payload into the target cell. Second strand synthesis occurs so that therapeutic gene expression is driven from a dsDNA episome. Not every AAV2 vector that enters a cell will achieve nuclear transfer of its genome, however. Some are phosphorylated by protein kinases, such as epidermal growth factor receptor tyrosine kinase (EGFR-TK) and subsequently tagged for proteasomal degradation via ubiquitination. Antigenic capsid peptides are subsequently loaded onto major histocompatibility complex type I proteins, which present viral epitopes to cytotoxic CD8+ T-cells.

When inside the cytosol, AAV can be phosphorylated and ubiquitinated by host cell protein tyrosine kinases and ubiquitin ligases, which facilitates degradation of the capsid by the proteasome, thereby preventing transduction. This occurs at specific residues, termed phosphodegrons, which can be mutated in order to inhibit cytosolic degradation of AAV, thereby increasing transduction [198]. Considering the connection between proteasomal degradation of capsid antigen and the presentation of epitopes to CD8 T-cells on MHC c. I, a triple phosphodegron mutant AAV2 capsid, AAV2 (Y444F, Y500F, Y730F) has been shown to reduce killing of transduced hepatocytes by cross-primed CD8 T-cells in a mouse model [194]. Of note however, the authors used a $rag^{-/-}$ mouse, which lacks T-cell and B-cell function and therefore has dramatically reduced dendritic cell function which collectively limit the ability of $rag^{-/-}$ mice to express antigen on MHC c. II and induce adaptive immune responses [199]. Further, the paper did not report on neutralising antibody (NAb) levels, nor activation of innate immune pathways. Considering the overarching objective of this thesis, repeated gene transfer to the inner retina, it was asked whether phosphodegron mutant AAV2 could be used to circumvent NAb production as a possible means of facilitating repeated vector injections by enabling robust transduction at low vector doses.

Figure 4.2: Known biology of phosphodegron mutant capsids

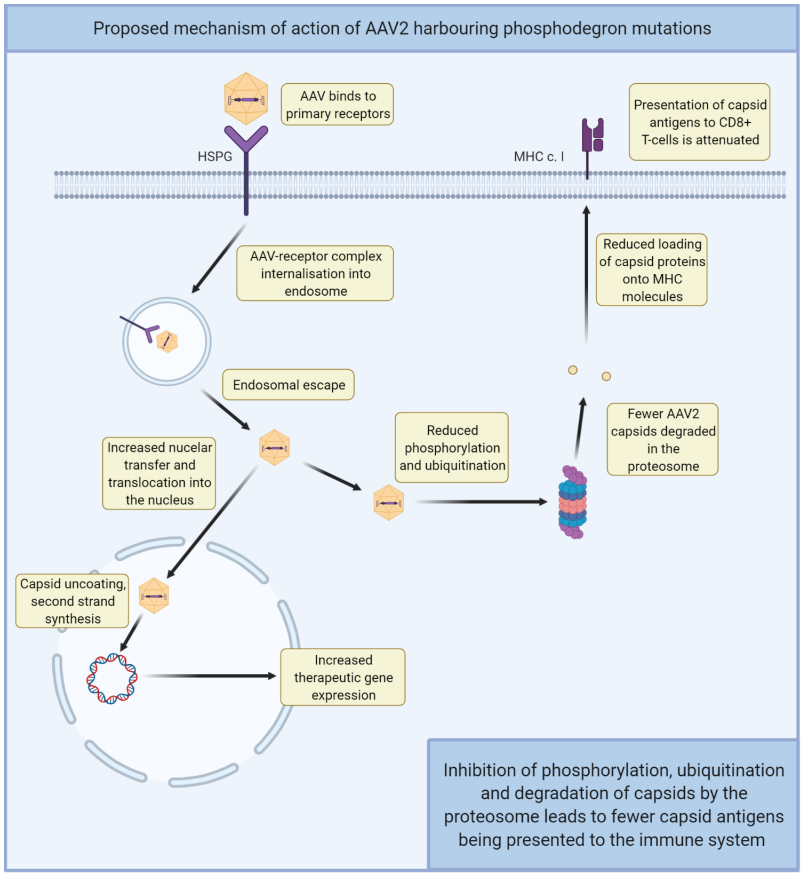

AAV2 can be engineered to avoid phosphorylation, ubiquitination and proteasomal degradation via rational design. Here, regions of AAV capsids that are known to be either phosphorylated or ubiquitinated by intracellular machinery can be mutated. This results in a higher rate of nuclear transfer and concomitant therapeutic gene expression. Reports have also suggested that the inhibition of proteasome-mediated degradation of capsid antigens may in turn limit presentation of AAV epitopes to CD8 T-cells, possibly reducing cytotoxic killing of transduced hepatocytes.

4.4 Overview of study plan

A detailed description of the materials and methods used in this chapter is given in Chapter 2. An overview of the study plan and experimental design is given below. Briefly, mutations were selected for analysis and used to manufacture AAV2 containing phosphodegron mutated residues. Capsids were injected bilaterally (into both eyes) into wild-type C57BL6/J mice via IVT. After three weeks, ERG was performed and samples were extracted for analysis.

Figure 4.3: Overview of study plan for Chapter 4

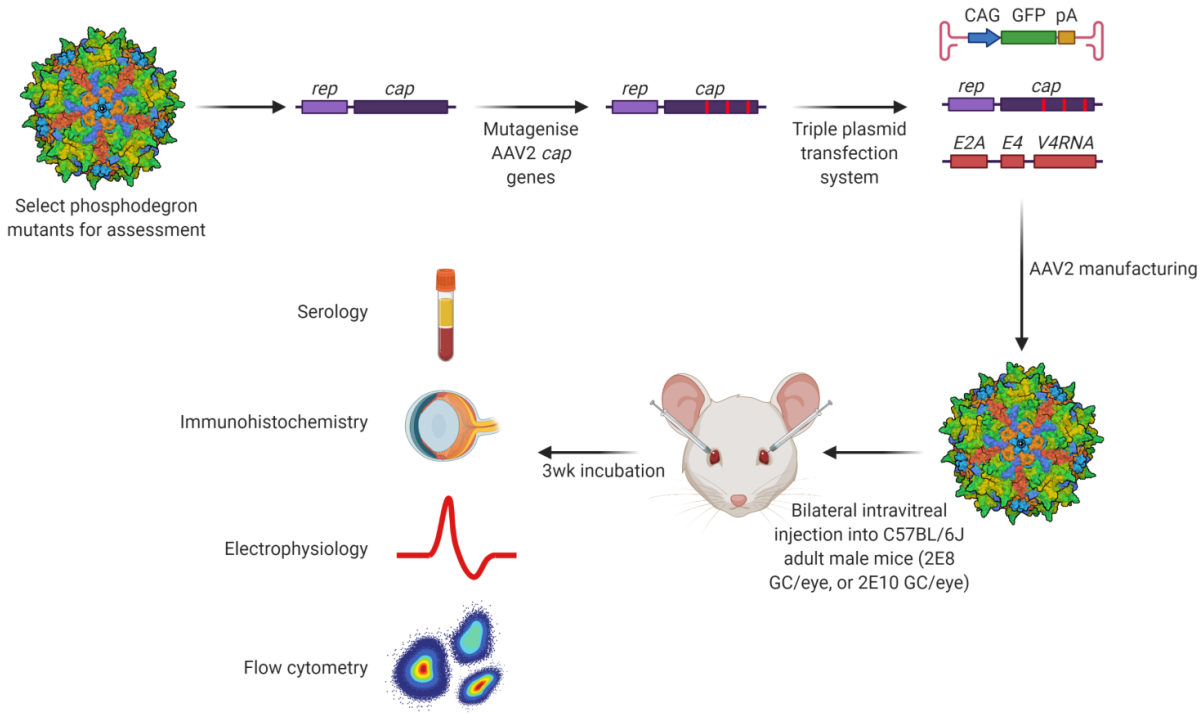

Capsid phosphodegron mutations were selected and AAV2 rep/cap plasmids were mutagenised. The triple plasmid transfection system was used to manufacture WT and mutant AAV2. Bilateral intravitreal injections into C57BL/6J adult male mice were performed. After a 3wk incubation period, blood samples were taken for assessment of NAb levels. Eyes were enucleated, fixed and sectioned for immunohistochemical analysis. Electroretinography was performed to assess the possibility of functional damage to the retina. Spleens were harvested, dissociated, stained, and analysed for changes in lymphocyte populations using flow cytometry.

4.5 Results

4.5.1 Phosphodegron mutant AAV2 vectors induce higher levels of retinal transduction than wild-type AAV2 following intravitreal injection to the murine retina

Three previously described phosphodegron mutations were selected for assessment in accordance with two criteria. First, in their capacity to increase transduction of target cell types, and second, in that the functional viral titre was not affected by possible structural perturbations due to changes to the AAV2 capsid structure [198, 200, 201].

The AAV2 phosphodegron mutants were tested in their ability to transduce the retina following intravitreal injection of 2E8 GC/eye. Injection of AAV2 (Y444F) resulted in a higher percentage of GFP+ RBPMS+ regions-of-interest (ROIs) when compared to WT AAV2 (24.98 ±4.41 vs. 2.72 ±1.05% SEM; $p < 0.001$). Increases in mean fluorescence intensity (measured in relative fluorescence units, RFUs) per RBPMS+ ROI were also observed (20.93 ±1.80 vs. 5.02 ±1.62 RFUs SEM; $p < 0.0001$). Injection of AAV2 (K556E) resulted in increases in the percentage of GFP+ RBPMS+ ROIs compared to WT AAV2 (19.35 ±2.79 vs. 2.72 ±1.05% SEM; $p < 0.01$), and the mean GFP fluorescence intensity per RBPMS+ ROI (16.50 ±2.00 vs. 5.02 ±1.62 RFUs SEM; $p < 0.001$) was also seen in comparison with mice receiving intravitreal injections of WT AAV2. Injection of S662V resulted in an elevated percentage of GFP+ RBPMS+ ROIs/FOV vs. WT AAV2 injections (13.73 ±1.69 vs. 2.72 ±1.05% SEM; $p < 0.05$). Mice receiving S662V injections also exhibited increased mean GFP fluorescence intensity per RBPMS+ ROI (15.10 ±1.15 vs. 5.02 ±1.62 RFUs SEM; $p < 0.01$). Assessing GFP immunoreactivity in all RBPMS+ ROIs, similar trends were apparent where all phosphodegron mutant AAV2 vectors increased transduction vs. WT AAV2 controls. In summary, all selected phosphodegron mutant AAV2 vectors exhibited greater levels of transduction of the murine retina following IVT.

Figure 4.4: Phosphodegron mutant AAV2 vectors induce higher levels of retinal transduction than wild-type AAV2 following intravitreal injection to the murine retina

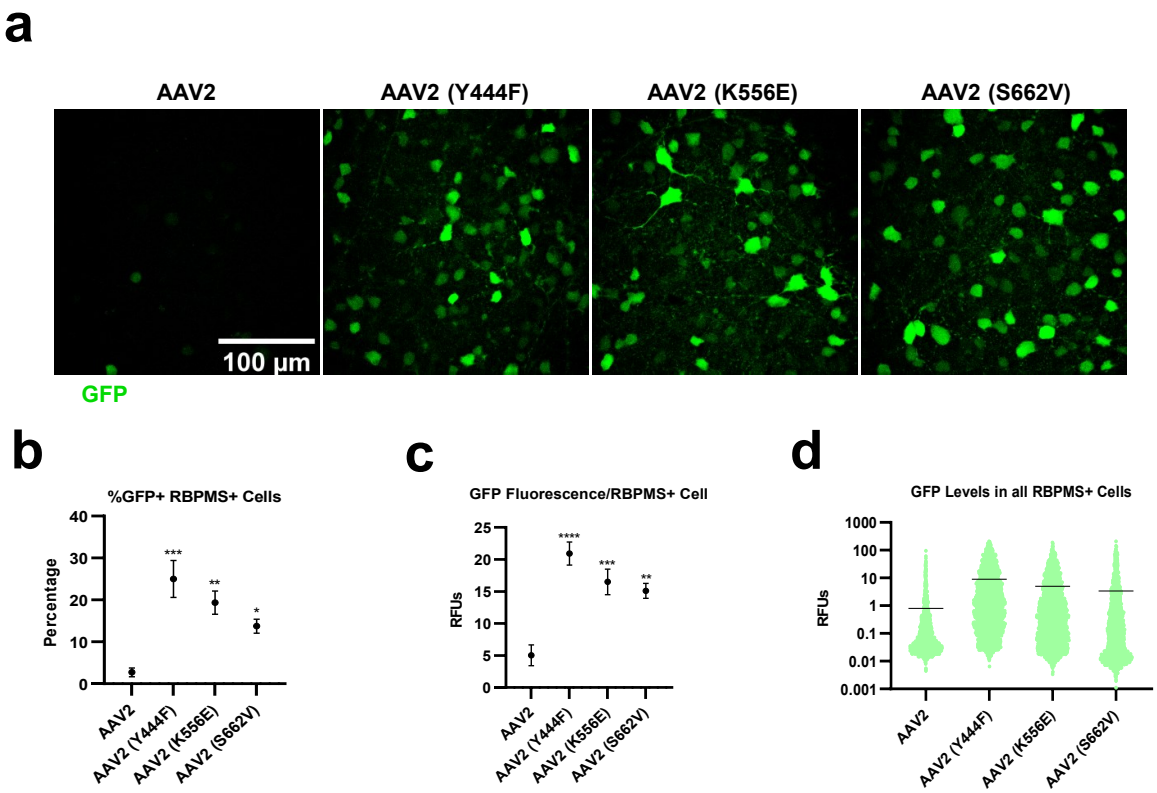

(a) Representative images of retinal wholemounts depicting increased levels of GFP in the phosphodegron mutant groups compared to AAV2 WT control three weeks after bilateral intravitreal injection of 2E8 GC/eye. Quantification of GFP expression levels in wholemounted retina samples was performed in Volocity.

(b) Percentage of GFP+ RBPMS+ cells, (c) mean GFP immunofluorescence/RBPMS+ ROI/FOV, and (d) mean GFP immunofluorescence/all RBPMS+ ROIs were calculated. To assess statistically significant differences between groups, parametric ANOVAs and Dunnett's posthoc tests were used. * = $p < 0.05$, ** = $p < 0.01$, *** = $p < 0.001$, n=6 per group.

4.5.2 Validation of a triple phosphodegron mutant AAV2 capsid *in vitro*

Having validated the transduction potential of the single phosphodegron mutant AAV2 capsids, a triple phosphodegron mutant AAV2 capsid variant was created , AAV2 (Y444F, K556E, S662V), termed AAV2 (TM) for the remainder of this thesis. First the ability of AAV2 (TM) to transduce two cell lines, HEK-239T and ARPE-19 cells, was examined with flow cytometry. AAV2 (TM) incubation increased the percentage of GFP+ cells in HEK293T (25.7 ±0.54 vs. 2.78 ±0.12% SEM; $p < 0.0001$) and ARPE-19 (27.1 ±0.41 vs. 2.78 ±0.12% SEM; $p < 0.0001$) cells when compared to prototypical AAV2 vectors.

Figure 4.5: Validation of a triple phosphodegron mutant AAV2 capsid *in vitro*

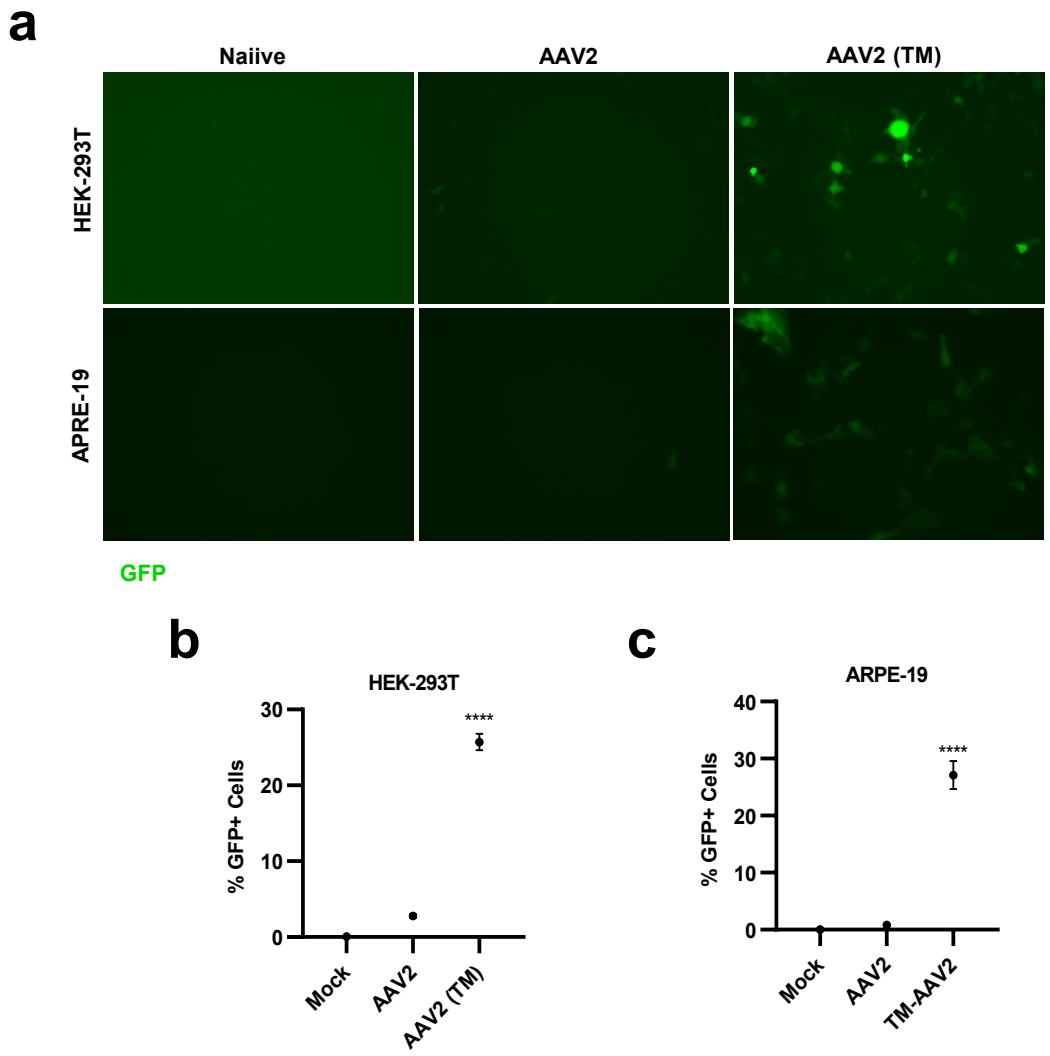

(a) Representative images of GFP expression levels following a 24h incubation with the triple phosphodegron mutant AAV2 and WT AAV2 and Mock (DMEM-only). Here, 5E7 VP/mL was used for the HEK-293T cell line, 2E8 VP/mL for the ARPE-19 cell line.
(b & c) Flow cytometry analysis of GFP expression in (b) HEK-293T cells and (c) ARPE-19 cells. **** = $p < 0.0001$, two-tailed Student's t-test, n=4 per group.

4.5.3 Validation of a triple phosphodegron mutant AAV2 capsid *in vivo*

These findings were then translated into an *in vivo* model. Adult male C57BL/6J mice were injected with 2E8 GC/eye of AAV2, AAV2 (Y444F), AAV2 (TM), or 2E10 GC/eye AAV2 (high titre; 2E10 GC/eye), or PBS vehicle as a control. Analysis of the levels of GFP expression after three weeks showed that injection with AAV2 (Y444F) increased RFUs/FOV (4.55 ±0.84 vs. 1.49 ±0.31 RFUs/FOV; $p < 0.05$) vs. WT AAV2. In the AAV2 (TM) group, an in increase in the mean fluorescence intensity/FOV was observed when compared to the WT AAV2 group (7.80 ±1.01 vs. 1.49 ±0.31 RFUs/FOV; $p < 0.01$). An even greater increase in mean fluorescence intensity/FOV was seen after administration of AAV2 (high titre) vs. WT AAV2 (24.11 ±2.24 vs. 1.49 ±0.31 RFUs/FOV; $p < 0.01$).

Figure 4.6: Validation of a triple phosphodegron mutant AAV2 capsid *in vivo* with cryosections

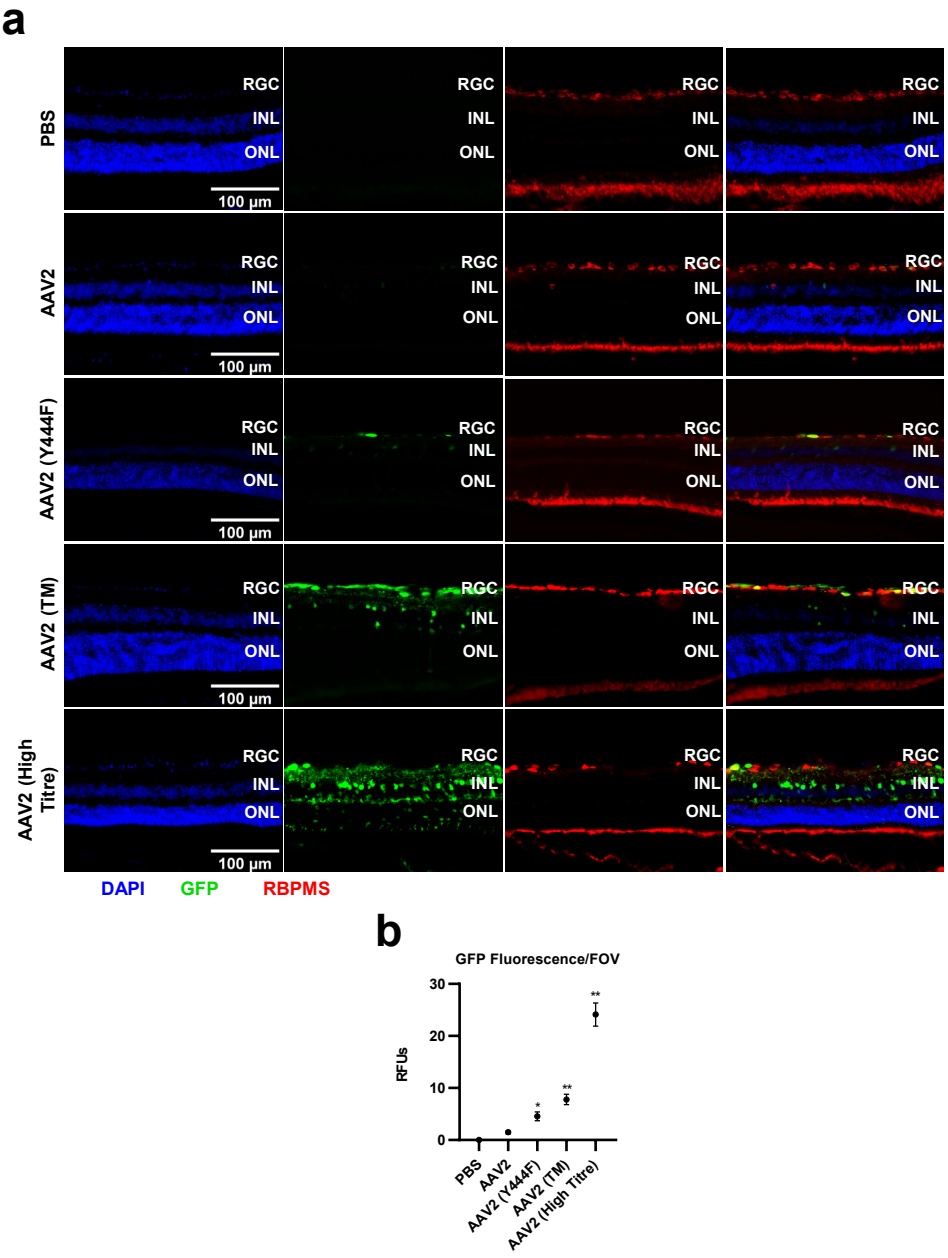

(a) Representative 40x epifluorescence microscope images of retinal sections transduced with AAV2, phosphodegron mutant capsid AAV2, or high titre AAV2. RGC = retinal ganglion cell layer, INL = inner nuclear layer, ONL = outer nuclear layer.

(b) Quantification was performed in ImageJ. Here, mean GFP fluorescence levels/FOV was calculated. * = $p < 0.05$, ** = $p < 0.01$, **** = $p < 0.0001$, Kruskal-Wallis and Dunn's posthoc tests, n=6 per group.

In a separate set of experiments, AAV2, AAV2 (Y444F), AAV2 (TM) and AAV2 (high titre) were injected via IVT. After three weeks, eyes were taken and retinal wholemounts (RWMs) were prepared. This experiment validated the data obtained from the retinal wholemounts. AAV2 (Y444F) induced a higher level of transduction than wild-type AAV2, and AAV2 (TM) induced a higher level of GFP expression than AAV2 (Y444F). However, expression was much greater with AAV2 (high titre) than all other vectors tested.

Figure 4.7: Validation of a triple phosphodegron mutant AAV2 capsid *in vivo* with RWMs

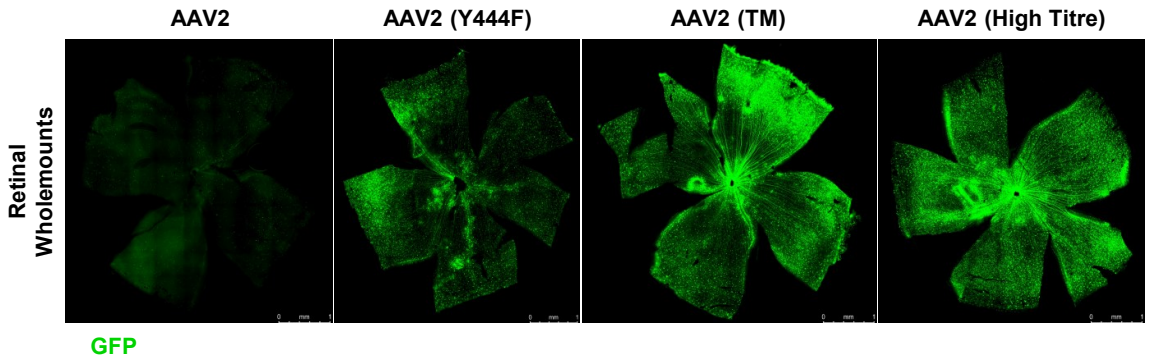

Representative tilescan images showing wholemounted retinas from mice receiving 2E8 GC/eye wild-type AAV2, AAV2 (Y444F) and AAV2 (TM). RWMs from mice receiving AAV2 (high titre) are also included for reference.

4.5.4 AAV2 (TM) induces higher humoral immune responses than wild-type AAV2 after IVT

The validation experiments showed that the rationally-designed AAV2 capsids improved transduction in the murine retina when compared to wild-type AAV2 vector. In the next set of experiments, the effect of incorporating phosphodegron mutations into AAV2 capsid in terms of the induction of humoral immune responses was tested. First, C57BL6/J mice were injected via IVT with wild-type AAV and mutated AAV2 at the stated titres. After three weeks, serum samples were collected and NAb and TAb assays were performed. This was to identify neutralising activity in the serum samples, and also to confirm that this activity was due to the presence of anti-AAV2 immunoglobulin molecules, and not another potentially confounding factor, such as complement factors which may play a role in neutralising AAV *in vivo* [87].

In mice that received wild-type AAV2 injections, no neutralising activity was observed up to serum dilutions of 1:59. When AAV2 (Y444F) was delivered via IVT however, the presence of NAbs could be seen at around 1:1,000, as the remaining infectivity began to decline at this concentration of serum. Even higher levels of NAbs were evident in mice that received AAV2 (TM) IVTs, and neutralising activity was detected at serum dilution of around 1:5,000. In the AAV2 (high titre) group, the highest level of NAb were evident, where reductions in remaining infectivity at 1:10,000 dilutions were seen.

This dataset was subsequently converted into IC50 values (concentration of serum that yields a 50% reduction in reporter levels i.e. remaining infectivity). AAV2 (Y444F) IVTs yielded a higher mean IC50 value than wild-type AAV2 (2,062 ±645.1 vs. 68.8 ±9.8 AUs SEM, $p = 0.370$), although this difference was not statistically significant. In mice that received IVTs of AAV2 (TM), serum NAb titres were significantly elevated compared to those from the wild-type AAV2 group (5,098 ±981.9 vs. 68.8 ±9.8 AUs SEM, $p < 0.01$). Mice who were injected with AAV2 (high titre) displayed the greatest increase in NAb levels vs. wild-type AAV2 controls (12,244 ±1,694 vs. 68.8 ±9.8 AUs SEM, $p < 0.01$).

This was further analysed by investigating changes in the area-under-the-curve (AUC) between groups. In this analysis, a lower AUC is associated with higher levels of NAbs. A statistically significant decrease in AUC was seen between AAV2 (Y444F) and wild-type AAV2 groups (54,026 ±978.2 vs. 64,306 ±1,309 AUs SEM, $p < 0.01$). An even greater decrease was seen when comparing mice who received AAV2 (TM) and wild-type AAV2 IVTs (48,168 ±1,555 vs. 64,306 ±1,309 AUs SEM, $p < 0.0001$). The largest decrease in AUC was observed when comparing the AAV2 (high titre) and wild-type AAV2 groups (37,273 ±2,449 vs. 64,306 ±1,309 AUs SEM, $p < 0.0001$).

In summary, these assays demonstrated that the incorporation of phosphodegron mutations into AAV2 capsids may induce a higher level of NAbs after injection to the murine

retina via IVT. To validate these findings, demonstrate that the neutralising activity observed was immunoglobulin-dependent, and to identify the main antibody isotype responsible for the neutralising effect, TAb assays were performed. Here, serum samples were analysed using ELISA, with secondary antibodies specific to certain subclasses of immunoglobulin molecules.

Changes were seen in IgG levels. In mice that received AAV2 (Y444F), IgG levels were greater than in those injected with wild-type AAV2, although this change was not statistically significant (0.080 ±0.048 vs. 0.009 ±0.002 SEM AUs, $p = 0.33$). When AAV2 (TM) was delivered via IVT however, statistically significant increases in IgG levels were seen compared to mice receiving IVTs of wild-type AAV2 (0.227 ±0.051 vs. 0.009 ±0.002 SEM AUs, $p < 0.0001$). The greatest changes in IgG titres were observed when comparing AAV2 (high titre) and wild-type AAV2 (0.685 ±0.034 vs. 0.009 ±0.002 SEM AUs, $p < 0.0001$).

No statistically significant changes in IgG1 were seen between groups, although a small increase in mean values was observed between AAV2 (high titre) and wild-type AAV2 groups (0.091 ±0.029 vs. 0.016 ±0.012 SEM AUs, $p = 0.281$).

Changes in IgG2b were evident between groups, however. An increase in the mean IgG2b level was seen when comparing AAV2 (Y444F) and wild-type AAV2 injected groups (0.092 ±0.062 vs. 0.007 ±0.001 SEM AUs, $p = 0.194$) although the difference was not statistically significant. In mice that received an IVT of AAV2 (TM), however, a significant increase in IgG2b levels was observed when comparing to wild-type AAV2 (0.290 ±0.075 vs. 0.007 ±0.001 SEM AUs, $p < 0.0001$). Similarly, an increase was seen in the AAV2 (high titre) group compared to the wild-type AAV2 group (0.797 ±0.054 vs. 0.007 ±0.001 SEM AUs, $p < 0.0001$).

Similar trends were also evident when analysing the levels of IgG2c. Increased mean IgG2c levels were seen when AAV2 (Y444F) and wild-type AAV2 groups were compared, although these differences were not statistically significant (0.032 ±0.024 vs. 0.009 ±0.001 SEM AUs, $p = 0.929$). When AAV2 (TM) was delivered to the murine vitreous, however, statistically significant increases in IgG2c levels could be observed (0.179 ±0.043 vs. 0.009 ±0.001 SEM AUs, $p < 0.01$). The greatest increase in IgG2c was evident when comparing AAV2 (high titre) and wild-type AAV2 groups (0.655 ±0.033 vs. 0.009 ±0.001 SEM AUs, $p < 0.0001$).

When the levels of IgM were compared between groups, however, no changes were seen. To summarise, this set of experiments showed that higher levels of IgG2b and IgG2c (both subclasses of IgG) were observed in mice who received IVTs of AAV2 (TM) compared to wild-type AAV2. This data corroborated that of the NAb experiments and further substantiated the idea that incorporation of phosphodegron mutations into AAV2 capsids may lead to

increased antibody synthesis upon injection to the vitreous cavity of mouse models.

Figure 4.8: AAV2 (TM) induces higher humoral immune responses than wild-type AAV2 after IVT

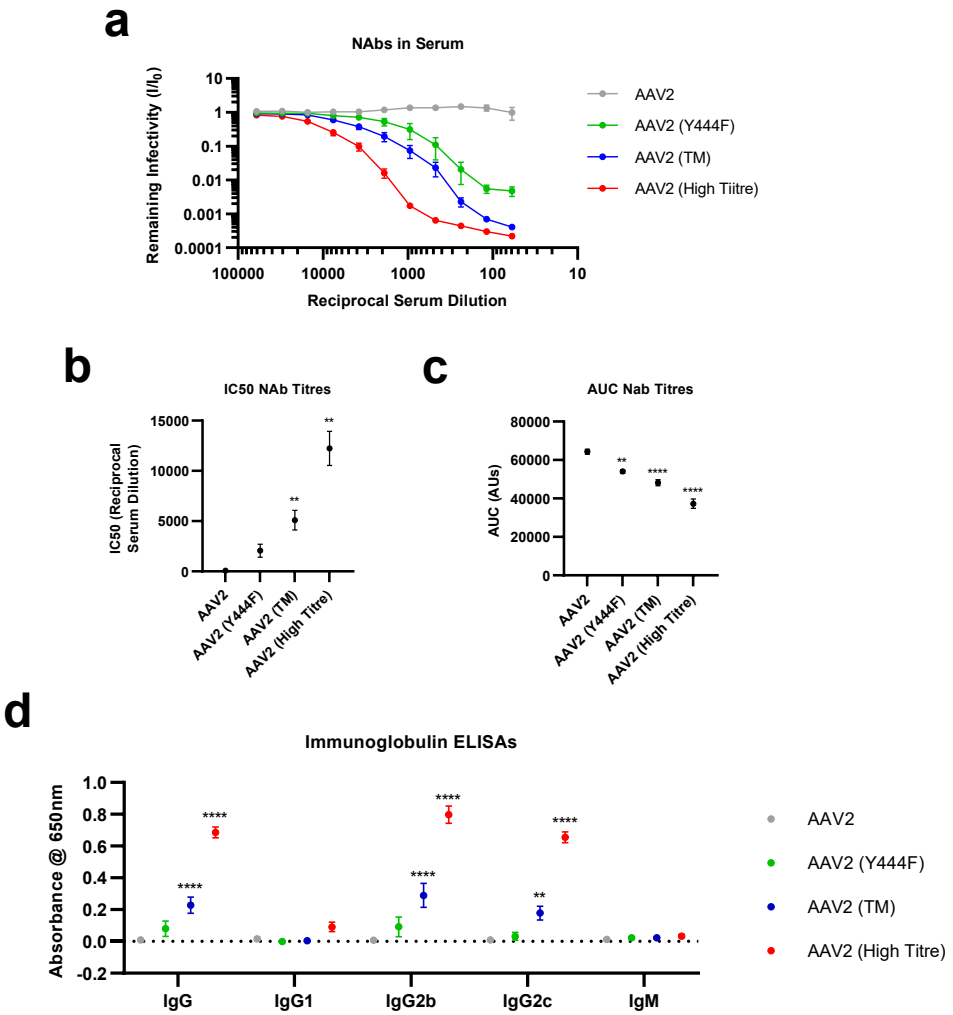

Intravitreal injection of a triple phosphodegron mutant AAV2 induces higher NAb and TAb levels than wild-type AAV2. Vectors were injected and serum samples were taken three weeks later for analysis. All data is presented as column graphs showing the mean value for each group +/- SEM. All statistical analyses are vs. the AAV2 group. N=6 per group.

(a) NAb titres were assessed using a HEK-293T/AAV2.CMV.Luciferase system. Remaining infectivity was defined as the luminescent signal in each well divided by 'Control' values.

(b) IC50 values for each group were calculated using non-linear regression (variable slope, four parameters) in GraphPad. ** = $p < 0.01$, Brown-Forsythe ANOVA and Dunnett's posthoc tests.

(c) Area-under-the-curve (AUC) values were calculated in GraphPad. ** = $p < 0.01$, **** = $p < 0.0001$, one-way ANOVA and Dunnett's posthoc tests.

(d) Immunoglobulin ELISA assays were performed to assess the antibody isotypes responsible for the neutralising effect. ** = $p < 0.01$, **** = $p < 0.0001$, two-way ANOVA and Dunnett's posthoc tests.

4.5.5 Elevated T-cell infiltration arising from IVT of AAV2 (TM)

In the next set of experiments, the possibility that IVT of phosphodegron mutant AAV2 may cause higher immune responses than wild-type AAV2 was investigated further. Here, an assessment of whether injection of the vectors resulted in increased or decreased levels of T-cell infiltration into the retina was made. Mice were injected with vectors and eyes were taken after three weeks. Cryosections were prepared and stained for CD4 and CD8, and cells/FOV counted.

A small increase in the levels of CD4 T-cells was seen when comparing AAV2 (Y444F) and wild-type AAV2 groups, however, the difference was not statistically significant (0.194 $\pm$0.109 vs. 0.074 $\pm$0.029 SEM CD4+ ROIs/FOV, $p > 0.99$). After an injection of AAV (TM), however, increases in the mean levels of CD4 T-cells infiltrating into the retina did increase when compared to wild-type AAV2 levels (1.61 $\pm$0.78 vs. 0.074 $\pm$0.029 CD4+ ROIs/FOV SEM, $p < 0.05$). Finally, the levels of CD4 T-cells in the retina following IVT of AAV2 (high titre) was the greatest of all the groups tested and significantly greater than wild-type AAV2 levels (2.63 $\pm$0.55 vs. 0.074 $\pm$0.029 SEM CD4+ ROIs/FOV, $p < 0.001$).

Figure 4.9: IVT of AAV2 (TM) induces higher levels of CD4 T-cell infiltration into the retina the wild-type AAV2

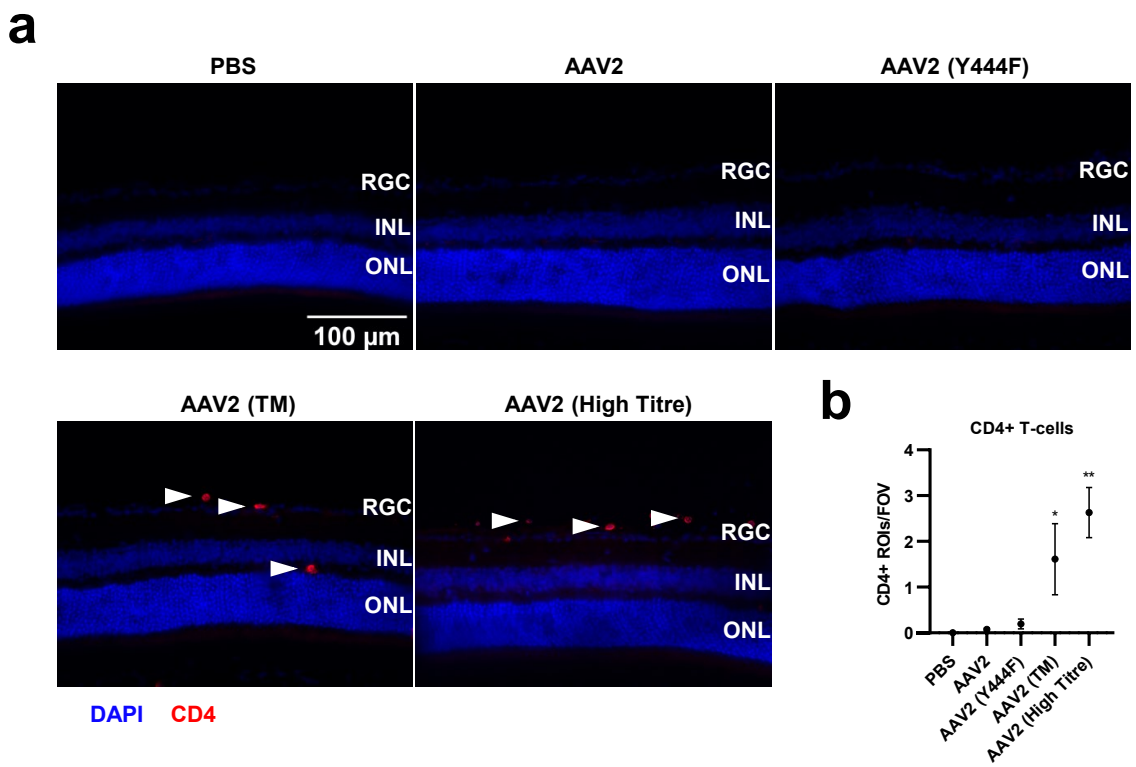

Intravitreal injection of a triple phosphodegron mutant AAV2 and high dose AAV2 induces T-cell infiltration into the retina. Vectors were injected and blood and tissue samples were taken three weeks later for analysis. Data is presented as a column graph showing the mean value for each group +/- SEM. Statistical analyses are vs. the AAV2 group.

(a) Representative 40x magnification epifluorescence microscope images showing that intravitreal injection of triple phosphodegron mutant AAV2 and high titre AAV2 is associated with the presence of CD4+ T-cells in the retina.

(b) Quantification of dataset was undertaken via counting of the number of CD4+ ROIs/FOV in ImageJ. * = $p < 0.05$, ** = $p < 0.01$, Kruskal-Wallis and Dunn's posthoc tests, n=8 per group.

Having shown changes in the levels of CD4 T-cells after IVT of the vectors, the possibility that injection of AAV2 (TM) may induce greater levels of CD8 T-cell infiltration into the retina was also assessed. When comparing AAV2 (Y444F) and wild-type AAV2, no changes in the levels of CD8 T-cells was observed. In mice that received an IVT of AAV2 (TM) however, a statistically significant increase in CD8 T-cell infiltration was observed when comparing to mice that received wild-type AAV2 injections (1.20 $\pm$0.34 vs. 0.00 $\pm$0.00 CD8+ ROIs/FOV SEM, $p < 0.01$). A greater increase in CD8 T-cell infiltration was seen in the AAV2 (high titre) group compared to the wild-type AAV2 group (2.58 $\pm$1.08 vs. 0.00 $\pm$0.00 CD8+ ROIs/FOV SEM, $p < 0.05$).

Figure 4.10: IVT of AAV2 (TM) induces higher levels of CD8 T-cell infiltration into the retina the wild-type AAV2

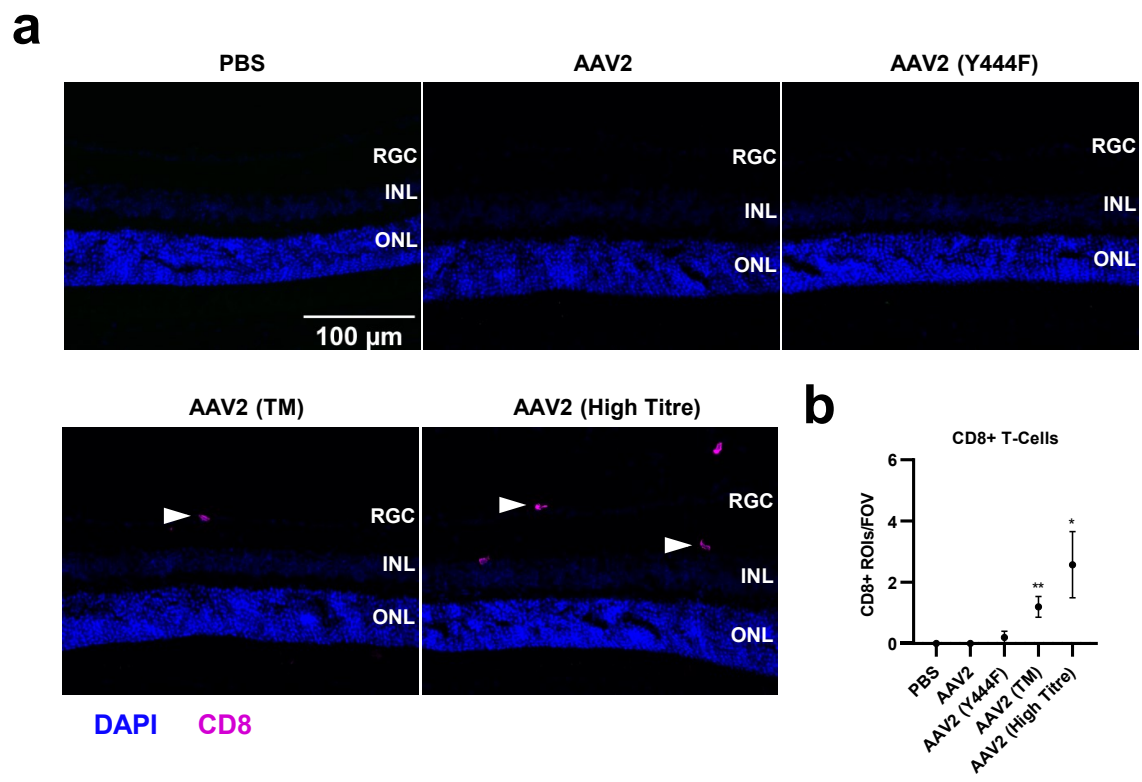

Intravitreal injection of a triple phosphodegron mutant AAV2 and high dose AAV2 induces cellular adaptive immune responses. Vectors were injected and blood and tissue samples were taken three weeks later for analysis. Data is presented as a column graph showing the mean value for each group +/- SEM. Statistical analyses are vs. the AAV2 group.

(a) Representative 40x magnification epifluorescence microscope images showing that intravitreal injection of triple phosphodegron mutant AAV2 and high titre AAV2 is associated with the presence of CD8+ T-cells in the retina.

(b) Quantification of dataset was undertaken via counting of the number of CD8+ ROIs/FOV in ImageJ. * = $p < 0.05$, ** = $p < 0.01$, Kruskal-Wallis and Dunn's posthoc tests, n=8-10 per group.

4.5.6 Increased follicular T-cell levels after IVT of AAV2 (TM) vs. wild-type AAV2

Recent reports examining the immune response to AAV have shown a substantial number of genome copies present in the spleen weeks after intraocular vector injection, even if the levels of AAV genomes in the liver was limited [202].

Considering this data, a set of experiments were undertaken to assess whether IVT of AAV2 and phosphodegron mutant vectors would induce changes in lymphocyte populations in the spleens. Here, spleens were extracted three weeks after IVT and stained with a cocktail of antibodies to examine T- and B-cell and dendritic cell populations.

No changes were observed in the levels of effector CD4+ T-cell (CD3+ CD4+ CD8- $CD62L_{lo}$ $CD44_{hi}$) between mice who received IVTs of wild-type AAV2, AAV2 (Y444F) and AAV2 (TM). Similarly, the levels of effector CD8+ T-cell (CD3+ CD4- CD8+ $CD62L_{lo}$ $CD44_{hi}$) were unchanged between these three groups. Assessment of the levels of follicular helper T-cells (Tfh) ((CD3+ CD4+ $CXCR5_{hi}$ $PD\text{-}1_{hi}$) did yield statistically significant changes between some of the groups, however. Whilst mice injected with AAV2 (Y444F) showed no increase in Tfh levels vs. those injected with wild-type AAV2 (0.262 $\pm$0.037% vs. 0.276 $\pm$0.053% SEM %Thf/CD4 cells, $p = 0.97$), when AAV2 (TM) was administered, a 3.3-fold increase in Tfh levels was observed vs. wild-type AAV2 IVTs (0.910 $\pm$0.12% vs. 0.276 $\pm$0.053% SEM %Thf/CD4 cells, $p < 0.01$).

Figure 4.11: Increased follicular helper T-cell levels after IVT of AAV2 (TM) vs. wild-type AAV2

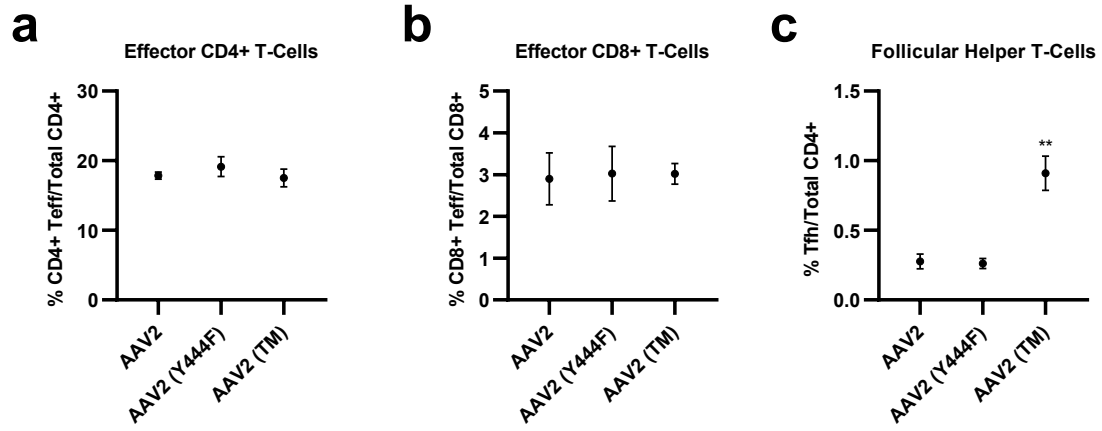

Intravitreal injection of AAV2 (TM) induces changes in splenic lymphocyte populations. Vectors were injected via IVT and spleens were harvested for analysis after three weeks. Data is displayed as column graphs, and show the mean for each group +/- SEM. Statistical analyses are vs. the AAV2 group. N=6 per group.

(a) Effector CD4+ T-cell (CD3+ CD4+ CD8- $CD62L_{lo}$ $CD44_{hi}$) levels expressed as a percentage of total CD4+ T-cell levels.

(b) Effector CD8+ T-cell (CD3+ CD4- CD8+ $CD62L_{lo}$ $CD44_{hi}$) levels expressed as a percentage of total CD8+ T-cell levels.

(c) Follicular helper CD4+ T-cell (CD3+ CD4+ $CXCR5_{hi}$ $PD\text{-}1_{hi}$) levels expressed as a percentage of all CD4+ cells. ** = $p < 0.01$, Brown-Forsythe ANOVA and Dunnett's T3 posthoc tests.

4.5.7 Splenic germinal centre reactions induced by IVT of AAV2 (TM)

These investigations continued with an assessment of whether IVT of the vectors induced changes in germinal centre (GC) B-cells (CD19+ IgM+/$_{lo}$ IgD$_{lo}$ CD95$_{hi}$ GL7+). First, the levels of GC B-cells were assessed, as B-cells are known to migrate to GCs in response to a new infection. No changes were observed between mice receiving an IVT of AAV2 (Y444F) when compared to wild-type AAV2 (0.143 $\pm$0.043% vs. 0.084 $\pm$0.013% SEM %GC B-cells/total splenic lymphocytes, p = 0.93). When AAV2 (TM) was delivered via IVT however, a statistically significant increase in GC B-cells was seen vs. mice that were injected with wild-type AAV2 (0.676 $\pm$0.097 SEM vs. 0.084 $\pm$0.013 SEM %GC B-cells/total splenic lymphocytes, p $<$ 0.001).

Next, the levels of MHC c. II on GC B-cells was investigated. MHC c. II is a marker for activation of B-cells, which occurs when a mature B-cell encounters an antigen that its B-cell receptor binds to[203].

After delivery of AAV2 (Y444F), no significant changes in GC B-cell MHC c. II levels were observed vs. wild-type injections (12,035 $\pm$1,646 vs. 11,087 $\pm$1,782 SEM RFUs, p = 0.87). Following an IVT of AAV2 (TM) however, a statistically significant increase in MHC c. II levels was seen when compared to mice that received wild-type AAV2 injections (18,632 $\pm$1,111 vs. 11,087 $\pm$1,782 SEM RFUs, p $<$ 0.01).

Lastly, the percentage of class-switched B-cells (IgM$_{lo}$ IgD$_{lo}$) in the germinal centres was assessed. Class-switching occurs as GC reactions progress to change the structure of the immunoglobulin molecules produced by B-cells thus eliciting a broad range of antibody effector functions [204].

When comparing mice that received AAV2 (Y444F) to wild-type AAV2 injections, no significant difference in B-cell class-switching could be seen (49.3 $\pm$6.82 vs. 49.2 $\pm$8.01 SEM IgM$_{lo}$ IgD$_{lo}$B-cells/GC B-cells, p = 0.99). When mice were injected with AAV2 (TM), however, a statistically significant increase in the levels of class-switched B-cells was observed compared to the wild-type AAV2 group (77.1 $\pm$3.1 vs. 49.2 $\pm$8.01 SEM IgM$_{lo}$ IgD$_{lo}$B-cells/GC B-cells, p $<$ 0.05).

In summary, this set of experiments showed that injection of a triple phosphodegron mutant induced a greater level of splenic B-cell activation and class-switching than wild-type AAV2 vectors.

Figure 4.12: Splenic germinal centre reactions induced by IVT of AAV2 (TM)

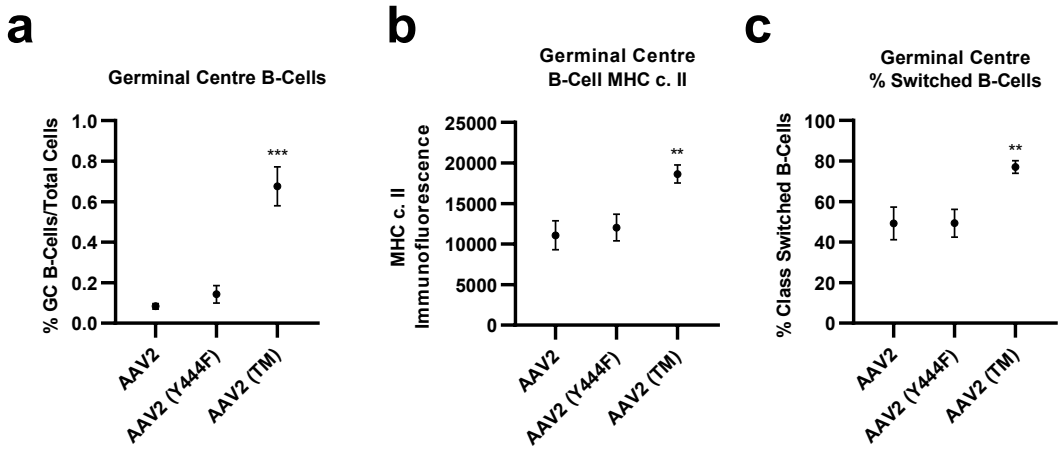

Intravitreal injection of AAV2 (TM) induces changes in splenic lymphocyte populations. Vectors were injected via IVT and spleens were harvested for analysis after three weeks. Data is displayed as column graphs, and show the mean for each group +/- SEM. Statistical analyses are vs. the AAV2 group. N=6 per group.

(a) Germinal centre B-cell (CD19+ IgM+/$_{lo}$ IgD$_{lo}$ CD95$_{hi}$ GL7+) levels as a percentage of all splenic lymphocytes. *** = $p < 0.001$, Kruskal-Wallis test and Dunn's posthoc tests.

(b) Levels of MHC c. II expressed on GC B-cells. ** = $p < 0.01$, one-way ANOVA and Dunnett's posthoc tests.

(c) Percentage of class-switched B-cells (IgM$_{lo}$ IgD$_{lo}$) in the germinal centres, as a percentage of all GC B-cells. ** = $p < 0.01$, one-way ANOVA and Dunnett's posthoc tests.

4.5.8 Increased dendritic cell activation induced by IVT of AAV2 (TM) vs. wild-type AAV2

In the next set of experiments, conventional and plasmacytoid dendritic cell activation was assessed by measuring the levels of MHC c. II on the cell surface. Dendritic cells (DCs) inhibit degradation of MHC c. II from the cell surface when they are activated by an antigen, therefore increased MHC c. II expression is a marker of DC activation [205].

First, the levels of MHC c. II on conventional DCs subset 1 (cDC1; $CD11c_{hi}$ CD8a+ XCR1+) was examined. No changes were observed between mice receiving AAV2 (Y444F) or wild-type AAV2 injections (15,960 $\pm$871 vs. 15,266 $\pm$605 SEM RFUs, $p = 0.71$). When AAV2 (TM) was delivered intravitreally, however, a statistically significant increase in cDC1 MHC c. II expression was observed compared to mice who were injected with wild-type AAV2 (17,305 $\pm$591 SEM vs. 15,266 $\pm$605 SEM RFUs, $p < 0.05$).

Similarly, when assessing activation of conventional DCs subset 2 (cDC2; $CD11c_{hi}$ CD11b+), no changes were evident between AAV2 (Y444F) and wild-type AAV2 groups (15,029 $\pm$1,645 vs. 14,517 $\pm$1,383 SEM RFUs, $p = 0.95$). In mice that received IVT of AAV2 (TM), however, a statistically significant increase in cDC2 MHC c. II expression was observed compared to that seen in the wild-type AAV2 group (18,533 $\pm$1,087 vs. 14,517 $\pm$1,383 SEM RFUs, $p < 0.05$).

Lastly, MHC c. II levels were analysed in plasmacytoid dendritic cells (pDCs; CD11c+ SiglecH+). In contrast to the other DC subsets assessed however, no significant increases in MHC c. II levels were seen between AAV2 (Y444F) and wild-type AAV2 (1,225 $\pm$116 vs. 1,144 $\pm$153 SEM RFUs, $p = 0.90$), nor between AAV2 (TM) and wild-type AAV2 groups (1,338 $\pm$119 vs. 1,144 $\pm$153 SEM RFUs, $p = 0.56$).

In summary, this set of experiments showed that IVT of AAV2 (TM) induced activation of cDC1 and cDC2 subsets when compared to wild-type AAV2 injected mice, but these changes were not seen with the pDC subset.

Figure 4.13: Dendritic cell activation induced by IVT of AAV2 (TM)

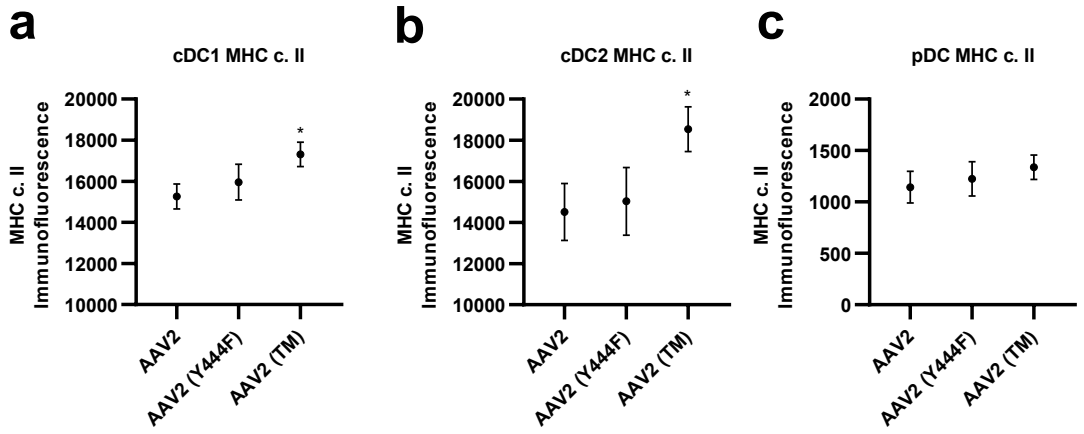

Intravitreal injection of AAV2 (TM) induces changes in splenic lymphocyte populations. Vectors were injected via IVT and spleens were harvested for analysis after three weeks. Data is displayed as column graphs, and show the mean for each group +/- SEM. Statistical analyses are vs. the AAV2 group. N=6 per group.

(a) MHC c. II expression on conventional DCs subset 1 (cDC1) ($CD11c_{hi}$ CD8a+ XCR1+) dendritic cells. * = $p < 0.05$, one-way ANOVA and Dunnett's posthoc tests.

(b) MHC c. II expression on conventional DCs subset 2 (cDC1) ($CD11c_{hi}$ CD11b+) dendritic cells. * = $p < 0.05$, Student's t-test.

(c) MHC c. II expression on plasmacytoid (CD11c+ SiglecH+) dendritic cells.

4.5.9 Elevated microglia activation after AAV2 (TM) vs. wild-type AAV2 IVT

Having characterised the cellular and humoral arms of the adaptive immune system, a set of experiments was undertaken to understand how an IVT of AAV2 (TM) may induce higher innate immune response in different glia cell populations in the retina. This began with an assessment of whether IBA1 (ionized calcium-binding adapter molecule 1) levels were altered in the retina post-injection of the vectors. IBA1 is a marker for activated microglia cells and is commonly used as a tool for investigating immune responses in the eye [206].

Comparing mice who were injected with AAV2 (Y444F) with those who received a wild-type AAV2 IVT, a small but statistically non-significant increase in IBA1 levels was seen (101,047 $\pm$31,974 SEM vs. 13,560 $\pm$3,333 SEM RFUs, $p = 0.66$). When AAV2 (TM) was delivered to the vitreous, however, a 40-fold increase in IBA1 immunofluorescence was observed compared to the wild-type AAV2 group (425,428 $\pm$78,004 vs. 13,560 $\pm$3,333 SEM RFUs, $p < 0.05$). In mice that were in the AAV2 (high titre) group, the greatest fold increase in IBA1 immunofluorescence was seen, compared to the wild-type AAV2 group (680,342 $\pm$297,679 vs. 13,560 $\pm$3,333 SEM RFUs, $p < 0.01$). In summary, these experiments showed that injection of AAV2 (TM) induces a higher level of microglia activation than injection of wild-type AAV2.

Figure 4.14: Microglia activation induced by IVT of AAV2 (TM)

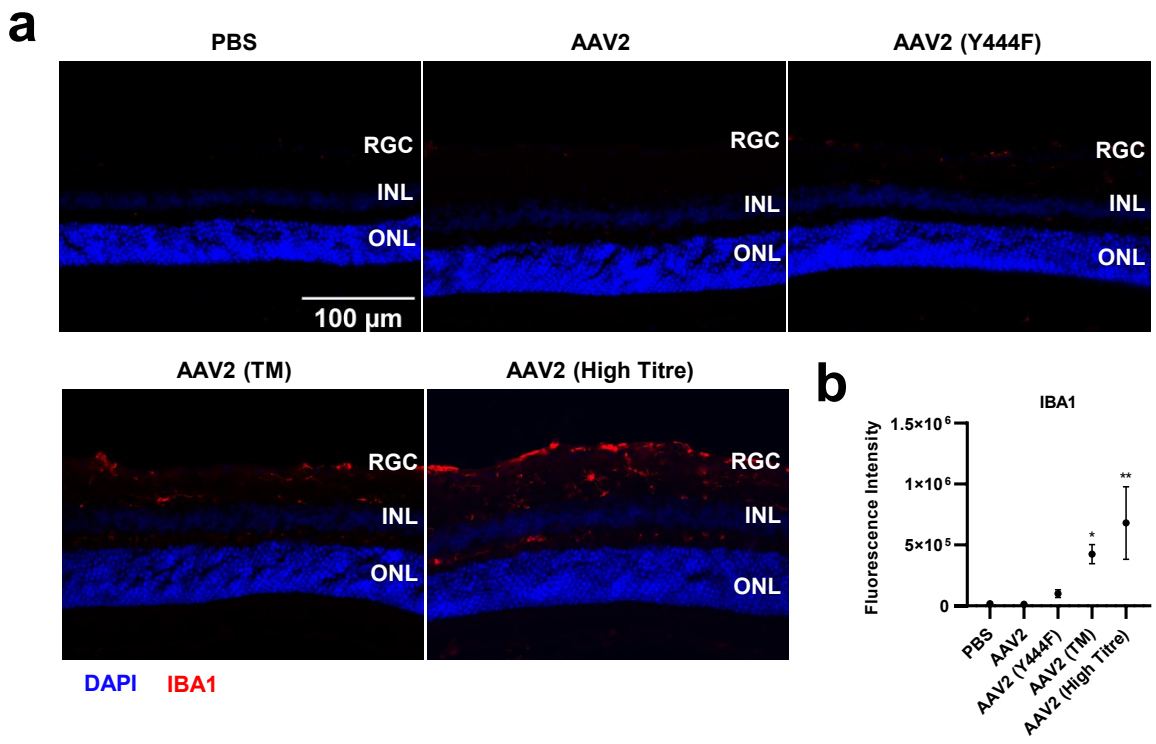

Intravitreal injection of a phosphodegron mutant AAV2 and high titre AAV2 leads to gliosis in the murine retina. Vectors were injected via IVT and retinas were extracted for analysis after three weeks. Data is presented as a column graph, with the mean value for each group shown +/- SEM. Statistical analyses are vs. the AAV2 group. RGC, retinal ganglion cell layer; INL, inner nuclear layer; ONL, outer nuclear layer.

(a) Representative 40x objective epifluorescence microscopy images of retinal cryosections showing IBA1 immunoreactivity in groups receiving phosphodegron mutant AAV2 and high titre AAV2 injections.

(b) Corresponding quantification performed in ImageJ shows the level of IBA1 immunoreactivity per field of view (FOV). A Kruskal-Wallis ANOVA and Dunn's posthoc test was used to determine whether differences between groups were statistically significant. * = $p < 0.05$, ** = $p < 0.01$, n=8-10 per group.

4.5.10 Increased Muller glia activation in AAV2 (TM) vs. wild-type AAV2 treated mice

Having demonstrated increased microglia activation in AAV2 (TM) injected mice, the possibility that Muller glia activation may also be induced by IVT of some of the vector groups was investigated. GFAP (glial fibrilary acidic protein) immunofluorescence was used to assess Muller glia activation, as GFAP is thought to be upregulated in response to a variety of proinflammatory stimuli in the retina [207]. To quantify the dataset, Simple Neurite Tracer was used to trace neurites individually and avoid quantifying overall GFAP immunofluorescence per field-of-view, which would include astrocyte-derived GFAP immunofluorescence, thereby confounding interpretation of the results.

First, the length of the GFAP positive fibrils was assessed, as this was expected to increase as a result of possible vector-induced immune activation. Mice that received AAV2 (Y444F) vector via IVT did not demonstrate a statistically significant increase in GFAP fibril length vs. those that were injected with wild-type AAV2 (29.35 $\pm$3.15 vs. 23.66 $\pm$3.37μm SEM, p = 0.51). In the AAV2 (TM) group, however, a statistically significant increase in GFAP fibril length was observed when compared to mice in the wild-type AAV2 group (35.65 $\pm$2.84 vs. 23.66 $\pm$3.37μm SEM, p <0.05). The greatest GFAP fibril length was seen in the AAV2 (high titre) group vs. mice injected with wild-type AAV2 (38.69 $\pm$2.77 vs. 23.66 $\pm$3.37μm SEM, p <0.05).

Next, the mean GFAP fluorescence intensity per GFAP+ fibril was measured, which was also expected to increase in groups that induced an immune response upon IVT. In mice that were injected with AAV2 (Y444F), no change in fibril GFAP fluorescence intensity was seen compared to mice receiving wild-type AAV2 IVTs (80.30 $\pm$20.91 vs. 79.23 $\pm$21.12 RFUs SEM, p = 0.99). When AAV2 (TM) was injected, however, a statistically significant increase in GFAP fibril immunofluorescence was observed vs. mice injected with wild-type AAV2 (219.0 $\pm$31.66 vs. 79.23 $\pm$21.12 RFUs SEM, p < 0.05). An even greater increase was seen in mice in the AAV2 (high titre) group vs. wild-type AAV2 group (263.2 $\pm$36.33 vs. 79.23 $\pm$21.12 RFUs SEM, p < 0.01).

In summary, these experiments showed that Muller glia activation was greater in mice who received IVT of AAV2 (TM) than wild-type AAV2.

Figure 4.15: Muller glia activation following IVT of AAV2 (TM)

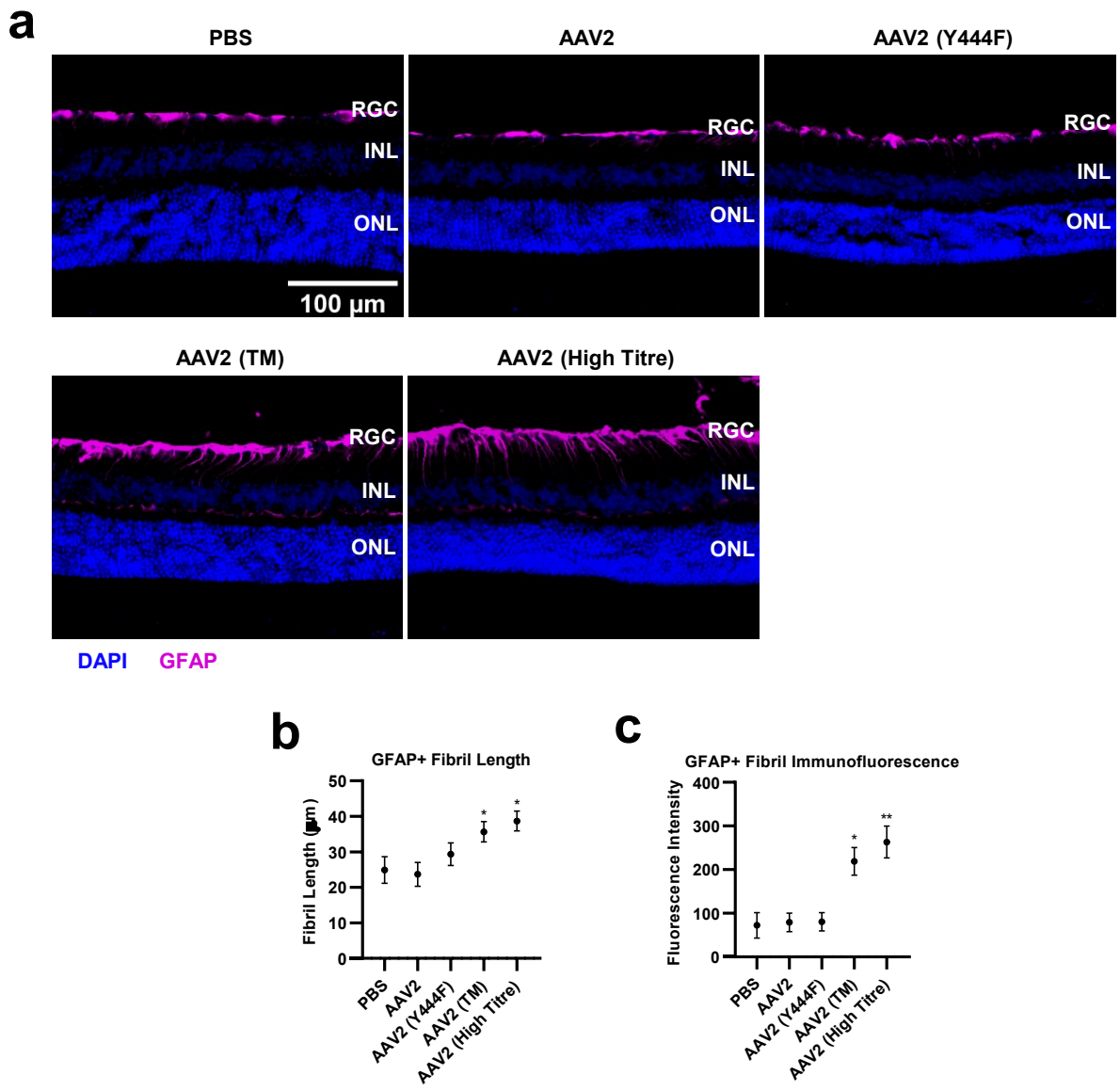

Intravitreal injection of a phosphodegron mutant AAV2 and high titre AAV2 leads to gliosis in the murine retina. Vectors were injected via IVT and retinas were extracted for analysis after three weeks. Data is presented as a column graph, with the mean value for each group shown +/- SEM. Statistical analyses are vs. the AAV2 group. RGC, retinal ganglion cell layer; INL, inner nuclear layer; ONL, outer nuclear layer.

(a) Representative 40x objective epifluorescence microscopy images of retinal cryosections showing GFAP immunoreactivity in groups receiving phosphodegron mutant AAV2 and high titre AAV2 injections.

(b & c) Corresponding quantification was performed using Single Neurite Tracer, an ImageJ plugin (https://imagej.net/SNT). Each GFAP+ fibril was identified in each FOV and the length of each fibril (b) and its fluorescence intensity (c) and was measured. * = $p < 0.05$, ** = $p < 0.01$, one-way ANOVA and Dunnett's posthoc tests, n=4 per group.

4.5.11 Increased astrocyte dendritic arbour complexity induced by AAV2 (TM) vs. wild-type AAV2 IVT

To continue the investigation into the innate immune responses induced by AAV2 (TM), the possibility of astrocyte activation was assessed. Astrocytes are a glial cell type present in the retinal ganglion cell layer in the retina. Reports examining the immune response in the brain and CNS have shown that the complexity of astrocytic dendritic arbours increases in response to a multitude of infections, inflammatory stimuli and neurodegenerative pathologies [208]. However, the role that astrocytes may play in the immune response to AAV2 injections into the eye has not been explored. To examine this, retinal wholemounts were stained with GFAP antibodies to delineate astrocytic dendritic arbours. In contrast to published work, the staining highlighted a highly interconnected network of astrocytic processes, within which it was difficult to distinguish individual astrocytes and the boundaries between their respective dendritic arbours. This precluded the opportunity to analyse the dataset with Strahler, Scholl or Fractal analysis, which are commonly cited methods for analysing the shapes of glial cells. As such, images were skeletonised and certain properties of the skeletons measured, such as the number of junctions (where two points in the skeleton meet) or the number of quadruple points (a convergence of four lines of the skeleton).

First, the number of junctions was analysed. After injection of AAV2 (Y444F), no change in the numbers of junctions was evident compared to mice that were injected with wild-type AAV2 vectors (1,064 $\pm$69.70 vs. 1,062 $\pm$46.44 junctions SEM, $p = 0.99$). In mice that received an injection of AAV2 (TM), however, a statistically significant increase in the number of junctions was seen compared to those in the wild-type AAV2 group (1,380 $\pm$51.94 vs. 1,062 $\pm$46.44 junctions SEM, $p < 0.05$). Similar to the changes observed with the microglia and Muller glia analysis, the greatest increase in dendritic arbour complexity was evident in the AAV2 (high titre) group vs. wild-type AAV2 (1,522 $\pm$146.4 vs. 1,062 $\pm$46.44 junctions SEM, $p < 0.01$).

The number of quadruple points in the skeletonised images was also measured. In the AAV2 (Y444F) group, no change in the number of quadruple points was seen vs. wild-type AAV2 controls (225.9 $\pm$15.02 vs. 226.7 $\pm$8.95 quadruple points SEM, $p = 0.99$). In the AAV2 (TM) group, a clear increase in the number of quadruple points was observed compared to mice that were injected with wild-type AAV2, however, this effect was not quite statistically significant (281.3 $\pm$10.01 vs. 226.7 $\pm$8.95 SEM quadruple points, $p = 0.0583$). The largest comparative increase in the number of quadruple points in the dataset was between mice who received AAV2 (high titre) and wild-type AAV2 IVTs (322.3 $\pm$28.79 vs. 226.7 $\pm$8.95 SEM quadruple points, $p < 0.01$).

In summary, this set of experiments corroborated previous findings pertaining to microglia

and Muller glia activation and showed that the complexity of astrocytic dendritic arbours in the retina may be increased in response to inflammatory stimuli, in this instance, IVT of AAV2 (TM) or AAV2 (high titre).

Figure 4.16: Astrocytic dendritic arbour complexity increased after IVT of AAV2 (TM)

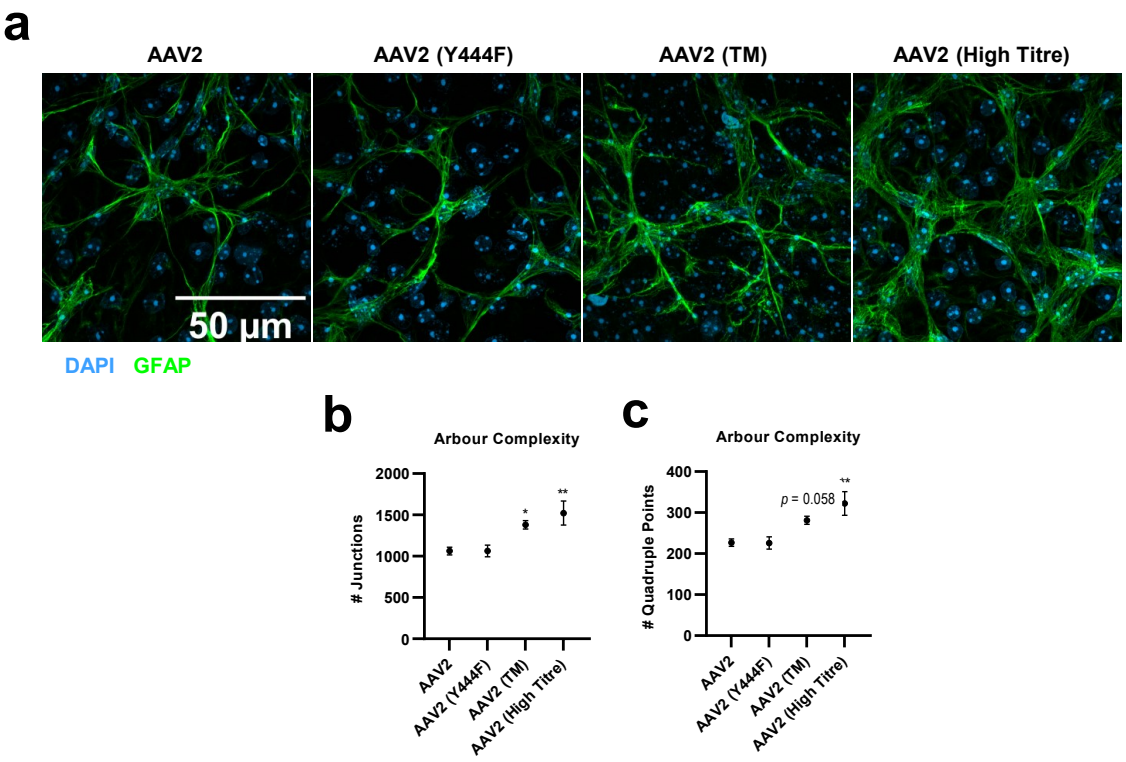

Intravitreal injection of a phosphodegron mutant AAV2 and high titre AAV2 leads to gliosis in the murine retina. Vectors were injected via IVT and retinas were extracted for analysis after three weeks. Data is presented as a column graph, with the mean value for each group shown +/- SEM. Statistical analyses are vs. the AAV2 group. N=8-10 per group.

(a) Representative 63x images acquired on an Leiss Airyscan Confocal microscope showing increased complexity of astrocytic dendritic arbours in AAV2 (TM) and AAV2 (high titre) groups.

(b & c) Data was analysed in ImageJ using by assessing the number of junctions (b) and quadruple points (c) of skeletonised images. * = $p < 0.05$, ** = $p < 0.01$, one-way ANOVA and posthoc Dunnett's tests.

4.5.12 Identification of activated microglia morphologies after injection of AAV2 (TM)

Further to the identification of increased astrocytic dendritic arbour complexity in whole-mounted retina tissue, a set of experiments was undertaken to identify possible changes in microglia morphology upon IVT delivery of wild-type and phosphodegron mutant AAV2 capsids. IBA1 antibodies were used to delineate the morphology of microglia cells in the retinal ganglion cell layer. After an injection of wild-type AAV2, no discernible IBA1 signal could be seen. After IVT of AAV2 (Y444F), some IBA1 immunoreactivity was evident, which highlighted a small number of microglia cells exhibiting a 'ramified' morphology. When AAV2 (TM) was injected however, the appearance of the 'bushy' microglia in the retinal ganglion cell layer was evident, a finding that supported the statistically significant elevation of IBA1 immunoreactivity previously identified (see above). In contrast to previous reports [209], however, the lack of IBA1 immunoreactivity in the wild-type AAV2 group precluded the opportunity to analyse the disparate microglia morphologies in more detail. Here, analytical tools such as Strahler, Scholl, and Fractal analysis were considered, which would have enabled a more in depth and quantitative evaluation of changes in microglia morphology that arise after IVT of AAV2 wild-type and mutant vectors. Different microglia/macrophage stains, such as CD11b, were also considered as possible a means to delineate 'ramified' microglia cells. However, the quality of the signal with this stain, whilst acceptable in a retinal cryosection with citrate buffer-mediated antigen retrieval, was very poor in wholemounted retinal tissue.

Figure 4.17: Activated microglia morphologies identified in AAV2 (TM) injected retinal wholemounts

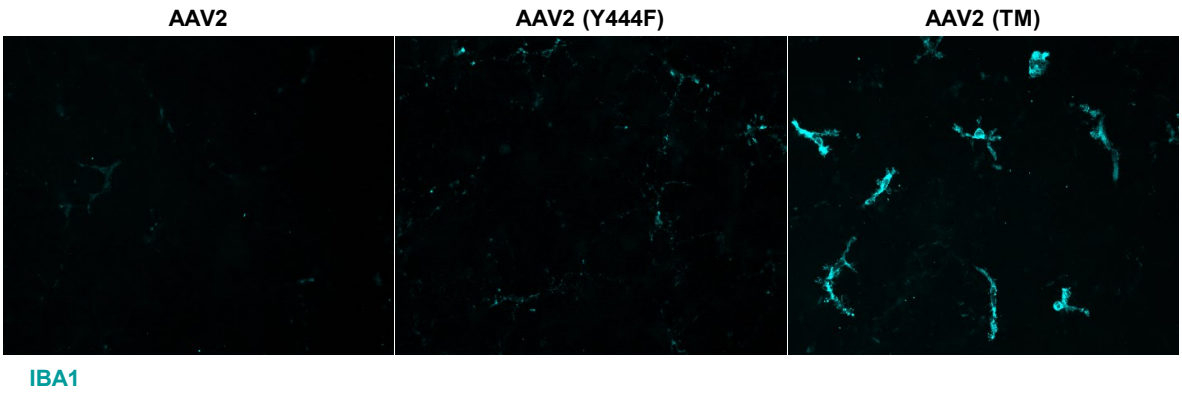

Changes in microglia IBA1 staining identified in murine retinal wholemounts. Vectors were injected via IVT and tissue was taken for analysis after three weeks. IBA1 antibodies were used to delineate the morphologies of microglia cells. Representative 40x objective epifluorescence microscopy images are shown from each group.

4.5.13 IBA1+ MHC c. II+ co-immunolabelled cells identified in the vitreous after IVT of AAV2 (TM) and AAV2 (high titre)

When assessing retinal cryosections in this study, a cluster of DAPI+ cells towards the periphery of the retina, close to the ciliary body, could be observed. Previous analysis had shown that these cells were not CD4 or CD8 T-cells. Considering recent reports in the literature [210] in which IVT of AAV2 in mice was correlated with the infiltration of macrophages into the ocular compartment, a co-immunolabelling experiment was performed to identify the possible cellular identity of the cluster of cells observed in the peripheral retina. IBA1 is a marker of activated microglia cells, but is also expressed by macrophages in the eye [211]. MHC c. II is a marker of activated antigen presenting cells (as discussed above) and also exhibits upregulated expression in activated macrophages. As such, IBA1/MHC c. II co-immunolabelling was used to identify the cluster of cells seen at the peripheral retina as activated macrophages. Injections of wild-type AAV2 and AAV2 (Y444F) was not associated with the presence of IBA1+ MHC c. II+ cells at the peripheral retina. In mice that received an injection of AAV2 (TM), however, a population of the co-immunolabelled cells was evident. This IBA1+ MHC c. II+ population was also observed in mice that were injected with AAV2 (high titre). Most of the co-immunolabelled cellular population were located in the vitreous, however, consistent with reports in the literature [212], some IBA1+ MHC c. II+ cells could be seen in the ciliary body, which may have been ciliary macrophages.

Figure 4.18: IBA1+ MHC c. II+ co-immunolabelled cells identified in the vitreous after IVT of AAV2 (TM) and AAV2 (high titre)

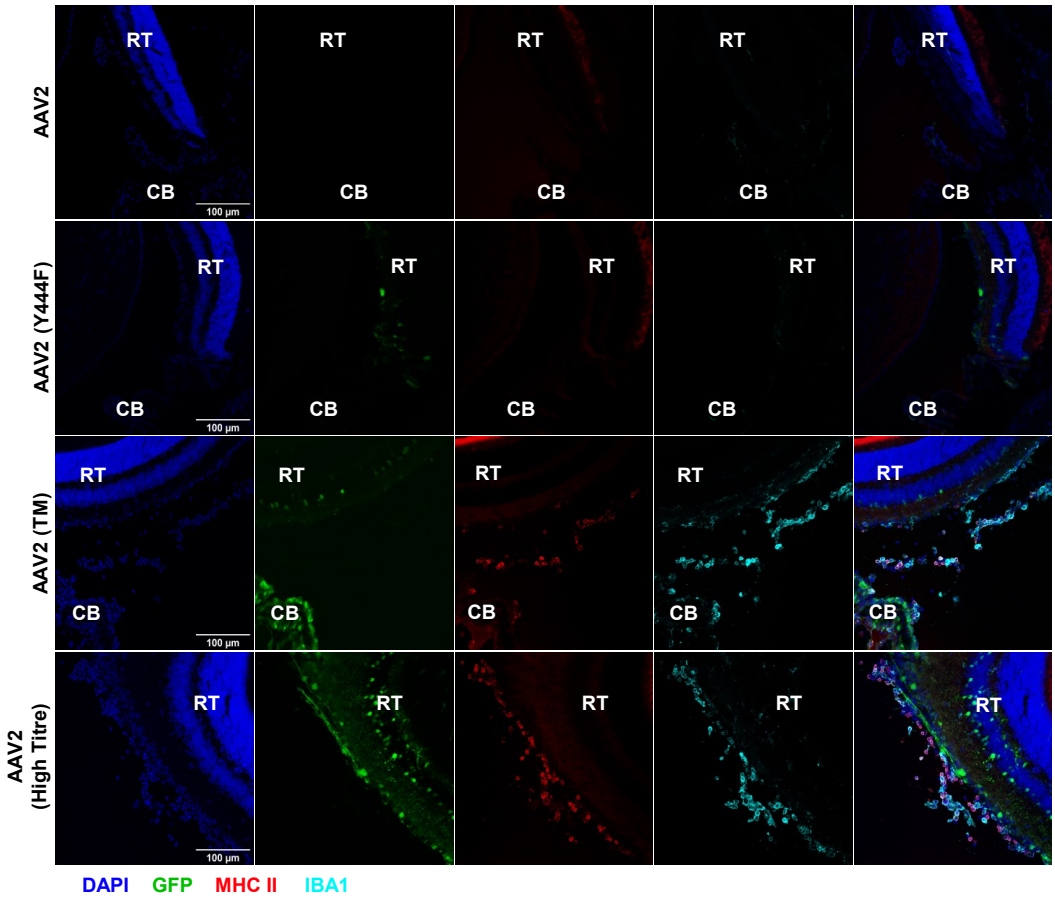

MHC c. II/IBA1 co-immunolabelling at the peripheral retina identifies possible activated macrophages in the eye after IVT of a triple phosphodegron mutant AAV2 and a high titre dose of AAV2. Vectors were injected and tissue was harvested after three weeks for analysis. Representative 20x confocal images are shown at the periphery of the retina (RT), close to the ciliary body (CB). Accumulation of MHC c. II+/IBA1+ co-immunolabelled cells can be seen in these regions, which may be activated (MHC c. II+) macrophage (IBA1+) cells.

4.5.14 Incorporation of phosphodegron mutations into AAV2 capsids induces a modest rescue from neutralisation by anti-AAV2 NAbs and heparan sulphate

The experiments describe above demonstrated that the incorporation of phosphodegron mutations into AAV2 capsids led to elevated humoral and cellular adaptive immune responses, in addition to an increase in the innate immune response. In the next set of experiments, the effect of mutating these residues was further explored. Here, recent reports were considered in which the introduction of combinations of phosphodegron mutations in AAV2 capsids was correlated with a slight attenuation of binding affinity to AAV2's primary attachment receptor, heparan sulphate (HS) [213]. First, the proximity of the three mutations selected for analysis was compared to canonical HS binding residues (R484, R487, K532, R585, R588) [214]. This qualitative assessment was performed in PyMol using 6ih9, a cryoelectron microscopy-derived structure of AAV2's VP3 monomer. In accordance with reports from Boye et. al., it was observed that the three mutations (Y444F, K556E, S662V) lay distal to the HS receptor attachment site. The AAV receptor (AAV-R) binding residues were also highlighted in this analysis for reference, although no further investigation into the possible effects of mutating phosphodegron residues and binding affinity to AAV-R was undertaken in this thesis.

Figure 4.19: Proximity of phosphodegron mutations to canonical HS binding residues

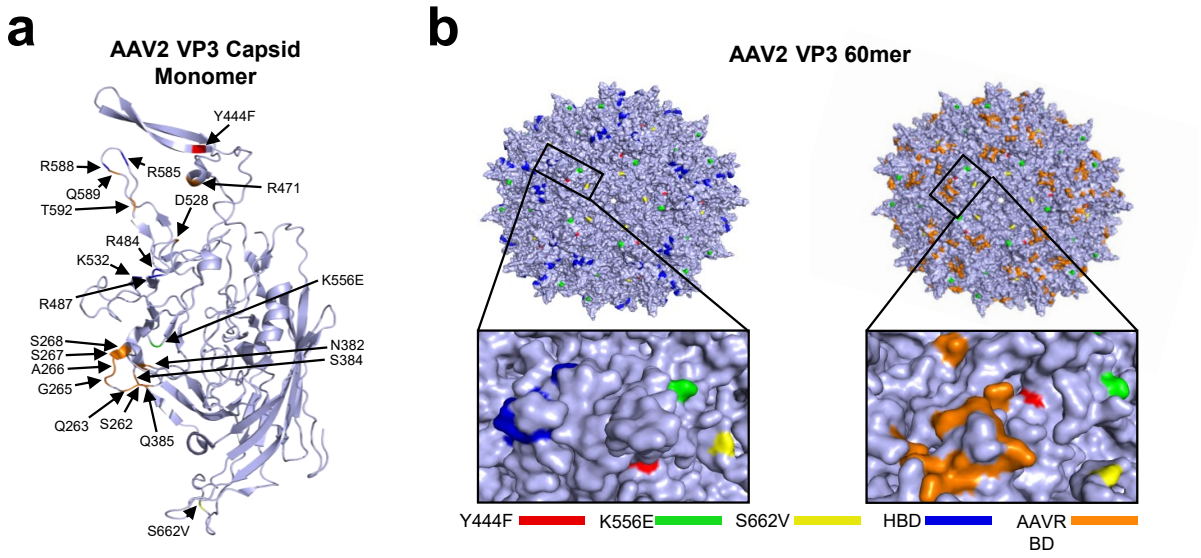

(a) VP3 capsid monomer showing the positioning of the three phosphodegron mutants, the five residues thought to mediate the binding affinity of AAV2 capsids to heparin (blue) and the 14 residues thought to mediate binding of AAV2 to the AAV receptor (orange) (AAV-R), KIAA0319. This model was generated in PyMol using 6ih9, a 2.8Å resolution cryoelectron microscopy-derived structure of the AAV2 VP3 monomer.

(b) AAV2 full 60mer capsid structure with highlighted phosphodegron mutations and heparin binding domains. Red = Y444F, Green = K556E, Yellow = S662V, Blue = R484, R487, K532, R585, and R588 heparin binding domains (HBDs), Orange = R471, D528, Q589, T592, S262, Q263, G265, A266, S267, N268, H271, N382 and Q385 AAV-R binding domains (AAV-R BDs).

Further to the assessment undertaken in PyMol, a RIVEM chart was produced by Dr. Suzanne Scott (University of Sydney). This stereographic projection of the three phosphodegrons mutations, canonical HS binding and AAV-R binding residues on the AAV2 capsid depicted the phosphodegrons positioned distal to the canonical HS binding site(s). PyMol's mutagenesis wizard was also used to suggest possible conformations of the mutant residues, which was achieved by mutating the appropriate residue *in silico* and selecting the rotamer with the highest confidence score (PyMol's estimation that the rotameric conformation of a particular residue is consistent with the local protein conformation, e.g. no immediately adjacent hydrophobic amino acid backbones). Several *in silico* modelling software packages were also used in an attempt to predict possible conformational changes that may have been induced by the incorporation of the mutations into AAV2 capsids. First, SWISS-MODEL was utilised, but yielded low Q-mean values, indicating a low confidence score for the predicted structures. trRossetta was also tested, which assigned TM-scores ranging from ~0.6 to 0.8, indicating a 'high' or 'very high' confidence score for the wild-type and mutant capsid sequences. However, when the predicted structures were loaded into PyMol and each mutant capsid structure was compared to the wild-type counterpart, gross structural changes were observed that appeared to be unrelated to the mutation being studied. This suggested that trRossetta had not accurately predicted the protein structure despite the assignment of high TM-scores to the respective coordinate files. Further work in this regard may seek to determine the protein structure of each capsid monomer using cryoelectron microscopy. This could be combined with the HS and NAb work discussed below to understand how AAV2 capsid mutation affects interaction with its primary receptor and neutralising factors, using a process similar to that outlined by O'Donnell et. al. [215]. A summary of the trRossetta work is given in Appendix A.1.2. Here, RMSD (root mean squared deviation) is a measurement of the degree of structural misalignment exhibited by two protein structures.

Figure 4.20: Positioning and rotameric conformations of phosphodegron mutations under investigation

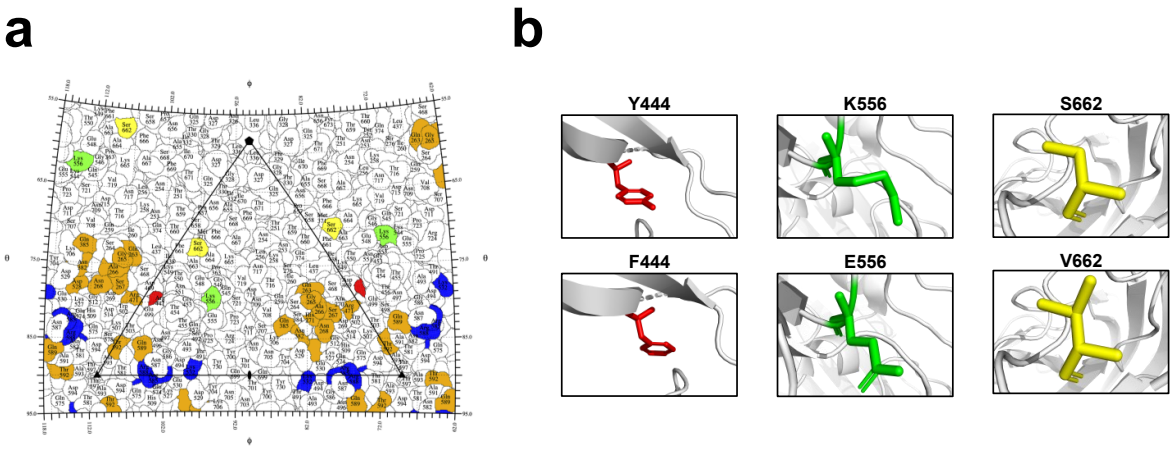

(a) RIVEM plot showing the positioning of the three phosphodegron mutants and their proximity to HBDs and AAV-R BDs (using 6ih9 AAV2 coordinates, see figure above for colouring).
(b) Schematic representation of mutations represented in PyMol. Mutations were introduced using PyMol's Mutagenesis Wizard, and the optimal rotamer confirmation was selected in accordance with the software's prediction.

Having shown the proximity of the three mutations to the heparan binding domains of AAV2, a set of experiments was undertaken to understand how, in accordance with the work of Boye et. al., incorporation of multiple phosphodegron mutations into the capsid may affect neutralisation of the vectors by HS and anti-AAV2 NAb serum. To assess this, vectors were incubated with HS or serum for 1h, then added to HEK-293T cell cultures, and transduction efficiency was assessed after 24h with flow cytometry. In this set of experiments, a higher remaining infectivity is indicative of reduced neutralisation by either HS or anti-AAV2 NAb containing serum.

In the AAV2 (Y444F) group, a statistically significant increase in remaining infectivity was observed compared to the wild-type AAV2 group in the presence of HS (0.227 $\pm$0.01 vs. 0.151 $\pm$0.01 RUs SEM, $p < 0.05$). When the AAV2 (K556E) vector was incubated with HS, a small but statistically non-significant increase in remaining infectivity was seen compared to the wild-type AAV2 group (0.194 $\pm$0.02 vs. 0.151 $\pm$0.01 RUs SEM, $p = 0.18$). The AAV2 (S662V) vector demonstrated a two-fold increase in remaining infectivity in the presence of HS compared to wild-type AAV2 vectors (0.295 $\pm$0.01 vs. 0.151 $\pm$0.01 RUs SEM, $p < 0.0001$). The greatest increase in remaining infectivity, i.e. the highest level of escape from neutralisation by HS, was seen in the AAV2 (TM) group, in which a three-fold increase was observed when compared to the wild-type AAV2 vector group (0.484 $\pm$0.03 vs. 0.151 $\pm$0.01 RUs SEM, $p < 0.0001$). These experiments therefore corroborated those of Boye et. al. [213] and showed that the introduction of phosphodegron mutations into AAV2 capsids elicits a slight escape from neutralisation by HS, suggesting that attachment to the primary receptor *in vivo*, heparan sulphate proteoglycan (HSPG), may be attenuated upon injection into the vitreous, possibly via inducing conformational changes in the heparan binding footprint.

In the next set of experiments, the concept that mutation of phosphodegron residues may lead to conformational changes in AAV2 structure was further explored. The data suggesting a possible conformational change in capsid structure was used to hypothesise that incorporation of the phosphodegrons may elicit changes in neutralising antibody epitopes recognised by anti-AAV2 NAb containing serum. As such, it was predicted that remaining infectivity of the mutant capsids would follow similar patterns to that seen in the HS experiments. When AAV2 (Y444F) vectors were incubated with anti-AAV2 NAb containing serum, a statistically significant increase in remaining infectivity was seen compared to the wild-type AAV2 group (0.200 $\pm$0.01 vs. 0.093 $\pm$0.01 RUs SEM, $p < 0.01$). Similarly, the AAV2 (K556E) group demonstrated a 2.5-fold increase in remaining infectivity vs. wild-type AAV2 capsids (0.159 $\pm$0.03 vs. 0.093 $\pm$0.01 RUs SEM, $p < 0.05$). When AAV2 (S662V) vectors were incubated in the serum, a 3-fold increase in remaining infectivity was seen vs. the wild-type vector group (0.325 $\pm$0.02 vs. 0.093 $\pm$0.01 RUs SEM, $p < 0.001$). Finally, the greatest increase

in remaining infectivity in the presence of anti-AAV2 NAb-containing serum was observed when comparing the AAV2 (TM) and wild-type AAV2 groups, where a statistically significant seven-fold increase was seen (0.730 $\pm$0.01 vs. 0.093 $\pm$0.01 RUs SEM, $p < 0.0001$).

In summary, this set of experiments corroborated reports in the literature that mutation of phosphodegron residues in AAV2 capsids can lead to a slight attenuation of binding affinity to HS. It also demonstrated that the possible conformational changes induced by the mutations may elicit a slight escape from neutralisation by anti-AAV2 NAbs.

Figure 4.21: Escape from neutralisation by HS and anti-AAV2 NAbs by phosphodegron mutant vectors

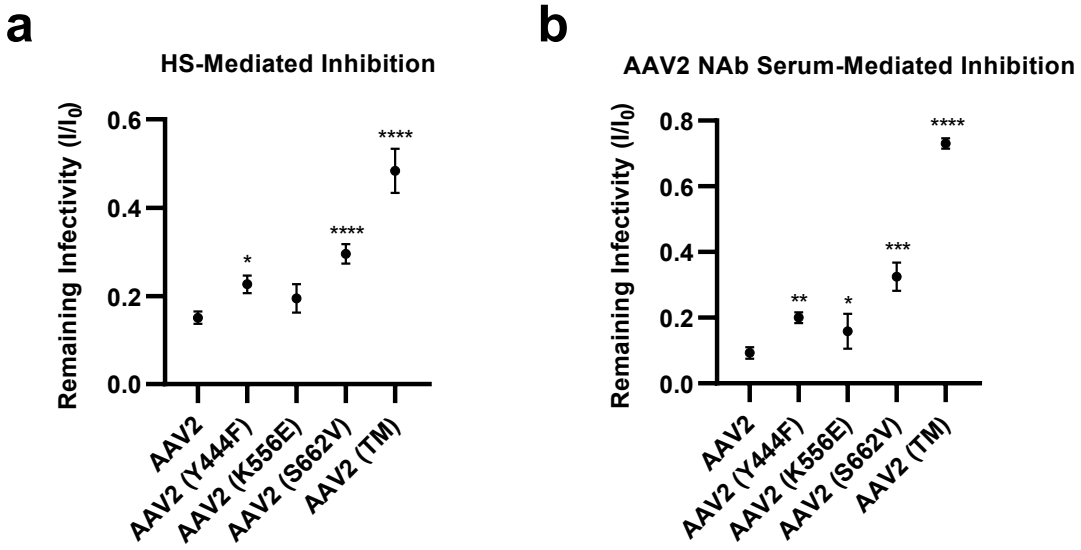

Mutation of AAV2 capsids at selected phosphodegron regions attenuates neutralisation by HS, and anti-AAV2 NAb-containing serum. Data is presented as column graphs, with the mean value for each group shown +/- SEM. All statistical analyses are vs. the AAV2 group. N=4 per group.

(a) Mutation of phosphodegron residues attenuates neutralisation by HS. AAV2 and mutant capsids were incubated with HS for 1h, prior to addition to HEK293T cell media. Number of GFP+ cells was normalised to –HS controls for each vector group, allowing calculation of remaining infectivity (I/I_0). * = $p < 0.05$, **** = $p < 0.0001$, one-way ANOVA and a Dunnett's posthoc tests

(b) Mutation of phosphodegron residues partially rescues neutralisation by AAV2 NAbs. AAV2 and mutant capsids were incubated with serum extracted from animals that had previously been injected intravitreally with AAV2 (High Titre), and the samples were tested to confirm the presence of NAbs. Calculation of remaining infectivity (I/I_0) was performed as in (a). * = $p < 0.05$, ** = $p < 0.01$, *** = $p < 0.001$, **** = $p < 0.0001$, one-way ANOVA and a Dunnett's posthoc tests.

4.5.15 Electrophysiological activity following intravitreal injection of phosphodegron mutant AAV2 capsids

Having investigated the immune response that arises from IVT of the wild-type and mutant AAV2 vectors, electroretinography (ERG) was performed. Briefly, ERG assesses the electrophysiological activity of the retina. pSTR (retinal ganglion cell), B-wave (rod bipolar cell) and A-wave (rod photoreceptor) recordings are taken, and represent the induction of action potentials in these neuronal cell populations in response to stimulation with light (expressed as a log light intensity value, units of cd.s/m^2). In a degenerate or inflamed retina, ERG recordings are affected, and thus serve as a useful protocol for assessing functional changes in the retina with gene therapies. Note that in this set of experiments, an AAV2.CAG.Null (high titre) group was included to determine whether any changes in ERG recordings were due to the overexpression of fluorescent reporters. A 250ng lipopolysaccharide (LPS) group (injected 24h before ERG) was also included to serve as a positive control for inducing an immunological reaction in the retina.

First, representative waveforms from each group were produced, and showed no evidence of electrophysiological changes between any of the vector groups in terms of pSTR (-4.37 cd.s/m^2), B-wave (-1.90 cd.s/m^2) or A-wave recordings (1.29 cd.s/m^2) (see Appendix). Next, the ERG recordings from all seven pSTRs, four B-waves and four A-waves were plotted as column graphs. Whilst some noise (slight variation in signal between groups) could be seen, a two-way ANOVA demonstrated that no statistically significant differences were observed between any of the vector groups at any of the light intensities tested, whilst significant differences vs. the LPS control group were evident.

This assessment showed that, whilst an immune response in the retina was induced by the triple phosphodegron mutant and high titre AAV2 groups, these reactions were not associated with a functional deficit in the neural retina.

Figure 4.22: ERG recordings after IVT of wild-type and mutant vector groups

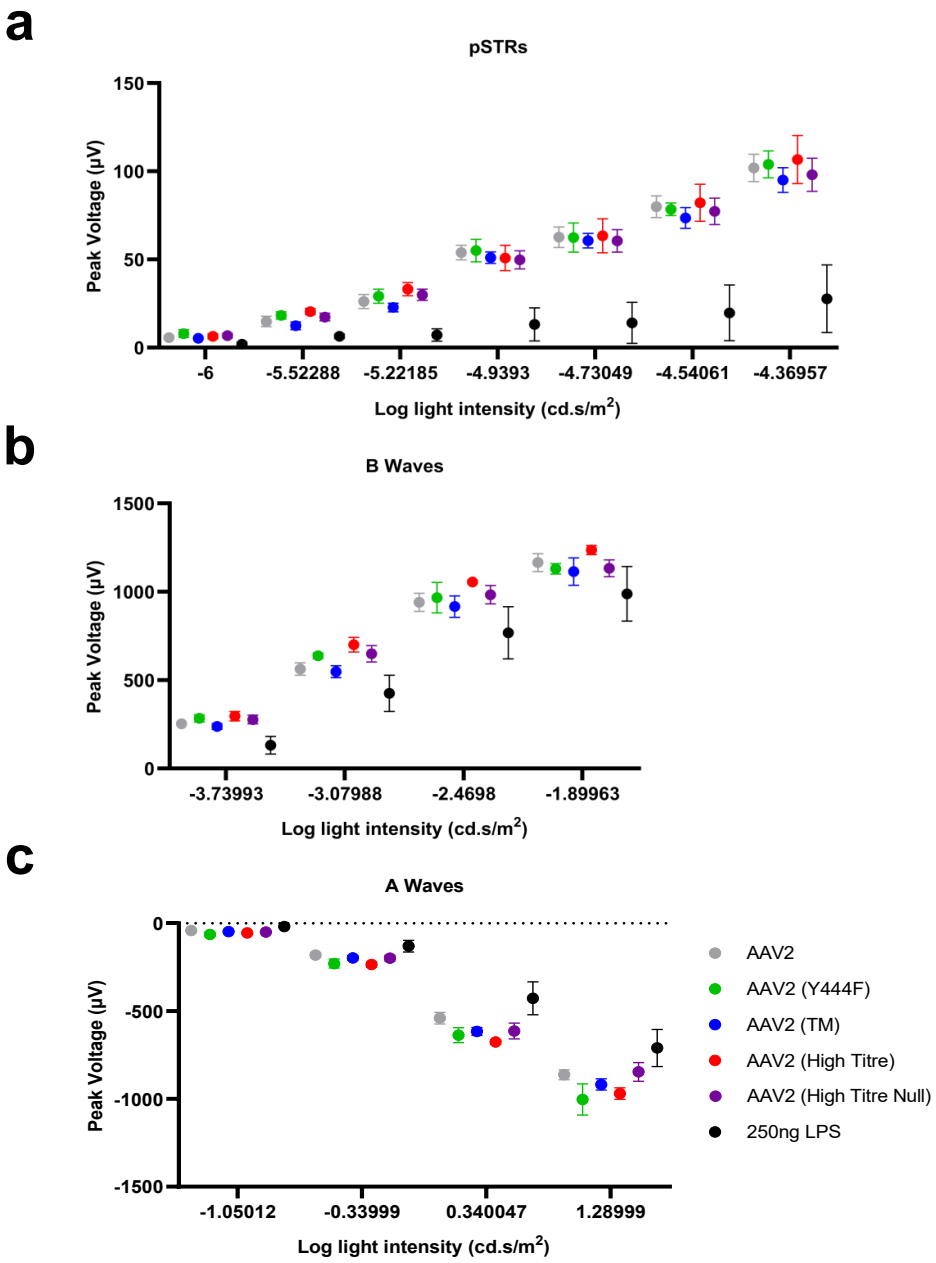

Injection of phosphodegron mutant vectors is not associated with changes in electrophysiological function in the murine retina. Vectors were injected via IVT and ERG was performed after three weeks. 250ng of lipopolysaccharide (LPS) 24h prior to ERG. Column charts showing peak voltages across a range of light intensities for each treatment group. Data is presented as the mean value +/- SEM. N=6-12 per group.

4.5.16 Tuj1+ retinal ganglion cells in wild-type and mutant vector injected groups

The tissue from the ERG experiment was taken and stained for Tuj1, a retinal ganglion cell marker, to support the ERG analysis. In all of the vector injected groups, no changes in the number of Tuj1+ cells were apparent. In the LPS injected group, however, some loss of Tuj1+ cells could be seen. The data in this experiment therefore supported the ERG data and suggested that, whilst an immune response was observed in the vector-treated retinas, this is not apparently associated with functional or anatomical/histological damage. Note that only representative Tuj1 images were included in this assessment given the difficulties in automating Tuj1+ cell counting. If differences had been evident between vector injected groups, then manual counting would have been used.

Figure 4.23: Tuj1+ retinal ganglion cells in vector and LPS-treated retinal wholemounts

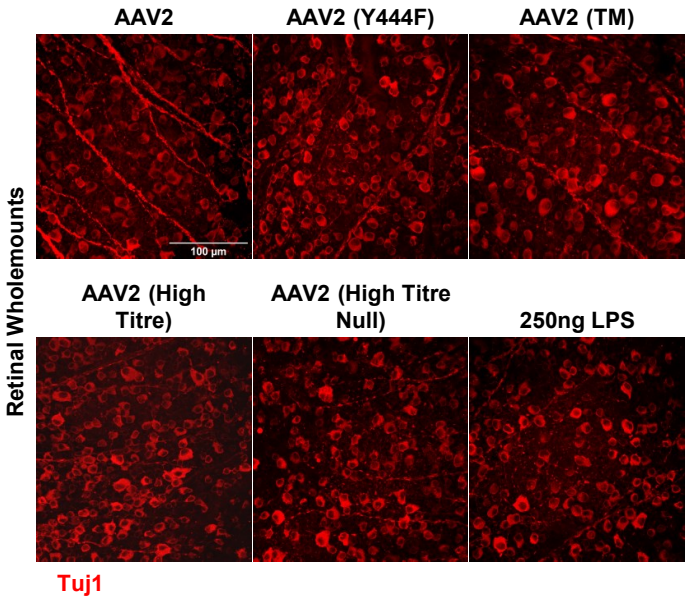

Injection of phosphodegron mutant vectors is not associated with changes in Tuj1+ retinal ganglion cell levels in the murine retina. Vectors were injected via IVT and ERG was performed after three weeks. 250ng of lipopolysaccharide (LPS) 24h prior to ERG.

4.6 Summary of Results

In this chapter, the immune response to a triple phosphodegron mutant AAV2 capsid, AAV2 (TM), was assessed. Having shown that AAV2 (TM) increases transduction efficiency compared to wild-type AAV2 capsids, activation of the humoral and cellular arms of the adaptive immune system was analysed. Increased levels of NAbs and TAbs were seen after IVT of AAV2 (TM) vs. wild-type AAV2, and elevated infiltration of CD4 and CD8 T-cells into the retina was also observed. The possibility of increased innate immune activation was then tested. Increased levels of microglia and Muller glia activation was seen in mice injected with AAV2 (TM) compared to those who received wild-type AAV2. A slight increase in the complexity of astrocyte dendritic arbours was also evident when comparing these two groups, and possible changes in the morphology of microglia cells was also seen in wholemounted retina tissue. In accordance with previous reports, the location of the three mutations was assessed and proved distal to the canonical heparan binding domains of AAV2 capsids. Nonetheless, a slight attenuation in binding affinity to HS was demonstrated, and this finding also correlated with a slight escape in neutralisation by anti-AAV2 NAbs. Lastly, no electrophysiological or anatomical changes were observed between the different vector groups. In summary, these results showed that mutation of phosphodegron residues in AAV2 capsids may be associated with increased immune activation after IVT. The study highlights novel aspects of phosphodegron mutant AAV2 immunobiology but suggests this strategy may not be appropriate for circumventing NAb responses to AAV gene therapies and enabling repeated gene transfer to the inner retina.

Chapter 5

Perioperative prednisolone administration attenuates immune activation following intravitreal injection of AAV2, but fails to enable repeated gene transfer to the inner retina

5.1 Declaration

The material in this chapter has not yet been published, however, we are preparing a manuscript for submission. This work was funded by a Pump Priming Grant from Novo Nordisk Research Foundation UK (G103197; £9,000) Addenbrookes Charitable Trust Small Grant Award (G109216; £8,200), both of which were written by the author of this thesis with feedback from Dr. Patrick Yu Wai Man and Professor Keith Martin.

The scientific hypotheses tested in this chapter were those of the author of this thesis with input from Dr. Patrick Yu Wai Man and Professor Keith Martin. All of the data presented was the work of the author, with the exception of the flow cytometry (performed by Dr. Andrew Sage, see Chapter 2).

5.2 Chapter synopsis

The objective of this chapter was to further the previous investigations into the nature of the immune response to intravitreally-delivered AAV2 vectors in murine mouse models. In this study, perioperative prednisolone was tested as a possible agent to circumvent the immune response to repeated bilateral injections of AAV2 IVTs, with the aim of enabling repeated gene transfer to the inner retina. The immunosuppressant was found to reduce NAb and TAb levels at two of the sampled timepoints. Mechanistically, it was demonstrated that this may have been via the inhibition of splenic germinal centre reactions and follicular B-cell class-switching. Significant reductions in CD4 and CD8 T-cell infiltration into the retina was also found to occur in prednisolone- vs. PBS-treated mice, however, no significant changes in microglia activation was observed. Despite lowering NAb and TAb levels, prednisolone-mediated immunosuppression was not sufficient to lift the blocking effect induced by post-IVT NAb synthesis and enable repeated gene transfer to the inner retina. Further, the data revealed that repeated bilateral IVTs of AAV2 may be associated with reduced electrophysiological activity in the retina, suggesting functional damage may be induced by multiple AAV2 injections. In summary, the data presented in this chapter suggested that perioperative prednisolone administration is a promising strategy for circumventing anti-AAV2 immune activation, but further immunosuppression may be required to enable repeated gene transfer to the inner retina.

5.3 Introduction

The injection of AAV gene therapy vectors to immune competent sites, such as intramuscular and intravenous administration, is associated with the induction of NAb synthesis that may limit the opportunity to perform a repeated injection [216]. The literature detailing NAb synthesis that may arise after an intraocular injection is more nuanced, however. After subretinal (SRT) injections of AAV2, a minority of patients exhibit increased NAb titres (possibly due to leakage of some of the vector from the subretinal 'bleb' created during surgery), and three patients have been successfully redosed into the contralateral eye [125]. After an intravitreal injection however, a greater proportion of patients may develop NAbs than those enrolled in SRT trials. Crucially, whilst some of the patients that received IVTs of AAV2 vectors were treated with prednisolone, a proportion of these still developed NAbs against AAV2, suggesting that steroid monotherapy may be ineffective at enabling repeated gene transfer in all patients [216]. However, there is currently little literature to support the use of prednisolone in attenuating anti-AAV2 NAb titres after IVT, either in terms of the possible cellular and molecular mechanisms underpinning its therapeutic efficacy, or in terms of its capacity to circumvent the NAb response and enable a repeated AAV2 IVT. Further, there is little evidence to suggest how repeated bilateral injections of AAV2 via the intravitreal route may be associated with deleterious functional consequences, such as electrophysiological changes or degeneration of synapses, and whether this may be rescued by prednisolone.

Briefly, prednisolone is an FDA-approved glucocortiosteroid (GC) immunosuppressant. The lipophillic molecule is capable of crossing the cell membrane and binding to glucocorticoid receptors (GRs) in the cytoplasm, which causes it to dissociate from a complex of chaperone proteins. This allows the GC/GR complex to enter the nucleus where it associates with DNA or co-activator complexes. As a result, the GC/GR complex can activate expression of anti-inflammatory genes or decrease expression of pro-inflammatory genes via transactivation and transrepression respectively. The GC/GR complex has also been reported to interact with NFκB, reducing its activity as a means of exerting its anti-inflammatory mechanism-of-action [217]. Given that the GR is expressed in almost every cell in the body [218], prednisolone has a very broad-acting effect when dampening the immune response. For instance, it can inhibit the proliferation and activation of T-cells by downregulating the activity of interleukin-2 (IL-2) [219], a finding that may support its apparent effectiveness at limiting the cytotoxic CD8 T-cell response in haemophilia B trials and enabling long-term expression of factor IX [220]. Further, it has been posited to have a downregulatory effect on B-cell function, highlighting possible application in terms of circumventing NAb responses to AAV2 [221].

The objective of this chapter was to determine whether perioperative prednisolone administration could be used to circumvent the anti-AAV2 NAb response after IVT and study the

possible cellular and molecular mechanisms by which the glucocorticoid drug functions.

5.4 Overview of study plan

In this study, the effect of perioperative (before, during and after surgery) prednisolone administration on attenuating multiple arms of the immune response to AAV2 was assessed. Mice were divided into four groups. In Group A, PBS vehicle was injected as a control, whilst in Group B, 0.75mg/kg/day prednisolone was injected intraperitoneally. In groups A & B, mice received bilateral IVTs of 1E10 GC/eye AAV2.CAG.GFP on day 0 and a second set of bilateral IVTs of 1E10 GC/eye AAV2.CMV.mCherry at day 21. Group C and Group D were control groups, and both were injected with PBS vehicle instead of prednisolone. Group C received two IVTs of PBS on day 0 and 21, and Group D received a PBS injection on day 0 and an IVT of 1E10 GC/eye AAV2.CMV.mCherry at day 21. Blood samples were collected on days 21 and 42, and centrifuged to collect serum for NAb and TAb assays. ERG was performed on day 42 to assess possible functional damage that may have been induced by the repeated bilateral injections. Mice were sacrificed immediately post-ERG and spleens and eyes were extracted for analysis of lymphocyte populations by flow cytometry, and multiple immune markers by immunohistochemistry respectively.

Figure 5.1: Overview of study plan

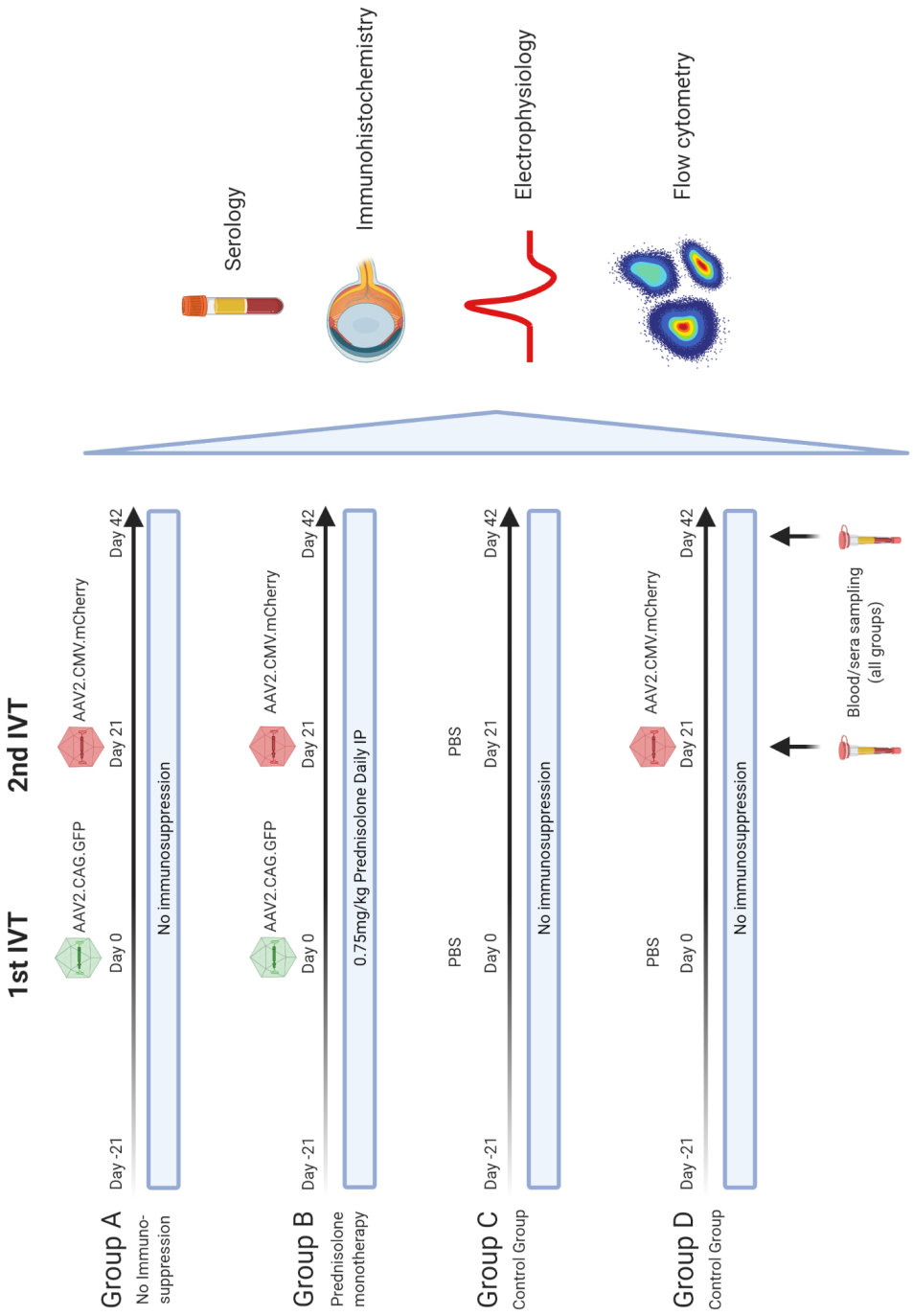

Overview of experimental design. Wild-type C75BL6/J mice were divided into four groups. Groups A and B received a 1E10 GC/eye AAV2.CAG.GFP IVT on day 0, and a 1E10 GC/eye IVT of AAV2.CMV.mCherry on day 21. Group B received a daily IP injection of 0.75mg/kg prednisolone throughout the study pe-

riod, starting 21 days before the first set of IVTs. Group C received PBS IVTs at days 0 and 21. Group D received a PBS injection at day 0 and a 1E10 GC/eye IVT at day 21. Neither group C or D received any immunosuppression. Blood samples were collected at day 21 via a saphenous vein bleed, and by cardiac puncture at day 42 for serological tests. Electroretinography was performed on day 42. Mice were sacrificed immediately and spleen and eye tissue was extracted for analysis by flow cytometry and immunohistochemistry respectively.

5.5 Results

5.5.1 Prednisolone attenuates NAb and TAb titres in mice challenged with a single set of bilateral AAV2 IVTs (day 21 data)

The study began with an assessment of whether prednisolone administration increased or decreased the levels of NAbs and TAbs after repeated bilateral IVTs of AAV2. The first set of blood samples were taken at day 21 and centrifuged to acquire serum for analysis. In Group C, there was no evidence of a reduction in remaining infectivity at any of the serum dilutions tested, confirming that these samples did not contain any detectable NAbs. In Group A, however, reductions in remaining infectivity were evident at serum dilutions of around 1:10,000, and in Group B, evidence of neutralising activity was observed at higher dilutions, suggesting mice who received prednisolone developed lower NAb responses.

This dataset was converted into IC50 values as described in Chapter 2, which showed that prednisolone had a statistically significant effect in terms of attenuating NAb titres. Here, mice in Group A had a 3.8-fold higher NAb titre than those in Group B (5,712 $\pm$1,245 vs. 1,520 $\pm$390 AUs SEM, $p < 0.01$). The data was also used to compute area-under-the-curve (AUC; where a lower value denotes higher neutralising activity) values, thus enabling a quantitative comparison between samples with no detectable NAbs and those with high levels of NAbs. When comparing mice in Group A and B, a statistically significant increase in AUC was seen, demonstrating that prednisolone-treated Group B samples contained fewer NAbs (28,893 $\pm$3,078 vs. 37,605 $\pm$2,129 AUs SEM, $p < 0.05$). Further, a comparison between Group B (prednisolone treated) and Group C (PBS IVTs) showed that there was not a statistically significant difference between these two groups (37,605 $\pm$2,129 vs. 40,674 $\pm$1,262 AUs SEM, $p = 0.77$). In summary, this analysis showed that prednisolone was effective at reducing the levels of NAbs in mice receiving IVTs of AAV2, however, there were still higher levels of neutralising activity observed in these samples compared to mice in the PBS IVTs control group (Group C).

These samples were further analysed with TAb assays. In accordance with the results of the previous chapter, changes in IgG, IgG2b and IgG2c levels were seen after IVT of AAV2, however, no changes in IgG1 and IgM isotypes were evident. In the IgG analysis, a statistically significant decrease in 650nm absorbance was observed between mice who received no immunosuppression (Group A) and those in the prednisolone group (Group B) (0.543 $\pm$0.12 vs. 0.114 $\pm$0.04 AUs SEM, $p < 0.0001$). Prednisolone was not completely effective at attenuating IgG levels however, and increased absorbance in Group B compared to Group C was evident, although the difference was not statistically significant (0.114 $\pm$0.04 vs. 0.0170 $\pm$0.004 AUs SEM, $p = 0.19$). Similar trends were evident when assessing IgG2b levels. A

four-fold, statistically significant decrease in 650nm absorbance between Group A and Group B was observed, providing evidence that prednisolone was effective at decreasing synthesis of this immunoglobulin isotype (0.371 $\pm$0.074 vs. 0.080 $\pm$0.037 AUs SEM, $p < 0.01$). There was, however, evidence of some residual IgG2b in prednisolone-treated mice in that the mean absorbance in Group B was higher than Group C, although the difference was not statistically significant (0.080 $\pm$0.037 vs. 0.007 $\pm$0.002 AUs SEM, $p = 0.31$). These trends were recapitulated in the assessment of IgG2c levels between groups. There was a four-fold, statistically significant decrease in IgG2c levels when mice in Group A and Group B were compared (0.213 $\pm$0.040 vs. 0.056 $\pm$0.014 AUs SEM, $p < 0.05$). However, some IgG2c remained in the prednisolone-treated mice and the levels of this antibody subclass remained higher than that seen in Group C, although this difference was not quite statistically significant (0.056 $\pm$0.014 vs. 0.006 $\pm$0.002 AUs SEM, $p = 0.089$).

In summary, these TAb experiments corroborated the findings of the NAb assays at the day 21 timepoint. These data showed that prednisolone was effective at attenuating the synthesis of anti-AAV2 antibodies after a single set of bilateral IVTs. However, the efficacy of the glucocorticoid was limited to a partial effect, and some anti-AAV2 NAbs and TAbs were seen in Group B compared to mice in Group C who received PBS IVTs.

Figure 5.2: Prednisolone reduces NAb and TAb levels in AAV2-treated mice (day 21 data)

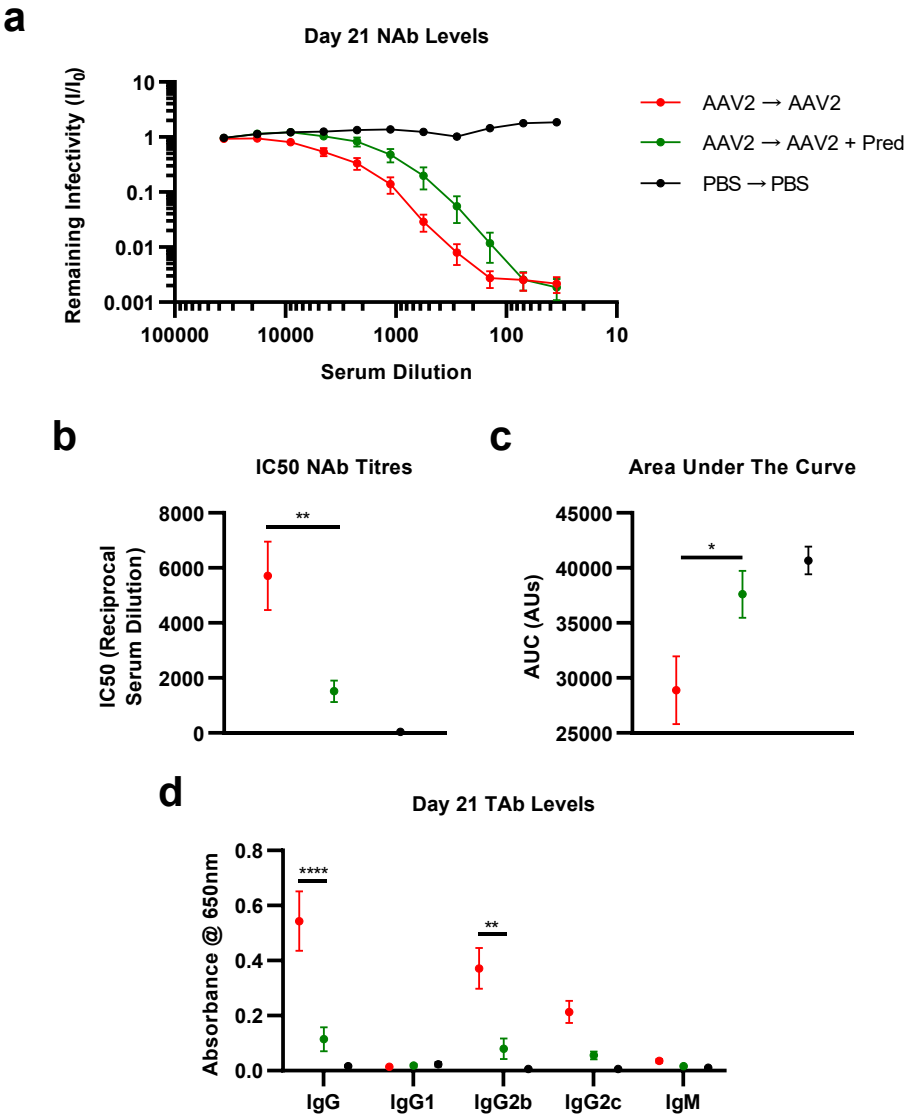

Perioperative prednisolone administration reduces neutralising and total antigen binding antibody levels in mice receiving a single set of bilateral IVTs of AAV2. All data is presented as column graphs showing the mean value for each group +/- SEM. All statistical analyses are between AAV2 → AAV2 and AAV2 → AAV2 + Pred groups. N=4-8 per group.

(a) Day 21 NAb levels.

(b) IC50 values for day 21 NAb levels. ** = $p < 0.01$, Kruskal-Wallis Wallis and Dunn's posthoc test.

(c) AUC values for day 21 NAb levels. * = $p < 0.05$, Welch's t-test.

(d) Day 21 TAb levels. ** = $p < 0.01$, **** = $p < 0.0001$, two-way ANOVA and Tukey's posthoc testing.

5.5.2 Prednisolone attenuates NAb and TAb titres in mice challenged with repeated bilateral AAV2 IVTs (day 42 data)

To continue this investigation, serum samples were collected at day 42, after the repeated bilateral injections of AAV2 or control agents. First, the levels of NAbs were assessed. Similar to the trends observed in the previous figure, no neutralising activity was seen in Group C mice who received PBS IVTs. In Group A, the highest levels of neutralising activity was observed, where reductions in remaining infectivity were seen at the lowest serum dilutions. In Group B, lower levels of neutralising activity were seen compared to Group A, where reductions in remaining infectivity were only seen at higher serum dilutions. There was little difference between Groups B and D, in which changes in remaining infectivity were observed at roughly equitable serum dilutions.

As per the previous figure, this data was used to calculate IC50 values for each group. When Group A and Group B were compared, it was found that prednisolone-treated mice exhibited a 2.3-fold decreased IC50 value, an effect that was statistically significant (21,785 $\pm$5,161 vs. 8,295 $\pm$1,661 AUs SEM, $p < 0.05$). Interestingly, the IC50 mean value in Group B and D were not significantly different (8,295 $\pm$1,661 vs. 11,906 $\pm$3,092 AUs SEM, $p = 0.99$), suggesting that administration of prednisolone only reduced the levels of NAbs after the repeated bilateral injections to that arising from a single set of bilateral AAV2 IVTs. Further, there was an increase in the IC50 values when Group D and Group A were compared, however, this was not a statistically significant effect (11,906 $\pm$3,092 vs. 21,785 $\pm$5,161 AUs SEM, $p = 0.18$). The remaining infectivity dataset was also used to compute AUC values as described above, which corroborated the findings of the IC50 analysis. When comparing Group A and Group B, a 33% increase in AUC values was seen, a difference that was statistically significant (74,899 $\pm$6,356 vs. 99,644 $\pm$6,961 AUs SEM $p < 0.05$). Further to the findings of the IC50 analysis, no statistically significant difference between Group B and Group D (PBS $\rightarrow$AAV2) was observed (99,644 $\pm$6,961 vs. 101,090 $\pm$6,593 AUs SEM, $p = 0.99$). In contrast to the IC50 analyses, the AUC data did show a statistically significant decrease when Group D and Group A were compared, indicating higher neutralising activity in mice receiving repeated AAV2 IVTs vs. a single set of AAV2 IVTs (101,090 $\pm$6,593 vs. 74,899 $\pm$6,356 AUs SEM, $p < 0.05$).

In summary, analysis of this dataset corroborated the findings outlined in the previous figure and showed that perioperative administration of prednisolone was effective at reducing the levels of NAbs in mice that received repeated bilateral IVTs of AAV2, however, there was clear evidence of residual neutralising activity in these samples compared to mice that were in the PBS IVT control Group C.

Next, the levels of TAbs were assessed. Similar to the results obtained at day 21, the great-

est fold changes in TAb levels were observed in the IgG, IgG2b and IgG2c immunoglobulin isotypes. When assessing IgG levels, a statistically significant decrease in IgG titre was observed between Group A and prednisolone-treated mice in Group B (0.421 $\pm$0.049 vs. 0.244 $\pm$0.056 AUs SEM, $p < 0.05$). However, the levels of IgG remaining in Group B samples were greater than those in the PBS IVT control Group C (0.244 $\pm$0.056 vs. 0.008 $\pm$0.001 AUs SEM, $p < 0.01$). Further, in support of the AUC data outlined above, there was a statistically significant 1.8-fold decrease in IgG levels in in Group D compared to Group A (0.243 $\pm$0.55 vs. 0.421 $\pm$0.049 AUs SEM, $p < 0.05$).

In accordance with the data obtained from the day 21 samples, there were no significant changes in the levels of IgG1 immunoglobulin observed between the different groups.

The results from the IgG2b isotype analysis were at variance with those obtained from the day 21 samples. No changes were seen in IgG2b titres between Groups A, B and D. However, a clear increase in IgG2b levels in all of these groups was evident when compared to the PBS IVT control Group C.

Analysis of the IgG2c subtype mirrored that obtained from the IgG assessment. A statistically significant 40% decrease in IgG2c levels was seen when comparing mice in Group A and prednisolone-treated mice in Group B (0.432 $\pm$0.056 vs. 0.259 $\pm$0.051 AUs SEM, $p < 0.05$). However, a clear fraction of AAV2-binding IgG2c remained in these samples when compared to mice in the PBS IVTs control Group C (0.259 $\pm$0.051 vs. 0.016 $\pm$0.002 AUs SEM, $p < 0.01$). In accordance with the IgG analysis, a statistically significant increase in IgG2c levels was seen between Group D and Group A (0.222 $\pm$0.050 vs. 0.432 $\pm$0.056 AUs SEM, $p < 0.01$).

Interestingly, when comparing IgM levels, some changes in antibody titre were evident. For instance, administration of prednisolone in Group B appeared to increase IgM levels three-fold compared to mice in Group A. Whilst this effect was statistically significant with a standalone t-test, this assessment was not included in this analysis to control type I error in the grouped dataset. Note that higher concentrations of serum to further this assessment were considered but not deemed useful to the investigation, as the initial optimisation of serum dilutions for TAb assays showed that even very high (1:25 dilutions) of serum yielded very low detection of IgM (see Material and Methods chapter).

In summary, analysis of day 42 serum samples showed that administration of prednisolone in mice receiving repeated bilateral IVTs of AAV2 reduced IgG, IgG2b and IgG2c TAb levels in accordance with the attenuation of neutralising activity described above.

Figure 5.3: Prednisolone reduces NAb and TAb levels in repeated bilateral IVT AAV2-treated mice (day 42 data)

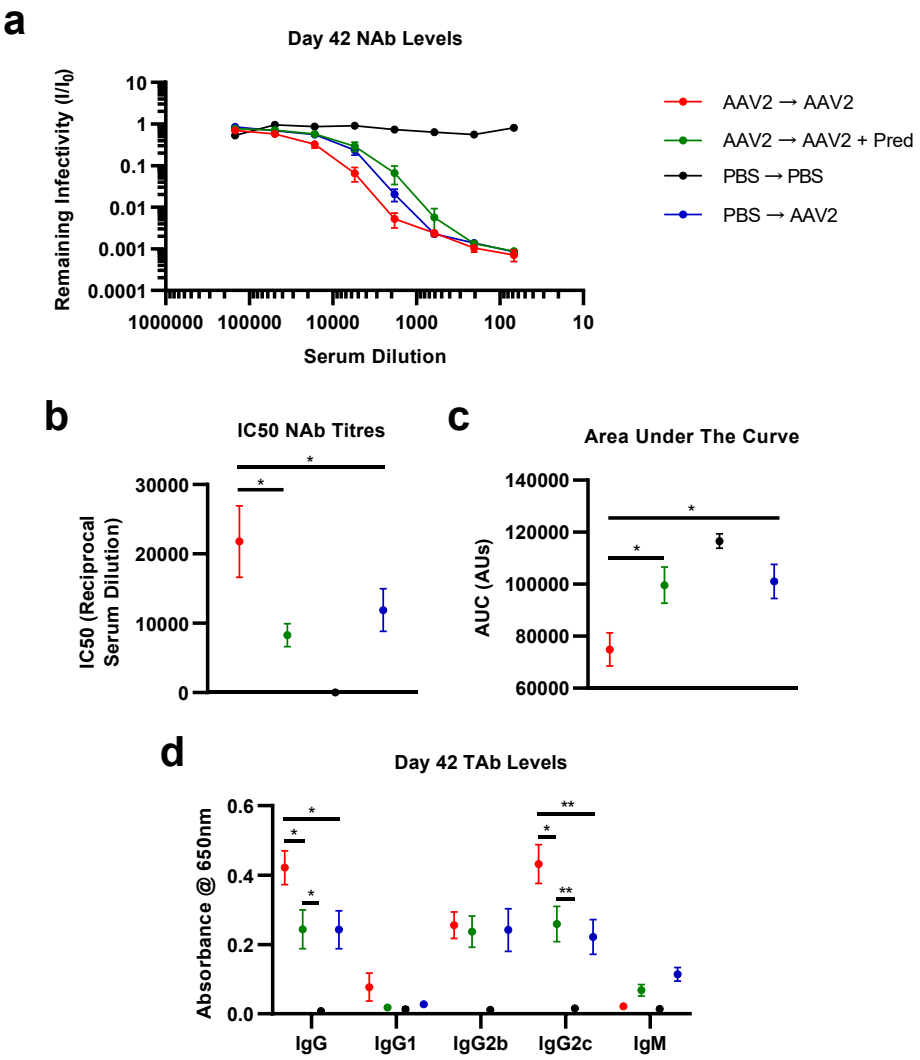

Perioperative prednisolone administration reduces NAb and TAb levels in mice receiving repeated bilateral IVTs of AAV2. All data is presented as column graphs showing the mean value for each group +/- SEM. Statistical analyses are between the labelled groups. N=4-8 per group.

(a) Day 42 NAb levels.

(b) IC50 values for day 42 NAb levels. * = $p < 0.05$, Mann-Whitney test.

(c) AUC values for 42 day NAb levels. * = $p < 0.05$, Student's t-test.

(d) Day 42 TAb levels. * = $p < 0.05$, two-way ANOVA and Tukey's posthoc testing.

5.5.3 Perioperative prednisolone administration inhibits germinal centre reactions in AAV2 challenged mice

The experiments outlined above showed that perioperative prednisolone administration was effective with regards to dampening the NAb and TAb response to intravitreally-delivered AAV2. This investigation was subsequently expanded to examine the underlying cellular mechanisms that may be driving the apparent efficacy of prednisolone. Spleens were harvested at day 42 and processed for analysis, stained with a cocktail of antibodies and analysed with flow cytometry.

First, the levels of Treg cells (CD25+ CD4+) were assessed. Although an additional marker, such as FoxP3, was absent from this analysis, around 90% of Treg cells are thought to express CD25, suggesting this co-immunolabelling was an adequate tool for measuring Treg levels. Interestingly, no differences were observed between mice in Group A and the prednisolone-treated mice in Group B. Similarly, no differences were evident between Groups A and B and mice who received a single AAV2 IVT in Group D. Statistically significant changes were observed between mice who received repeated bilateral PBS IVTs in Group C and the other three groups, however. Mice in Group A exhibited a ~40% higher level of Tregs than Group C mice (10.19 $\pm$0.46 vs. 6.85 $\pm$0.35% SEM, $p < 0.001$). Similarly, mice in the prednisolone-treated group (Group B) had a ~40% higher Treg levels than Group C control (10.25 $\pm$0.58 vs. 6.85 $\pm$0.35% SEM, $p < 0.01$). Group D mice also exhibited the same fold increase in Tregs compared to Group C (10.53 $\pm$0.49 vs. 6.85 $\pm$0.35% SEM, $p < 0.01$). This experiment showed that elevated splenic Treg levels are associated with AAV2 IVTs, however no prednisolone-dependent Treg response could be detected in this experiment.

The second T-cell subset that was analysed was follicular helper CD4+ cells (Tfh; CD3+ CD4+ $CXCR5_{hi}$ $PD\text{-}1_{hi}$). These cells are thought to interact with antigen-presenting DCs and cognate B-cells in splenic GCs, and provide signals to these cell types to facilitate activation and immunoglobulin class-switching toward the generation of high potency neutralising antibodies [222]. A statistically significant decrease in the levels of Tfh was evident when comparing mice in Group A and prednisolone-treated mice in Group B (1.76 $\pm$0.17 vs. 0.80 $\pm$0.13% SEM, $p < 0.01$). However, there was still a higher level of Tfh cells in Group B than the PBS injected mice in control Group C, suggesting prednisolone administration alone was insufficient to completely curtail Tfh responses, however, this difference was not statistically significant (0.80 $\pm$0.13 vs. 0.36 $\pm$0.08% SEM, $p = 0.42$). The levels of Tfh cells in Group A were also 2.2-fold higher than that observed in Group D, an effect that was also statistically significant (1.76 $\pm$0.17 vs. 0.68 $\pm$0.23% SEM, $p < 0.01$).

Following the analysis of Treg and Tfh populations, the effect of perioperative prednisolone administration on B-cell populations was assessed. First, the levels of GC B-cells

(CD19+ IgM+/$_{lo}$ IgD$_{lo}$ CD95$_{hi}$ GL7+) was measured, as B-cells are known to migrate to GCs during an infection. Compared to mice treated with no immunosuppression, it was found that administration of prednisolone reduced the levels of GC B-cells three-fold (0.906 $\pm$0.175 vs. 0.310 $\pm$0.065% SEM, $p < 0.05$). Further, prednisolone was found to reduce GC B-cell levels to that observed in mice who received PBS IVTs (Group C) (0.310 $\pm$0.065 vs. 0.333 $\pm$0.074% SEM). Interestingly, the levels of GC B-cells were not higher in Group A than Group D, a finding that may have been at variance with that observed in the NAb and TAb analyses, and assessment of Tfh levels (0.906 $\pm$0.175 vs. 1.023 $\pm$0.180).

Next, the effect of prednisolone on inhibiting B-cell class-switching was observed. First, the levels of GC unswitched B-cells (CD19+ IgM+ IgD+ CD95$_{hi}$ GL7+) was assessed. When comparing Group A and Group B, administration of prednisolone was found to increase unswitched B-cell levels by 30% (51.6 $\pm$2.83 vs. 65.3 $\pm$5.28% SEM, $p < 0.05$). As a result, the levels of unswitched B-cells were not changed compared to those in Group B and mice in the PBS IVT control Group C (65.3 $\pm$5.28 vs. 67.4 $\pm$2.53% SEM). The levels of class-switched B-cells (CD19+ IgM$_{lo}$ IgD$_{lo}$ CD95$_{hi}$ GL7+) was then analysed. Administration of prednisolone was found to reduce the levels of class-switched B-cells when mice in Group A and Group B were compared (49.5 $\pm$3.08 vs. 34.4 $\pm$4.37% SEM, $p < 0.05$). However, the levels of class-switched B-cells was still slightly higher than that observed in PBS IVT controls (34.4 $\pm$4.37 vs. 28.5 $\pm$5.28% SEM). Further, there was no significant change in class-switched B-cell levels when Groups A and D were compared (49.5 $\pm$3.08 vs. 42.1 $\pm$6.66% SEM).

In summary, analysis of splenic lymphocyte populations in this study showed that perioperative administration of prednisolone may and inhibit germinal centre reactions to reduce NAb and TAb titres in mice receiving repeated bilateral IVTs of AAV2, which may be independent of inducing a Treg response.

Figure 5.4: Perioperative prednisolone administration inhibits germinal centre reactions in AAV2 challenged mice

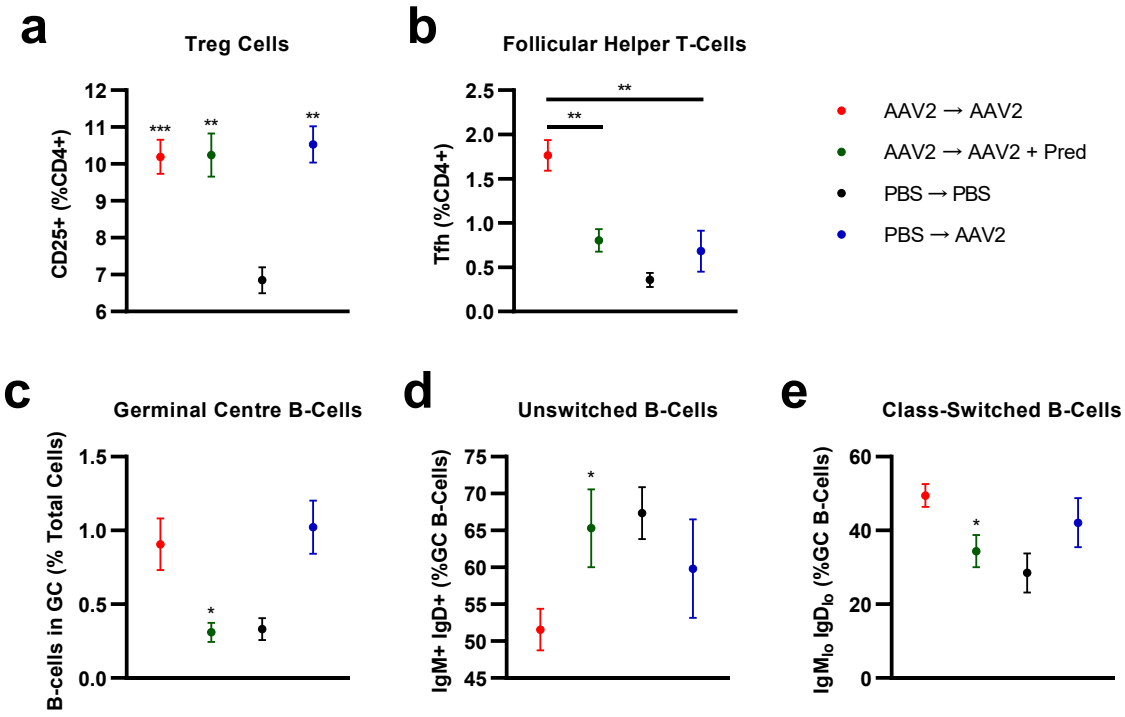

Spleens were extracted on day 42, processed into a single cell suspension, then stained with a cocktail of fluorescently tagged antibodies, and analysed via flow cytometry. All data is presented as column graphs showing the mean value for each group +/- SEM. All statistical analyses are between AAV2 → AAV2 + Pred and AAV2 → AAV2 groups unless otherwise stated. N=4-8 per group.

(a) Regulatory CD4 T-cell (Treg) levels (CD25+ CD4+ cells expressed as a percentage of all CD4+ T-cells). ** = $p < 0.01$, *** = $p < 0.001$, One-way ANOVA and Dunnett's posthoc tests. Here, all groups were compared against the PBS → PBS group.

(b) Follicular helper T-cells (CD3+ CD4+ $CXCR5_{hi}$ $PD\text{-}1_{hi}$)cells expressed as a percentage of all CD4+ T-cells). ** = $p < 0.01$, One-way ANOVA and Dunnett's posthoc tests.

(c) GC B-cells (CD19+ $IgM+/_{lo}$ IgD_{lo} $CD95_{hi}$ GL7+) cells expressed as a percentage of all splenocytes). * = $p < 0.05$, Brown-Forsythe ANOVA and Dunnett's T3 posthoc tests.

(d) Unswitched B-cell levels (CD19+ IgM+ IgD+ $CD95_{hi}$ GL7+) cells expressed as a percentage of all GC B-cells). * = $p < 0.05$, Student's t-test.

(e) Class-switched B-cell levels (CD19+ IgM_{lo} IgD_{lo} $CD95_{hi}$ GL7+) cells expressed as a percentage of all GC B-cells). * = $p < 0.05$, Student's t-test.

5.5.4 Prednisolone administration attenuates CD4+ T-cell infiltration after repeated bilateral AAV2 IVTs

The data presented above demonstrated the ability of prednisolone to attenuate NAb and TAb synthesis in AAV2 challenged mice via a mechanism that may involve inhibition of GC reactions. It was previously shown that infiltration of the retina by CD4+ T-cells may arise in response to AAV2 IVTs. Therefore to further the investigation into the possible benefits of prednisolone administration, the presence of CD4 T-cells in the retina at the endpoint of the study was assessed.

When comparing mice in Group A and prednisolone-treated mice in Group B, a statistically significant two-fold decrease in CD4+ T-cell levels in the retina was observed (3.49 $\pm$0.66 vs. 1.80 $\pm$0.41 CD4+ ROIs/FOV SEM, $p < 0.05$). Similar to the trends observed when assessing NAb and TAb titres however, there was still a higher level of CD4+ T-cells in Group B than PBS IVT control Group C (1.80 $\pm$0.41 vs. 0.27 $\pm$0.18 CD4+ ROIs/FOV SEM). Interestingly, in this experiment, the highest CD4+ T-cell level was seen in Group D, where a two-fold greater level of ROIs were identified compared to Group A (7.42 $\pm$0.63 vs. 3.49 $\pm$0.66 CD4+ ROIs/FOV SEM).

Figure 5.5: Prednisolone administration attenuates CD4+ T-cell infiltration after repeated bilateral AAV2 IVTs

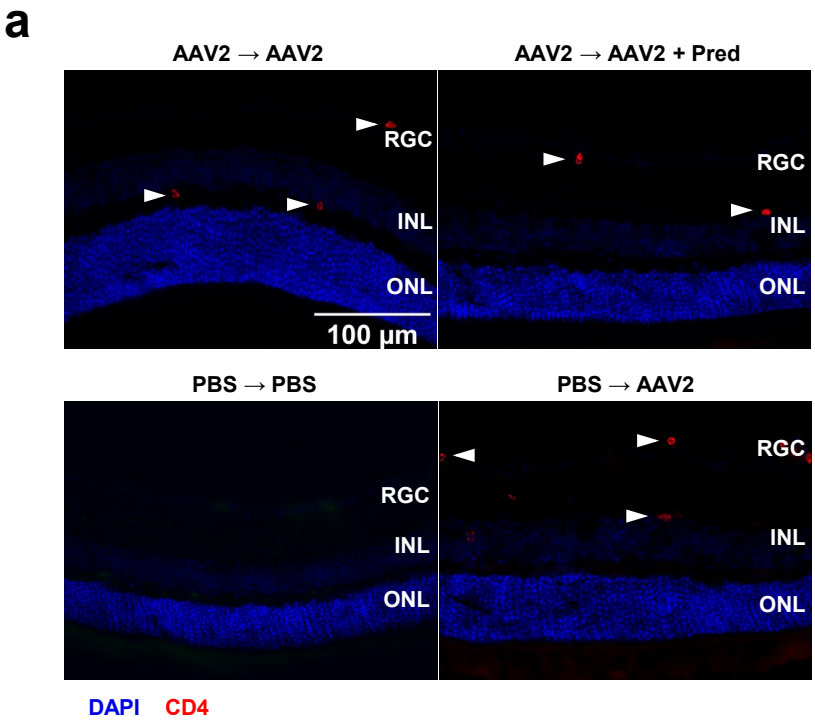

Eyes were enucleated on day 42, processed into 13µm cryosections and stained for the presence of CD4 (marker for helper T-cells). Data is presented as column graphs showing the mean value for each group +/- SEM. Statistical analysis is between AAV2 → AAV2 + Pred and AAV2 → AAV2 groups. RGC, retinal ganglion cell layer; INL, inner nuclear layer; ONL, outer nuclear layer.

(a) Representative 40x epifluorescence images showing CD4+ T-cells in the murine retina.

(b) Quantification of the number of CD4+ regions-of-interest (ROIs) per FOV. * = $p < 0.05$, Mann-Whitney test, n=8-12 per group.

5.5.5 Prednisolone administration attenuates CD8+ T-cell infiltration after repeated bilateral AAV2 IVTs

Having demonstrated a significant reduction in the levels of CD4 T-cells in prednisolone-treated mice, the levels of CD8 T-cells in the retina was measured to assess whether the steroid immunosuppressant may limit infiltration of cytolytic T-cells into the retina in response to challenge by AAV2 IVTs. Mice in Group A were found to have a six-fold higher level of CD8+ T-cells in the retina compared to prednisolone-treated mice in Group B (1.48 $\pm$0.55 vs. 0.23 $\pm$0.06 CD8+ ROIs/FOV SEM, $p < 0.01$). The mean number of CD8+ T-cells in Group B was marginally higher than that observed in the PBS IVT control Group C (0.23 $\pm$0.06 vs. 0.042 $\pm$0.042 CD8+ ROIs/FOV SEM). Similar to the trends seen with the analysis of CD4+ T-cell levels, the highest levels of CD8+ T-cells were seen in Group D, and this was two-fold higher than that observed in Group A mice (2.67 $\pm$0.59 vs. 1.48 $\pm$0.55 CD8+ ROIs/FOV SEM).

Figure 5.6: Prednisolone administration attenuates CD8+ T-cell infiltration after repeated bilateral AAV2 IVTs

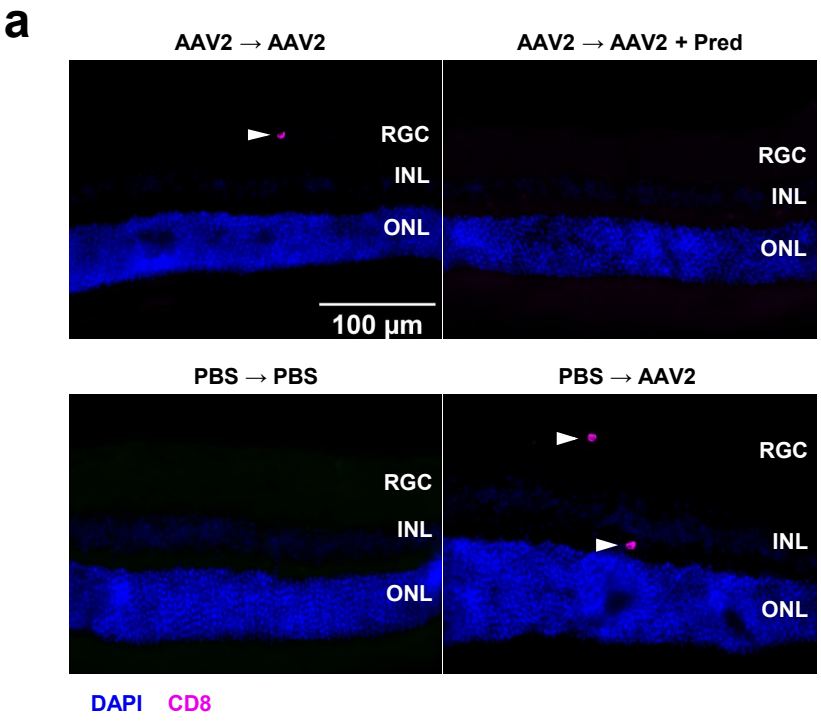

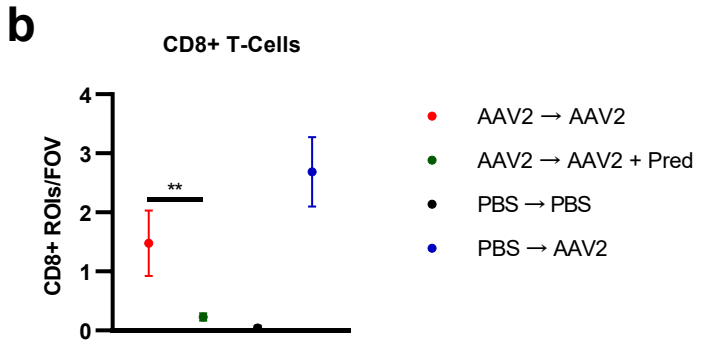

Eyes were enucleated on day 42, processed into 13μm cryosections and stained for the presence of CD8 (marker for cytolytic T-cells). Data is presented as column graphs showing the mean value for each group +/- SEM. Statistical analysis is between AAV2 → AAV2 + Pred and AAV2 → AAV2 groups. RGC, retinal ganglion cell layer; INL, inner nuclear layer; ONL, outer nuclear layer.
(a) Representative 40x epifluorescence microscopy images showing CD8+ T-cells in the murine retina.
(b) Quantification of the number of CD4+ regions-of-interest (ROIs) per FOV. ** = $p < 0.01$, Mann-Whitney test, n=8-12 per group.

5.5.6 Changes in microglia activation arising from repeated bilateral IVTs of AAV2

The experiments outlined above showed that prednisolone administration successfully attenuated the levels of CD4 and CD8 T-cell infiltration into the retina following repeated bilateral AAV2 injections. Having shown this dampening effect on the cellular arms of the adaptive immune system, the possibility that the immunosuppressant may reduce activation of the innate cellular immune response, specifically activation of microglia cells, was tested. Comparing mice in Group A and the prednisolone-treated mice in Group B, a reduction in IBA1 immunoreactivity was observed, however, this difference was not statistically significant (105,315 $\pm$20,715 vs. 62,311 $\pm$11,645 AUs SEM, p = 0.09). Interestingly, in accordance with the analysis outlined above pertaining to CD4 and CD8 T-cell infiltration, the highest level of microglia activation was seen in Group D mice, wherein the levels of IBA1 immunoreactivity in this group was three-fold higher than that seen in Group A (305,753 $\pm$57,830 vs. 105,315 $\pm$20,715 AUs SEM).

Figure 5.7: Changes in microglia activation arising from repeated bilateral IVTs of AAV2

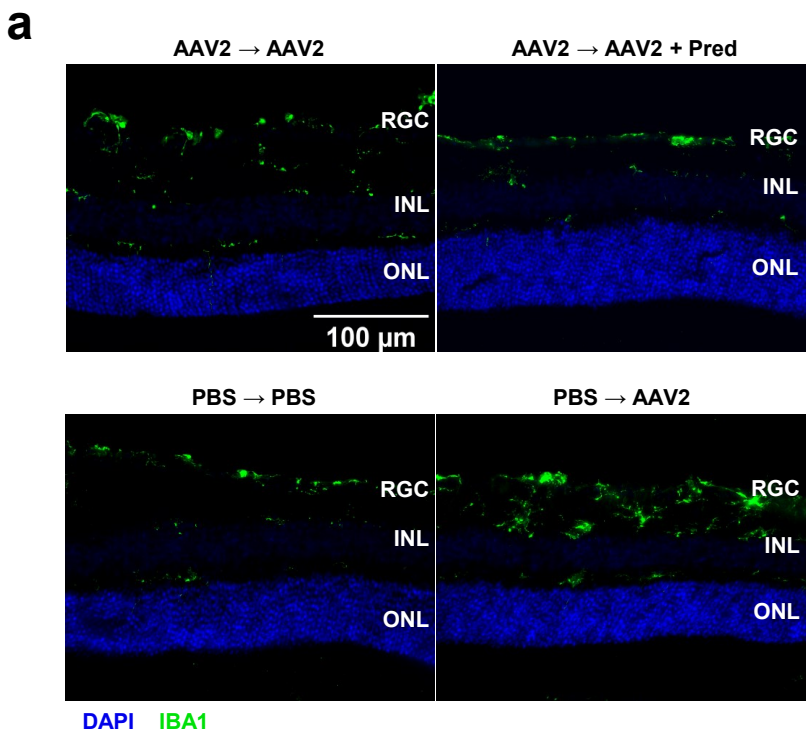

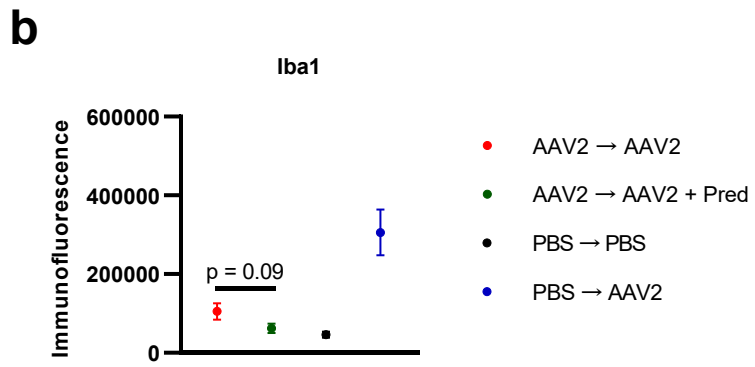

Eyes were enucleated on day 42, processed into 13μm cryosections and stained for the presence of IBA1 (marker for activated microglia cells). Data is presented as a column graph showing the mean value for each group +/- SEM. Statistical analysis is between AAV2 → AAV2 + Pred and AAV2 → AAV2 groups. RGC, retinal ganglion cell layer; INL, inner nuclear layer; ONL, outer nuclear layer.
(a) Representative 40x epifluorescence microscopy images showing IBA1+ microglia in the murine retina.
(b) Quantification of IBA1 immunoreactivity/FOV. Changes in IBA1 levels between mice receiving prednisolone and no immunosuppression were not statistically significant. p = 0.09, Student's t-test, n=8-12 per group.

5.5.7 Perioperative prednisolone-mediated immunosuppression fails to enable repeated gene transfer to the inner retina with repeated bilateral IVTs of AAV2

The data described in this chapter showed that mice treated with prednisolone exhibited lower NAb and TAb titres via a mechanism that may involve the inhibition of GC B-cell responses, and that this immunosuppression was also associated with reduced T-cell infiltration into the retina. The ability of prednisolone to enable repeated gene transfer to the inner retina was subsequently assessed. Briefly, as described in the study plan at the beginning of this chapter, mice in Groups A and B received a first IVT of AAV2.CAG.GFP and a second IVT three weeks later of AAV2.CMV.mCherry, with Group B mice being treated with daily IPs of prednisolone and Group A mice receiving PBS IPs as a control.

First, the levels of GFP expression were assessed, and mice in Group A and B demonstrated robust GFP expression in the retina, in line with expectation. Further, no GFP expression was seen in Group C and D mice who received PBS IVTs at day 0.

Next, mCherry immunoreactivity in the retina was analysed. No mCherry expression was seen in Group A and B mice, at any location in the retina nor in any of the samples tested, suggesting the mCherry-expressing AAV2 given at the three week timepoint may have been neutralised even in the prednisolone-treated group. No mCherry expression was seen in Group C PBS IVT controls. However, robust mCherry immunoreactivity was seen in Group D mice retinae. In summary, this analysis showed that prednisolone monotherapy may be insufficient to lift the blocking effect imposed by NAbs that arise from AAV2 IVTs in murine models.

Figure 5.8: Perioperative prednisolone-mediated immunosuppression fails to enable repeated gene transfer to the inner retina with repeated bilateral IVTs of AAV2

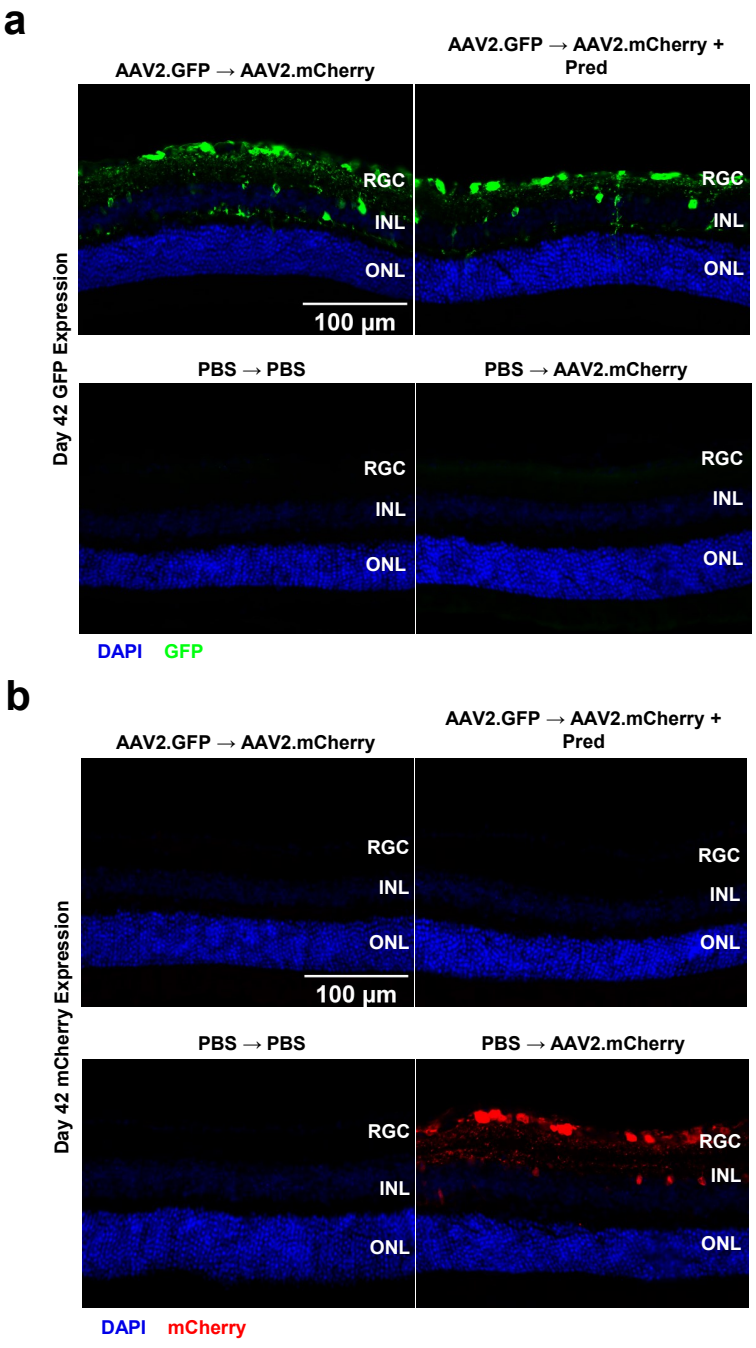

Perioperative prednisolone administration fails to enable repeated gene transfer to the murine retina following repeated bilateral IVTs of AAV2. Eyes were enucleated on day 42, processed into 13μm cryosections, and stained for GFP and mCherry. RGC, retinal ganglion cell layer; INL, inner nuclear layer; ONL, outer nuclear layer.

(a) Representative 40x epifluorescence microscope images showing GFP immunoreactivity in the murine retina.

(b) Representative 40x epifluorescence microscope images showing mCherry immunoreactivity in the murine retina.

5.5.8 Repeated bilateral IVTs of AAV2 may be associated with reduced electrophysiological activity in the retina (average waveforms)

The results described in this chapter showed that prednisolone failed to enable repeated gene transfer to the inner retina, in spite of a demonstrated ability to attenuate synthesis of NAbs. It the previous chapter it was shown that IVTs of wild-type and mutant AAV2 was not associated with electrophysiological perturbations in the murine retina. However, the possibility of ERG deficits arising from repeated bilateral IVTs of AAV2 had not been explored at the time of writing this thesis. Therefore, prior to termination of the study at day 42, ERG was performed on all mice to assess whether functional damage may have arisen as a possible consequence of AAV2-mediated immunological reactions. First, average pSTR, B- and A-waveforms for Groups A-D were assessed (derived from log light intensities of -4.37, -1.90 and 1.29 cd.s/m^2 respectively).

Assessment of pSTRs (RGC function) showed that no observable differences were apparent between Group A and Group B mice, despite the data previously outlined in this chapter in which prednisolone treatment was shown to attenuate cellular infiltration to the retina. Interestingly, both Group A and Group B pSTR values were lower than that seen in Group C PBS IVT control mice, indicating possible electrophysiological changes arising from repeated administration of AAV2. Further, the lowest mean average pSTR values were seen in Group D, a finding which may have correlated with the highest levels of CD4 and CD8 T-cell infiltration and microglia activation that were previously observed.

Similar trends were evident when analysing changes in B-waveforms (rod bipolar cell function). There was no observable difference between mice in Group A and prednisolone-treated mice in Group B. In contrast to the trends observed with the pSTR values, there was no changes in B-wave amplitude between Groups A & B and Group D mice. However, mice in the PBS IVT control Group C had the highest B-wave amplitudes compared to the other three groups.

The trends seen with the B-waveforms were recapitulated in the A-waveforms (rod photoreceptor function). No changes were evident when comparing mice in Group A, B or D. However, the greatest A-wave amplitudes (most negative values) were observed in the PBS IVT control Group C.

Figure 5.9: Repeated bilateral IVTs of AAV2 may be associated with reduced electrophysiological activity in the retina (average waveforms)

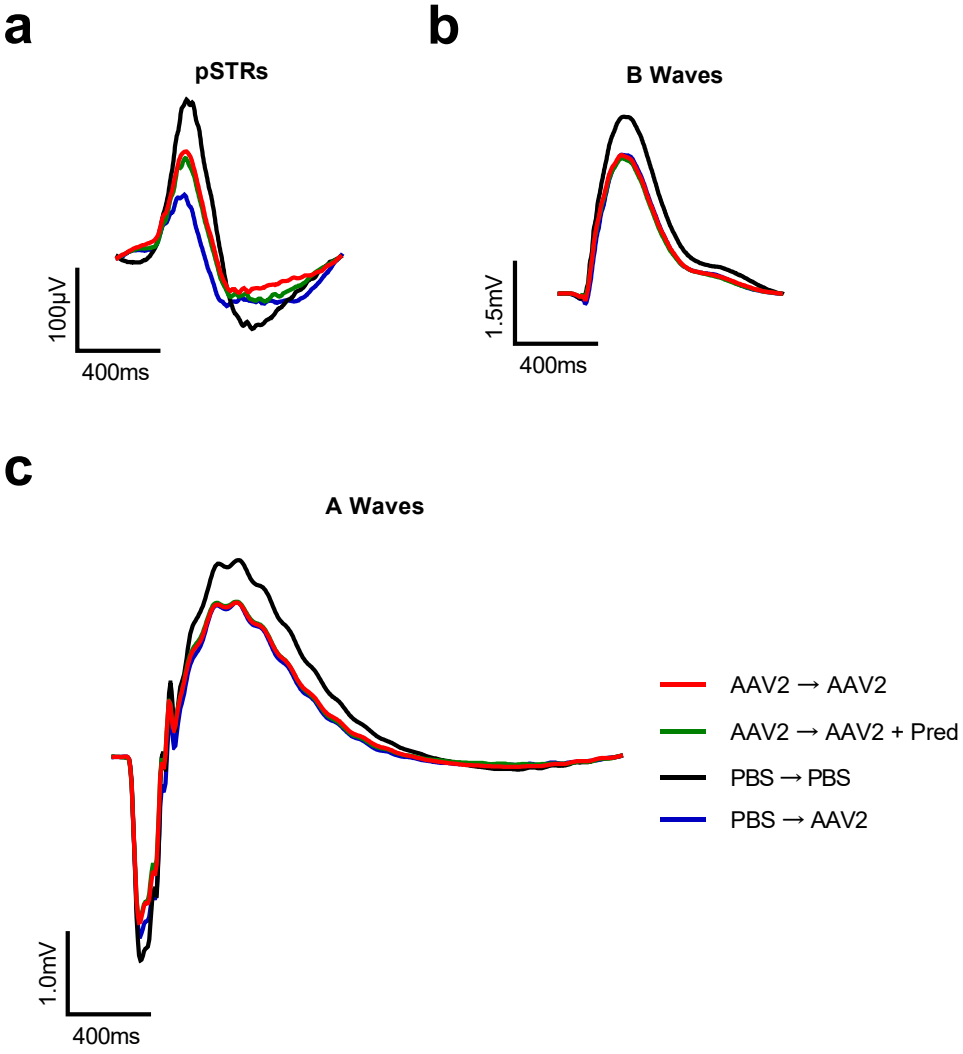

Electrophysiological changes arising from repeated bilateral IVTs of AAV2. ERG was performed on day 42 immediately prior to animal sacrifice and tissue extraction.
(a) Average pSTR waveforms at -4.37 log light intensity (cd.s/m^2)
(b) Average B waveforms at -1.90 log light intensity (cd.s/m^2)
(c) Average A waveforms at 1.29 log light intensity (cd.s/m^2)

5.5.9 Repeated bilateral IVTs of AAV2 may be associated with reduced electrophysiological activity in the retina (quantitative analysis across all light intensities)

This analysis was extended to the maximum peak amplitude of every sample in each group across all 15 light intensities tested, thus enabling a quantitative and statistical analysis of differences between groups.

When assessing the seven pSTRs included in the ERG protocol, significant differences were observed at log light intensities of -4.94, -4.73, -4.54 and -4.37 cd.s/m^2. For brevity, only the data at -4.37 cd.s/$m^2$are described. No differences were observed between mice in Group A and Group B. However, the mean peak pSTR voltage was 50% greater in the PBS IVT Group C than Group A mice (75.4 $\pm$8.95 vs. 50.8 $\pm$3.02 μV SEM, $p < 0.0001$). Further, the lowest peak pSTR voltage was observed in Group D, which was 40% lower than that seen in Group A (31.3 $\pm$2.97 vs. 50.8 $\pm$3.02 μV SEM, $p < 0.001$), a finding that may relate to the levels of T-cell infiltration and microglia activation observed in this group.

Similar trends were observed in the B-wave dataset, in which significant differences between groups were evident at log light intensities of -3.08, -2.47 and -1.90 cd.s/m^2. At -1.90 cd.s/m^2, no changes were seen between Group A and prednisolone-treated Group B mice. In contrast to the pSTR analysis, no changes were evident between these two groups and Group D mice. However, significant changes were seen between the peak B-wave amplitudes of Group A, B and D mice and those in the PBS IVT control Group C. In particular, Group C peak B-wave amplitudes were 22% higher than that observed in Group A mice (1068.4 $\pm$43.6 vs. 834.9 $\pm$31.9 μV SEM, $p < 0.0001$).

Finally, peak A-wave amplitudes were assessed across four log light intensities, two of which (0.34 and 1.29 cd.s/m^2), yielded statistically significant differences between groups. At 1.29 cd.s/m^2 log light intensity, no statistically significant changes between Group A, B or D mice were observed, similar to the trends seen in the B-wave analysis. However, differences were observed when mice in PBS IVT control Group C and mice in Groups A, B, and D were compared. Specifically, Group C peak A-wave amplitudes were 18% higher than those recorded in Group A (-816.2 $\pm$25.3 vs. -666.2 $\pm$24.5 μV SEM, $p < 0.0001$).

In summary, this analysis showed that repeated bilateral IVTs of AAV2 may be associated with electrophysiological perturbations in the murine retina, and that these changes might not be rescued by administration of prednisolone immunosuppression. Interestingly, the greatest decrease in RGC ERG pSTR activity was seen in Group D, where mice received an IVT of PBS followed by AAV2 three weeks later, a finding that may reflect the timings of the induction and resolution of immune responses to viral vectors in the vitreous.

Figure 5.10: Repeated bilateral IVTs of AAV2 may be associated with reduced electrophysiological activity in the retina (quantitative analysis across all light intensities)

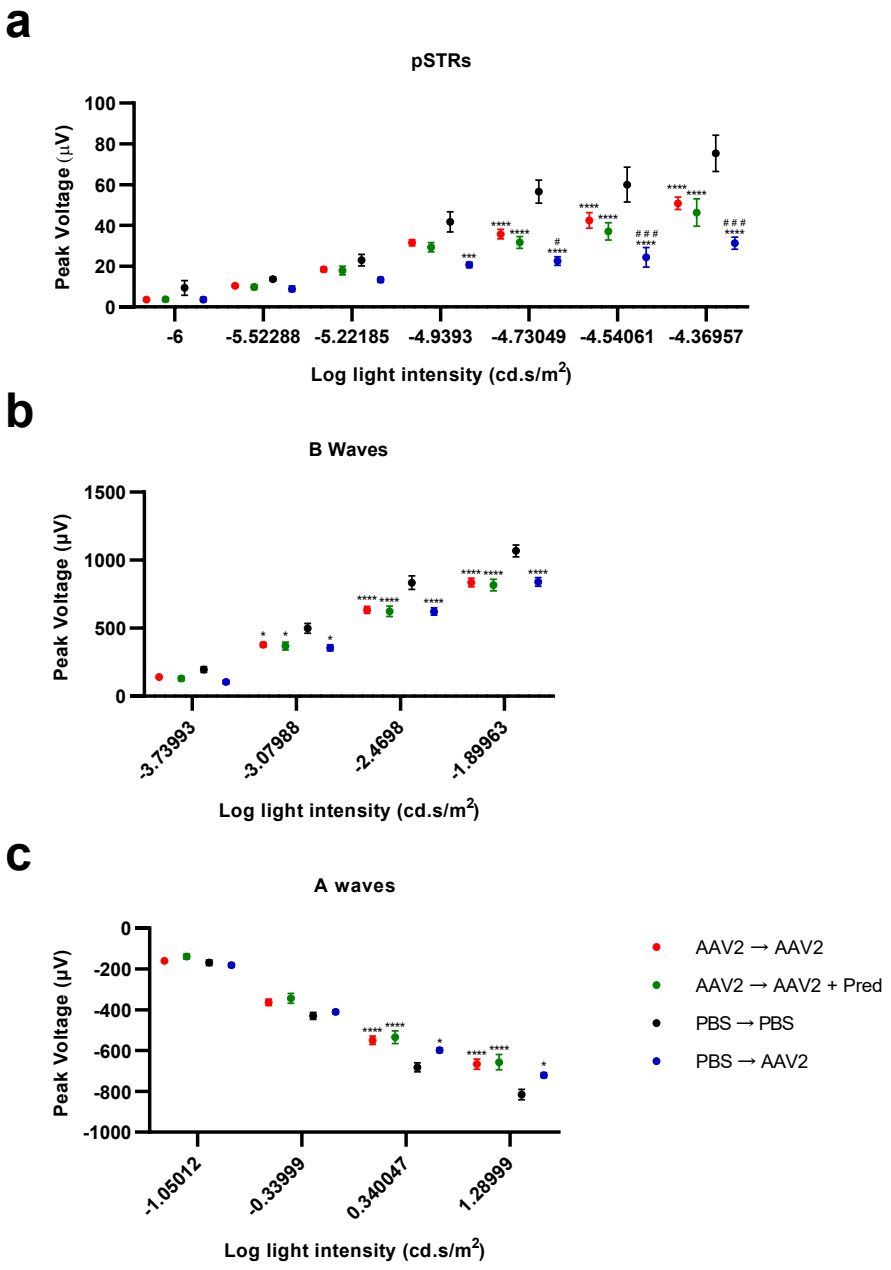

Electrophysiological changes arising from repeated bilateral IVTs of AAV2. ERG was performed on day 42 immediately prior to animal sacrifice and tissue extraction. All data is presented as column graphs showing the mean value for each group +/- SEM. Statistical analyses are comparisons are between groups as outlined below. N=8-16 per group.

(a) pSTR values across seven light intensities. *** = $p < 0.001$, **** = $p < 0.0001$ (comparing Group C vs. all other groups), # = $p < 0.05$, ### = $p < 0.001$ (comparing Group A and Group D cohorts), two-way ANOVA and Dunnett's posthoc tests.

(b) B wave values across four light intensities. * = $p < 0.05$, *** = $p < 0.001$, **** = $p < 0.0001$, two-way ANOVA and Dunnett's posthoc tests.

(c) A wave values across four light intensities. * = $p < 0.05$, **** = $p < 0.0001$, two-way ANOVA and Dunnett's posthoc tests.

5.6 Summary of results

In this chapter, the effect of prednisolone glucocorticoid immunosuppression on dampening immune responses arising from repeated bilateral IVTs of AAV2 was investigated. Specifically, it was asked whether prednisolone monotherapy would be sufficient to reduce NAb synthesis to a level that would be permissive of a second AAV2 IVT.

First, prednisolone was found to reduce NAb and IgG TAb levels by around four- and five-fold respectively after a single set of AAV2 IVTs (day 21). When investigating day 42 NAb and TAb levels following repeated bilateral AAV2 IVTs, prednisolone attenuated NAb levels by around 2.5-fold and IgG TAb levels by around two-fold. The underlying cellular mechanisms dictating this attenuating effect on antibody synthesis were tested, and it was found that administration of the immunosuppressant was associated with the inhibition of GC reactions and B-cell class-switching.

Further benefits to prednisolone administration were also characterised, wherein the immunosuppressant was found to reduce infiltration of the retina by CD4 and CD8 T-cells. However, no significant changes in microglia activation were observed at the timepoints tested.

The possibility that perioperative prednisolone administration may be able to lift the blocking effect imposed by anti-AAV2 NAbs that proceeds an IVT was then investigated, however, this showed that the beneficial effects of prednisolone monotherapy alone may be insufficient in enabling repeated gene transfer to the inner retina.

Lastly, analysis of ERG data showed that repeated bilateral IVTs of AAV2 may be associated with a slight reduction in RGC, rod bipolar and rod photoreceptor electrophysiological activity in the retina.

In summary, this chapter suggested that, whilst administration of prednisolone may be beneficial in partially circumventing anti-AAV2 immune activation, further optimisation of immunosuppression protocols may be required to ensure safe and effective gene delivery to the inner retina.

Chapter 6

Discussion

6.1 Review of thesis aims and objectives

In the first part of this thesis, a comprehensive review was provided of the role that pre-existing and induced NAbs play in the context of gene delivery to the eye. This analysis suggested that a subset of patients receiving AAV vectors via the SRT or IVT routes develop anti-AAV NAbs that may present a barrier to readministration of the gene therapy. Whilst readministration of an AAV-based gene therapy to the contralateral eye had been shown [125], a small number of preclinical studies had suggested that readministration via IVT may be more challenging, which may highlight disparities between the subretinal and vitreal cavities with respect to inducing tolerogenic immune responses [97, 133]. The literature review concluded that a comprehensive and multifaceted approach may be required to enable repeated gene transfer to the inner retina via IVT. Specifically, a combination of small molecule immunosuppressants, B- and T-cell modulators and AAV capsid engineering may be needed to prevent neutralisation by pre-existing NAbs and also to limit the generation of NAbs upon injection.

To this end, this thesis sought to characterise whether engineered AAV vectors or glucocorticoid prednisolone administration could be used to reduce anti-AAV NAb titres, which may have highlighted their possible utility as components of the comprehensive/multifaceted strategy outlined in Chapter 1.

6.2 Immunology of a rationally-designed AAV2 capsid mutant in the ocular compartment

The first strategy that was tested was whether the incorporation of phosphodegron mutations could be used to reduce the synthesis of NAbs upon IVT in a murine models by enabling robust transduction at a low vector dose. Recent reports that systemic injection of a triple phosphodegron mutant capsid (tY-F) was associated with reduced CD8 T-cell killing of transduced hepatocytes led the authors to suggest that reduced phosphorylation/ubiquitination and subsequent proteasomal degradation of capsid protein reduced presentation of those antigens on MHC c. I to CD8 T-cells [194]. However, the potential impact of mutating phosphodegron residues in terms of limiting NAb synthesis is less clear, given that viral antigen in APCs is loaded onto MHC c. II molecules following degradation in endosomal compartments, a process that may be sequestered away from cytosolic kinases and proteasomal machinery [223]. Considering reports that phosphodegron mutant AAV2 vectors increase transduction of the murine retina [224], it was deemed a reasonable hypothesis to test whether low dose IVT of a phosphodegron mutant AAV2 could enable robust transduction whilst limiting the anti-capsid NAb response.

6.2.1 Transduction efficiency of phosphodegron mutant AAV2 in murine retina

First, the transduction efficiency of the vectors was tested. It was shown that each mutation induced higher levels of transduction in the retina after IVT, a finding that is consistent with previous reports that reduced intracellular degradation of capsids may be associated with elevated rates of nuclear transfer and concomitant gene expression [198, 201].

The three mutants were then combined into a single capsid, termed AAV2 (TM), which was initially tested for transduction efficiency in HEK293T and ARPE19 cell lines. This experiment demonstrated that the mutant AAV2 capsids tolerated incorporation of the three selected mutations (gross structural perturbations may have resulted in aberrant genome packaging etc, leading to very low viral titres or no transduction at all), and induced a higher level of gene expression than wild-type AAV2 *in vitro*.

Expanding these findings into an *in vivo* model, AAV2 (Y444F) was found to induce a higher level of retina transduction than wild-type AAV2 in accordance with previous reports in the literature [224]. Further, IVT of the triple phosphodegron mutant AAV2 capsid developed in this study resulted in a greater level of transgene expression than AAV2 (Y444F), demonstrating a synergistic effect between the three point mutations selected for analysis. These

findings were then corroborated by a second set of IVTs in which transduction efficiency was measured qualitatively via assessments of retinal wholemounts.

One question that remains to be addressed with regards to the transduction efficiency of phosphodegron mutant AAV2 capsids after IVT is the extent to which the increase in gene expression observed is due to reducing intracellular degradation of the vector, or the attenuation of binding to the primary attachment receptor, HSPG, in the ILM. Interestingly, recent work by Boye et. al. showed that combinations of phosphodegron mutations in AAV2 are associated with reduced binding to HSPG [213], a finding consistent with data generated in this thesis (discussed later). The authors draw an interesting distinction between the transduction efficiency of phosphodegron mutant AAV2s *in vitro* and *in vivo* in relation to their binding affinity to HSPG. Specifically, that lower affinity HSPG binding is associated with lower transduction *in vitro*, but higher transduction *in vivo* with phosphodegron mutant capsids [225]. Boye et. al. posit that phosphodegron mutant AAV2 particles permeate towards deeper layers of the retina, possibly because of reduced sequestration in the HSPG-rich ILM, a conclusion similar to that outlined in recent work from the Lisowski group (albeit in a different organ/route of administration) [226]. Therefore the relative contribution of reduced intracellular degradation vs. attenuated HSPG binding in the ILM in relation to increasing transduction efficiency after IVT remains to be determined, but reports in the literature do suggest that mechanisms additional to reducing cytosolic degradation of capsid antigen may be involved. Later, the possible role of reduced HSPG binding in the ILM will be discussed in the context of possible mechanisms of increased immune activation identified in this thesis.

6.2.2 AAV2 (TM) induces a greater humoral immune response compared with wild-type AAV2

The first arm of the immune system that was tested after IVT of the vectors was the generation of NAbs and TAbs, as they were most relevant to the key research question/hypothesis, and are likely generated independently of possible immune activation induced by GFP expression in the retina.

IVT of AAV2 (TM) and, to a lesser extent AAV2 (Y444F), was associated with higher levels of NAbs and TAbs than mice who were injected with wild-type AAV2 vectors. This was shown with IC50 analysis, and corroborated with an AUC assessment. Further, in terms of the key immunoglobulin isotypes correlated with the neutralising activity, IgG, IgG2b and IgG2c were the TAbs where significant differences were seen, a finding partially in accordance with previous reports in the literature in which IgG1 and IgG2 TAbs were deemed the key isotypes involved, however these disparities may be explained by the different species (human

vs. mouse) studied [85].

These findings suggested that mutation of phosphodegron residues on AAV2 capsids may be a useful tool for circumventing NAb generation after injection to the vitreous. To explain this, a number of disparities between the work presented in this thesis and the findings by Mingozzi and colleagues [194] will be highlighted. Aside from the obvious difference, which is route of administration and target organ (Martino et. al. injected systemically to target the liver), previous reports of reduced hepatocyte killing by AAV2 (tY-F) were observed in a $rag^{-/-}$mouse, which cannot generate T- and B-cell receptors, meaning they exhibit abrogated T- and B-cell function [227], and dramatically reduced dendritic cell function [199]. As such, the model utilised in their study harbours no endogenous mechanisms for antigen presentation via the MHC c. II pathway on APCs, nor cDC-mediated cross-presentation to CD8 T-cells via MHC c. I. Moreover, a close examination of the pathways involved in processing antigens for presentation on MHC c. II in APCs (the pathway that drives NAb synthesis via B-cell activation) shows that this occurs via cathepsin-mediated degradation in endosomal compartments in APCs, which may be sequestered away from the cytosolic protein tyrosine/serine kinases, ubiquitin ligases and proteasomal machinery to which the canonical phosphodegron hypothesis of reduced cytosolic degradation may be more relevant [223]. The next question to be addressed was why the NAb and TAb levels (and other arms of the immune system) were increased with AAV2 (TM) vs. wild-type capsids. A number of possible explanations is provided below. Briefly, these can be summarised as (i) attenuated binding to HSPG may increase vector shedding to secondary lymphoid organs like the spleen, (ii) retinal inflammation attracted APCs like dendritic cells which increased antigen presentation to B-cells after recirculation to splenic/lymph node tissue, and may also be linked to (iii) increased vector shedding to the circulation caused by increased vascular permeability arising from retinal inflammation. Later, the observed increase in MHC c. II expression in splenic cDC1 & 2 subsets is discussed, highlighting a possible mechanism of antigen-dependent activation of APCs in support of the hypothesis that increased vector shedding to the spleen may have been responsible for increased humoral immune activation with AAV2 (TM) vs. wild-type capsids. The identification of IBA1+ MHC c. II+ co-immunolabelled cells in the vitreous, which may have been activated macrophage cells [228], is also discussed, highlighting a possible increase in APC infiltration after IVT of AAV2 (TM).

6.2.3 Increased CD4 and CD8 T-cell infiltration to the retina after IVT of AAV2 (TM) vs. wild-type AAV2

In the next set of experiments, the levels of CD4 and CD8 T-cell infiltration into the retina after IVT of AAV2 (TM), AAV2 (Y444F) and wild-type AAV2 was assessed. Statistically significant increases in CD4 and CD8 T-cell levels were observed in the AAV2 (TM) group when compared to mice who were injected with wild-type AAV2 capsids. Further, no elevation of T-cell infiltration was seen after IVT of AAV2 (Y444F) vs. wild-type AAV2 and the highest infiltration levels were seen after high titre injections of wild-type AAV2, in accordance with the trends observed in the NAb and TAb datasets. The findings of this assessment were largely in support of reports in the literature in which CD4 and CD8 T-cells have been identified in the retina following injection of wild-type AAV2 via IVT [210]. To explain why increased infiltration was observed with AAV2 (TM) vs. wild-type AAV2, an assessment of CD4 and CD8 activation by splenic cDC1 APCs is required, which will be detailed in the next section of this chapter.

In terms of future research questions pertaining to these findings, an assessment of whether the CD4 and CD8 T-cells are exhibiting an activated or exhausted phenotype [229] will be important in understanding the role that T-cells play upon infiltration to the retina. If the latter is true and the effector functionality of these cells (cytokine production by CD4 T-cells and cytotoxic activity of CD8 T-cells) is significantly diminished in the retina, this may prove a key facet of AAV immunobiology in the eye and could support the safety profile of this gene therapy vector. Another aspect of CD4 and CD8 T-cell activation states that has not been studied in depth is the propensity of antigen-presenting microglia cells to reactivate infiltrating T-cells via presentation of viral antigen on MHC molecules, a facet of immunobiology that has been demonstrated in a number of neurodegenerative pathologies [230]. In this thesis, activation of microglia cells was identified after IVT of AAV2 vectors. Further research to characterise possible interactions between microglia and infiltrating T-cells in the context of understanding T-cell activation/exhaustion with techniques like spatial multiomics [231] or immunopeptidomics [232] may prove fruitful here.

6.2.4 Splenic lymphocyte populations modulated by IVT of AAV2 (TM) vs. wild-type AAV2

First, changes in the levels of splenic T-cells in AAV2 (TM), AAV2 (Y444F) and wild-type AAV2 injected mice was studied. No differences were observed with effector CD4 and CD8 T-cells between the three different groups. However, this might be due to inadequate sensitivity of this assay, and future work could seek to identify AAV2-reactive CD4 and CD8

T-cells in splenic tissue after IVT using ELISPOT assays, for example. Further, identification of the precise CD4 T-cell subsets, such as Th1, Th2 etc, are induced by IVTs of AAV2 and mutant AAV2 capsids, and a detailed characterisation of these subsets using single cell RNA sequencing [233] and T-cell repertoire sequencing [234] would prove a useful addition to the field. For instance, identification of the key T-cell receptors implicated in anti-AAV2 immunobiology could be leveraged to achieve antigen-selective depletion of specific T-cell clones as a means of mitigating anti-vector immune responses without the risks associated with general immunosuppression [235].

Significant differences were observed in Tfh levels between AAV2 (TM) and wild-type AAV2 injected mice (but no changes were seen when AAV2 (Y444F) and wild-type AAV2 were compared). This finding was therefore largely in accordance with the NAb and TAb data in which increased antibody synthesis was evident in the AAV2 (TM) group vs. wild-type control capsids. These data support a model in which B-cell activation, class-switching, and antibody synthesis are facilitated by Tfh cells in splenic GCs [222]. A possible role for cDC2 cells in priming Tfh cells identified in this study is outlined below. Further research into the interaction between Tfh and GC B-cells may involve the identification and characterisation of molecular factors underpinning the facilitation of B-cell activation and class-switching by Tfhs, which could be inhibited as a means of preventing anti-AAV2 NAb synthesis. For instance, inhibition of SLAMF6, which has been identified as a possible molecular player involved in facilitating Tfh-mediated B-cell help (e.g. by upregulating class-switch recombination) could be explored to this end, however, this strategy would need to carefully consider possible off-target effects arising from ablation of SLAMF6 activity, principally, that generalised attenutation of humoral immunity could be associated with increased risk of opportunistic infections.

Next, changes in B-cell lymphocyte populations were assessed. When comparing AAV2 (TM) to wild-type AAV2 capsids, a significant elevation in the number of GC B-cells was observed, although no differences were seen when comparing AAV2 (Y444F) and wild-type AAV2 injected mice. This finding could be consistent with a model of increased migration of splenic B-cells into the GCs in response to detecting a new infection [236], and may be explained by an increase in vector shedding to the spleen/peripheral lymph nodes with AAV2 (TM) vs. wild-type capsids as outlined above. The data may also be consistent with the increase in Tfh cells described above, which are thought to induce GC B-cell proliferation via cytokine secretion.

The level of MHC c. II expression in GC B-cells was also assessed, as this serves as a marker of B-cell activation [237]. An increase in MHC c. II level on GC B-cells was seen after IVT of AAV2 (TM) vs. wild-type capsids, thus providing evidence of increased B-cell

activation in this group. This finding may reflect an increase in antigen-dependent B-cell activation, for instance, if an increase in vector shedding increased vector biodistribution in the spleen via membrane-bound peptide-MHC c. II complexes on APCs, or soluble AAV2 antigen draining to the spleen via the circulation. The B-cell activation observed in this study may have been partially driven by antigen-independent pathways as well, for instance, an increase in Tfh induction by cDC2s may have activated B-cells by CD40L-CD40 interactions and secretion of cytokines such as IL-21 [222].

The final B-cell population that was analysed was the percentage of class-switched B-cells. Consistent with a model of increased humoral immune activation, more switched GC B-cells were evident after IVT of AAV2 (TM) vs. wild-type AAV2, but not AAV2 (Y444F) vs. wild-type AAV2. The increase in the percentage of switched B-cells was therefore in accordance with the increased levels of NAbs and TAbs, Tfh cells, and GC B-cell MHC c. II expression observed in this study. Future research may seek to prevent B-cell class-switching as a means of reducing the levels of anti-AAV2 immunoglobulins with high neutralising activity, which could be advantageous in terms of circumventing humoral immunity to AAV gene therapies. However, inhibition of genes that facilitate class-switching would likely ablate the capacity of the immune system to produce functional B- and T-cells. Therefore, a strategy that seeks to deplete Tfh cells (ideally in an antigen-specific fashion) may be preferable, for instance by targeting AAV-specific T-cell receptors as a means of immunomodulation.

Lastly, the levels of MHC c. II on APCs in the spleens was assessed. Here, cDC1, cDC2 and pDC populations were analysed. Similar to B-cell activation mechanisms, dendritic cells upregulate MHC c. II expression when they are activated by soluble antigen in the spleen and peripheral lymph nodes [238]. This is thought to arise from reduced cycling of MHC c. II from the cell surface into degradative endosome/lysosome complexes in non-activated dendritic cells [205]. Significant increases in MHC c. II expression on cDC1 was observed between AAV2 (TM) and wild-type AAV2 injected mice. cDC1 are thought to be involved in the activation of Th1 responses which are a crucial component of the anti-viral immune response [239]. As discussed above, a significant increase in CD4+ T-cells were observed after IVT of AAV2 (TM) vs. wild-type AAV2, which may have been driven by increased cDC1-mediated Th1 induction in the spleen, however, further work is needed to delineate the precise helper T-cell subsets that are induced by IVTs of AAV2. cDC1s are also key regulators of CD8 T-cell priming [239], and as such, one possible explanation for the increase in CD8+ T-cells observed in AAV2 (TM) injected mouse retinae involves increased antigen-dependent activation of cDC1 arising from increased vector shedding/biodistribution as outlined above. However, providing a possible explanation for CD8+ T-cell activation by dendritic cells in this study requires additional analysis, as the mechanism of phosphodegron mutations involves

reducing cytosolic degradation of capsid antigen thereby reducing its display by MHC c. I [194]. A possible reason is that whilst phosphodegrons do partially reduce peptide display on MHC c. I (reducing CD8 T-cell priming), this was offset/overcompensated for in this study by increased vector shedding/biodistribution in the spleen (increasing CD8 T-cell priming). Further, increased CD4 T-cell activation (which may have been elevated in the AAV2 (TM) group) that supports CD8 T-cell priming may have counteracted the effect that phosphodegrons have on attenuating capsid antigen presentation via MHC c. I.

Next, an increase in MHC c. II expression in cDC2s was seen when AAV2 (TM) and wild-type AAV2 injected mice were compared. cDC2 cells are important for activating Tfh responses [239]. Therefore, the increase in cDC2 activation observed in this study was consistent with the elevation of Tfh cell numbers and upregulated GC reactions (increased B-cell activation and class-switching in the AAV2 (TM) group), which may have been due to an increase in vector shedding/biodistribution in the spleen and peripheral lymph nodes caused by attenuated binding affinity to AAV2's primary attachment receptor, HSPG (discussed in more detail below).

The final dendritic cell population to be analysed was pDCs, which are thought to be an important dendritic cell subtype involved in the antiviral response. No differences were observed in MHC c. II expression in splenic pDCs between the three vector groups tested. However, this may be explained by the differences in MHC c. II expression between pDCs and cDC1/2s, which has been described in a number of reports and reviews in the literature [240, 241]. This is not to suggest that the pDCs did not play a role in the anti-viral response described in this study however. In fact, pDCs are thought to be a key cellular player in the anti-viral response, in part due to their ability to sense unmethylated CpG motifs in viral genomes and secrete IFNγ to potentiate Th1 differentiation [242]. Further research is needed to better understand the role that pDCs play in response to AAV gene therapy in the eye. Interestingly, a recent paper utilised TLR9-inhibiting io1 sequences as a means of dampening innate and adaptive immune responses to multiple AAV capsids across a range of delivery routes. However, no reduction in the levels of NAbs induced after systemic administration of the engineered vectors was observed, despite the demonstration of reduced innate immune responses in human pDCs *in vitro* [209]. Therefore, whilst the benefits of reducing TLR9 sensing of viral genomes may be beneficial in partially limiting immune responses against AAV gene therapies, additional strategies to circumvent pDC responses to limit NAb synthesis are clearly required.

6.2.5 Increased glial cell activation following AAV2 (TM) vs. wild-type capsid IVT

In the next set of experiments, the possibility that AAV2 (TM) may induce higher levels of gliosis in the retina than wild-type AAV2 capsids was tested. First, IBA1 immunoreactivity was measured, which is considered to be a marker of activated microglia cells [206]. Higher levels of IBA1 were seen in AAV2 (TM) retinae than those mice who received wild-type AAV2 injections, and microglia cells exhibiting a "bushy" morphology were also observed in AAV2 (TM) injected mice. Next, GFAP was assessed in retinal cryosections to assess whether Muller glia cells were activated by the vector injected groups. Here, significant increases in GFAP fibril length and immunofluorescence were seen in AAV2 (TM) vs. wild-type AAV2 injected mice, which is consistent with reports of Muller glia activation in the retina [243]. This analysis was then extended to include GFAP+ astrocyte cells in the retinal ganglion cell layer, which was analysed via staining and imaging of wholemounted retinal tissue and assessment of skeletonised GFAP+ dendritic arbours. Further to the results outlined above, significant differences were observed when AAV2 (TM) and wild-type AAV2 injected mice were compared, however, the effect size with these analyses was smaller than that seen with the IBA1 and Muller glia GFAP analysis.

These data therefore showed that, further to increasing the humoral and cellular arms of the adaptive immune system, innate immune activation in the retina may also be increased after IVT of AAV2 (TM). To explain this, the work of Boye et. al. [213] is highly relevant in which the authors argue that a possible reason that phosphodegron mutant capsids exhibit increased transduction of the outer retina after IVT vs. wild-type AAV2 is due to attenuated binding affinity to HSPG in the ILM at the vitreoretinal interface. The data outlined in this thesis goes a step further and asks what the possible consequences of this may be in terms of innate immune activation and reactive gliosis in the retina. Here, a number of possible models are considered. First, it may be that reduced capture of vector in HSPG-rich ILM (which is been postulated as a barrier to transduction of the retina [244]) drives an increase in transduction by increasing the infection of retinal neurons, such as RGCs and amacrine cells. As such, increased levels of vector are sensed by intracellular arms of the innate immune system, such as TLR9 that responds to endosomal viral unmethylated CpG motifs. In support of this hypothesis, type I interferon responses in neurones have been documented arising from infection by viruses [245], a finding that may be relevant to the neuronal cells that are infected/transduced after IVT of AAV2. An alternative explanation is that the increased permeation into the retina exhibited by some phosphodegron mutant AAV2 capsids [213] that arises from attenuated HSPG binding/capture in the ILM may be related to the interaction between the viral particles and the resident immune cells of the CNS, microglia cells, which are thought to reside in

their resting state in the inner and outer plexiform layers [246]. One possible model is that increased permeation of AAV2 (TM) into the retina vs. wild-type capsids resulted in elevated antigen-dependent activation of microglia cells via a mechanism similar to that described with other viral infections [247]. Whilst transduction of microglia is usually considered rare after an IVT of AAV2, recent reports have suggested that entry of capsid to endosomes/cytosol may occur (positive qPCR signal for AAV genomes) although concomitant nuclear transfer of AAV genomes and gene expression may be blocked by intracellular machinery whose role is to degrade viral capsids [248]. Thus, work reviewed by Maes et. al. provides a possible reason why microglia may be the key cell type underpinning the increased immune activation observed after IVT of AAV2 (TM) vs. wild-type control capsids, where increased antigen-dependent activation of these cells may have occurred in the absence of detectable transduction (in this case, expression of GFP).

Microglia cells harbour a documented capacity to secrete type I interferons if they are activated by viral infections [249]. Therefore one possible explanation that links the microglia, Muller glia and astrocyte activation observed in this thesis begins with increased antigen-dependent activation of microglia, which in turn increases TLR9-mediated sensing of unmethylated CpG dinucleotide sequences in AAV genomes [209]. This in turn could have facilitated increased type I interferon (IFNα/β) production via the interferon response factor 7 (IRF7) pathway [250]. In turn, type I interferon production drives NFκB- and STAT-dependent synthesis of proinflammatory cytokines like TNFα and IL1β in addition to chemokines like MCP1 and MIP1 [251]. Further, increased TLR2 sensing of capsid proteins at the cell surface of the microglia cells have played a role [252]. As a result, the proinflammatory cytokine microenvironment may have induced the gliosis described above in accordance with a number of recent publication linking cytokines like TNFα to microglia activation [253] and astrocyte activation [254]. However, significantly more research will be required before a precise explanation (e.g. a detailed spatio-temporal model) of the mechanisms underpinning innate immune activation after IVT of AAV2 (and many mutant/designer capsids) can be provided. For instance, a recent review highlighted reports of transduction of astrocytes and Muller glia cells by several AAV serotypes [255], which may have caused TLR9-mediated type I interferon signalling and antigen-independent activation of microglia cells. In reality, a network of discrete glial cell activation events likely occurs via antigen-dependent and -independent mechanisms which culminates in gliosis in the retina after AAV2 IVT. However, the relative contribution that activation of different glial populations to inducing gliosis requires further investigation. Future investigations may also seek to characterise the transcriptomes of infected microglia cells via single cell RNA sequencing compared to PBS injected control retinae. As highlighted above, immunopeptidomics could be utilised to highlight a possible role of capsid

antigen presentation in activated microglia cells, and possibly astrocytes as well given reports that this glial cell population may harbour antigen-presenting capacity [256, 257]. Finally, spatial multiomics techniques [231] could be used to identify a possible role for microglia-mediated reactivation of infiltrating T-cells if a role for capsid antigen presentation by microglia/astrocytes was determined.

Another role for the innate immune response and glial cell activation that remains to be determined, and one that was not directly investigated in this thesis, was the possible impact that chemokine synthesis and secretion played in facilitating the recruitment of circulating lymphocytes into the retina, which has been documented in comparable examples of retinal inflammation involving chemokine receptor 5 (CCR5) expressing Th1 T-cells [258]. A recent review by Bucher et. al. highlighted an interesting role for proinflammatory cytokines like TNFα and IL1β in facilitating increased vascular permeability, thus potentiating the infiltration of the retina by lymphocytes and APCs [259]. These findings may be highly relevant to the development of gene therapies [260] for disease in which compromised blood-retinal barrier functionality is well-documented, such as age-related macular degeneration [261] and diabetic macular oedema [262], where AAV2 administration may transiently worsen disease pathology before substantial levels of a therapeutic transgene are expressed. In terms of the work discussed in this thesis, however, cytokine-mediated increases in vascular permeability (e.g. that driven by activated microglia cells) may have played a role in facilitating lymphocyte (CD4 and CD8 T-cell) recruitment to the retina. As discussed below, increases in microglia-mediated vascular permeability could also have been linked to increased intravasation of vector in the AAV2 (TM) group vs. wild-type AAV2, which may explain the increases in cDC1 & 2 activation and concomitant NAb synthesis.

Further, if there had been an increase in APCs infiltrating to the retina [210], then recirculating to the spleen and lymph nodes and activating B-cell responses, this may also have been involved in increasing NAb and TAb responses in AAV2 (TM) injected eyes vs. wild-type AAV2 injected eyes. In support of this, IBA1+ MHC c. II+ co-immunolabelled cells were observed in the vitreous after IVT of AAV2 (TM) eyes, which may have been macrophages which harbour antigen presenting capacity. Interestingly, in a recent publication, the role of microglia and macrophages was studied in an experimental autoimmune uveitis (EAU) model, and it was posited that microglia may be responsible for the initiation of the innate immune response, in part via the facilitating extravasation of infiltrating MHC c. II+ APCs, which may include monocytes/macrophages. Depletion of microglia after the onset of EAU however had little effect on the duration or severity of inflammation, leading the authors to suggest that the infiltrating APCs were responsible for reprocessing and presentation of autoantigen to infiltrating CD4 T-cells and the onset of EAU [206]. Closer examination of these pathways in the

context of AAV2-induced intraocular inflammation may therefore prove useful in determining the initial steps that drive the immune response against various capsid components, which could be achieved via depletion of microglia using PLX5622 at various timepoints post-IVT. Crucially, given that depletion of microglia prior to immunisation in the Okunuki et. al. paper blocked development of EAU [206], strategies to target activation and function of this glia cell type in AAV gene therapy studies may be beneficial.

6.2.6 AAV2 (TM) exhibits reduced neutralisation by heparan sulphate and anti-AAV2 NAbs vs. wild-type control capsids

Previous reports have demonstrated that the incorporation of phosphodegron mutations into AAV2 capsids may be associated with the attenuation of binding affinity to HSPG, AAV2's primary attachment receptor, which was correlated with increased permeation of vector particles into the retina [213]. As discussed above, this could lead to increased activation of glial cells and retinal neurones via antigen-dependent and -independent mechanisms. To demonstrate that AAV2 (TM) exhibits reduced HSPG affinity, a heparan sulphate (HS) neutralisation assay was used. Here, vector was incubated with HS and HEK293T cells, and reduced neutralisation (i.e. increased remaining infectivity) in the AAV2 (TM) group (a slight reduction in neutralisation was also identified in AAV2 (Y444F), AAV2 (K556E) and AAV2 (S662V) groups) was observed. These findings therefore corroborated the findings of Boye et. al. [213], however, further work to characterise the attenuation of HSPG binding with AAV2 (TM) using heparin chromatography would likely be beneficial to the investigation. Possible explanations linking attenuated HSPG binding to increased immune activation are outlined above in the relevant sections. Below, further justification and key literature reports are provided in support of the hypothesis that attenuated HSPG binding may correlate to greater immune activation.

The work of the Lisowski group may be relevant [226]. In their recent publication, the authors outlined a functional model by which AAV2 mutants with attenuated HSPG binding increase liver transduction. After systemic intravascular administration, they suggested that reduced HSPG capture in the extracellular matrices surrounding the liver results in an increase in free vector levels, which increases biodistribution of the capsid, leading to increased hepatocyte transduction via a process that may be partially HSPG-independent [226] (this may be supported by reports in the retina in which some mutants exhibit high levels of photoreceptor transduction despite displaying ablated binding affinity to HSPG [263]). The presence of AAV vector genomes in the spleen after IVT [264] and suprachoroidal administration [202] has been characterised. This suggests that vectors delivered to the eye may travel via the blood to this secondary lymphoid organ, and a substantial number of AAV genomes have been iden-

tified in the blood after IVT (464-fold greater levels than that observed after SRT in the NHP study) [264].

Another publication relevant to the discussion is a recent report of an evolved AAV capsid exhibiting increased photoreceptor transduction after systemic administration and IVT [265]. This study sought to develop capsids capable crossing biological barriers such as the extracellular matrix in the ILM. Both capsids that were identified as exhibiting increased transduction of the retina also demonstrated reduced binding affinity to HS in a heparin chromatography assay. The authors comment that, due to the initial systemic injection used to screen for novel AAVs after 24h, the vectors had to penetrate through the blood vessel endothelium to enter the retina and transduce photoreceptors (however, they acknowledge that intracellular processes may also explain their data). One possible explanation here is that vectors exhibiting reduced HSPG binding were more effective at crossing the blood retinal barrier due to the high levels of HSPG-rich extracellular matrix present in blood vessel endothelium [266].

More research will be required to link these findings to the increased immune activation exhibited by AAV2 (TM). One possible explanation is that AAV2 (TM) is more readily able to drain to the spleen once it has accessed the circulation, similar to the patterns observed with HSPG binding mutants in heparin chromatography assays in which elution of mutant capsids occurs at lower buffer concentrations than wild-type capsids [213, 226]. Here, a synergistic effect between increased extravasation of vector (driven by increased microglia activation) and increased vector shedding may explain the elevation in cDC1 & 2 activation between AAV2 (TM) and wild-type AAV2, which may explain the differences in NAb and TAb levels outlined above.

An important question to address with AAV2 (TM) is why the phosphodegron mutations induced changes in heparan binding. Notably, this question was not addressed in the Boye et. al. paper [213], possibly highlighting the fact that such an assessment can only be reliably performed using cryoelectron microscopy. However, the positioning of the mutations can be visualised in silico and the proximity of these residues to canonical HSPG binding motifs can be considered using PyMol and RIVEM. This assessment suggested that the three residues identified for analysis in this study lay distal to the main HSPG binding residues. As such, it may be unlikely mutating these areas of the capsid induced a conformational change in AAV2 monomers to the extent that HSPG binding was reduced. An alternative hypothesis is that the mutations may have modulated the overall oligomeric structure of 60mer AAV capsids by affecting interactions between individual monomer subunits of the virus, thus eliciting conformational changes between adjacent HSPG binding motifs at the three-fold axis of symmetry [215]. For instance, mutation of a polar serine residue at position 662 to a non-polar valine residue at the periphery of the AAV2 monomer may have modulated ionic interactions with

adjacent monomers, possibly inducing an overall structural change in the oligomeric 60mer capsid.

Having demonstrated reduced neutralisation of AAV2 (TM) by HS in an *in vitro* model, it was hypothesised that escape from neutralisation by anti-AAV2 NAbs may also be induced by the incorporation of the phosphodegron mutations. This hypothesis was partly derived from the fact that some neutralising epitopes are thought to be present at the three-fold axis of symmetry [267], which may have been altered in AAV2 (TM) vs. wild-type AAV2 capsids, in addition to recent reports that AAV vectors exhibiting attenuated HSPG binding may be less susceptible to neutralisation by anti-AAV2 NAbs [265]. To this end, wild-type and mutant vectors were incubated with anti-AAV2 NAb-containing serum and HEK293T cells. Remaining infectivity was subsequently calculated, which showed that whilst AAV2 (Y444F), AAV2 (K556E) and AAV2 (S662V) only elicited a slight escape from neutralisation, AAV2 (TM) demonstrated a 7-fold increase in remaining infectivity vs. wild-type capsids. This may prove a relevant finding pertaining to recent evidence that IVT of a phosphodegron mutant AAV2 capsid did not appear to be impacted by the presence of pre-existing NAbs in NHPs [268], and may explain why patients with high pre-existing NAb titres in clinical studies utilising IVT of phosphodegron mutant AAV2 demonstrated improvements in vision [98]. Therefore, one possible benefit of utilising phosphodegron mutant capsids in ocular gene therapy trials may be to assist in overcoming pre-existing NAb responses.

6.2.7 Analysis of electrophysiological activity in the retina following vector IVTs

IVT of AAV2 (TM) and also AAV2 (high titre) was associated with glial cell activation and T-cell infiltration in the retina. To assess whether these immune responses may have induced electrophysiological perturbations, ERG was performed. In this study, no changes in RGC, rod bipolar or rod photoreceptor ERG activity were detected. This suggested that although some inflammation was observed, this did not appear to affect the ability multiple retinal subsets to depolarise/hyperpolarise and induce action potentials 3wk after IVT. One weakness of this assessment however is that only a single timepoint was tested. It is possible that ERG deficits were present at earlier timepoints, for instance, 1-2 weeks post IVT where innate immune cell infiltration may be at a maximum [210]. Further, these data were arguably at variance with later ERG data described in Chapter 5, in which electrophysiological deficits were observed in mice who received a PBS IVT followed by an AAV2 IVT. Clearly, a key disparity between the two studies was the number of IVTs being performed, however, differences in the age of the mice may also provide a possible explanation, which will be discussed

later in this chapter.

6.2.8 Summary of immune responses induced by AAV2 (TM) vs. wild-type AAV2

In this chapter, NAbs, TAbs, retinal T-cell infiltration, splenic GC reactions (Tfh levels and GC B-cell changes), and DC activation were all found to be increased after an IVT of AAV2 (TM) vs. wild-type capsids. Further, elevated activation of microglia, Muller glia and astrocytes were identified. Interestingly, escape from neutralisation by anti-AAV2 NAb-containing serum was demonstrated, highlighting a possible benefit to the clinical application of phosphodegron mutant AAV2.

Elucidation of the underlying mechanisms by which this occurred will require further research, specifically, whether the reduction in binding affinity to HSPG (discussed further below) may correlate with an increase in vector shedding from the eye/increased biodistribution in the spleen and lymph nodes (possibly due to reduced capture in ECM or via microglia-mediated intravasation). The data discussed above may be consistent with a model in which increased viral load in the spleen is associated with elevated cDC1 and cDC2 activation, which drive CD4/CD8 T-cell and Tfh responses respectively. As a result, increased T-cell infiltration to the site of infection and increased Tfh/GC B-cell-driven NAb and TAb synthesis occurs. To identify increased vector shedding/biodistribution in the spleen and lymph nodes, and presentation of AAV2 antigen on cDC1/2 MHC c. I and c. II, immunopeptidomics could be employed [232]. Further, isolation of cDC1 and cDC2 endosomes and subsequent analysis of the number of endosomal AAV2 genomes via qPCR could also be beneficial [269]. Identification of elevated vector genomes in the blood after IVT of mutant and wild-type capsid would also assist in identifying increased vector shedding as a possible cause of increased adaptive immune responses. An alternative explanation is that increased permeation of AAV2 (TM) into the retina elevated interactions between the capsid and glial cell populations in the retina, which caused gliosis via antigen-dependent and -independent mechanisms. This may have facilitated recruitment of APCs, such as DCs, which could have engulfed antigen and circulated to the spleen and lymph nodes to present AAV2 capsid antigen to B-cells and T-cells, in addition to the reactivation of infiltrating CD4 T-cells [206], thus potentiating a self-amplifying feedback loop of leukocyte activation and antigen presentation. Further evaluation of this hypothesis could involve assessment of APC populations after IVT of AAV2 (TM) and wild-type capsids in accordance with published strategies [210]. Considering the observation of IBA1+ MHC c. II+ cells in the vitreous after AAV2 IVTs in this study, monocyte/macrophage depletion via administration of clodronate could be utilised to further investigate the role that these

cells play in response to intravitreally-injected gene therapies [270].

In summary, this chapter sought to assess whether the incorporation of phosphodegron mutations into AAV2 capsids could be a useful strategy to boost transduction of the retina whilst limiting NAb synthesis, thus identifying a possible component of the comprehensive strategy outlined in Chapter 1 that could be used to enable repeated gene transfer. Although increases in immune activation were observed, the study highlighted novel aspects of AAV vector immunobiology arising from incorporation of phosphodegron mutations, which may be of relevance to their clinical application.

6.3 Perioperative prednisolone administration attenuates immune activation following intravitreal injection of AAV2, but fails to enable repeated gene transfer to the inner retina

The analysis in Chapter 1 outlined the need for a comprehensive and multifaceted approach to circumvent NAb responses to AAV gene therapies. One component of this will likely entail the administration of small molecule immunosuppressants, such as glucocorticoid steroids. An advantage of this approach vs. the use of lymphocyte-depleting antibodies, for example, is that steroids like prednisolone have been used for decades in patients and exhibit a strong safety profile provided they are used for a short duration [271]. Interestingly, in the first gene therapy studies utilising IVT of AAV2 to treat diseases of the optic nerve, prednisolone was not administered to patients, but has been used in more recent studies utilising IVT and SRT modes of delivery [216]. Whilst prednisolone has demonstrated efficacy in reducing the CD8 T-cell response to transduced hepatocytes in patients [54, 272], the effect of the drug on attenuating NAb synthesis after IVT of AAV2 has not been documented as a possible solution to enabling repeated gene transfer. In this study, perioperative administration of prednisolone was found to reduce NAb and TAb synthesis in mice who received repeated bilateral injections of AAV2, which may have been due to the inhibition of splenic GC reactions. Prednisolone also reduced CD4 and CD8 T-cell infiltration into the retina, however, no changes in microglia activation were observed. Interestingly, electrophysiological changes affecting RGCs, rod bipolar cells and rod photoreceptors were evident between different groups. However, prednisolone monotherapy was insufficient in lifting the blocking effect imposed by anti-AAV2 NAbs, suggesting further optimisation to the immunosuppressive regimens may be required to enable repeated gene transfer.

6.3.1 Prednisolone limits induction of NAb and TAb synthesis

Blood samples were extracted three weeks after the first set of IVTs and assessed for the presence of NAbs and TAbs. In mice that were treated with prednisolone, reduced NAb and TAb levels were observed. As highlighted in the discussion below, this may have been driven by the inhibition of GC reactions. Similar to the results outlined in Chapter 4, the main immunoglobulin isotypes that appeared to be responsible for the neutralising activity detected were IgG, specifically, IgG2b and IgG2c.

Similar results were obtained at the end of the study (6wk timepoint) wherein prednisolone-

treated mice exhibited reduced NAb and TAb levels. Notably, the fold change between Group A (no immunosuppression) and Group B (prednisolone) mice in NAb IC50s and TAb levels was lower at the 6wk timepoint than the 3wk timepoint, which may suggest that steroid administration was more effective at attenuating humoral immune activation after the first IVT of AAV2 than the second. Another interesting observation is that the levels of NAbs and TAbs were higher in Group A mice, who received two AAV2 IVTs vs. Group D mice who received one AAV2 IVT. This suggested that, although the second vector injection was likely neutralised by NAbs in the vitreous (see discussion below), antibody-bound AAV2 was still processed by APCs and presented to B-cells, thereby eliciting further antibody production. This data is supported by the increase in GC reactions observed between these two groups, which is outlined below.

Notably, there was a possible exception in IgG2b TAb levels, in that there was no apparent difference observed between Group A and B mice with this immunoglobulin subtype, although a disparity was evident with IgG and IgG2c isotypes. The reason for this is not completely clear, especially when considered in conjunction with the 3wk TAb data in which IgG2b levels were reduced when comparing Group A and Group B samples. Further work should seek to validate these findings and confirm that this is the pattern of IgG2b expression. An investigation into the changes in immunoglobulin isotype synthesis over a greater number of timepoints could assist in furthering our understanding of the humoral immune response to AAV2.

The patterns of IgM levels between groups was also interesting. Although these differences were not significant when analysed with a two-way ANOVA, clear differences in the mean values between Group A and prednisolone-treated mice in Group B were evident, which may provide evidence for the inhibition of GC reactions/class-switching induced by the immunosuppressant. Further, elevated IgM levels were observed in Group D mice, which suggests that the innate B-cell response [273] was still active in this group at the end point of the study, 3wk after they received an AAV2 IVT. This is slightly different to the data obtained in Chapter 4 in which no IgM was detected in samples obtained 3wk after AAV2 IVT, however, the age of the mice in the study at the time of vector administration may have been responsible, where decreased class-switching in older mice has been described in the literature [274].

6.3.2 Inhibition of GC reactions identified as a possible mechanism of action underpinning the effect of prednisolone on antibody synthesis

Having shown that prednisolone reduces NAb and TAb synthesis in AAV2 injected mice, splenic lymphocyte populations were analysed to examine possible cellular mechanisms underlying the steroids effects. First, Treg levels were assessed, which were elevated in prednisolone-treated mice, but also Group A and Group D mice who received no immunosuppression compared to control Group C mice. This may have reflected the ability of the immune system to induce Treg responses when encountering a new infection as a means of controlling immune activation and dampening the potentially deleterious activity of conventional helper T-cells [275]. Interestingly, no differences in Treg levels were observed between Group A and prednisolone-treated Group B mice, who both received repeated AAV2 bilateral IVTs. This suggested that the mechanism by which prednisolone attenuated NAb and TAb synthesis may not have involved the induction of a Treg response, a finding that could be at variance with reports in the literature investigating autoimmune disorders [276] and rejection of transplanted organs [277]. In this experiment, CD25 was used as a marker to delineate Treg cells [278], however, further research into the Treg response induced by IVT of AAV2 could expand upon this by analysing FoxP3, CD127 and CTLA4 [278]. In addition, *in vitro* Treg suppression assays [279] could be employed to determine the immunosuppressive activity of the Treg population in different scenarios, for instance, in mice injected with AAV2 and treated with prednisolone. It is possible that, although no differences in Treg levels were observed in this study, the AAV-specific Tregs in the prednisolone treatment group were more immunosuppressive than those in mice who did not receive any immunosuppression. If a significant role for Tregs was determined in terms of dampening anti-AAV immune activation, one possible translational line of investigation could seek to administer AAV-specific Tregs as a means of reducing humoral immune activation and enabling repeated gene transfer, similar to a recent strategy outlined in the literature in which an autoantibody-mediated immune disorder was treated [280]. An advantage of this approach may be that it avoids the risks associated with general immunosuppression, such as potentiating opportunistic infection and dampening anti-tumour T-cell responses.

The next lymphocyte population that was analysed was Tfh cells, which are a T-cell subset that facilitate dendritic cell interactions with B-cells in splenic GCs in order to upregulate antibody synthesis by promoting survival and class-switching of B-cells [281]. Reduced Tfh levels were seen in the prednisolone-treated mice, suggesting that the reductions in NAbs and TAbs observed in this group vs. mice who did not receive any immunosuppression may

have been partly due to reduced Tfh activity in the spleens, a finding similar to that reported in studies investigating autoantibody-mediated disorders [282]. To determine the molecular mechanisms by which prednisolone may reduce Tfh levels in the spleen, sorting of Tfh cells and a characterisation of cellular transcriptomes could be used. For instance, steroids have been shown to block CD28-mediated cell cycle entry via upregulation of CTLA4 mRNA in CD4 T-cells as a means of inhibiting the proliferation of these cells, and a similar mechanism could have been involved here [283]. Interestingly, higher Tfh levels were seen in Group A (AAV2 →AAV2) mice vs. Group D (PBS →AAV2) mice, suggesting that AAV2 vectors in Group A were still capable of inducing GC reactions despite being neutralised in the vitreous after the 2nd IVT, possibly because the antibody-bound virions were engulfed by APCs in the retina or spleen, leading to Tfh priming. This observation may therefore be in agreement with reports of NAb-coated AAV vectors accumulating in the spleen [86].

Analysis of the changes induced in B-cell populations by prednisolone administration began by quantifying the levels of splenic GC B-cells. B-cells are known to migrate to the GCs in response to a new infection where they proliferate and undergo somatic hypermutation prior to selection based upon the affinity of their B-cell receptor to a particular antigen [236]. GC B-cell levels were lower in prednisolone-treated mice, suggesting that the steroid immunosuppressant may have inhibited proliferation of the cells in accordance with reports in the literature [284], possibly by binding to GRs on B-cell surfaces and inducing cell cycle arrest via repressing expression of CDK4/cyclin D3, and cMyc/E2F-1, the latter of which are key transcription factors mediating the G1 to S phase transition [285]. Interestingly, the levels of GC B-cells were equitable when comparing Group A (AAV2 →AAV2) and Group D (PBS →AAV2). The reasons for this were not completely clear, however, it is possible that GC B-cell levels in Group A (AAV2 →AAV2) mice began to decline due to GC reaction progression/resolution [286].

Lastly, changes in B-cell class-switching were assessed by analysing the expression of IgM and IgD. Briefly, class-switch recombination (CSR) is a process that proceeds somatic hypermutation (mutation of antigen binding domains) in B-cell GCs. CSR is driven by activation-induced cytidine deaminase (AID)-mediated mutation of 'switch' regions between immunoglobulin constant regions. These mutations induce the formation of single- and double-stranded DNA breaks that enable the excision of immunoglobulin constant region DNA mediated by recombinase enzymes. Thus, transcription of IgM mRNA can be changed to IgG mRNA, effectively switching the antibodies produced by that B-cell from IgM to high affinity IgG molecules with new effector functions, such as antibody-dependent cytotoxicity (ADCC) and antibody-dependent phagocytosis (ADP) [204, 287]. In this study, the levels of unswitched IgM+ IgD+ GC B-cells was increased in prednisolone-treated mice, and in parallel, switched

IgM_{lo} IgD_{lo} GC B-cell levels were increased in mice who were treated with the immunosuppressant. Thus, one possible reason that NAb and TAb levels were reduced in prednisolone-treated mice is that the drug acted to inhibit CSR, a finding that be in accordance with reports in the literature suggesting that AID mRNA synthesis may be reduced by administration of glucocorticoids [221]. As discussed above, however, prednisolone treatment also limited GC B-cell levels and Tfh levels, suggesting the cellular and molecular mechanisms governing the effect of the steroid on antibody synthesis may have been multifaceted in which a number of inhibitory pathways acted synergistically to attenuate NAb and TAb synthesis. Comparing the patterns of B-cell CSR between Group A (AAV2 →AAV2) and Group D (PBS →AAV2) also yielded interesting findings, in which CSR appeared to be higher in mice that received repeated bilateral AAV2 IVTs vs. a single set of bilateral IVTs, suggesting that CSR could still be upregulated by AAV2 vectors that had likely been neutralised upon injection into the vitreous by NAbs. Further work will be required to understand the pathways involved here, however, similar patterns were observed with Tfh levels in these groups, highlighting that increased DC-mediated priming of Tfh cells in Group A may have been involved, which could be assessed via expression of MHC c. II on cDC1 and cDC2 subsets with flow cytometry. Whether increased DC activation was driven by the infiltration of the cells to the retina [210] or draining of soluble antigen via the circulation to the spleen [264] remains to be determined, however.

To summarise, this set of experiments suggested that prednisolone inhibited GC reactions in AAV2 challenged mice which may explain the reductions in NAb and TAb titres described earlier. Whilst no change in Treg levels was observed in steroid-treated and -untreated animals, further work could implicate AAV-specific Treg responses as a possible cellular player underpinning prednisolone-mediated immunosuppression.

6.3.3 Prednisolone limits CD4 and CD8 T-cell infiltration into the retina in AAV2-challenged mice

Previous reports have demonstrated that CD4 and CD8 T-cells can infiltrate into the retina after IVT of AAV2 [210]. Having shown that prednisolone administration was associated with reduced NAb and TAb titres in AAV2-challenged mice, the possibility that the immunosuppressant may inhibit CD4 and CD8 T-cell infiltration into the retina was tested. Mice in the prednisolone treatment arm (Group B) demonstrated reduced CD4 and CD8 T-cell levels compared to mice in Group A who received no immunosuppression. These findings may therefore be in support of reports that CD4 infiltration may be modulated by glucocorticoid administration in studies examining T-cell levels in adrenocortical carcinoma [288]. Overall, however,

there has been little evidence to date suggesting that steroids may limit CD4 T-cell infiltration to inflamed tissues in response to viral infections. Given the capacity of CD4 T-cells to secrete proinflammatory cytokines, and possibly, eliminate infected cells in rare instances via cytolytic activity, this broad class of T-cell clearly plays an important role in antiviral immunity [289], and the findings of this study suggest that prednisolone may attenuate CD4 activity at the site of infection as well as in the spleens. The mechanism by which prednisolone inhibited CD4 T-cell infiltration may require further investigation, however. It is possible that the steroid acted via direct and indirect mechanisms. For instance, apoptosis of activated lymphocytes may have played a role [290], and upregulation of miR-98 may have been induced by the drug as a means of suppressing CD4 T-cell functionality [291]. Both of these possible aspects of prednisolone immunobiology have only been described in fields outside of AAV gene therapy, yet they provide a useful starting point for aiding future lines of inquiry.

There was also a significant reduction in the levels of CD8 T-cells infiltrating into the retina in the prednisolone-treated group, and this reduction appeared to be more pronounced than the differences observed with the CD4 T-cell analysis, suggesting that the drug may have had a bigger impact on the CD8 T-cell subset than the CD4 subset. This data therefore suggested that steroid administration may be beneficial in attenuating the infiltration of cytolytic cells, which may clear transduced cells expressing AAV antigen to CD8 T-cells via MHC c. I [292], however, this has not been demonstrated in the retina. As with the CD4 analysis, more research will clearly be need to establish a precise model for prednisolone-mediated immunosuppressive effects on CD8 T-cells. There is, however, some literature pertaining to the effect of glucocorticoids on CD8 T-cell subset function that may assist in explaining the results outlined in this study. Interestingly, this seemingly involves ablation of naiive CD8 T-cells via the induction of apoptosis in herpes simplex virus infections, as opposed to a mechanism affecting activated CD8 T-cells, in which the susceptibility to apoptosis of the T-cells was correlated with NR3C1 protein expression [293]. It is therefore possible that a similar effect occurred in this study, in which prednisolone ablated the naiive CD8 T-cell pool, thereby reducing the number of cells with T-cell receptors capable of recognising AAV epitopes presented on APCs, without altering the activation of primed CD8 T-cells (which has been demonstrated in melanoma models) [294]. One possible line of investigation that could be employed to this end would involve the sequencing of the T-cell repertoire based on a prior understanding of the sequence of anti-AAV T-cell receptors, in addition to flow cytometry analysis of circulating, splenic, lymph node and thymic naiive CD8 T-cells [295].

One aspect of T-cell infiltration to the retina that may require further study is the role that innate immune activation and concomitant release of cytokines that elevate vascular permeability could play [259]. As discussed above, it is possible that AAV-microglia interactions

upon IVT results in increased levels of proinflammatory cytokines in the retina, which may temporarily compromise the blood retinal barrier, thus potentiating leukocyte transmigration into the retina [296]. Considering the findings outlined in a recent review in which glucocorticoids were posited to elicit a downregulatory effect on vascular hyperpermeability [297] and another study investigating steroid administration in VEGF-challenged retinae (in which reduced blood vessel leakage was attributed to inhibition of signalling pathways downstream of the VEGF receptor) [298], one possible explanation for the attenuation of CD4 and CD8 T-cell infiltration into the retina exhibited by prednisolone-treated mice was that reduced vascular permeability limited the transmigration of lymphocytes. An interesting future line of investigation could be to test whether steroid administration can limit APC infiltration into the retina, thereby highlighting a possible mechanism by which prednisolone attenuated NAb and TAb synthesis in addition to the inhibition of GC reactions as outlined above.

One key observation of the assessment of CD4 and CD8 T-cells was that the highest levels of the infiltrating lymphocytes were seen in Group D (PBS $\rightarrow$ AAV2) mice. This may reflect the timings of adaptive immune responses to IVT AAV2, which have been shown to resolve over time [210]. It is possible that AAV2 vectors in Group A and B mice were neutralised in the vitreous after the second injection, negating a secondary T-cell response to the antigen. However, this seems unlikely given reports that neutralised AAV vectors accumulate in the spleen and lymph nodes [86] which could be linked to cDC1-mediated T-cell priming [239] and subsequent localisation to the site of infection at the retina. Another possible explanation, in accordance with recent reports is that the T-cell response in an AAV-primed mouse (one previously exposed to AAV antigen) occurs at a faster rate compared to animals naiive to AAV antigen [210]. Therefore, at the timepoints examined in this study, the T-cell response had begun to resolve in Groups A and B, but not yet in Group D, leading to the observation of higher T-cell levels in the retina at the endpoint of the study. As discussed in more depth below, it is possible that the disparities in T-cell levels between Group A/B and Group D mice could explain the differences in electrophysiological activity exhibited by these groups.

To summarise, this set of experiments suggested that prednisolone administration may inhibit the infiltration of T-cells in to the retina, however, further research will be required to understand whether this occurred via direct modulation of T-cell activity/induction of apoptosis, or by mediating vascular permeability. The study also provided possible insights into the role of vector neutralisation in the vitreous, however, it also remains unclear whether NAbs inhibit secondary T-cell responses, or prior exposure to AAV facilitate faster T-cell responses.

6.3.4 Prednisolone administration is not associated with a detectable change in retinal microglia activation in mice receiving AAV2 IVTs

The next set of experiments sought to establish whether prednisolone administration would affect microglia activation in AAV2-injected mice. Here, IBA1 immunoreactivity was measured at the end of the study, however, there was not a statistically significant difference seen between mice who were treated with prednisolone (Group B) and those who did not receive any immunosuppression (Group A). This may be because prednisolone did not have any impact on the activation of microglia cells, however, this would not be consistent with reports that administration of corticosteroid drugs is associated with a reduction in microglia activation [299], and further, microglia cells are known to express glucocorticoid receptors [300]. An alternative explanation relates to the resolution of the retinal immune response to AAV2, which has been described in recent literature reports [210]. It is possible that microglia activation levels were higher in Group A vs. Group B mice at earlier timepoints (e.g. 1-2wk after the 2nd IVT), however, microglia activation had declined by the 6wk timepoint at which IBA1 expression was assessed. A useful future line of investigation here could be to assess microglia activation in the days and 1-2wks proceeding the 2nd IVT, and in addition to whether this is attenuated in prednisolone-treated animals. This may prove valuable information in understanding whether neutralised AAV2 can elicit innate immune activation in the retina. Whilst it is possible that antibody-bound AAV2 cannot infect neuronal cells (via blocking of binding to cell surface receptors, see below), opsonised viral particles can be engulfed by phagocytic cells, such as microglia cells [301], which express Fcγ receptors [302], and possibly the IBA1+/MHC c. II+ co-immunolabelled macrophages in the vitreous as discussed above. Therefore it is possible that neutralised AAV2 can still activate microglia/macrophage responses in the retina, possibly because the engulfed/endocytosed viral particles activate TLR9-mediated MyD88/NFκB responses via unmethylated CpG sensing [303]. Notably, AAV2-primed mice (via intramuscular injection) were recently reported to exhibit higher microglia levels than AAV2-naiive counterparts after IVT of AAV2, suggesting that pre-exposure to the virus may exert a positive effect on microglia activation/function [210]. Whilst the reasons for this remain unclear, the interaction between microglia and infiltrating CD4 T-cells could be involved and requires further characterisation [230].

Interestingly, the highest level of IBA1 immunoreactivity was observed in Group D mice (PBS $\rightarrow$AAV2), which was similar to the trends observed with the levels of CD4 and CD8 T-cell infiltration discussed above. This may reflect the fact that the innate immune response to intravitreally-delivered AAV2 vectors gradually resolves over time in accordance with recent reports [210]. Given that AAV2 was likely neutralised in the vitreous after the 2nd IVT in Groups A and B, but not in Group D, then the assessment of IBA1 immunoreactivity ef-

fectively occurred 6wk after the introduction of the inflammatory stimuli in Groups A and B, but only 3wk in Group D. Hence, the innate immune response had begun to resolve in Groups A and B but not in Group D, which may provide a possible explanation for the patterns of microglia activation observed. Considering the capacity of activated microglia cells to secrete proinflammatory cytokines [304] and engulf synapses in neurodegenerative pathologies [305], both of which may have a detrimental affect on the electrophysiological activity of the retina, the patterns of microglia activation observed in this experiment may provide a possible explanation for the ERG perturbations exhibited between the groups in this study, which is further discussed below.

6.3.5 Immunosuppression via prednisolone monotherapy is insufficient in enabling repeated gene transfer to the inner retina with AAV2 vectors

The experiments discussed above demonstrated that perioperative prednisolone administration is associated with a reduction in adaptive immune activation in response to intravitreally-delivered AAV2 vectors, in particular, the compound elicited significant reductions in NAb and TAb levels.

It was then tested whether this would be sufficient to enable repeated gene transfer, i.e. the reduction in NAb and TAb levels would be to an extent that the 2nd IVT of AAV2 would not be neutralised in the vitreous, resulting in robust mCherry expression levels in prednisolone-treated Group B mice.

First, the levels of GFP expression (1st set of IVTs were GFP-expressing AAV2 vectors) was assessed. This showed that robust GFP synthesis was present in Group A and Group B mice, which was in line with expectations. Next, the levels of mCherry expression (2nd set of IVTs were mCherry-expressing AAV2 vectors) was analysed. No mCherry expression was seen in Group A or Group B mice, however, high levels of mCherry synthesis was seen in Group D mice. This experiment therefore showed that prednisolone monotherapy was insufficient in lifting the blocking effect imposed by anti-AAV2 NAbs, and suggests that further improvements could be required so that gene therapy vectors can be repeatedly (and safely) readministered to the vitreous compartment. These findings may therefore support the conclusions of the literature review in Chapter 1 in which a comprehensive strategy could be needed to enable repeated injections of AAV2.

A possible future line of investigation here could seek to combine the findings of Chapter 4 and 5, by assessing whether readministration of AAV2 (TM), which was found to be more resistant to neutralisation to anti-AAV2 NAbs, may be possible in prednisolone-treated

animals who received an initial IVT of wild-type AAV2. In the Appendix (A.2.1) an experiment in which an initial IVT of wild-type AAV2 was followed by a 2nd IVT of AAV-DJ is outlined. AAV-DJ is a mutant capsid that was derived by 'shuffling' the cap genes of multiple wild-type AAV serotypes to develop a library of AAV cap genes. Following selection in a mouse model, AAV-DJ was identified as a capsid capable of increased liver transduction and reduced sensitivity to neutralisation by anti-AAV2 NAbs [143]. Work by Lerch et. al. showed that binding of a key anti-AAV NAb, A20, was limited in AAV-DJ incubations due to changes in the VR-I region of the capsid [306]; a change depicted in Appendix Figure A.2.1. For this reason, AAV-DJ was selected as a mutant capsid that may be able to circumvent the blocking effect imposed by anti-AAV2 NAbs that proceeds IVT. Whilst no rescue of mCherry expression was seen in the AAV-DJ group in this experiment, it is possible that prednisolone immunosuppression combined with a capsid shuffling strategy or the incorporation of phosphodegron mutations into AAV2 capsids could be sufficient to bypass the NAb response to intravitreally-delivered vector protein.

6.3.6 Repeated bilateral injections of AAV2 may be associated with electrophysiological perturbations in the murine retina

The results outlined above showed that T-cell infiltration and microglia activation may be induced by injections of AAV2. As a result, it was then tested whether this immune activation may be associated with electrophysiological changes in the murine retina. Assessment of ERG recordings showed that pSTR (RGC function) values were lower in Group A and B mice than PBS IVT control Group C mice. Further, the lowest pSTR values were observed in Group D (PBS $\rightarrow$AAV2) mice. These trends were largely recapitulated in the B-wave (rod bipolar function) and A-wave (rod photoreceptor function) datasets, wherein reduced electrophysiological activity was detected in Group A and B mice compared to Group C mice in the PBS IVT control group. However, when assessing B-wave and A-wave data, no significant differences were observed between Group A/B and Group D mice. These data may therefore suggest that the repeated bilateral IVTs of AAV2 were associated reduced electrophysiological function in the retina, and that the immune response induced by the gene therapy vectors may have elicited a degenerative effect on RGC, rod bipolar and rod photoreceptor function. For instance, the induction of microglia activation may have increased the pruning/engulfment of synaptic junctions in the RGC layer, inner plexiform layer (IPL) and outer plexiform layer (OPL). Whilst microglia-mediated synaptic pruning is an important aspect of regulating the architecture of neuronal circuits during development under non-pathological conditions, excessive pruning is a common facet of neurodegeneration [307] and may be associated with aberrant synap-

tic function [308]. However, determining the precise cellular and molecular pathways that provide a possible link between synaptic pruning and reduced electrophysiological activity in the retina would require further investigations. Another possibility is that the production of proinflammatory cytokines arising from the AAV2 IVTs was responsible. Activated microglia cells, for example, are thought to upregulate release of cytokines like TNFα,which has been associated with the induction of apoptosis in neuronal cell types [309]. Microglia may not have been the only cell type responsible however, as elevated TNFα production has been described in astrocytes and neurones in response to inflammatory stimuli [310]. Therefore another possibility for the reduced ERG recordings observed may relate to the induction of neuronal apoptosis by proinflammatory cytokines however, further work would be required to establish this as a mechanism underpinning perturbed electrophysiological function. For instance, qPCR or ELISA could be used to establish elevated TNFα and IL1β levels and immunohistochemistry to identify changes in expression of apoptotic markers like BAX or caspase-3 could be beneficial. It is possible that inflammation in the retina modulated electrophysiological activity in the retina through other mechanisms, however. Several reports have documented reduced electrophysiological activity in neuronal cells arising from TNFα [310, 311] and interleukin-6 (IL-6) exposure [312], which may be relevant to the inflammation observed in this study. However, the relationship between increased cytokine levels and neuroelectrophysiology is clearly complicated, where in some scenarios, elevated TNFα and IL1β have been linked with elevated excitatory glutamatergic transmission and downregulated inhibitory GABAergic transmission in seizure/epilepsy models [313].

An alternative source of cytokines that may have affected ERG recordings was the infiltration of CD4 T-cells outlined above. In response to a viral infection, CD4 T-cells can elicit pro-apoptotic signalling by secreting FAS and TRAIL ligands which bind to cognate receptors on virally-infected cells [314]. The infiltration of the retina by CD8 T-cells may also have played a role, given the documented capacity of these cells to induce cytotoxicity in MHC c. I+ virally-infected cells [315]. However, a precise delineation of the role of T-cell-mediated killing of virally-infected cells in response to AAV2 IVTs would require further experimentation, for instance, starting with an assessment of whether the infiltrating cells are exhibiting effector functionality as outlined above. Initially, this could be achieved via sorting for a particular population of cells and analysing differential gene expression levels with single cell RNA sequencing technologies. This could be subsequently expanded to a spatial multiomics approach in which the co-localisation of a cytolytic CD8 T-cell and a virally-infected RGC could be used to describe a possible role for these cells in eliciting apoptosis, which may explain reduced pSTR ERG recordings, for example. Another approach that could be tested to this end is a synapse engulfment assay, in which the expression of lysosome-associated mark-

ers (like CD68) in microglia cells is co-localised with pre- and post-synapse markers [316].

A key issue arising from the assessment of ERG perturbations induced by AAV2 IVTs in this thesis was the apparent disparity between the results of Chapter 4 and Chapter 5. In Chapter 4, the IVTs were not associated with ERG deficits across any of the injection groups, nor population of retinal neuron (pSTR, B- and A-wave etc). In Chapter 5 however, significant differences between PBS-injected and AAV2-injected mice were detected. Clearly, one key difference between these two studies is that mice in Chapter 4 were injected once with AAV2 whilst mice in Chapter 5 received repeated bilateral injections of the virus. The age of the mice enrolled in the studies may also have played a role. Mice in Chapter 4 were six weeks old when IVTs were performed, however in Chapter 5, the 1st set of IVTs were performed at ten weeks and the 2nd set at 13 weeks. In humans, age-related changes in immune function has been described, and this may involve an increase in the intensity and duration of innate immune responses [317], and reports in the literature focussing on mouse models have demonstrated elevated microglia activation in older mice in response to the injection of inflammatory stimuli into the hippocampus [318], which may be due to elevated MHC c. II expression [319] in addition to increased toll-like receptor expression [320]. However, whether an increase in the innate immune response in the older animals enrolled in Chapter 5 vs Chapter 4 was responsible for the differences in ERG recordings will require further investigation. An interesting set of experiments in this regard could be to undertake a direct comparison of the innate immune response arising from AAV2 IVTs in aged vs. young mice, in terms of severity/magnitude and duration/time to resolution, and to test whether this correlates to changes in ERG recordings similar to that outlined in Chapter 5. This may be of relevance to complex non-genetic diseases of the retina, such as glaucoma and diabetic eye disease, in which the innate immune response to the vectors may be greater, highlighting a possible safety issue to ocular gene therapy in these patients. To validate the perturbations in electrophysiological function observed in this study, immunohistochemical analysis of synapse markers, such as VGlut1, synaptotagmin-1, and PSD-95 etc could be used. Ideally, a synapse coupling assay would be employed in which a dendrite (MAP2) counterstain is used to delineate RGC dendrites and a pre- and post-synapse markers are co-localised using tools like Puncta Analyser, thus enabling accurate quantification of synaptic damage [321].

6.3.7 Summary of effects of prednisolone on attenuating immune activation in AAV2-challenged mice

The results from this study showed that perioperative prednisolone administration limited the induction of a humoral immune response to intravitreally delivered AAV2 vectors. Mech-

anistically, this was shown to be via the inhibition of GC reactions, specifically, reductions in Tfh/GC B-cell levels and inhibition of B-cell class-switching. Prednisolone also reduced the levels of infiltrating CD4 and CD8 T-cells into the retina, although no changes in microglia activation were observed, possibly due to the timing of the innate and adaptive immune response to the vectors. Whilst significant reductions in NAb and TAb levels were seen, the effect of prednisolone monotherapy was insufficient to enable repeated gene transfer to the inner retina, indicating that the optimal immunosuppression protocols need to be further evaluated. Finally, repeated bilateral injections of AAV2 were associated with electrophysiological perturbations in the murine retina. Further work from independent research groups will be important to validate these findings, for instance, by assessing possible synaptic changes that may have been facilitated by activated microglia cells.

6.4 Summary of the findings of this thesis

This thesis began with a literature review of clinical and preclinical studies investigating the generation of humoral immune responses to intraocular injections of AAV gene therapies, and possible solutions to circumvent this problem. This analysis concluded that a comprehensive and multifaceted strategy may be needed in order to repeatedly and safely administer AAV to the inner retina, and possibly to other organs as well. This was deemed an important problem to address given the possible benefits of achieving repeated gene transfer in patients, namely, (i) the ability to treat complex pathologies by injecting multiple therapeutic constructs, (ii) the potential to increase the therapeutic effect if clinical benefits diminished over time, and (iii) the need to safely and effectively inject into the contralateral eye in ocular gene therapy trials. As such, two possible components of the comprehensive strategy outlined in Chapter 1 were tested. First, a capsid mutagenesis strategy was utilised, in which phosphodegron residues were mutated to prevent cytosolic degradation of vector protein and enable robust transduction at low vector dose. However, these designer capsids elicited an increase in humoral and cellular adaptive responses and glial cell activation vs. wild-type counterparts. Further, attenuated binding to AAV2's primary receptor was identified as a possible facet of phosphodegron capsid biology that could provide insight into the mechanisms underpinning the increase in immune activation. These possible changes in AAV2 oligomeric conformation was also linked to a slight escape from neutralisation by anti-AAV2 NAbs, highlighting a possible utility in overcoming pre-existing humoral immunity to the capsids. Second, the benefits of a small molecule immunosuppressant, prednisolone, were assessed in the context of depleting anti-AAV2 NAb titres in responses to repeated bilateral IVTs. Perioperative administration of the compound was found to reduce NAb and TAb levels, possibly via the inhibition of splenic GC reactions. In addition, reduced CD4 and CD8 T-cell infiltration into the retina was observed, although no detectable changes in microglia activation were evident in prednisolone treated mice. However, prednisolone monotherapy alone proved insufficient in lifting the blocking effect imposed by anti-AAV2 NAbs, suggesting further optimisation to immunosuppression protocols may be required. Nonetheless, this study demonstrated that perioperative prednisolone administration could be a useful means of enabling repeated gene transfer if used in conjunction with other means of circumventing humoral immunity. In summary, this thesis outlined the need for a comprehensive strategy to enable repeated gene transfer in patients, highlighted novel aspects of AAV2 phosphodegron mutant capsid immunobiology and identified prednisolone administration as a possible tool that could be used to reduce NAb responses to vector protein.

Bibliography

[1] Eric Hastie and R. Jude Samulski. Adeno-Associated Virus at 50: A Golden Anniversary of Discovery, Research, and Gene Therapy Success - A Personal Perspective. *Human Gene Therapy*, 26(5):257–265, 2015.

[2] A Srivastava, E W Lusby, and K I Berns. Nucleotide sequence and organization of the adeno-associated virus 2 genome. *Journal of Virology*, 45(2):555–564, 1983.

[3] J. A. Rose, K. I. Berns, M. D. Hoggan, and F. J. Koczot. Evidence for a single-stranded adenovirus-associated virus genome: formation of a DNA density hybrid on release of viral DNA. *Proceedings of the National Academy of Sciences of the United States of America*, 64(3):863–869, nov 1969.

[4] S K McLaughlin, P Collis, P L Hermonat, and N Muzyczka. Adeno-associated virus general transduction vectors: analysis of proviral structures. *Journal of Virology*, 62(6):1963–1973, 1988.

[5] C. A. Laughlin, H. Westphal, and B. J. Carter. Spliced adenovirus-associated virus RNA. *Proceedings of the National Academy of Sciences of the United States of America*, 76(11):5567–5571, 1979.

[6] Dong Soo Im and Nicholas Muzyczka. The AAV origin binding protein Rep68 is an ATP-dependent site-specific endonuclease with DNA helicase activity. *Cell*, 61(3):447–457, 1990.

[7] S P Becerra, F Koczot, P Fabisch, and J A Rose. Synthesis of adeno-associated virus structural proteins requires both alternative mRNA splicing and alternative initiations from a single transcript. *Journal of Virology*, 62(8):2745–2754, 1988.

[8] R. Jude Samulski and Nicholas Muzyczka. AAV-mediated gene therapy for research and therapeutic purposes. *Annual Review of Virology*, 1(1):427–451, 2014.

[9] Anna C. Maurer, Simon Pacouret, Ana Karla Cepeda Diaz, Jessica Blake, Eva Andres-Mateos, and Luk H. Vandenberghe. The Assembly-Activating Protein Promotes Stability and Interactions between AAV's Viral Proteins to Nucleate Capsid Assembly. *Cell Reports*, 23(6):1817–1830, 2018.

[10] Zhijian Wu, Hongyan Yang, and Peter Colosi. Effect of genome size on AAV vector packaging. *Molecular Therapy*, 18(1):80–86, 2010.

[11] Vivian W. Choi, Douglas M. McCarty, and R. Jude Samulski. Host Cell DNA Repair Pathways in Adeno-Associated Viral Genome Processing. *Journal of Virology*, 80(21):10346–10356, 2006.

[12] S. Pillay, N. L. Meyer, A. S. Puschnik, O. Davulcu, J. Diep, Y. Ishikawa, L. T. Jae, J. E. Wosen, C. M. Nagamine, M. S. Chapman, and J. E. Carette. An essential receptor for adeno-associated virus infection. *Nature*, 530(7588):108–112, 2016.

[13] P.-J. Xiao and R. J. Samulski. Cytoplasmic Trafficking, Endosomal Escape, and Perinuclear Accumulation of Adeno-Associated Virus Type 2 Particles Are Facilitated by Microtubule Network. *Journal of Virology*, 86(19):10462–10473, 2012.

[14] Joseph M. Kelich, Jiong Ma, Biao Dong, Qizhao Wang, Mario Chin, Connor M. Magura, Weidong Xiao, and Weidong Yang. Super-resolution imaging of nuclear import of adeno-associated virus in live cells. *Molecular Therapy - Methods & Clinical Development*, 2:15047, 2015.

[15] Garrett Edward Berry and Aravind Asokan. Cellular transduction mechanisms of adeno-associated viral vectors. *Current Opinion in Virology*, 21:54–60, dec 2016.

[16] Arianna Moiani, Ylenia Paleari, Daniela Sartori, Riccardo Mezzadra, Annarita Miccio, Claudia Cattoglio, Fabienne Cocchiarella, Maria Rosa Lidonnici, Giuliana Ferrari, and Fulvio Mavilio. Lentiviral vector integration in the human genome induces alternative splicing and generates aberrant transcripts. *Journal of Clinical Investigation*, 122(5):1653–1666, 2012.

[17] Arun Srivastava. In vivo tissue-tropism of adeno-associated viral vectors. *Current Opinion in Virology*, 21:75–80, dec 2016.

[18] Pasqualina Colella, Giuseppe Ronzitti, and Federico Mingozzi. Emerging Issues in AAV-Mediated In Vivo Gene Therapy. *Molecular Therapy - Methods & Clinical Development*, 8:87–104, mar 2018.

[19] Hanen Khabou, Chloé Cordeau, Laure Pacot, Sylvain Fisson, and Deniz Dalkara. Dosage Thresholds and Influence of Transgene Cassette in Adeno-Associated Virus-Related Toxicity. *Human Gene Therapy*, 29(11):1235–1241, 2018.

[20] Sangamo Biosciences. Ascending Dose Study of Genome Editing by the Zinc Finger Protein (ZFP) Therapeutic SB-FIX in Severe Hemophilia B - Full Text View - ClinicalTrials.gov, 2016.

[21] Ultragenyx Pharmaceutical Inc. Ultragenyx Announces Positive Topline Cohort 2 Results from Phase 1 / 2 Clinical Study of DTX301 Gene Therapy in Ornithine Transcarbamylase (OTC) Deficiency and Progression to Higher Dose, 2018.

[22] A Fabry Disease Gene Therapy Study, jul 2019.

[23] Stylianos Michalakis, Christian Schön, Elvir Becirovic, and Martin Biel. Gene therapy for achromatopsia. *Journal of Gene Medicine*, 19(3):2944, mar 2017.

[24] Gerard A. Rodrigues, Evgenyi Shalaev, Thomas K. Karami, James Cunningham, Nigel K.H. Slater, and Hongwen M. Rivers. Pharmaceutical Development of AAV-Based Gene Therapy Products for the Eye. *Pharmaceutical Research*, 36(2):29, feb 2019.

[25] Roman Teo Oliynyk. Future preventive gene therapy of polygenic diseases from a population genetics perspective. *International Journal of Molecular Sciences*, 20(20):5013, oct 2019.

[26] Alireza Shahryari, Marie Saghaeian Jazi, Saeed Mohammadi, Hadi Razavi Nikoo, Zahra Nazari, Elaheh Sadat Hosseini, Ingo Burtscher, Seyed Javad Mowla, and Heiko Lickert. Development and clinical translation of approved gene therapy products for genetic disorders. *Frontiers in Genetics*, 10(SEP):868, sep 2019.

[27] Samiah Al-Zaidy, A. Simon Pickard, Kavitha Kotha, Lindsay N. Alfano, Linda Lowes, Grace Paul, Kathleen Church, Kelly Lehman, Douglas M. Sproule, Omar Dabbous, Benit Maru, Katherine Berry, W. David Arnold, John T. Kissel, Jerry R. Mendell, and Richard Shell. Health outcomes in spinal muscular atrophy type 1 following AVXS-101 gene replacement therapy. *Pediatric Pulmonology*, 54(2):179–185, 2019.

[28] Vamshi K. Rao, Daniel Kapp, and Mary Schroth. Gene therapy for spinal muscular atrophy: An emerging treatment option for a devastating disease. *Journal of Managed Care and Specialty Pharmacy*, 24:S3–S16, 2018.

[29] Frans P.M. Cremers, José A.J.M. van den Hurk, and Anneke I. den Hollander. Molecular genetics of Leber congenital amaurosis. *Human Molecular Genetics*, 11(10):1169–1176, 2002.

[30] Stephen Russell, Jean Bennett, Jennifer A. Wellman, Daniel C. Chung, Zi-Fan Yu, Amy Tillman, Janet Wittes, Julie Pappas, Okan Elci, Sarah McCague, Dominique Cross, Kathleen A. Marshall, Jean Walshire, Taylor L. Kehoe, Hannah Reichert, Maria Davis, Leslie Raffini, Lindsey A. George, F. Parker Hudson, Laura Dingfield, Xiaosong Zhu, Julia A. Haller, Elliott H. Sohn, Vinit B. Mahajan, Wanda Pfeifer, Michelle Weckmann, Chris Johnson, Dina Gewaily, Arlene Drack, Edwin Stone, Katie Wachtel, Francesca Simonelli, Bart P. Leroy, J. Fraser Wright, Katherine A. High, and Albert M. Maguire. Efficacy and safety of voretigene neparvovec (AAV2-hRPE65v2) in patients with RPE65 -mediated inherited retinal dystrophy: a randomised, controlled, open-label, phase 3 trial. *The Lancet*, 390(10097):849–860, aug 2017.

[31] Albert M. Maguire, Stephen Russell, Jennifer A. Wellman, Daniel C. Chung, Zi Fan Yu, Amy Tillman, Janet Wittes, Julie Pappas, Okan Elci, Kathleen A. Marshall, Sarah McCague, Hannah Reichert, Maria Davis, Francesca Simonelli, Bart P. Leroy, J. Fraser Wright, Katherine A. High, and Jean Bennett. Efficacy, Safety, and Durability of Voretigene Neparvovec-rzyl in RPE65 MutationâAssociated Inherited Retinal Dystrophy: Results of Phase 1 and 3 Trials. *Ophthalmology*, 126(9):1273–1285, 2019.

[32] P. Yu-Wai-Man, M. Votruba, A. T. Moore, and P. F. Chinnery. Treatment strategies for inherited optic neuropathies: Past, present and future. *Eye (Basingstoke)*, 28(5):521–537, 2014.

[33] et al. Yu-Wai-Man P, Moster M, Sadun A. Efficacy of rAAV2/2-ND4 Gene Therapy for Leber Hereditary Optic Neuropathy: 96-Week Data From the Phase 3 RESCUE Trial. San Francisco, 2019.

[34] Céline Bouquet, Catherine Vignal Clermont, Anne Galy, Serge Fitoussi, Laure Blouin, Marion R. Munk, Sonia Valero, Sandrine Meunier, Barrett Katz, José Alain Sahel, and Nitza Thomasson. Immune Response and Intraocular Inflammation in Patients with Leber Hereditary Optic Neuropathy Treated with Intravitreal Injection of Recombinant Adeno-Associated Virus 2 Carrying the ND4 Gene: A Secondary Analysis of a Phase 1/2 Clinical Trial. *JAMA Ophthalmology*, 137(4):399–406, 2019.

[35] Trine H. Mogensen. Pathogen recognition and inflammatory signaling in innate immune defenses. *Clinical Microbiology Reviews*, 22(2):240–273, 2009.

[36] Céline Vandamme, Oumeya Adjali, and Federico Mingozzi. Unraveling the Complex Story of Immune Responses to AAV Vectors Trial After Trial. *Human Gene Therapy*, 28(11):1061–1074, 2017.

[37] Nathan D. Pennock, Jason T. White, Eric W. Cross, Elizabeth E. Cheney, Beth A. Tamburini, and Ross M. Kedl. T cell responses: Naïve to memory and everything in between. *American Journal of Physiology - Advances in Physiology Education*, 37(4):273–283, 2013.

[38] Weiguo Cui and Susan M. Kaech. Generation of effector CD8+ T cells and their conversion to memory T cells. *Immunological Reviews*, 236(1):151–166, 2010.

[39] Julie Tellier and Stephen L. Nutt. Plasma cells: The programming of an antibody-secreting machine. *European Journal of Immunology*, 49(1):30–37, 2019.

[40] M. T. Dorak. Basic Immunology: Functions and Disorders of the Immune System. *American Journal of Epidemiology*, 155(2):185–186, 2002.

[41] Anita Kruzik, Damir Fetahagic, Bettina Hartlieb, Sebastian Dorn, Herwig Koppensteiner, Frank M. Horling, Friedrich Scheiflinger, Birgit M. Reipert, and Maurus de la Rosa. Prevalence of Anti-Adeno-Associated Virus Immune Responses in International Cohorts of Healthy Donors. *Molecular Therapy - Methods & Clinical Development*, 14:126–133, sep 2019.

[42] Jean Charles Nault, Shalini Datta, Sandrine Imbeaud, Andrea Franconi, Maxime Mallet, Gabrielle Couchy, Eric Letouzé, Camilla Pilati, Benjamin Verret, Jean Frédéric Blanc, Charles Balabaud, Julien Calderaro, Alexis Laurent, Mélanie Letexier, Paulette Bioulac-Sage, Fabien Calvo, and Jessica Zucman-Rossi. Recurrent AAV2-related insertional mutagenesis in human hepatocellular carcinomas. *Nature Genetics*, 47(10):1187–1193, 2015.

[43] Jean Charles Nault, Iadh Mami, Tiziana La Bella, Shalini Datta, Sandrine Imbeaud, Andrea Franconi, Maxime Mallet, Gabrielle Couchy, Eric Letouzé, Camilla Pilati, Benjamin Verret, Jean Frédéric Blanc, Charles Balabaud, Julien Calderaro, Alexis Laurent, Mélanie Letexier, Paulette Bioulac-Sage, Fabien Calvo, and Jessica Zucman-Rossi. Wild-type AAV insertions in hepatocellular carcinoma do not inform debate over genotoxicity risk of vectorized AAV. *Molecular Therapy*, 24(4):660–661, 2016.

[44] S. Nayak and R. W. Herzog. Progress and prospects: Immune responses to viral vectors. *Gene Therapy*, 17(3):295–304, 2010.

[45] Lauren E. Mays, Lili Wang, Jianping Lin, Peter Bell, Alison Crawford, E. John Wherry, and James M. Wilson. AAV8 induces tolerance in murine muscle as a result of poor APC transduction, T cell exhaustion, and minimal MHCI upregulation on target cells. *Molecular Therapy*, 22(1):28–41, 2014.

[46] Axel Rossi, Léa Dupaty, Ludovic Aillot, Liang Zhang, Célia Gallien, Michael Hallek, Margarete Odenthal, Sahil Adriouch, Anna Salvetti, and Hildegard Büning. Vector uncoating limits adeno-associated viral vector-mediated transduction of human dendritic cells and vector immunogenicity. *Scientific Reports*, 9(1):3631, dec 2019.

[47] William Wold and Karoly Toth. Adenovirus Vectors for Gene Therapy, Vaccination and Cancer Gene Therapy. *Current Gene Therapy*, 13(6):421–433, 2014.

[48] Marianna Hösel, Mathias Broxtermann, Hanna Janicki, Knud Esser, Silke Arzberger, Pia Hartmann, Sonja Gillen, Jörg Kleeff, Dirk Stabenow, Margarete Odenthal, Percy Knolle, Michael Hallek, Ulrike Protzer, and Hildegard Büning. Toll-like receptor 2-mediated innate immune response in human nonparenchymal liver cells toward adeno-associated viral vectors. *Hepatology*, 55(1):287–297, 2012.

[49] Geoffrey L. Rogers, Jamie L. Shirley, Irene Zolotukhin, Sandeep R.P. Kumar, Alexandra Sherman, George Q. Perrin, Brad E. Hoffman, Arun Srivastava, Etiena Basner-Tschakarjan, Mark A. Wallet, Cox Terhorst, Moanaro Biswas, and Roland W. Herzog. Plasmacytoid and conventional dendritic cells cooperate in crosspriming AAV capsid-specific CD8+ T cells. *Blood*, 129(24):3184–3195, 2017.

[50] Scott N. Ashley, Suryanarayan Somanathan, April R. Giles, and James M. Wilson. TLR9 signaling mediates adaptive immunity following systemic AAV gene therapy. *Cellular Immunology*, 346:103997, dec 2019.

[51] Roland W. Herzog, Mario Cooper, George Q. Perrin, Moanaro Biswas, Ashley T. Martino, Laurence Morel, Cox Terhorst, and Brad E. Hoffman. Regulatory T cells and TLR9 activation shape antibody formation to a secreted transgene product in AAV muscle gene transfer. *Cellular Immunology*, 342:103682, aug 2019.

[52] Jamie L. Shirley, Geoffrey D. Keeler, Alexandra Sherman, Irene Zolotukhin, David M. Markusic, Brad E. Hoffman, Laurence M. Morel, Mark A. Wallet, Cox Terhorst, and Roland W. Herzog. Type I IFN Sensing by cDCs and CD4+ T Cell Help Are Both Requisite for Cross-Priming of AAV Capsid-Specific CD8+ T Cells. *Molecular Therapy*, 28(3):758–770, 2020.

[53] Wenwei Shao, Lauriel F. Earley, Zheng Chai, Xiaojing Chen, Junjiang Sun, Ting He, Meng Deng, Matthew L. Hirsch, Jenny Ting, R. Jude Samulski, and Chengwen Li. Double-stranded RNA innate immune response activation from long-term adeno-associated virus vector transduction. *JCI Insight*, 3(12):120474, jun 2018.

[54] Helena Costa Verdera, Klaudia Kuranda, and Federico Mingozzi. AAV Vector Immunogenicity in Humans: A Long Journey to Successful Gene Transfer. *Molecular Therapy*, 28(3):723–746, 2020.

[55] Daniel J. Hui, Shyrie C. Edmonson, Gregory M. Podsakoff, Gary C. Pien, Lacramioara Ivanciu, Rodney M. Camire, Hildegund Ertl, Federico Mingozzi, Katherine A. High, and Etiena Basner-Tschakarjan. AAV capsid CD8+ T-cell epitopes are highly conserved across AAV serotypes. *Molecular Therapy - Methods & Clinical Development*, 2:15–29, 2015.

[56] Klaudia Kuranda, Priscilla Jean-Alphonse, Christian Leborgne, Romain Hardet, Fanny Collaud, Solenne Marmier, Helena Costa Verdera, Giuseppe Ronzitti, Philippe Veron, and Federico Mingozzi. Exposure to wild-type AAV drives distinct capsid immunity profiles in humans. *Journal of Clinical Investigation*, 128(12):5267–5279, 2018.

[57] Gary C. Pien, Etiena Basner-Tschakarjan, Daniel J. Hui, Ashley N. Mentlik, Jonathan D. Finn, Nicole C. Hasbrouck, Shangzhen Zhou, Samuel L. Murphy, Marcela V. Maus, Federico Mingozzi, Jordan S. Orange, and Katherine A. High. Capsid antigen presentation flags human hepatocytes for destruction after transduction by adeno-associated viral vectors. *Journal of Clinical Investigation*, 119(6):1688–1695, 2009.

[58] Federico Mingozzi, Marcela V. Maus, Daniel J. Hui, Denise E. Sabatino, Samuel L. Murphy, John E.J. Rasko, Margaret V. Ragni, Catherine S. Manno, Jurg Sommer, Haiyan Jiang, Glenn F. Pierce, Hildegund C.J. Ertl, and Katherine A. High. CD18+ T-cell responses to adeno-associated virus capsid in humans. *Nature Medicine*, 13(4):419–422, 2007.

[59] Jian Chen, Qi Wu, Ping Ar Yang, Hui Chen Hsu, and John D. Mountz. Determination of specific CD4 and CD8 T cell epitopes after AAV2- and AAV8-hF.IX gene therapy. *Molecular Therapy*, 13(2):260–269, 2006.

[60] Catherine S. Manno, Valder R. Arruda, Glenn F. Pierce, Bertil Glader, Margaret Ragni, John Rasko, Margareth C. Ozelo, Keith Hoots, Philip Blatt, Barbara Konkle, Michael

Dake, Robin Kaye, Mahmood Razavi, Albert Zajko, James Zehnder, Hiroyuki Nakai, Amy Chew, Debra Leonard, J. Fraser Wright, Ruth R. Lessard, Jürg M. Sommer, Michael Tigges, Denise Sabatino, Alvin Luk, Haiyan Jiang, Federico Mingozzi, Linda Couto, Hildegund C. Ertl, Katherine A. High, and Mark A. Kay. Successful transduction of liver in hemophilia by AAV-Factor IX and limitations imposed by the host immune response. *Nature Medicine*, 12(3):342–347, 2006.

[61] Mark L. Brantly, Jeffrey D. Chulay, Lili Wang, Christian Mueller, Margaret Humphries, L. Terry Spencer, Farshid Rouhani, Thomas J. Conlon, Roberto Calcedo, Michael R. Betts, Carolyn Spencer, Barry J. Byrne, James M. Wilson, and Terence R. Flotte. Sustained transgene expression despite T lymphocyte responses in a clinical trial of rAAV1-AAT gene therapy. *Proceedings of the National Academy of Sciences of the United States of America*, 106(38):16363–16368, 2009.

[62] Mark L. Brantly, L. Terry Spencer, Margaret Humphries, Thomas J. Conlon, Carolyn T. Spencer, Amy Poirier, Wendy Garlington, Dawn Baker, Sihong Song, Kenneth I. Berns, Nicholas Muzyczka, Richard O. Snyder, Barry J. Byrne, and Terence R. Flotte. Phase I trial of intramuscular injection of a recombinant adeno-associated virus serotype 2 α1-antitrypsin (AAT) vector in AAT-deficient adults. *Human Gene Therapy*, 17(12):1177–1186, 2006.

[63] Christian Mueller, Jeffrey D. Chulay, Bruce C. Trapnell, Margaret Humphries, Brenna Carey, Robert A. Sandhaus, Noel G. McElvaney, Louis Messina, Qiushi Tang, Farshid N. Rouhani, Martha Campbell-Thompson, Ann D. Fu, Anthony Yachnis, David R. Knop, Guo Jie Ye, Mark Brantly, Roberto Calcedo, Suryanarayan Somanathan, Lee P. Richman, Robert H. Vonderheide, Maigan A. Hulme, Todd M. Brusko, James M. Wilson, and Terence R. Flotte. Human treg responses allow sustained recombinant adeno-associated virus-mediated transgene expression. *Journal of Clinical Investigation*, 123(12):5310–5318, 2013.

[64] Natalie F. Nidetz, Michael C. McGee, Longping V. Tse, Chengwen Li, Le Cong, Yunxing Li, and Weishan Huang. Adeno-associated viral vector-mediated immune responses: Understanding barriers to gene delivery. *Pharmacology & Therapeutics*, 207:425–453, mar 2020.

[65] Jerry R. Mendell, Katherine Campbell, Louise Rodino-Klapac, Zarife Sahenk, Chris Shilling, Sarah Lewis, Dawn Bowles, Steven Gray, Chengwen Li, Gloria Galloway, Vinod Malik, Brian Coley, K. Reed Clark, Juan Li, Xiao Xiao, Jade Samulski, Scott W. McPhee, R. Jude Samulski, and Christopher M. Walker. Dystrophin Immunity in

Duchenne's Muscular Dystrophy. *New England Journal of Medicine*, 363(15):1429–1437, 2010.

[66] Marc Tardieu, Michel Zérah, Marie Lise Gougeon, Jérome Ausseil, Stéphanie de Bournonville, Béatrice Husson, Dimitrios Zafeiriou, Giancarlo Parenti, Philippe Bourget, Béatrice Poirier, Valérie Furlan, Cécile Artaud, Thomas Baugnon, Thomas Roujeau, Ronald G. Crystal, Christian Meyer, Kumaran Deiva, and Jean Michel Heard. Intracerebral gene therapy in children with mucopolysaccharidosis type IIIB syndrome: an uncontrolled phase 1/2 clinical trial. *The Lancet Neurology*, 16(9):712–720, 2017.

[67] William Hoffman, Fadi G. Lakkis, and Geetha Chalasani. B cells, antibodies, and more. *Clinical Journal of the American Society of Nephrology*, 11(1):137–154, 2016.

[68] Matthew D. Thomas, Bhaskar Srivastava, and David Allman. Regulation of peripheral B cell maturation. *Cellular Immunology*, 239(2):92–102, 2006.

[69] Gabriel D. Victora and Michel C. Nussenzweig. Germinal centers. *Annual Review of Immunology*, 30(1):429–457, apr 2012.

[70] Mark J. Shlomchik and Florian Weisel. Germinal center selection and the development of memory B and plasma cells. *Immunological Reviews*, 247(1):52–63, 2012.

[71] Masamichi Muramatsu, Kazuo Kinoshita, Sidonia Fagarasan, Shuichi Yamada, Yoichi Shinkai, and Tasuku Honjo. Class switch recombination and hypermutation require activation-induced cytidine deaminase (AID), a potential RNA editing enzyme. *Cell*, 102(5):553–563, 2000.

[72] Jayanta Chaudhuri and Frederick W. Alt. Class-switch recombination: Interplay of transcription, DNA deamination and DNA repair. *Nature Reviews Immunology*, 4(7):541–552, 2004.

[73] Alan Schmaljohn. Protective Antiviral Antibodies that Lack Neutralizing Activity: Precedents and Evolution of Concepts. *Current HIV Research*, 11(5):345–353, 2013.

[74] P. Brioen, D. Dekegel, and A. Boeyé. Neutralization of poliovirus by antibody-mediated polymerization. *Virology*, 127(2):463–468, 1983.

[75] Raquel Hernandez, Angel Paredes, and Dennis T. Brown. Sindbis Virus Conformational Changes Induced by a Neutralizing Anti-E1 Monoclonal Antibody. *Journal of Virology*, 82(12):5750–5760, 2008.

[76] P. J. Klasse and Q. J. Sattentau. Occupancy and mechanism in antibody-mediated neutralization of animal viruses. *Journal of General Virology*, 83(9):2091–2108, 2002.

[77] Per Johan Klasse, Rogier W. Sanders, Andrea Cerutti, and John P. Moore. How can HIV-type-1-Env immunogenicity be improved to facilitate antibody-based vaccine development? *AIDS Research and Human Retroviruses*, 28(1):1–15, 2012.

[78] RunâTao âT He, Songli Wang, Robert Anderson, Bruce L. Innis, Ananda Nisalak, Wipawee Usawattanakul, and Siripen Kalayanarooj And. Antibodies that block virus attachment to vero cells are a major component of the human neutralizing antibody response against dengue virus type 2. *Journal of Medical Virology*, 45(4):451–461, 1995.

[79] Frank P. Booy, Richard B.S. Roden, Heather L. Greenstone, John T. Schiller, and Benes L. Trus. Two antibodies that neutralize papillomavirus by different mechanisms show distinct binding patterns at 13 Å resolution. *Journal of Molecular Biology*, 281(1):95–106, 1998.

[80] F M Ruggeri and H B Greenberg. Antibodies to the trypsin cleavage peptide VP8 neutralize rotavirus by inhibiting binding of virions to target cells in culture. *Journal of Virology*, 65(5):2211–2219, 1991.

[81] Eve de Rosny, Russell Vassell, Shibo Jiang, Renate Kunert, and Carol D. Weiss. Binding of the 2F5 Monoclonal Antibody to Native and Fusion-Intermediate Forms of Human Immunodeficiency Virus Type 1 gp41: Implications for Fusion-Inducing Conformational Changes. *Journal of Virology*, 78(5):2627–2631, 2004.

[82] Michelle W. Wien, David J. Filman, Enrico A. Stura, Sophie Guillot, Francis Delpeyroux, Radu Crainic, and James M. Hogle. Structure of the complex between the fab fragment of a neutralizing antibody for type 1 poliovirus and its viral epitope. *Nature Structural Biology*, 2(3):232–243, 1995.

[83] Yoshiyuki Ishii, Keiko Tanaka, Kazunari Kondo, Takamasa Takeuchi, Seiichiro Mori, and Tadahito Kanda. Inhibition of nuclear entry of HPV16 pseudovirus-packaged DNA by an anti-HPV16 L2 neutralizing antibody. *Virology*, 406(2):181–188, 2010.

[84] Donna L. Mallery, William A. McEwan, Susanna R. Bidgood, Greg J. Towers, Chris M. Johnson, and Leo C. James. Antibodies mediate intracellular immunity through tripartite motif-containing 21 (TRIM21). *Proceedings of the National Academy of Sciences*, 107(46):19985–19990, nov 2010.

[85] Samuel L. Murphy, Hojun Li, Federico Mingozzi, Denise E. Sabatino, Daniel J. Hui, Shyrie A. Edmonson, and Katherine A. High. Diverse IgG subclass responses to adeno-associated virus infection and vector administration. *Journal of Medical Virology*, 81(1):65–74, 2009.

[86] Zachary Fitzpatrick, Christian Leborgne, Elena Barbon, Elisa Masat, Giuseppe Ronzitti, Laetitia van Wittenberghe, Alban Vignaud, Fanny Collaud, Séverine Charles, Marcelo Simon Sola, Fabienne Jouen, Olivier Boyer, and Federico Mingozzi. Influence of Pre-existing Anti-capsid Neutralizing and Binding Antibodies on AAV Vector Transduction. *Molecular Therapy - Methods & Clinical Development*, 9:119–129, jun 2018.

[87] Anne K. Zaiss, Matthew J. Cotter, Lindsay R. White, Sharon A. Clark, Norman C. W. Wong, V. Michael Holers, Jeffrey S. Bartlett, and Daniel A. Muruve. Complement Is an Essential Component of the Immune Response to Adeno-Associated Virus Vectors. *Journal of Virology*, 82(6):2727–2740, 2008.

[88] Federico Mingozzi, Janneke J. Meulenberg, Daniel J. Hui, Etiena Basner-Tschakarjan, Nicole C. Hasbrouck, Shyrie A. Edmonson, Natalie A. Hutnick, Michael R. Betts, John J. Kastelein, Erik S. Stroes, and Katherine A. High. AAV-1-mediated gene transfer to skeletal muscle in humans results in dose-dependent activation of capsid-specific T cells. *Blood*, 114(10):2077–2086, 2009.

[89] Sylvie Boutin, Virginie Monteilhet, Philippe Veron, Christian Leborgne, Olivier Benveniste, Marie Françoise Montus, and Carole Masurier. Prevalence of serum IgG and neutralizing factors against adeno-associated virus (AAV) types 1, 2, 5, 6, 8, and 9 in the healthy population: Implications for gene therapy using AAV vectors. *Human Gene Therapy*, 21(6):704–712, 2010.

[90] Roberto Calcedo, Luk H. Vandenberghe, Guangping Gao, Jianping Lin, and James M. Wilson. Worldwide epidemiology of neutralizing antibodies to adeno-associated viruses. *Journal of Infectious Diseases*, 199(3):381–390, 2009.

[91] Roberto Calcedo and James M. Wilson. Humoral Immune Response to AAV. *Frontiers in Immunology*, 4:341, 2013.

[92] Wolfgang Miesbach, Karina Meijer, Michiel Coppens, Peter Kampmann, Robert Klamroth, Roger Schutgens, Marco Tangelder, Giancarlo Castaman, Joachim Schwäble, Halvard Bonig, Erhard Seifried, Federica Cattaneo, Christian Meyer, and Frank W.G. Lee-

beek. Gene therapy with adeno-associated virus vector 5âhuman factor IX in adults with hemophilia B. *Blood*, 131(9):1022–1031, 2018.

[93] Annette Von Drygalski, Adam Giermasz, Giancarlo Castaman, Nigel S. Key, Susan Lattimore, Frank W.G. Leebeek, Wolfgang Miesbach, Michael Recht, Alison Long, Robert Gut, Eileen K. Sawyer, and Steven W. Pipe. Etranacogene dezaparvovec (AMT-061 phase 2b): Normal/near normal FIX activity and bleed cessation in hemophilia B. *Blood Advances*, 3(21):3241–3247, 2019.

[94] Catherine S. Manno, Amy J. Chew, Sylvia Hutchison, Peter J. Larson, Roland W. Herzog, Valder R. Arruda, Shing Jen Tai, Margaret V. Ragni, Arthur Thompson, Margareth Ozelo, Linda B. Couto, Debra G.B. Leonard, Frederick A. Johnson, Alan McClelland, Ciaran Scallan, Erik Skarsgard, Alan W. Flake, Mark A. Kay, Katherine A. High, and Bertil Glader. AAV-mediated factor IX gene transfer to skeletal muscle in patients with severe hemophilia B. *Blood*, 101(8):2963–2972, 2003.

[95] Virginia Haurigot, Sara Marcó, Albert Ribera, Miguel Garcia, Albert Ruzo, Pilar Villacampa, Eduard Ayuso, Sònia Añor, Anna Andaluz, Mercedes Pineda, Gemma García-Fructuoso, Maria Molas, Luca Maggioni, Sergio Muñoz, Sandra Motas, Jess Ruberte, Federico Mingozzi, Martí Pumarola, and Fatima Bosch. Whole body correction of mucopolysaccharidosis IIIA by intracerebrospinal fluid gene therapy. *Journal of Clinical Investigation*, 123(8):3254–3271, 2013.

[96] S. J. Gray, S. Nagabhushan Kalburgi, T. J. McCown, and R. Jude Samulski. Global CNS gene delivery and evasion of anti-AAV-neutralizing antibodies by intrathecal AAV administration in non-human primates. *Gene Therapy*, 20(4):450–459, 2013.

[97] M. A. Kotterman, L. Yin, J. M. Strazzeri, J. G. Flannery, W. H. Merigan, and D. V. Schaffer. Antibody neutralization poses a barrier to intravitreal adeno-associated viral vector gene delivery to non-human primates. *Gene Therapy*, 22(2):116–126, 2015.

[98] William J. Feuer, Joyce C. Schiffman, Janet L. Davis, Vittorio Porciatti, Phillip Gonzalez, Rajeshwari D. Koilkonda, Huijun Yuan, Anil Lalwani, Byron L. Lam, and John Guy. Gene therapy for leber hereditary optic neuropathy initial results. *Ophthalmology*, 123(3):558–570, 2016.

[99] John Guy, William J. Feuer, Janet L. Davis, Vittorio Porciatti, Phillip J. Gonzalez, Rajeshwari D. Koilkonda, Huijun Yuan, William W. Hauswirth, and Byron L. Lam. Gene Therapy for Leber Hereditary Optic Neuropathy: Low- and Medium-Dose Visual Results. *Ophthalmology*, 124(11):1621–1634, 2017.

[100] Jeffrey S. Heier, Saleema Kherani, Shilpa Desai, Pravin Dugel, Shalesh Kaushal, Seng H. Cheng, Cheryl Delacono, Annie Purvis, Susan Richards, Annaig Le-Halpere, John Connelly, Samuel C. Wadsworth, Rafael Varona, Ronald Buggage, Abraham Scaria, and Peter A. Campochiaro. Intravitreous injection of AAV2-sFLT01 in patients with advanced neovascular age-related macular degeneration: a phase 1, open-label trial. *The Lancet*, 390(10089):50–61, 2017.

[101] Amit C. Nathwani, Edward G.D. Tuddenham, Savita Rangarajan, Cecilia Rosales, Jenny McIntosh, David C. Linch, Pratima Chowdary, Anne Riddell, Arnulfo Jaquilmac Pie, Chris Harrington, James O'Beirne, Keith Smith, John Pasi, Bertil Glader, Pradip Rustagi, Catherine Y.C. Ng, Mark A. Kay, Junfang Zhou, Yunyu Spence, Christopher L. Morton, James Allay, John Coleman, Susan Sleep, John M. Cunningham, Deokumar Srivastava, Etiena Basner-Tschakarjan, Federico Mingozzi, Katherine A. High, John T. Gray, Ulrike M. Reiss, Arthur W. Nienhuis, and Andrew M. Davidoff. Adenovirus-Associated Virus VectorâMediated Gene Transfer in Hemophilia B. *New England Journal of Medicine*, 365(25):2357–2365, 2011.

[102] Terence R. Flotte, Bruce C. Trapnell, Margaret Humphries, Brenna Carey, Roberto Calcedo, Farshid Rouhani, Martha Campbell-Thompson, Anthony T. Yachnis, Robert A. Sandhaus, Noel G. McElvaney, Christian Mueller, Louis M. Messina, James M. Wilson, Mark Brantly, David R. Knop, Guo Jie Ye, and Jeffrey D. Chulay. Phase 2 clinical trial of a recombinant adeno-associated viral vector expressing α 1-antitrypsin: Interim results. *Human Gene Therapy*, 22(10):1239–1247, 2011.

[103] Erik S. Stroes, Melchior C. Nierman, Janneke J. Meulenberg, Remco Franssen, Jaap Twisk, C. Pieter Henny, Mario M. Maas, Aeilko H. Zwinderman, Colin Ross, Eleonora Aronica, Katherine A. High, Marcel M. Levi, Michael R. Hayden, John J. Kastelein, and Jan Albert Kuivenhoven. Intramuscular administration of AAV1-lipoprotein lipaseS447X lowers triglycerides in lipoprotein lipase-deficient patients. *Arteriosclerosis, Thrombosis, and Vascular Biology*, 28(12):2303–2304, 2008.

[104] D. Gaudet, J. Méthot, S. Déry, D. Brisson, C. Essiembre, G. Tremblay, K. Tremblay, J. De Wal, J. Twisk, N. Van Den Bulk, V. Sier-Ferreira, and S. Van Deventer. Efficacy and long-term safety of alipogene tiparvovec (AAV1-LPL S447X) gene therapy for lipoprotein lipase deficiency: An open-label trial. *Gene Therapy*, 20(4):361–369, 2013.

[105] Valerie Ferreira, Jaap Twisk, Karin Kwikkers, Eleonora Aronica, Diane Brisson, Julie Methot, Harald Petry, and Daniel Gaudet. Immune responses to intramuscular administration of alipogene tiparvovec (AAV1-LPLS447X) in a phase II Clinical trial

of lipoprotein lipase deficiency gene therapy. *Human Gene Therapy*, 25(3):180–188, 2014.

[106] Luk H. Vandenberghe. AAV Engineering Identifies a Species Barrier That Highlights a Portal to the Brain. *Molecular Therapy*, 27(5):901–903, 2019.

[107] Eloise Hudry, Eva Andres-Mateos, Eli P. Lerner, Adrienn Volak, Olivia Cohen, Bradley T. Hyman, Casey A. Maguire, and Luk H. Vandenberghe. Efficient Gene Transfer to the Central Nervous System by Single-Stranded Anc80L65. *Molecular Therapy - Methods & Clinical Development*, 10:197–209, sep 2018.

[108] Juliette Hordeaux, Qiang Wang, Nathan Katz, Elizabeth L. Buza, Peter Bell, and James M. Wilson. The Neurotropic Properties of AAV-PHP.B Are Limited to C57BL/6J Mice, 2018.

[109] Jerry R. Mendell, Samiah Al-Zaidy, Richard Shell, W. Dave Arnold, Louise R. Rodino-Klapac, Thomas W. Prior, Linda Lowes, Lindsay Alfano, Katherine Berry, Kathleen Church, John T. Kissel, Sukumar Nagendran, James L'Italien, Douglas M. Sproule, Courtney Wells, Jessica A. Cardenas, Marjet D. Heitzer, Allan Kaspar, Sarah Corcoran, Lyndsey Braun, Shibi Likhite, Carlos Miranda, Kathrin Meyer, K.D. Foust, Arthur H.M. Burghes, and Brian K. Kaspar. Single-Dose Gene-Replacement Therapy for Spinal Muscular Atrophy. *New England Journal of Medicine*, 377(18):1713–1722, 2017.

[110] Linda P. Lowes, Lindsay N. Alfano, W. David Arnold, Richard Shell, Thomas W. Prior, Markus McColly, Kelly J. Lehman, Kathleen Church, Douglas M. Sproule, Sukumar Nagendran, Melissa Menier, Douglas E. Feltner, Courtney Wells, John T. Kissel, Samiah Al-Zaidy, and Jerry Mendell. Impact of Age and Motor Function in a Phase 1/2A Study of Infants With SMA Type 1 Receiving Single-Dose Gene Replacement Therapy. *Pediatric Neurology*, 98:39–45, sep 2019.

[111] Christian Hinderer, Nathan Katz, Elizabeth L. Buza, Cecilia Dyer, Tamara Goode, Peter Bell, Laura K. Richman, and James M. Wilson. Severe Toxicity in Nonhuman Primates and Piglets Following High-Dose Intravenous Administration of an Adeno-Associated Virus Vector Expressing Human SMN. *Human Gene Therapy*, 29(3):285–298, mar 2018.

[112] Lluis Samaranch, Azucena Pérez-Cañamás, Beatriz Soto-Huelin, Vivek Sudhakar, Jerónimo Jurado-Arjona, Piotr Hadaczek, Jesús Ávila, John R. Bringas, Josefina Casas,

Haifeng Chen, Xingxuan He, Edward H. Schuchman, Seng H. Cheng, John Forsayeth, Krystof S. Bankiewicz, and María Dolores Ledesma. Adeno-associated viral vector serotype 9-based gene therapy for Niemann-Pick disease type A. *Science Translational Medicine*, 11(506):3738, aug 2019.

[113] José Cunha-Vaz, Rui Bernardes, and Conceição Lobo. Blood-retinal barrier. *European Journal of Ophthalmology*, 21(SUPPL.6):3–9, 2011.

[114] Defne Amado, Federico Mingozzi, Daniel Hui, Jeannette L. Bennicelli, Zhangyong Wei, Yifeng Chen, Erin Bote, Rebecca L. Grant, Jeffrey A. Golden, Kristina Narfstrom, Nasreen A. Syed, Stephen E. Orlin, Katherine A. High, Albert M. Maguire, and Jean Bennett. Safety and efficacy of subretinal readministration of a viral vector in large animals to treat congenital blindness. *Science Translational Medicine*, 2(21):2116, mar 2010.

[115] L. Martínez-Alcantar, D.K. Talavera-Carrillo, J.U. Pineda-Salazar, M. Ávalos-Viveros, G. Gutiérrez-Ospina, B.V. Phillips-Farfán, A.L. Fuentes-Farías, and E. Meléndez-Herrera. Anterior chamber associated immune deviation to cytosolic neural antigens avoids self-reactivity after optic nerve injury and polarizes the retinal environment to an anti-inflammatory profile. *Journal of Neuroimmunology*, 333:464–76, aug 2019.

[116] Hiroshi Keino, Shintaro Horie, and Sunao Sugita. Immune Privilege and Eye-Derived T-Regulatory Cells. *Journal of Immunology Research*, 2018:1–12, 2018.

[117] A. W. Taylor. Ocular immune privilege. In *Eye*, volume 23, pages 1885–1889, 2009.

[118] Ru Zhou and Rachel R. Caspi. Ocular immune privilege. *F1000 Biology Reports*, 2(1), jan 2010.

[119] James W.B. Bainbridge, Alexander J. Smith, Susie S. Barker, Scott Robbie, Robert Henderson, Kamaljit Balaggan, Ananth Viswanathan, Graham E. Holder, Andrew Stockman, Nick Tyler, Simon Petersen-Jones, Shomi S. Bhattacharya, Adrian J. Thrasher, Fred W. Fitzke, Barrie J. Carter, Gary S. Rubin, Anthony T. Moore, and Robin R. Ali. Effect of Gene Therapy on Visual Function in Leber's Congenital Amaurosis. *New England Journal of Medicine*, 358(21):2231–2239, 2008.

[120] James W.B. Bainbridge, Manjit S. Mehat, Venki Sundaram, Scott J. Robbie, Susie E. Barker, Caterina Ripamonti, Anastasios Georgiadis, Freya M. Mowat, Stuart G. Beattie, Peter J. Gardner, Kecia L. Feathers, Vy A. Luong, Suzanne Yzer, Kamaljit Balaggan, Ananth Viswanathan, Thomy J.L. de Ravel, Ingele Casteels, Graham E. Holder, Nick

Tyler, Fred W. Fitzke, Richard G. Weleber, Marko Nardini, Anthony T. Moore, Debra A. Thompson, Simon M. Petersen-Jones, Michel Michaelides, L. Ingeborgh van den Born, Andrew Stockman, Alexander J. Smith, Gary Rubin, and Robin R. Ali. Long-Term Effect of Gene Therapy on Leber's Congenital Amaurosis. *New England Journal of Medicine*, 372(20):1887–1897, 2015.

[121] William W. Hauswirth, Tomas S. Aleman, Shalesh Kaushal, Artur V. Cideciyan, Sharon B. Schwartz, Lili Wang, Thomas J. Conlon, Sanford L. Boye, Terence R. Flotte, Barry J. Byrne, and Samuel G. Jacobson. Treatment of Leber congenital amaurosis due to RPE65 mutations by ocular subretinal injection of adeno-associated virus gene vector: Short-term results of a phase I trial. *Human Gene Therapy*, 19(10):979–990, 2008.

[122] Samuel G. Jacobson, Artur V. Cideciyan, Ramakrishna Ratnakaram, Elise Heon, Sharon B. Schwartz, Alejandro J. Roman, Marc C. Peden, Tomas S. Aleman, Sanford L. Boye, Alexander Sumaroka, Thomas J. Conlon, Roberto Calcedo, Ji Jing Pang, Kirsten E. Erger, Melani B. Olivares, Cristina L. Mullins, Malgorzata Swider, Shalesh Kaushal, William J. Feuer, Alessandro Iannaccone, Gerald A. Fishman, Edwin M. Stone, Barry J. Byrne, and William W. Hauswirth. Gene therapy for leber congenital amaurosis caused by RPE65 mutations: Safety and efficacy in 15 children and adults followed up to 3 years. *Archives of Ophthalmology*, 130(1):9–24, 2012.

[123] Albert M. Maguire, Francesca Simonelli, Eric A. Pierce, Edward N. Pugh, Federico Mingozzi, Jeannette Bennicelli, Sandro Banfi, Kathleen A. Marshall, Francesco Testa, Enrico M. Surace, Settimio Rossi, Arkady Lyubarsky, Valder R. Arruda, Barbara Konkle, Edwin Stone, Junwei Sun, Jonathan Jacobs, Lou Dell'Osso, Richard Hertle, Jianxing Ma, T. Michael Redmond, Xiaosong Zhu, Bernd Hauck, Olga Zelenaia, Kenneth S. Shindler, Maureen G. Maguire, J. Fraser Wright, Nicholas J. Volpe, Jennifer Wellman McDonnell, Alberto Auricchio, Katherine A. High, and Jean Bennett. Safety and Efficacy of Gene Transfer for Leber's Congenital Amaurosis. *New England Journal of Medicine*, 358(21):2240–2248, 2008.

[124] Albert M. Maguire, Katherine A. High, Alberto Auricchio, J. Fraser Wright, Eric A. Pierce, Francesco Testa, Federico Mingozzi, Jeannette L. Bennicelli, Gui shuang Ying, Settimio Rossi, Ann Fulton, Kathleen A. Marshall, Sandro Banfi, Daniel C. Chung, Jessica IW Morgan, Bernd Hauck, Olga Zelenaia, Xiaosong Zhu, Leslie Raffini, Frauke Coppieters, Elfride De Baere, Kenneth S. Shindler, Nicholas J. Volpe, Enrico M. Surace, Carmela Acerra, Arkady Lyubarsky, T. Michael Redmond, Edwin Stone, Jun-

wei Sun, Jennifer Wellman McDonnell, Bart P. Leroy, Francesca Simonelli, and Jean Bennett. Age-dependent effects of RPE65 gene therapy for Leber's congenital amaurosis: a phase 1 dose-escalation trial. *The Lancet*, 374(9701):1597–1605, nov 2009.

[125] Jean Bennett, Manzar Ashtari, Jennifer Wellman, Kathleen A. Marshall, Laura L. Cyckowski, Daniel C. Chung, Sarah McCague, Eric A. Pierce, Yifeng Chen, Jeannette L. Bennicelli, Xiaosong Zhu, Gui Shuang Ying, Junwei Sun, J. Fraser Wright, Alberto Auricchio, Francesca Simonelli, Kenneth S. Shindler, Federico Mingozzi, Katherine A. High, and Albert M. Maguire. Gene therapy: AAV2 gene therapy readministration in three adults with congenital blindness. *Science Translational Medicine*, 4(120):15, feb 2012.

[126] Guylène Le Meur, Pierre Lebranchu, Fanny Billaud, Oumeya Adjali, Sébastien Schmitt, Stéphane Bézieau, Yann Péréon, Romain Valabregue, Catherine Ivan, Christophe Darmon, Philippe Moullier, Fabienne Rolling, and Michel Weber. Safety and Long-Term Efficacy of AAV4 Gene Therapy in Patients with RPE65 Leber Congenital Amaurosis. *Molecular Therapy*, 26(1):256–268, 2018.

[127] Nicola G. Ghazi, Emad B. Abboud, Sawsan R. Nowilaty, Hisham Alkuraya, Abdulrahman Alhommadi, Huimin Cai, Rui Hou, Wen Tao Deng, Sanford L. Boye, Abdulrahman Almaghamsi, Fahad Al Saikhan, Hassan Al-Dhibi, David Birch, Christopher Chung, Dilek Colak, Matthew M. LaVail, Douglas Vollrath, Kirsten Erger, Wenqiu Wang, Thomas Conlon, Kang Zhang, William Hauswirth, and Fowzan S. Alkuraya. Treatment of retinitis pigmentosa due to MERTK mutations by ocular subretinal injection of adeno-associated virus gene vector: results of a phase I trial. *Human Genetics*, 135(3):327–343, 2016.

[128] Elizabeth P. Rakoczy, Chooi May Lai, Aaron L. Magno, Matthew E. Wikstrom, Martyn A. French, Cora M. Pierce, Steven D. Schwartz, Mark S. Blumenkranz, Thomas W. Chalberg, Mariapia A. Degli-Esposti, and Ian J. Constable. Gene therapy with recombinant adeno-associated vectors for neovascular age-related macular degeneration: 1 year follow-up of a phase 1 randomised clinical trial. *The Lancet*, 386(10011):2395–2403, 2015.

[129] Ian J. Constable, Cora M. Pierce, Chooi-May Lai, Aaron L. Magno, Mariapia A. Degli-Esposti, Martyn A. French, Ian L. McAllister, Steve Butler, Samuel B. Barone, Steven D. Schwartz, Mark S. Blumenkranz, and Elizabeth P. Rakoczy. Phase 2a Randomized Clinical Trial: Safety and Post Hoc Analysis of Subretinal rAAV.sFLT-1 for Wet Age-related Macular Degeneration. *EBioMedicine*, 14:168–175, dec 2016.

[130] Xing Wan, Han Pei, Min Jian Zhao, Shuo Yang, Wei Kun Hu, Heng He, Si Qi Ma, Ge Zhang, Xiao Yan Dong, Chen Chen, Dao Wen Wang, and Bin Li. Efficacy and Safety of rAAV2-ND4 Treatment for Leberâ (tm) s Hereditary Optic Neuropathy. *Scientific Reports*, 6(1):21587, apr 2016.

[131] Vibha Anand, Narendra Chirmule, Madeleine Fersh, Albert M. Maguire, and Jean Bennett. Additional transduction events after subretinal readministration of recombinant adeno-associated virus. *Human Gene Therapy*, 11(3):449–457, 2000.

[132] Vibha Anand, Bethany Duffy, Zaixin Yang, Nadine S. Dejneka, Albert M. Maguire, and Jean Bennett. A deviant immune response to viral proteins and transgene product is generated on subretinal administration of adenovirus and adeno-associated virus. *Molecular Therapy*, 5(2):125–132, 2002.

[133] Qiuhong Li, Rehae Miller, Ping Yang Han, Jijing Pang, Astra Dinculescu, Vince Chiodo, and William W. Hauswirth. Intraocular route of AAV2 vector administration defines humoral immune response and therapeutic potential. *Molecular Vision*, 14:1760–1769, sep 2008.

[134] Deniz Dalkara, Leah C. Byrne, Ryan R. Klimczak, Meike Visel, Lu Yin, William H. Merigan, John G. Flannery, and David V. Schaffer. In vivo-directed evolution of a new adeno-associated virus for therapeutic outer retinal gene delivery from the vitreous. *Science Translational Medicine*, 5(189):176–89, jun 2013.

[135] Ruslan Grishanin, Brian Vuillemenot, Pallavi Sharma, Annahita Keravala, Judith Greengard, Claire Gelfman, Mark Blumenkrantz, Matthew Lawrence, Wenzheng Hu, Szilárd Kiss, and Mehdi Gasmi. Preclinical Evaluation of ADVM-022, a Novel Gene Therapy Approach to Treating Wet Age-Related Macular Degeneration. *Molecular Therapy*, 27(1):118–129, 2019.

[136] Philippe Veron, Christian Leborgne, Virginie Monteilhet, Sylvie Boutin, Samia Martin, Philippe Moullier, and Carole Masurier. Humoral and Cellular Capsid-Specific Immune Responses to Adeno-Associated Virus Type 1 in Randomized Healthy Donors. *The Journal of Immunology*, 188(12):6418–6424, 2012.

[137] Kasey L. Jackson, Robert D. Dayton, and Ronald L. Klein. AAV9 supports wide-scale transduction of the CNS and TDP-43 disease modeling in adult rats. *Molecular Therapy - Methods & Clinical Development*, 2:15–36, 2015.

[138] Luk H. Vandenberghe. 368. Optimizing Liver Transduction of the Low Seroprevalent AAV rh32.33. In *Molecular Therapy*, volume 18, pages S142–S143, may 2010.

[139] L. E. Mays, L. Wang, R. Tenney, P. Bell, H.-J. Nam, J. Lin, B. Gurda, K. Van Vliet, K. Mikals, M. Agbandje-McKenna, and J. M. Wilson. Mapping the Structural Determinants Responsible for Enhanced T Cell Activation to the Immunogenic Adeno-Associated Virus Capsid from Isolate Rhesus 32.33. *Journal of Virology*, 87(17):9473–9485, 2013.

[140] R. Thwaite, G. Pagès, M. Chillón, and A. Bosch. AAVrh.10 immunogenicity in mice and humans. Relevance of antibody cross-reactivity in human gene therapy. *Gene Therapy*, 22(2):196–201, 2015.

[141] Eric Zinn, Simon Pacouret, Vadim Khaychuk, Heikki T. Turunen, Livia S. Carvalho, Eva Andres-Mateos, Samiksha Shah, Rajani Shelke, Anna C. Maurer, Eva Maurer, Ru Xiao, and Luk H. Vandenberghe. In silico reconstruction of the viral evolutionary lineage yields a potent gene therapy vector. *Cell Reports*, 12(6):1056–1068, aug 2015.

[142] Melissa A. Kotterman and David V. Schaffer. Engineering adeno-associated viruses for clinical gene therapy. *Nature Reviews Genetics*, 15(7):445–451, 2014.

[143] Dirk Grimm, Joyce S. Lee, Lora Wang, Tushar Desai, Bassel Akache, Theresa A. Storm, and Mark A. Kay. In Vitro and In Vivo Gene Therapy Vector Evolution via Multispecies Interbreeding and Retargeting of Adeno-Associated Viruses. *Journal of Virology*, 82(12):5887–5911, 2008.

[144] M. A. Bartel, J. R. Weinstein, and D. V. Schaffer. Directed evolution of novel adeno-associated viruses for therapeutic gene delivery. *Gene Therapy*, 19(6):694–700, 2012.

[145] Longping V. Tse, Sven Moller-Tank, and Aravind Asokan. Strategies to circumvent humoral immunity to adeno-Associated viral vectors, 2015.

[146] Te Lang Wu, Hua Li, Susan M. Faust, Emily Chi, Shangzhen Zhou, Fraser Wright, Katherine A. High, and Hildegund C.J. Ertl. CD8+ T cell recognition of epitopes within the capsid of adeno-associated virus 8-based gene transfer vectors depends on vectors' genome. *Molecular Therapy*, 22(1):42–51, 2014.

[147] Longping Victor Tse, Kelli A. Klinc, Victoria J. Madigan, Ruth M.Castellanos Rivera, Lindsey F. Wells, L. Patrick Havlik, J. Kennon Smith, Mavis Agbandje-McKenna, and Aravind Asokan. Structure-guided evolution of antigenically distinct adeno-associated

virus variants for immune evasion. *Proceedings of the National Academy of Sciences of the United States of America*, 114(24):E4812–E4821, 2017.

[148] Amine Meliani, Florence Boisgerault, Zachary Fitzpatrick, Solenne Marmier, Christian Leborgne, Fanny Collaud, Marcelo Simon Sola, Severine Charles, Giuseppe Ronzitti, Alban Vignaud, Laetitia Van Wittenberghe, Beatrice Marolleau, Fabienne Jouen, Sisareuth Tan, Olivier Boyer, Olivier Christophe, Alain R. Brisson, Casey A. Maguire, and Federico Mingozzi. Enhanced liver gene transfer and evasion of preexisting humoral immunity with exosome-enveloped AAV vectors. *Blood Advances*, 1(23):2019–2031, 2017.

[149] E. Hudry, C. Martin, S. Gandhi, B. György, D. I. Scheffer, D. Mu, S. F. Merkel, F. Mingozzi, Z. Fitzpatrick, H. Dimant, M. Masek, T. Ragan, S. Tan, A. R. Brisson, S. H. Ramirez, B. T. Hyman, and C. A. Maguire. Exosome-associated AAV vector as a robust and convenient neuroscience tool. *Gene Therapy*, 23(4):380–392, 2016.

[150] Gary K. Lee, Narendra Maheshri, Brian Kaspar, and David V. Schaffer. PEG conjugation moderately protects adeno-associated viral vectors against antibody neutralization. *Biotechnology and Bioengineering*, 92(1):24–34, 2005.

[151] S. J. Beer, C. B. Matthews, C. S. Stein, B. D. Ross, J. M. Hilfinger, and B. L. Davidson. Poly (lactic-glycolic) acid copolymer encapsulation of recombinant adenovirus reduces immunogenicity in vivo. *Gene Therapy*, 5(6):740–746, 1998.

[152] G. Sailaja, H. HogenEsch, A. North, J. Hays, and S. K. Mittal. Encapsulation of recombinant adenovirus into alginate microspheres circumvents vector specific immune response. *Gene Therapy*, 9(24):1722–1729, 2002.

[153] Thai Thanh Hoang Thi, Emily H. Pilkington, Dai Hai Nguyen, Jung Seok Lee, Ki Dong Park, and Nghia P. Truong. The importance of Poly(ethylene glycol) alternatives for overcoming PEG immunogenicity in drug delivery and bioconjugation. *Polymers*, 12(2):298, feb 2020.

[154] Federico Mingozzi, Xavier M. Anguela, Giulia Pavani, Yifeng Chen, Robert J. Davidson, Daniel J. Hui, Mustafa Yazicioglu, Liron Elkouby, Christian J. Hinderer, Armida Faella, Carolann Howard, Alex Tai, Gregory M. Podsakoff, Shangzhen Zhou, Etiena Basner-Tschakarjan, John Fraser Wright, and Katherine A. High. Overcoming preexisting humoral immunity to AAV using capsid decoys. *Science Translational Medicine*, 5(194):192–94, jul 2013.

[155] Paul E. Monahan, Junjiang Sun, Tong Gui, Genlin Hu, William B. Hannah, David G. Wichlan, Zhijian Wu, Joshua C. Grieger, Chengwen Li, Thipparat Suwanmanee, Darrel W. Stafford, Carmen J. Booth, Jade J. Samulski, Tal Kafri, Scott W.J. McPhee, and R. Jude Samulski. Employing a gain-of-function factor IX variant R338L to advance the efficacy and safety of hemophilia B human gene therapy: Preclinical evaluation supporting an ongoing adeno-associated virus clinical trial. *Human Gene Therapy*, 26(2):69–81, 2015.

[156] Kai Gao, Mengxin Li, Li Zhong, Qin Su, Jia Li, Shaoyong Li, Ran He, Yu Zhang, Gregory Hendricks, Junzhi Wang, and Guangping Gao. Empty virions in AAV8 vector preparations reduce transduction efficiency and may cause total viral particle dose-limiting side effects. *Molecular Therapy - Methods & Clinical Development*, 1:9, 2014.

[157] Adrian M. Timmers, Judith A. Newmark, Heikki T. Turunen, Tanaz Farivar, Jilin Liu, Chunjuan Song, Guo Jie Ye, Steven Pennock, Chantelle Gaskin, David R. Knop, and Mark S. Shearman. Ocular Inflammatory Response to Intravitreal Injection of Adeno-Associated Virus Vector: Relative Contribution of Genome and Capsid. *Human Gene Therapy*, 31(1-2):80–89, 2020.

[158] R. H.W.M. Derksen, H. J. Schuurman, F. H.J.Gmelig Meyling, A. Struyvenberg, and L. Kater. The efficacy of plasma exchange in the removal of plasma components. *The Journal of Laboratory and Clinical Medicine*, 104(3):346–354, 1984.

[159] R. W. Erickson, W. A. Franklin, and W. Emlen. Treatment of hemorrhagic lupus pneumonitis with plasmapheresis. *Seminars in Arthritis and Rheumatism*, 24(2):114–123, 1994.

[160] S. B. Buzzigoli, M. Genovesi, P. Lambelet, C. Logi, S. Raffaelli, and D. Cattano. Plasmapheresis treatment in Guillain-Barré Syndrome: Potential benefit over intravenous immunoglobulin. *Anaesthesia and Intensive Care*, 38(2):387–389, 2010.

[161] Douglas Kazutoshi Sato, Dagoberto Callegaro, Marco Aurelio Lana-Peixoto, Patrick J. Waters, Frederico M. De Haidar Jorge, Toshiyuki Takahashi, Ichiro Nakashima, Samira Luisa Apostolos- Pereira, Natalia Talim Renata Faria Simm, Angelina Maria Martins Lino, Tatsuro Misu, Maria Isabel Leite, Masashi Aoki, and Kazuo Fujihara. Distinction between MOG antibodypositive and AQP4 antibody-positive NMO spectrum disorders. *Neurology*, 82(6):474–481, 2014.

[162] L. G. Chicoine, C. L. Montgomery, W. G. Bremer, K. M. Shontz, D. A. Griffin, K. N. Heller, S. Lewis, V. Malik, W. E. Grose, C. J. Shilling, K. J. Campbell, T. J. Preston,

B. D. Coley, P. T. Martin, C. M. Walker, K. R. Clark, Z. Sahenk, J. R. Mendell, and L. R. Rodino-Klapac. Plasmapheresis eliminates the negative impact of AAV antibodies on microdystrophin gene expression following vascular delivery. *Molecular Therapy*, 22(2):338–347, 2014.

[163] S. Vucic and L. Davies. Safety of plasmapheresis in the treatment of neurological disease. *Australian and New Zealand Journal of Medicine*, 28(3):301–305, 1998.

[164] Virginie Monteilhet, Samir Saheb, Sylvie Boutin, Christian Leborgne, Philippe Veron, Marie Françoise Montus, Philippe Moullier, Olivier Benveniste, and Carole Masurier. A 10 patient case report on the impact of plasmapheresis upon neutralizing factors against adeno-associated virus (AAV) types 1, 2, 6, and 8. *Molecular Therapy*, 19(11):2084–2091, 2011.

[165] Berangere Bertin, Philippe Veron, Christian Leborgne, Jack Yves Deschamps, Sophie Moullec, Yves Fromes, Fanny Collaud, Sylvie Boutin, Virginie Latournerie, Laetitia van Wittenberghe, Benoit Delache, Roger Le Grand, Nathalie Dereuddre-Bosquet, Olivier Benveniste, Philippe Moullier, Carole Masurier, Otto Merten, and Federico Mingozzi. Capsid-specific removal of circulating antibodies to adeno-associated virus vectors. *Scientific Reports*, 10(1):864, dec 2020.

[166] Victoria M. Velazquez, Aaron S. Meadows, Ricardo J. Pineda, Marybeth Camboni, Douglas M. McCarty, and Haiyan Fu. Effective Depletion of Pre-existing Anti-AAV Antibodies Requires Broad Immune Targeting. *Molecular Therapy - Methods & Clinical Development*, 4:159–168, mar 2017.

[167] Steven J. Gray, Stacey B. Foti, Joel W. Schwartz, Lavanya Bachaboina, Bonnie Taylor-Blake, Jennifer Coleman, Michael D. Ehlers, Mark J. Zylka, Thomas J. McCown, and R. Jude Samulski. Optimizing promoters for recombinant adeno-associated virus-mediated gene expression in the peripheral and central nervous system using self-complementary vectors. *Human Gene Therapy*, 22(9):1143–1153, 2011.

[168] Leonard A. Levin and Lynn K. Gordon. Retinal ganglion cell disorders: Types and treatments. *Progress in Retinal and Eye Research*, 21(5):465–484, 2002.

[169] Weidong Xiao, Narendra Chirmule, Michael A. Schnell, John Tazelaar, Joseph V. Hughes, and James M. Wilson. Route of Administration Determines Induction of T-Cell-Independent Humoral Responses to Adeno-Associated Virus Vectors. *Molecular Therapy*, 1(4):323–329, 2000.

[170] Sang Oh Han, Songtao Li, Elizabeth D. Brooks, Elisa Masat, Christian Leborgne, Suhrad Banugaria, Andrew Bird, Federico Mingozzi, Herman Waldmann, and Dwight Koeberl. Enhanced efficacy from gene therapy in Pompe disease using coreceptor blockade. *Human Gene Therapy*, 26(1):26–35, 2015.

[171] Christine L. Halbert, Thomas A. Standaert, Christopher B. Wilson, and A. Dusty Miller. Successful Readministration of Adeno-Associated Virus Vectors to the Mouse Lung Requires Transient Immunosuppression during the Initial Exposure. *Journal of Virology*, 72(12):9795–9805, 1998.

[172] J. H. McIntosh, M. Cochrane, S. Cobbold, H. Waldmann, S. A. Nathwani, A. M. Davidoff, and A. C. Nathwani. Successful attenuation of humoral immunity to viral capsid and transgenic protein following AAV-mediated gene transfer with a non-depleting CD4 antibody and cyclosporine. *Gene Therapy*, 19(1):78–85, 2012.

[173] Anne S. De Groot, Leonard Moise, Julie A. McMurry, Erik Wambre, Laurence Van Overtvelt, Philippe Moingeon, David W. Scott, and William Martin. Activation of natural regulatory T cells by IgG Fc-derived peptide "Tregitopes". *Blood*, 112(8):3303–3311, 2008.

[174] Daniel J. Hui, Etiena Basner-Tschakarjan, Yifeng Chen, Robert J. Davidson, George Buchlis, Mustafa Yazicioglu, Gary C. Pien, Jonathan D. Finn, Virginia Haurigot, Alex Tai, David W. Scott, Leslie P. Cousens, Shangzhen Zhou, Anne S. De Groot, and Federico Mingozzi. Modulation of CD8 + T cell responses to AAV vectors with IgG-derived MHC class II epitopes. *Molecular Therapy*, 21(9):1727–1737, 2013.

[175] Yolanda R. Carrasco and Facundo D. Batista. B cell recognition of membrane-bound antigen: an exquisite way of sensing ligands. *Current Opinion in Immunology*, 18(3):286–291, 2006.

[176] Naomi E. Harwood and Facundo D. Batista. New Insights into the Early Molecular Events Underlying B Cell Activation. *Immunity*, 28(5):609–619, 2008.

[177] Etiena Basner-Tschakarjan, Enoch Bijjiga, and Ashley T. Martino. Pre-Clinical Assessment of Immune Responses to Adeno-Associated Virus (AAV) Vectors. *Frontiers in Immunology*, 5(FEB), 2014.

[178] Jozsef Karman, Nathan K. Gumlaw, Jinhua Zhang, Ji Lei Jiang, Seng H. Cheng, and Yunxiang Zhu. Proteasome inhibition is partially effective in attenuating pre-existing

immunity against recombinant adeno-associated viral vectors. *PLoS ONE*, 7(4):34684, apr 2012.

[179] Mitchell R. Smith. Rituximab (monoclonal anti-CD20 antibody): Mechanisms of action and resistance. *Oncogene*, 22(47):7359–7368, 2003.

[180] F. Mingozzi, Y. Chen, S. C. Edmonson, S. Zhou, R. M. Thurlings, P. P. Tak, K. A. High, and M. J. Vervoordeldonk. Prevalence and pharmacological modulation of humoral immunity to AAV vectors in gene transfer to synovial tissue. *Gene Therapy*, 20(4):417–424, 2013.

[181] M. Corti, M. E. Elder, D. J. Falk, L. Lawson, B. K. Smith, S. Nayak, T. J. Conlon, N. Clément, K. Erger, E. Lavassani, M. M. Green, P. A. Doerfler, R. W. Herzog, and B. J. Byrne. B-cell depletion is protective against anti-AAV capsid immune response: A human subject case study. *Molecular Therapy - Methods and Clinical Development*, 1:14033, 2014.

[182] Federico Mingozzi, Yifeng Chen, Samuel L. Murphy, Shyrie C. Edmonson, Alex Tai, Sandra D. Price, Mark E. Metzger, Shangzhen Zhou, J. Fraser Wright, Robert E. Donahue, Cynthia E. Dunbar, and Katherine A. High. Pharmacological modulation of humoral immunity in a nonhuman primate model of AAV gene transfer for hemophilia B. *Molecular Therapy*, 20(7):1410–1416, 2012.

[183] Subhankar Chakraborty, Stefano R. Tarantolo, John Treves, David Sambol, Ralph J. Hauke, and Surinder K. Batra. Progressive multifocal leukoencephalopathy in a HIV-negative patient with small lymphocytic leukemia following treatment with rituximab. *Case Reports in Oncology*, 4(1):136–142, 2011.

[184] Maria J. Leandro. B-cell subpopulations in humans and their differential susceptibility to depletion with anti-CD20 monoclonal antibodies. *Arthritis Research & Therapy*, 15(Suppl 1):S3, 2013.

[185] Jonathan Skupsky, Yan Su, Tie-Chi Lei, and David Scott. Tolerance Induction by Gene Transfer to Lymphocytes. *Current Gene Therapy*, 7(5):369–380, 2007.

[186] Jennifer Müller and Lars Nitschke. The role of CD22 and Siglec-G in B-cell tolerance and autoimmune disease, 2014.

[187] Matthew S. Macauley, Fabian Pfrengle, Christoph Rademacher, Corwin M. Nycholat, Andrew J. Gale, Annette Von Drygalski, and James C. Paulson. Antigenic liposomes

displaying CD22 ligands induce antigen-specific B cell apoptosis. *Journal of Clinical Investigation*, 123(7):3074–3083, 2013.

[188] B. Greenberg, J. Butler, G. M. Felker, P. Ponikowski, A. A. Voors, J. M. Pogoda, R. Provost, J. Guerrero, R. J. Hajjar, and K. M. Zsebo. Prevalence of AAV1 neutralizing antibodies and consequences for a clinical trial of gene transfer for advanced heart failure. *Gene Therapy*, 23(3):313–319, 2016.

[189] Carmen Unzu, Sandra Hervás-Stubbs, Ana Sampedro, Itsaso Mauleón, Uxua Mancheño, Carlos Alfaro, Rafael Enríquez de Salamanca, Alberto Benito, Stuart G. Beattie, Harald Petry, Jesús Prieto, Ignacio Melero, and Antonio Fontanellas. Transient and intensive pharmacological immunosuppression fails to improve AAV-based liver gene transfer in non-human primates. *Journal of translational medicine*, 10(1):122, 2012.

[190] S. W.J. McPhee, C. G. Janson, C. Li, R. J. Samulski, A. S. Camp, J. Francis, D. Shera, L. Lioutermann, M. Feely, A. Freese, and P. Leone. Immune responses to AAV in a phase I study for Canavan disease. *Journal of Gene Medicine*, 8(5):577–588, 2006.

[191] Amine Meliani, Florence Boisgerault, Romain Hardet, Solenne Marmier, Fanny Collaud, Giuseppe Ronzitti, Christian Leborgne, Helena Costa Verdera, Marcelo Simon Sola, Severine Charles, Alban Vignaud, Laetitia van Wittenberghe, Giorgia Manni, Olivier Christophe, Francesca Fallarino, Christopher Roy, Alicia Michaud, Petr Ilyinskii, Takashi Kei Kishimoto, and Federico Mingozzi. Antigen-selective modulation of AAV immunogenicity with tolerogenic rapamycin nanoparticles enables successful vector re-administration. *Nature Communications*, 9(1):4098, dec 2018.

[192] Marina Moskalenko, Lili Chen, Melinda van Roey, Brian A. Donahue, Richard O. Snyder, James G. McArthur, and Salil D. Patel. Epitope Mapping of Human Anti-Adeno-Associated Virus Type 2 Neutralizing Antibodies: Implications for Gene Therapy and Virus Structure. *Journal of Virology*, 74(4):1761–1766, 2000.

[193] W. A. McEwan, F. Hauler, C. R. Williams, S. R. Bidgood, D. L. Mallery, R. A. Crowther, and L. C. James. Regulation of Virus Neutralization and the Persistent Fraction by TRIM21. *Journal of Virology*, 86(16):8482–8491, 2012.

[194] Ashley T. Martino, Etiena Basner-Tschakarjan, David M. Markusic, Jonathan D. Finn, Christian Hinderer, Shangzhen Zhou, David A. Ostrov, Arun Srivastava, Hildegund C.J.

Ertl, Cox Terhorst, Katherine A. High, Federico Mingozzi, and Roland W. Herzog. Engineered AAV vector minimizes in vivo targeting of transduced hepatocytes by capsid-specific CD8+ T cells. *Blood*, 121(12):2224–2233, 2013.

[195] Yuji Kashiwakura, Kenji Tamayose, Kazuhisa Iwabuchi, Yukihiko Hirai, Takashi Shimada, Kunio Matsumoto, Toshikazu Nakamura, Masami Watanabe, Kazuo Oshimi, and Hiroyuki Daida. Hepatocyte Growth Factor Receptor Is a Coreceptor for Adeno-Associated Virus Type 2 Infection. *Journal of Virology*, 79(1):609–614, 2005.

[196] Keyun Qing, Cathryn Mah, Jonathan Hansen, Shangzhen Zhou, Varavani Dwarki, and Arun Srivastava. Human fibroblast growth factor receptor 1 is a co-receptor for infection by adeno-associated virus 2. *Nature Medicine*, 5(1):71–77, 1999.

[197] Amanda M. Dudek, Nerea Zabaleta, Eric Zinn, Sirika Pillay, James Zengel, Caryn Porter, Jennifer Santos Franceschini, Reynette Estelien, Jan E. Carette, Guo Ling Zhou, and Luk H. Vandenberghe. GPR108 Is a Highly Conserved AAV Entry Factor. *Molecular Therapy*, 28(2):367–381, 2020.

[198] Li Zhong, Baozheng Li, Cathryn S. Mah, Lakshmanan Govindasamy, Mavis Agbandje-McKenna, Mario Cooper, Roland W. Herzog, Irene Zolotukhin, Kenneth H. Warrington, Kirsten A. Weigel-Van Aken, Jacqueline A. Hobbs, Sergei Zolotukhin, Nicholas Muzyczka, and Arun Srivastava. Next generation of adeno-associated virus 2 vectors: Point mutations in tyrosines lead to high-efficiency transduction at lower doses. *Proceedings of the National Academy of Sciences of the United States of America*, 105(22):7827–7832, 2008.

[199] Vijay Shreedhar, Angus M. Moodycliffe, Stephen E. Ullrich, Corazon Bucana, Margaret L. Kripke, and Leopoldo Flores-Romo. Dendritic cells require T cells for functional maturation in vivo. *Immunity*, 11(5):625–636, 1999.

[200] Baozheng Li, Wenqin Ma, Chen Ling, Kim Van Vliet, Lin Ya Huang, Mavis Agbandje-McKenna, Arun Srivastava, and George V. Aslanidi. Site-Directed Mutagenesis of Surface-Exposed Lysine Residues Leads to Improved Transduction by AAV2, But Not AAV8, Vectors in Murine Hepatocytes In Vivo. *Human Gene Therapy Methods*, 26(6):211–220, 2015.

[201] George V. Aslanidi, Angela E. Rivers, Luis Ortiz, Liujiang Song, Chen Ling, Lakshmanan Govindasamy, Kim Van Vliet, Mengqun Tan, Mavis Agbandje-McKenna, and Arun Srivastava. Optimization of the capsid of recombinant adeno-associated virus 2 (AAV2) vectors: the final threshold? *PloS one*, 8(3):42–59, mar 2013.

[202] Sook Hyun Chung, Iris Natalie Mollhoff, Alaknanda Mishra, Tzu Ni Sin, Taylor Ngo, Thomas Ciulla, Paul Sieving, Sara M. Thomasy, and Glenn Yiu. Host immune responses after suprachoroidal delivery of AAV8 in nonhuman primate eyes. *Human Gene Therapy*, 32(13-14):682–693, 2021.

[203] Lital N. Adler, Wei Jiang, Kartik Bhamidipati, Matthew Millican, Claudia Macaubas, Shu-chen Hung, and Elizabeth D. Mellins. The Other Function: Class II-Restricted Antigen Presentation by B Cells. *Frontiers in Immunology*, 8(MAR), mar 2017.

[204] Janet Stavnezer, Jeroen E.J. Guikema, and Carol E. Schrader. Mechanism and Regulation of Class Switch Recombination. *Annual Review of Immunology*, 26(1):261–292, apr 2008.

[205] Toine ten Broeke, Richard Wubbolts, and Willem Stoorvogel. MHC Class II Antigen Presentation by Dendritic Cells Regulated through Endosomal Sorting. *Cold Spring Harbor Perspectives in Biology*, 5(12):168–173, dec 2013.

[206] Yoko Okunuki, Ryo Mukai, Takeshi Nakao, Steven J. Tabor, Oleg Butovsky, Reza Dana, Bruce R. Ksander, and Kip M. Connor. Retinal microglia initiate neuroinflammation in ocular autoimmunity. *Proceedings of the National Academy of Sciences*, 116(20):9989–9998, may 2019.

[207] Rosa de Hoz, Blanca Rojas, Ana I. Ramírez, Juan J. Salazar, Beatriz I. Gallego, Alberto Triviño, and José M. Ramírez. Retinal Macroglial Responses in Health and Disease. *BioMed Research International*, 2016:1–13, 2016.

[208] Federico Giovannoni and Francisco J. Quintana. The Role of Astrocytes in CNS Inflammation. *Trends in Immunology*, 41(9):805–819, 2020.

[209] Ying Kai Chan, Sean K. Wang, Colin J. Chu, David A. Copland, Alexander J. Letizia, Helena Costa Verdera, Jessica J. Chiang, Meher Sethi, May K. Wang, William J. Neidermyer, Yingleong Chan, Elaine T. Lim, Amanda R. Graveline, Melinda Sanchez, Ryan F. Boyd, Thomas S. Vihtelic, Rolando Gian Carlo O. Inciong, Jared M. Slain, Priscilla J. Alphonse, Yunlu Xue, Lindsey R. Robinson-McCarthy, Jenny M. Tam, Maha H. Jabbar, Bhubanananda Sahu, Janelle F. Adeniran, Manish Muhuri, Phillip W L Tai, Jun Xie, Tyler B. Krause, Andyna Vernet, Matthew Pezone, Ru Xiao, Tina Liu, Wei Wang, Henry J. Kaplan, Guangping Gao, Andrew D. Dick, Federico Mingozzi, Maureen A. McCall, Constance L. Cepko, and George M. Church. Engineering adeno-associated viral vectors to evade innate immune and inflammatory responses. *Science Translational Medicine*, 13(580):34–38, feb 2021.

[210] Gayathri Tummala, Adam Crain, Jessica Rowlan, and Kathryn L. Pepple. Characterization of Gene Therapy Associated Uveitis Following Intravitreal Adeno-Associated Virus Injection in Mice. *Investigative ophthalmology & visual science*, 62(2):41, 2021.

[211] Samy Omri, Francine Behar-Cohen, Yvonne De Kozak, Florian Sennlaub, Lourena Mafra Verissimo, Laurent Jonet, Michle Savoldelli, Boubaker Omri, and Patricia Crisanti. Microglia/macrophages migrate through retinal epithelium barrier by a transcellular route in diabetic retinopathy: Role of PKCζ in the Goto Kakizaki rat model. *American Journal of Pathology*, 179(2):942–953, 2011.

[212] Stefanie G. Wohl, Christian W. Schmeer, Otto W. Witte, and Stefan Isenmann. Proliferative response of microglia and macrophages in the adult mouse eye after optic nerve lesion. *Investigative Ophthalmology and Visual Science*, 51(5):2686–2696, 2010.

[213] Sanford L. Boye, Antonette Bennett, Miranda L. Scalabrino, K. Tyler McCullough, Kim Van Vliet, Shreyasi Choudhury, Qing Ruan, James Peterson, Mavis Agbandje-McKenna, and Shannon E. Boye. Impact of Heparan Sulfate Binding on Transduction of Retina by Recombinant Adeno-Associated Virus Vectors. *Journal of Virology*, 90(8):4215–4231, 2016.

[214] A. Kern, K. Schmidt, C. Leder, O. J. Müller, C. E. Wobus, K. Bettinger, C. W. Von der Lieth, J. A. King, and J. A. Kleinschmidt. Identification of a Heparin-Binding Motif on Adeno-Associated Virus Type 2 Capsids. *Journal of Virology*, 77(20):11072–11081, 2003.

[215] Jason O'Donnell, Kenneth A. Taylor, and Michael S. Chapman. Adeno-associated virus-2 and its primary cellular receptor-Cryo-EM structure of a heparin complex. *Virology*, 385(2):434–443, 2009.

[216] Michael Whitehead, Andrew Osborne, Patrick Yu-Wai-Man, and Keith Martin. Humoral immune responses to AAV gene therapy in the ocular compartment. *Biological Reviews*, 96(4):1616–1644, 2021.

[217] Anne M. Schijvens, Rob ter Heine, Saskia N. de Wildt, and Michiel F. Schreuder. Pharmacology and pharmacogenetics of prednisone and prednisolone in patients with nephrotic syndrome. *Pediatric Nephrology*, 34(3):389–403, 2019.

[218] Robert H. Oakley and John A. Cidlowski. The biology of the glucocorticoid receptor: New signaling mechanisms in health and disease. *Journal of Allergy and Clinical Immunology*, 132(5):1033–1044, 2013.

[219] J. S. Goodwin, D. Atluru, S. Sierakowski, and E. A. Lianos. Mechanism of action of glucocorticosteroids. Inhibition of T cell proliferation and interleukin 2 production by hydrocortisone is reversed by leukotriene B4. *Journal of Clinical Investigation*, 77(4):1244–1250, 1986.

[220] George Q. Perrin, Roland W. Herzog, and David M. Markusic. Update on clinical gene therapy for hemophilia. *Blood*, 133(5):407–414, 2019.

[221] William J. Kovacs. To B or not to B? Glucocorticoid impact on B lymphocyte fate and function. *Endocrinology*, 155(2):339–341, 2014.

[222] Shane Crotty. T Follicular Helper Cell Differentiation, Function, and Roles in Disease. *Immunity*, 41(4):529–542, 2014.

[223] Janice S. Blum, Pamela A. Wearsch, and Peter Cresswell. Pathways of antigen processing. *Annual review of immunology*, 31:443–73, 2013.

[224] Hilda Petrs-Silva, Astra Dinculescu, Qiuhong Li, Seok Hong Min, Vince Chiodo, Ji Jing Pang, Li Zhong, Sergei Zolotukhin, Arun Srivastava, Alfred S. Lewin, and William W. Hauswirth. High-efficiency transduction of the mouse retina by tyrosine-mutant AAV serotype vectors. *Molecular Therapy*, 17(3):463–471, 2009.

[225] Renee C. Ryals, Sanford L Boye, Astra Dinculescu, William W. Hauswirth, and Shannon E. Boye. Quantifying transduction efficiencies of unmodified and tyrosine capsid mutant AAV vectors in vitro using two ocular cell lines. *Molecular vision*, 17:1090–102, apr 2011.

[226] Marti Cabanes-Creus, Adrian Westhaus, Renina Gale Navarro, Grober Baltazar, Erhua Zhu, Anais K. Amaya, Sophia H.Y. Liao, Suzanne Scott, Erwan Sallard, Kimberley L. Dilworth, Arkadiusz Rybicki, Matthieu Drouyer, Claus V. Hallwirth, Antonette Bennett, Giorgia Santilli, Adrian J. Thrasher, Mavis Agbandje-McKenna, Ian E. Alexander, and Leszek Lisowski. Attenuation of Heparan Sulfate Proteoglycan Binding Enhances In Vivo Transduction of Human Primary Hepatocytes with AAV2. *Molecular Therapy - Methods & Clinical Development*, 17:1139–1154, jun 2020.

[227] Peter Mombaerts, John Iacomini, Randall S. Johnson, Karl Herrup, Susumu Tonegawa, and Virginia E. Papaioannou. RAG-1-deficient mice have no mature B and T lymphocytes. *Cell*, 68(5):869–877, 1992.

[228] Jordi Xaus, Mònica Comalada, Marta Barrachina, Carmen Herrero, Eduard Goñalons, Concepció Soler, Jorge Lloberas, and Antonio Celada. The Expression of MHC Class

II Genes in Macrophages Is Cell Cycle Dependent. *The Journal of Immunology*, 165(11):6364–6371, 2000.

[229] E. John Wherry and Makoto Kurachi. Molecular and cellular insights into T cell exhaustion. *Nature Reviews Immunology*, 15(8):486–499, 2015.

[230] Sjoerd T. T. Schetters, Diego Gomez-Nicola, Juan J. Garcia-Vallejo, and Yvette Van Kooyk. Neuroinflammation: Microglia and T Cells Get Ready to Tango. *Frontiers in Immunology*, 8(JAN), jan 2018.

[231] Lei Tang. Multiomics sequencing goes spatial. *Nature Methods*, 18(1):31, 2021.

[232] Anthony W. Purcell, Sri H. Ramarathinam, and Nicola Ternette. Mass spectrometryâbased identification of MHC-bound peptides for immunopeptidomics. *Nature Protocols*, 14(6):1687–1707, 2019.

[233] Peter A. Szabo, Hanna Mendes Levitin, Michelle Miron, Mark E. Snyder, Takashi Senda, Jinzhou Yuan, Yim Ling Cheng, Erin C. Bush, Pranay Dogra, Puspa Thapa, Donna L. Farber, and Peter A. Sims. Single-cell transcriptomics of human T cells reveals tissue and activation signatures in health and disease. *Nature communications*, 10(1):4706, 2019.

[234] Janelle M. Montagne, Xuwen Alice Zheng, Iago Pinal-Fernandez, Jose C. Milisenda, Lisa Christopher-Stine, Thomas E. Lloyd, Andrew L. Mammen, and H. Benjamin Larman. Ultra-efficient sequencing of T Cell receptor repertoires reveals shared responses in muscle from patients with Myositis. *EBioMedicine*, 59:102–72, sep 2020.

[235] Daniel Tassone, Alexander Thompson, William Connell, Tanya Lee, Ryan Ungaro, Ping An, Yijuan Ding, and Nik S. Ding. Immunosuppression as a risk factor for COVID-19: a meta-analysis. *Internal Medicine Journal*, 51(2):199–205, 2021.

[236] Joost B. Beltman, Christopher D.C. Allen, Jason G. Cyster, and Rob J. De Boer. B cells within germinal centers migrate preferentially from dark to light zone. *Proceedings of the National Academy of Sciences of the United States of America*, 108(21):8755–8760, 2011.

[237] A. Haas, K. Zimmermann, and A. Oxenius. Antigen-Dependent and -Independent Mechanisms of T and B Cell Hyperactivation during Chronic HIV-1 Infection. *Journal of Virology*, 85(23):12102–12113, 2011.

[238] R. M. Steinman and H. Hemmi. Dendritic cells: translating innate to adaptive immunity. *Current topics in microbiology and immunology*, 311:17–58, 2006.

[239] Vivek Durai and Kenneth M. Murphy. Functions of Murine Dendritic Cells. *Immunity*, 45(4):719–736, 2016.

[240] Louise J. Young, Nicholas S. Wilson, Petra Schnorrer, Anna Proietto, Toine ten Broeke, Yohei Matsuki, Adele M. Mount, Gabrielle T. Belz, Meredith O'Keeffe, Mari Ohmura-Hoshino, Satoshi Ishido, Willem Stoorvogel, William R. Heath, Ken Shortman, and Jose A. Villadangos. Differential MHC class II synthesis and ubiquitination confers distinct antigen-presenting properties on conventional and plasmacytoid dendritic cells. *Nature Immunology*, 9(11):1244–1252, 2008.

[241] José A. Villadangos and Louise Young. Antigen-Presentation Properties of Plasmacytoid Dendritic Cells. *Immunity*, 29(3):352–361, 2008.

[242] David Vremec, Meredith O'Keeffe, Hubertus Hochrein, Martina Fuchsberger, Irina Caminschi, Mireille Lahoud, and Ken Shortman. Production of interferons by dendritic cells, plasmacytoid cells, natural killer cells, and interferon-producing killer dendritic cells. *Blood*, 109(3):1165–1173, 2007.

[243] Sarah L. Roche, Ana M. Ruiz-Lopez, Jennifer N. Moloney, Ashleigh M. Byrne, and Thomas G. Cotter. Microglial-induced Müller cell gliosis is attenuated by progesterone in a mouse model of retinitis pigmentosa. *Glia*, 66(2):295–310, 2018.

[244] Deniz Dalkara, Kathleen D. Kolstad, Natalia Caporale, Meike Visel, Ryan R. Klimczak, David V. Schaffer, and John G. Flannery. Inner limiting membrane barriers to aav-mediated retinal transduction from the vitreous. *Molecular Therapy*, 17(12):2096–2102, 2009.

[245] Sophie Delhaye, Sophie Paul, Gjon Blakqori, Muriel Minet, Friedemann Weber, Peter Staeheli, and Thomas Michiels. Neurons produce type I interferon during viral encephalitis. *Proceedings of the National Academy of Sciences of the United States of America*, 103(20):7835–7840, 2006.

[246] Khalid Rashid, Isha Akhtar-Schaefer, and Thomas Langmann. Microglia in Retinal Degeneration. *Frontiers in immunology*, 10:1975, aug 2019.

[247] Julie K. Olson, Ann M. Girvin, and Stephen D. Miller. Direct Activation of Innate and Antigen-Presenting Functions of Microglia following Infection with Theiler's Virus. *Journal of Virology*, 75(20):9780–9789, 2001.

[248] Margaret E. Maes, Gloria Colombo, Rouven Schulz, and Sandra Siegert. Targeting microglia with lentivirus and AAV: Recent advances and remaining challenges. *Neuroscience letters*, 707:134–144, 2019.

[249] Zhuangzhuang Chen, Di Zhong, and Guozhong Li. The role of microglia in viral encephalitis: a review. *Journal of neuroinflammation*, 16(1):76, apr 2019.

[250] Lionel B. Ivashkiv and Laura T. Donlin. Regulation of type i interferon responses. *Nature Reviews Immunology*, 14(1):36–49, 2014.

[251] Finlay McNab, Katrin Mayer-Barber, Alan Sher, Andreas Wack, and Anne O'Garra. Type I interferons in infectious disease. *Nature Reviews Immunology*, 15(2):87–103, 2015.

[252] Joseph Rabinowitz, Ying Kai Chan, and Richard Jude Samulski. Adeno-associated Virus (AAV) versus Immune Response. *Viruses*, 11(2):102, jan 2019.

[253] João Paulo Brás, Joana Bravo, Jaime Freitas, Mário Adolfo Barbosa, Susana Gomes Santos, Teresa Summavielle, and Maria Inês Almeida. TNF-alpha-induced microglia activation requires miR-342: impact on NF-kB signaling and neurotoxicity. *Cell death & disease*, 11(6):415, 2020.

[254] Michelle A. Sama, Diana M. Mathis, Jennifer L. Furman, Hafiz Mohmmad Abdul, Irina A. Artiushin, Susan D. Kraner, and Christopher M. Norris. Interleukin-1β-dependent signaling between astrocytes and neurons depends critically on astrocytic calcineurin/NFAT activity. *Journal of Biological Chemistry*, 283(32):21953–21964, 2008.

[255] Simon J. O'Carroll, William H. Cook, and Deborah Young. AAV Targeting of Glial Cell Types in the Central and Peripheral Nervous System and Relevance to Human Gene Therapy. *Frontiers in Molecular Neuroscience*, 13, jan 2021.

[256] Cris S. Constantinescu, Marie Tani, Richard M. Ransohoff, Maria Wysocka, Brendan Hilliard, Toshiki Fujioka, Sean Murphy, Patrick J. Tighe, Jayasri Das Sarma, Giorgio Trinchieri, and Abdolmohamad Rostami. Astrocytes as antigen-presenting cells: Expression of IL-12/IL-23. *Journal of Neurochemistry*, 95(2):331–340, 2005.

[257] Jinar Rostami, Grammatiki Fotaki, Julien Sirois, Ropafadzo Mzezewa, Joakim Bergström, Magnus Essand, Luke Healy, and Anna Erlandsson. Astrocytes have the capacity to act as antigen-presenting cells in the Parkinson's disease brain. *Journal of neuroinflammation*, 17(1):119, apr 2020.

[258] Isabel J. Crane, Heping Xu, Carol Wallace, Ayyakkannu Manivannan, Matthias Mack, Janet Liversidge, Gabriel Marquez, Peter F. Sharp, and John V. Forrester. Involvement of CCR5 in the passage of Th1-type cells across the blood-retina barrier in experimental autoimmune uveitis. *Journal of Leukocyte Biology*, 79(3):435–443, 2006.

[259] Kirsten Bucher, Eduardo Rodríguez-Bocanegra, Daniyar Dauletbekov, and M. Dominik Fischer. Immune responses to retinal gene therapy using adeno-associated viral vectors - Implications for treatment success and safety. *Progress in retinal and eye research*, 83:100–115, jul 2021.

[260] Thilo M. Buck and Jan Wijnholds. Recombinant adeno-associated viral vectors (RAAV)-vector elements in ocular gene therapy clinical trials and transgene expression and bioactivity assays. *International Journal of Molecular Sciences*, 21(12):1–52, 2020.

[261] Annamaria Tisi, Marco Feligioni, Maurizio Passacantando, Marco Ciancaglini, and Rita Maccarone. The Impact of Oxidative Stress on Blood-Retinal Barrier Physiology in Age-Related Macular Degeneration. *Cells*, 10(1), jan 2021.

[262] Michael Whitehead, Sanjeewa Wickremasinghe, Andrew Osborne, Peter Van Wijngaarden, and Keith R. Martin. Diabetic retinopathy: a complex pathophysiology requiring novel therapeutic strategies. *Expert Opinion on Biological Therapy*, 18(12):1257–1270, 2018.

[263] Kenton T. Woodard, Katharine J. Liang, William C. Bennett, and R. Jude Samulski. Heparan Sulfate Binding Promotes Accumulation of Intravitreally Delivered Adeno-associated Viral Vectors at the Retina for Enhanced Transduction but Weakly Influences Tropism. *Journal of Virology*, 90(21):9878–9888, 2016.

[264] Immanuel P. Seitz, Stylianos Michalakis, Barbara Wilhelm, Felix F. Reichel, G. Alex Ochakovski, Eberhart Zrenner, Marius Ueffing, Martin Biel, Bernd Wissinger, Karl U. Bartz-Schmidt, Tobias Peters, and M. Dominik Fischer. Superior retinal gene transfer and biodistribution profile of subretinal versus intravitreal delivery of AAV8 in non-human primates. *Investigative Ophthalmology and Visual Science*, 58(13):5792–5801, 2017.

[265] Marina Pavlou, Christian Schön, Laurence M Occelli, Axel Rossi, Nadja Meumann, Ryan F Boyd, Joshua T Bartoe, Jakob Siedlecki, Maximilian J Gerhardt, Sabrina Babutzka, Jacqueline Bogedein, Johanna E Wagner, Siegfried G Priglinger, Martin

Biel, Simon M PetersenâJones, Hildegard Büning, and Stylianos Michalakis. Novel AAV capsids for intravitreal gene therapy of photoreceptor disorders. *EMBO Molecular Medicine*, 13(4), 2021.

[266] Mark M. Fuster and Lianchun Wang. Endothelial heparan sulfate in angiogenesis. In *Progress in Molecular Biology and Translational Science*, volume 93, pages 179–212. 2010.

[267] Shanan N. Emmanuel, Mario Mietzsch, Yu Shan Tseng, James Kennon Smith, and Mavis Agbandje-Mckenna. Parvovirus Capsid-Antibody Complex Structures Reveal Conservation of Antigenic Epitopes across the Family. *Viral Immunology*, 34(1):3–17, 2021.

[268] AGTC. AGTC Presents Data Demonstrating Efficiency of its AAV Vectors for Ocular Gene Therapy Even in the Presence of Anti-AAV Antibodies, 2019.

[269] Sophie Duclos, Giovanna Clavarino, Gilles Rousserie, Guillaume Goyette, Jonathan Boulais, Voahirana Camossetto, Evelina Gatti, Sylvie LaBoissière, Philippe Pierre, and Michel Desjardins. The endosomal proteome of macrophage and dendritic cells. *Proteomics*, 11(5):854–864, 2011.

[270] David A. Ferenbach, Tara A. Sheldrake, Kevin Dhaliwal, Tiina M.J. Kipari, Lorna P. Marson, David C. Kluth, and Jeremy Hughes. Macrophage/monocyte depletion by clodronate, but not diphtheria toxin, improves renal ischemia/reperfusion injury in mice. *Kidney International*, 82(8):928–933, 2012.

[271] Muhammad Yasir, Amandeep Goyal, Pankaj Bansal, and Sidharth Sonthalia. *Corticosteroid Adverse Effects*. 2021.

[272] Federico Mingozzi and Katherine A. High. Immune responses to AAV vectors: Overcoming barriers to successful gene therapy. *Blood*, 122(1):23–36, 2013.

[273] Eric C.B. Milner, Jennifer Anolik, Amedeo Cappione, and Iñaki Sanz. Human innate B cells: A link between host defense and autoimmunity? *Springer Seminars in Immunopathology*, 26(4):433–452, 2005.

[274] Bonnie B. Blomberg and Daniela Frasca. Age effects on mouse and human B cells. *Immunologic Research*, 57(1-3):354–360, 2013.

[275] A. Corthay. How do regulatory t cells work? *Scandinavian Journal of Immunology*, 70(4):326–336, 2009.

[276] Alexis Mathian, Romain Jouenne, Driss Chader, Fleur Cohen-Aubart, Julien Haroche, Jehane Fadlallah, Laetitia Claër, Lucile Musset, Guy Gorochov, Zahir Amoura, and Makoto Miyara. Regulatory T cell responses to high-dose methylprednisolone in active systemic lupus erythematosus. *PLoS ONE*, 10(12), 2015.

[277] Charlotte Kötting, Linda Hofmann, Ramin Lotfi, Daphne Engelhardt, Simon Laban, Patrick J. Schuler, Thomas K. Hoffmann, Cornelia Brunner, and Marie Nicole Theodoraki. Immune-stimulatory effects of curcumin on the tumor microenvironment in head and neck squamous cell carcinoma. *Cancers*, 13(6):1–19, 2021.

[278] A. L. Rodríguez-Perea, E. D. Arcia, C. M. Rueda, and P. A. Velilla. Phenotypical characterization of regulatory T cells in humans and rodents. *Clinical and Experimental Immunology*, 185(3):281–291, 2016.

[279] Lauren W. Collison and Dario A A Vignali. In vitro Treg suppression assays. *Methods in molecular biology (Clifton, N.J.)*, 707:21–37, 2011.

[280] Christoph T. Ellebrecht, Vijay G. Bhoj, Arben Nace, Eun Jung Choi, Xuming Mao, Michael Jeffrey Cho, Giovanni Di Zenzo, Antonio Lanzavecchia, John T. Seykora, George Cotsarelis, Michael C. Milone, and Aimee S. Payne. Reengineering chimeric antigen receptor T cells for targeted therapy of autoimmune disease. *Science*, 353(6295):179–184, 2016.

[281] Jayendra Kumar Krishnaswamy, Samuel Alsén, Ulf Yrlid, Stephanie C. Eisenbarth, and Adam Williams. Determination of T Follicular Helper Cell Fate by Dendritic Cells. *Frontiers in immunology*, 9:2169, sep 2018.

[282] Xuebing Feng, Dandan Wang, Jingjing Chen, Lin Lu, Bingzhu Hua, Xia Li, Betty P. Tsao, and Lingyun Sun. Inhibition of aberrant circulating Tfh cell proportions by corticosteroids in patients with systemic lupus erythematosus. *PloS one*, 7(12), 2012.

[283] Amber J. Giles, Marsha-Kay N D Hutchinson, Heather M. Sonnemann, Jinkyu Jung, Peter E. Fecci, Nivedita M. Ratnam, Wei Zhang, Hua Song, Rolanda Bailey, Dionne Davis, Caitlin M. Reid, Deric M. Park, and Mark R. Gilbert. Dexamethasone-induced immunosuppression: mechanisms and implications for immunotherapy. *Journal for immunotherapy of cancer*, 6(1):51, 2018.

[284] Cindy Strehl, Lisa Ehlers, Timo Gaber, and Frank Buttgereit. Glucocorticoids-All-Rounders Tackling the Versatile Players of the Immune System. *Frontiers in immunology*, 10:1744, 2019.

[285] I Rogatsky, J M Trowbridge, and M J Garabedian. Glucocorticoid receptor-mediated cell cycle arrest is achieved through distinct cell-specific transcriptional regulatory mechanisms. *Molecular and Cellular Biology*, 17(6):3181–3193, 1997.

[286] Luka Mesin, Jonatan Ersching, and Gabriel D. Victora. Germinal Center B Cell Dynamics. *Immunity*, 45(3):471–482, 2016.

[287] Elisabeth A van Erp, Willem Luytjes, Gerben Ferwerda, and Puck B van Kasteren. Fc-Mediated Antibody Effector Functions During Respiratory Syncytial Virus Infection and Disease. *Frontiers in immunology*, 10(MAR):548, 2019.

[288] Laura Sophie Landwehr, Barbara Altieri, Jochen Schreiner, Iuliu Sbiera, Isabel Weigand, Matthias Kroiss, Martin Fassnacht, and Silviu Sbiera. Interplay between glucocorticoids and tumor-infiltrating lymphocytes on the prognosis of adrenocortical carcinoma. *Journal for immunotherapy of cancer*, 8(1), 2020.

[289] Susan L. Swain, K. Kai McKinstry, and Tara M. Strutt. Expanding roles for CD4 + T cells in immunity to viruses. *Nature Reviews Immunology*, 12(2):136–148, 2012.

[290] L. Lanza, M. Scudeletti, F. Puppo, O. Bosco, L. Peirano, G. Filaci, E. Fecarotta, G. Vidali, and F. Indiveri. Prednisone increases apoptosis in in vitro activated human peripheral blood T lymphocytes. *Clinical and Experimental Immunology*, 103(3):482–490, 1996.

[291] Trevor E. Davis, Katalin Kis-Toth, Attila Szanto, and George C. Tsokos. Glucocorticoids suppress T cell function by up-regulating microRNA-98. *Arthritis and Rheumatism*, 65(7):1882–1890, 2013.

[292] Hildegund C.J. Ertl. T Cell-Mediated Immune Responses to AAV and AAV Vectors. *Frontiers in Immunology*, 12, 2021.

[293] Dhaneshwar Kumar and Sharvan Sehrawat. Divergent effects of a transient corticosteroid therapy on virus-specific quiescent and effector CD8+T Cells. *Frontiers in Immunology*, 10(JULY), 2019.

[294] Christian S. Hinrichs, Douglas C. Palmer, Steven A. Rosenberg, and Nicholas P. Restifo. Glucocorticoids do not inhibit antitumor activity of activated CD8 + T cells. *Journal of Immunotherapy*, 28(6):517–524, 2005.

[295] Marco De Simone, Grazisa Rossetti, and Massimiliano Pagani. Single cell T cell receptor sequencing: Techniques and future challenges. *Frontiers in Immunology*, 9(JUL), jul 2018.

[296] Jason W. Griffith, Caroline L. Sokol, and Andrew D. Luster. Chemokines and chemokine receptors: positioning cells for host defense and immunity. *Annual review of immunology*, 32:659–702, 2014.

[297] Karolina A. Zielińska, Laura Van Moortel, Ghislain Opdenakker, Karolien De Bosscher, and Philippe E. Van den Steen. Endothelial response to glucocorticoids in inflammatory diseases. *Frontiers in Immunology*, 7(DEC):592, 2016.

[298] Jeffrey L. Edelman, David Lutz, and Marisol R. Castro. Corticosteroids inhibit VEGF-induced vascular leakage in a rabbit model of blood-retinal and blood-aqueous barrier breakdown. *Experimental Eye Research*, 80(2):249–258, 2005.

[299] S. Sugama, T. Takenouchi, M. Fujita, H. Kitani, B. Conti, and M. Hashimoto. Corticosteroids limit microglial activation occurring during acute stress. *Neuroscience*, 232:13–20, 2013.

[300] Francisco Ros-Bernal, Stéphane Hunot, Maria Trinidad Herrero, Sebastien Parnadeau, Jean Christophe Corvol, Lixia Lu, Daniel Alvarez-Fischer, María Angeles Carrillo De Sauvage, Françoise Saurini, Christiane Coussieu, Kiyoka Kinugawa, Annick Prigent, Günter Höglinger, Michel Hamon, François Tronche, Etienne C. Hirsch, and Sheela Vyas. Microglial glucocorticoid receptors play a pivotal role in regulating dopaminergic neurodegeneration in parkinsonism. *Proceedings of the National Academy of Sciences of the United States of America*, 108(16):6632–6637, 2011.

[301] Amanda Sierra, Oihane Abiega, Anahita Shahraz, and Harald Neumann. Janus-faced microglia: beneficial and detrimental consequences of microglial phagocytosis. *Frontiers in Cellular Neuroscience*, 7(JANUARY 2013), 2013.

[302] Priyanka Chauhan, Shuxian Hu, Wen S. Sheng, Sujata Prasad, and James R. Lokensgard. Modulation of Microglial Cell Fcγ Receptor Expression Following Viral Brain Infection. *Scientific reports*, 7, 2017.

[303] Geoffrey L. Rogers, Masataka Suzuki, Irene Zolotukhin, David M. Markusic, Laurence M. Morel, Brendan Lee, Hildegund C.J. Ertl, and Roland W. Herzog. Unique roles of TLR9- and MyD88-dependent and -independent pathways in adaptive immune responses to AAV-mediated gene transfer. *Journal of Innate Immunity*, 7(3):302–314, 2015.

[304] Joshua A. Smith, Arabinda Das, Swapan K. Ray, and Naren L. Banik. Role of pro-inflammatory cytokines released from microglia in neurodegenerative diseases. *Brain Research Bulletin*, 87(1):10–20, 2012.

[305] Soyon Hong, Lasse Dissing-Olesen, and Beth Stevens. New insights on the role of microglia in synaptic pruning in health and disease. *Current opinion in neurobiology*, 36:128–34, feb 2016.

[306] Thomas F. Lerch, Jason K. O'Donnell, Nancy L. Meyer, Qing Xie, Kenneth A. Taylor, Scott M. Stagg, and Michael S. Chapman. Structure of AAV-DJ, a retargeted gene therapy vector: Cryo-electron microscopy at 4.5 Å resolution. *Structure*, 20(8):1310–1320, 2012.

[307] Dorothy P. Schafer, Christopher T. Heller, Georgia Gunner, Molly Heller, Christopher Gordon, Timothy Hammond, Yochai Wolf, Steffen Jung, and Beth Stevens. Microglia contribute to circuit defects in Mecp2 null mice independent of microglia-specific loss of Mecp2 expression. *eLife*, 5(2016JULY), 2016.

[308] Megumi Andoh, Yuji Ikegaya, and Ryuta Koyama. Synaptic Pruning by Microglia in Epilepsy. *Journal of Clinical Medicine*, 8(12):2170, 2019.

[309] J. Guadagno, X. Xu, M. Karajgikar, A. Brown, and S. P. Cregan. Microglia-derived TNFα induces apoptosis in neural precursor cells via transcriptional activation of the Bcl-2 family member Puma. *Cell Death and Disease*, 4(3):538–538, mar 2013.

[310] Keigan M. Park and William J. Bowers. Tumor necrosis factor-alpha mediated signaling in neuronal homeostasis and dysfunction. *Cellular Signalling*, 22(7):977–983, 2010.

[311] Desheng Wang. Tumor Necrosis Factor-Alpha Alters Electrophysiological Properties of Rabbit Hippocampal Neurons. *Journal of Alzheimer's Disease*, 68(3):1257–1271, 2019.

[312] Thomas E. Nelson, Christina L. Ur, and Donna L. Gruol. Chronic interleukin-6 exposure alters electrophysiological properties and calcium signaling in developing cerebellar Purkinje neurons in culture. *Journal of Neurophysiology*, 88(1):475–486, 2002.

[313] Kiarash Riazi, Michael A. Galic, and Quentin J. Pittman. Contributions of peripheral inflammation to seizure susceptibility: Cytokines and brain excitability. *Epilepsy Research*, 89(1):34–42, 2010.

[314] Jason K. Whitmire. Induction and function of virus-specific CD4+ T cell responses, 2011.

[315] Joseph M. Kulinski, Vera L. Tarakanova, and James Verbsky. Regulation of antiviral CD8 T-cell responses. *Critical Reviews in Immunology*, 33(6):477–488, 2013.

[316] Dorothy P. Schafer, Emily K. Lehrman, Christopher T. Heller, and Beth Stevens. An engulfment assay: A protocol to assess interactions between CNS phagocytes and neurons. *Journal of Visualized Experiments*, (88), 2014.

[317] Cornelia M. Weyand and Jörg J. Goronzy. Aging of the immune system: Mechanisms and therapeutic targets. In *Annals of the American Thoracic Society*, volume 13, pages S422–S428, 2016.

[318] Daniel C. Lee, Claudia R. Ruiz, Lori Lebson, Maj Linda B. Selenica, Justin Rizer, Jerry B. Hunt, Rahil Rojiani, Patrick Reid, Sidharth Kammath, Kevin Nash, Chad A. Dickey, Marcia Gordon, and Dave Morgan. Aging enhances classical activation but mitigates alternative activation in the central nervous system. *Neurobiology of Aging*, 34(6):1610–1620, 2013.

[319] Christopher J. Henry, Yan Huang, Angela M. Wynne, and Jonathan P. Godbout. Peripheral lipopolysaccharide (LPS) challenge promotes microglial hyperactivity in aged mice that is associated with exaggerated induction of both pro-inflammatory IL-1β and anti-inflammatory IL-10 cytokines. *Brain, Behavior, and Immunity*, 23(3):309–317, 2009.

[320] M. Letiembre, W. Hao, Y. Liu, S. Walter, I. Mihaljevic, S. Rivest, T. Hartmann, and K. Fassbender. Innate immune receptor expression in normal brain aging. *Neuroscience*, 146(1):248–254, 2007.

[321] Dominic M. Ippolito and Cagla Eroglu. Quantifying synapses: An immunocytochemistry-based assay to quantify synapse number. *Journal of Visualized Experiments*, (45), 2010.

[322] Warren N. D'Souza, Kimberly S. Schluns, David Masopust, and Leo Lefrançois. Essential Role for IL-2 in the Regulation of Antiviral Extralymphoid CD8 T Cell Responses. *The Journal of Immunology*, 168(11):5566–5572, 2002.

[323] Mayilaadumveettil Nishana and Sathees C. Raghavan. Role of recombination activating genes in the generation of antigen receptor diversity and beyond. *Immunology*, 137(4):271–281, 2012.

[324] Xingfeng Bao, E. Ashley Moseman, Hideo Saito, Bronislawa Petryanik, Aude Thiriot, Shingo Hatakeyama, Yuki Ito, Hiroto Kawashima, Yu Yamaguchi, John B. Lowe, Ulrich H. von Andrian, and Minoru Fukuda. Endothelial heparan sulfate controls

chemokine presentation in recruitment of lymphocytes and dendritic cells to lymph nodes. *Immunity*, 33(5):817–829, 2010.

[325] Yeni H. Yücel, Miles G. Johnston, Tina Ly, Manoj Patel, Brian Drake, Ersin GümüÅ, Stephan A. Fraenkl, Sara Moore, Dalia Tobbia, Dianna Armstrong, Eva Horvath, and Neeru Gupta. Identification of lymphatics in the ciliary body of the human eye: A novel "uveolymphatic" outflow pathway. *Experimental Eye Research*, 89(5):810–819, 2009.

[326] David M. Markusic, Roland W. Herzog, George V. Aslanidi, Brad E. Hoffman, Baozheng Li, Mengxin Li, Giridhara R. Jayandharan, Chen Ling, Irene Zolotukhin, Wenqin Ma, Sergei Zolotukhin, Arun Srivastava, and Li Zhong. High-efficiency transduction and correction of murine hemophilia B using AAV2 vectors devoid of multiple surface-exposed tyrosines. *Molecular Therapy*, 18(12):2048–2056, 2010.

[327] Etsuko Sugawara and Hiroshi Nikaido. Properties of AdeABC and AdeIJK efflux systems of Acinetobacter baumannii compared with those of the AcrAB-TolC system of Escherichia coli. *Antimicrobial agents and chemotherapy*, 58(12):7250–7, dec 2014.

[328] Christian Leborgne, Elena Barbon, Jeffrey M. Alexander, Hayley Hanby, Sandrine Delignat, Daniel M. Cohen, Fanny Collaud, Saghana Muraleetharan, Dan Lupo, Joseph Silverberg, Karen Huang, Laetitia van Wittengerghe, Béatrice Marolleau, Adeline Miranda, Anna Fabiano, Victoria Daventure, Heena Beck, Xavier M. Anguela, Giuseppe Ronzitti, Sean M. Armour, Sebastien Lacroix-Desmazes, and Federico Mingozzi. IgG-cleaving endopeptidase enables in vivo gene therapy in the presence of anti-AAV neutralizing antibodies. *Nature Medicine*, 26(7):1096–1101, jul 2020.

[329] Stanley C. Jordan, Tomas Lorant, Jua Choi, Christian Kjellman, Lena Winstedt, Mats Bengtsson, Xiaohai Zhang, Torsten Eich, Mieko Toyoda, Britt-Marie Eriksson, Shili Ge, Alice Peng, Sofia Järnum, Kathryn J. Wood, Torbjorn Lundgren, Lars Wennberg, Lars Bäckman, Erik Larsson, Rafael Villicana, Joe Kahwaji, Sabrina Louie, Alexis Kang, Mark Haas, Cynthia Nast, Ashley Vo, and Gunnar Tufveson. IgG Endopeptidase in Highly Sensitized Patients Undergoing Transplantation. *New England Journal of Medicine*, 377(5):442–453, 2017.

[330] Lena Winstedt, Sofia Järnum, Emma Andersson Nordahl, Andreas Olsson, Anna Runström, Robert Bockermann, Christofer Karlsson, Johan Malmström, Gabriella Samuelsson Palmgren, Ulf Malmqvist, Lars Björck, and Christian Kjellman. Complete removal of extracellular IgG antibodies in a randomized dose-escalation

phase i study with the bacterial enzyme IdeS - A novel therapeutic opportunity. *PLoS ONE*, 10(7):0132011, jul 2015.

[331] Amine Meliani, Christian Leborgne, Sabrina Triffault, Laurence Jeanson-Leh, Philippe Veron, and Federico Mingozzi. Determination of anti-adeno-associated virus vector neutralizing antibody titer with an in vitro reporter system. *Human Gene Therapy Methods*, 26(2):45–53, 2015.

[332] Xi Chen, Meilin Lin, Shi Qian, Zining Zhang, Yajing Fu, Junjie Xu, Xiaoxu Han, Haibo Ding, Tao Dong, Hong Shang, and Yongjun Jiang. The early antibody-dependent cell-mediated cytotoxicity response is associated with lower viral set point in individuals with primary HIV infection. *Frontiers in Immunology*, 9(OCT):2322, oct 2018.

[333] Matthew Zirui Tay, Kevin Wiehe, and Justin Pollara. Antibody dependent cellular phagocytosis in antiviral immune responses. *Frontiers in Immunology*, 10(FEB):332, 2019.

[334] G. Hashimoto, P. F. Wright, and D. T. Karzon. Antibody-dependent cell-mediated cytotoxicity against influenza virus-infected cells. *Journal of Infectious Diseases*, 148(5):785–794, 1983.

[335] Gwladys Gernoux, James M. Wilson, and Christian Mueller. Regulatory and Exhausted T Cell Responses to AAV Capsid. *Human Gene Therapy*, 28(4):338–349, 2017.

[336] P NORMAN. Immunobiology: The immune system in health and disease. In *Journal of Allergy and Clinical Immunology*, volume 96, pages 274–274. 1995.

[337] Klaudia Kuranda, Priscilla Jean-Alphonse, Christian Leborgne, Romain Hardet, Fanny Collaud, Solenne Marmier, Helena Costa Verdera, Giuseppe Ronzitti, Philippe Veron, and Federico Mingozzi. Exposure to wild-type AAV drives distinct capsid immunity profiles in humans. *Journal of Clinical Investigation*, 128(12):5267–5279, 2018.

[338] Masataka Suzuki, Terry K. Bertin, Geoffrey L. Rogers, Racel G. Cela, Irene Zolotukhin, Donna J. Palmer, Philip Ng, Roland W. Herzog, and Brendan Lee. Differential type i interferon-dependent transgene silencing of helper-dependent adenoviral vs. adeno-associated viral vectors in vivo. *Molecular Therapy*, 21(4):796–805, 2013.

[339] Giridhara R. Jayandharan, George Aslanidi, Ashley T. Martino, Stephan C. Jahn, George Q. Perrin, Roland W. Herzog, and Arun Srivastava. Activation of the NF-κB pathway by adeno-associated virus (AAV) vectors and its implications in immune

response and gene therapy. *Proceedings of the National Academy of Sciences of the United States of America*, 108(9):3743–3748, 2011.

[340] Naomi E. Harwood and Facundo D. Batista. New Insights into the Early Molecular Events Underlying B Cell Activation. *Immunity*, 28(5):609–619, 2008.

[341] Candace Summerford and Richard Jude Samulski. Membrane-Associated Heparan Sulfate Proteoglycan Is a Receptor for Adeno-Associated Virus Type 2 Virions. *Journal of Virology*, 72(2):1438–1445, 1998.

[342] Narendra Maheshri, James T. Koerber, Brian K. Kaspar, and David V. Schaffer. Directed evolution of adeno-associated virus yields enhanced gene delivery vectors. *Nature Biotechnology*, 24(2):198–204, 2006.

[343] Samantha L. Ginn, Anais K. Amaya, Ian E. Alexander, Michael Edelstein, and Mohammad R. Abedi. Gene therapy clinical trials worldwide to 2017: An update. *Journal of Gene Medicine*, 20(5):3015, may 2018.

[344] Koh Hei Sonoda, Taiji Sakamoto, Hong Qiao, Toshio Hisatomi, Toru Oshima, Chikako Tsutsumi-Miyahara, Mark Exley, Steven P. Balk, Masaru Taniguchi, and Tatsuro Ishibashi. The analysis of systemic tolerance elicited by antigen inoculation into the vitreous cavity: Vitreous cavity-associated immune deviation. *Immunology*, 116(3):390–399, 2005.

[345] M. Dominik Fischer, G. Alex Ochakovski, Benjamin Beier, Immanuel P. Seitz, Yousof Vaheb, Constanze Kortuem, Felix F.L. Reichel, Laura Kuehlewein, Nadine A. Kahle, Tobias Peters, Aniz Girach, Eberhart Zrenner, Marius Ueffing, Robert E. MacLaren, Karl Ulrich Bartz-Schmidt, and Barbara Wilhelm. Efficacy and Safety of Retinal Gene Therapy Using Adeno-Associated Virus Vector for Patients with Choroideremia: A Randomized Clinical Trial. *JAMA Ophthalmology*, 137(11):1247–1254, 2019.

[346] Thomas L. Edwards, Jasleen K. Jolly, Markus Groppe, Alun R. Barnard, Charles L. Cottriall, Tanya Tolmachova, Graeme C. Black, Andrew R. Webster, Andrew J. Lotery, Graham E. Holder, Kanmin Xue, Susan M. Downes, Matthew P. Simunovic, Miguel C. Seabra, and Robert E. MacLaren. Visual Acuity after Retinal Gene Therapy for Choroideremia. *New England Journal of Medicine*, 374(20):1996–1998, 2016.

[347] Robert E. MacLaren, Markus Groppe, Alun R. Barnard, Charles L. Cottriall, Tanya Tolmachova, Len Seymour, K. Reed Clark, Matthew J. During, Frans P.M. Cremers, Graeme C.M. Black, Andrew J. Lotery, Susan M. Downes, Andrew R. Webster, and

Miguel C. Seabra. Retinal gene therapy in patients with choroideremia: Initial fi ndings from a phase 1/2 clinical trial. *The Lancet*, 383(9923):1129–1137, 2014.

[348] Jérôme Poupiot, Helena Costa Verdera, Romain Hardet, Pasqualina Colella, Fanny Collaud, Laurent Bartolo, Jean Davoust, Peggy Sanatine, Federico Mingozzi, Isabelle Richard, and Giuseppe Ronzitti. Role of Regulatory T Cell and Effector T Cell Exhaustion in Liver-Mediated Transgene Tolerance in Muscle. *Molecular Therapy - Methods and Clinical Development*, 15:83–100, 2019.

[349] Caroline Le Guiner, Laurent Servais, Marie Montus, Thibaut Larcher, Bodvaël Fraysse, Sophie Moullec, Marine Allais, Virginie François, Maeva Dutilleul, Alberto Malerba, Taeyoung Koo, Jean Laurent Thibaut, Béatrice Matot, Marie Devaux, Johanne Le Duff, Jack Yves Deschamps, Inès Barthelemy, Stéphane Blot, Isabelle Testault, Karim Wahbi, Stéphane Ederhy, Samia Martin, Philippe Veron, Christophe Georger, Takis Athanasopoulos, Carole Masurier, Federico Mingozzi, Pierre Carlier, Bernard Gjata, Jean Yves Hogrel, Oumeya Adjali, Fulvio Mavilio, Thomas Voit, Philippe Moullier, and George Dickson. Long-term microdystrophin gene therapy is effective in a canine model of Duchenne muscular dystrophy. *Nature Communications*, 8(1):16105, dec 2017.

[350] Guang Ping Gao, Mauricio R. Alvira, Lili Wang, Roberto Calcedo, Jule Johnston, and James M. Wilson. Novel adeno-associated viruses from rhesus monkeys as vectors for human gene therapy. *Proceedings of the National Academy of Sciences of the United States of America*, 99(18):11854–11859, 2002.

[351] Guangping Gao, Mauricio R. Alvira, Suryanarayan Somanathan, You Lu, Luk H. Vandenberghe, John J. Rux, Roberto Calcedo, Julio Sanmiguel, Zahra Abbas, and James M. Wilson. Adeno-associated viruses undergo substantial evolution in primates during natural infections. *Proceedings of the National Academy of Sciences of the United States of America*, 100(10):6081–6086, 2003.

[352] Stephen Russell, Jean Bennett, Jennifer A. Wellman, Daniel C. Chung, Zi Fan Yu, Amy Tillman, Janet Wittes, Julie Pappas, Okan Elci, Sarah McCague, Dominique Cross, Kathleen A. Marshall, Jean Walshire, Taylor L. Kehoe, Hannah Reichert, Maria Davis, Leslie Raffini, Lindsey A. George, F. Parker Hudson, Laura Dingfield, Xiaosong Zhu, Julia A. Haller, Elliott H. Sohn, Vinit B. Mahajan, Wanda Pfeifer, Michelle Weckmann, Chris Johnson, Dina Gewaily, Arlene Drack, Edwin Stone, Katie Wachtel, Francesca Simonelli, Bart P. Leroy, J. Fraser Wright, Katherine A. High, and Albert M. Maguire. Efficacy and safety of voretigene neparvovec (AAV2-hRPE65v2) in

patients with RPE65-mediated inherited retinal dystrophy: a randomised, controlled, open-label, phase 3 trial. *The Lancet*, 390(10097):849–860, 2017.

[353] Cell and Gene Therapy Catapult. Cell and Gene Therapy Catapult Clinical Trials Database 2019, 2019.

[354] MeiraGTx UK II. MeiraGTx Presents Preclinical Data on its Ocular Gene Therapy Studies for the Treatment of Leber's Congenital Amaurosis, Achromatopsia and X-Linked Retinitis Pigmentosa at ESGCT 2017 Congress in Berlin, 2017.

Appendix A

Appendix

A.1 Flow cytometry example flow plots for key cell populations

Figure A.1: Example flow plots of key cell populations

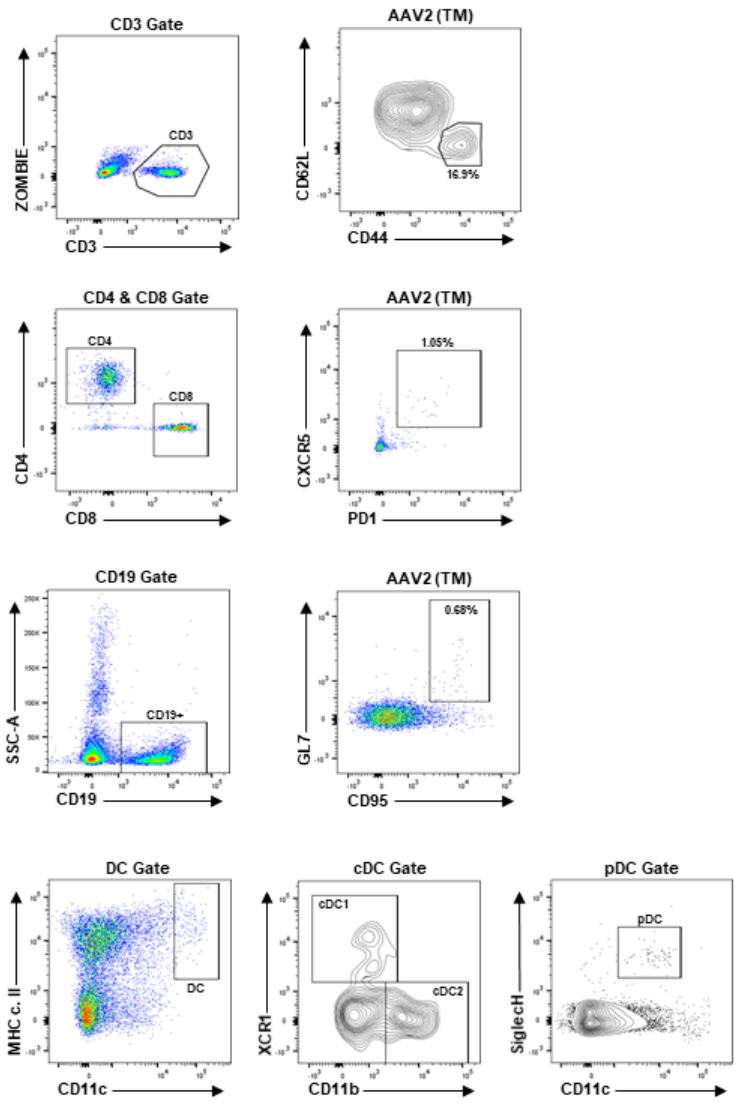

Example flow plots from flow cytometry experiments. Spleens were processed for analysis and gated for T-cell, B-cell or dendritic cell markers. These populations were further assessed for combinations of markers to delineate specific lymphocyte populations, such as Tfh cells, or pDCs.

A.2 Immunology of a rationally-designed AAV2 capsid mutant in the ocular compartment

A.2.1 Representative ERG waveforms after IVT of wild-type and mutant vectors

Figure A.2: Average ERG waveforms from phosphodegron mutant AAV study

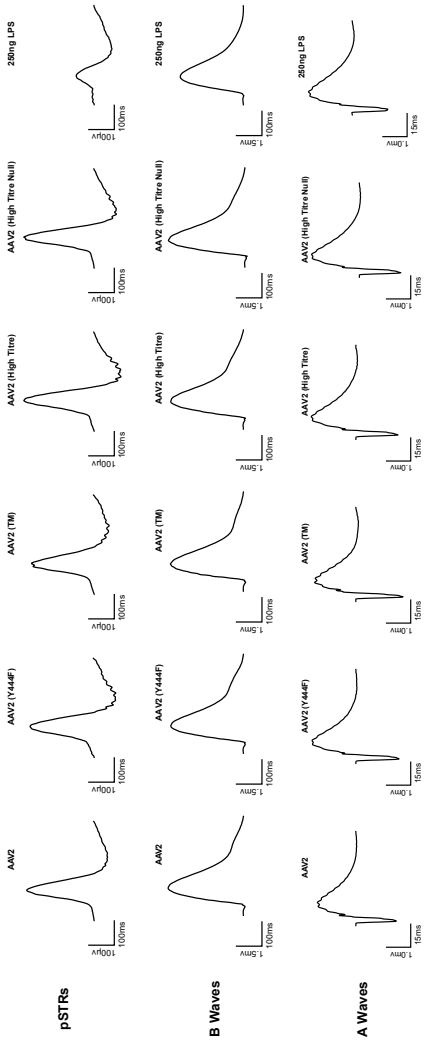

Injection of phosphodegron mutant vectors is not associated with changes in electrophysiological function in the murine retina. Vectors were injected via IVT and ERG was performed after three weeks. 250ng of lipopolysaccharide (LPS) 24h prior to ERG. Representative pSTRs, B-waves and A-waves from each treatment group are shown.

A.2.2 Summary of trRossetta work to delineate structure of AAV2 mutant and wild-type capsids

Figure A.3: Summary of trRossetta work to delineate structure of AAV2 mutant and wild-type capsids

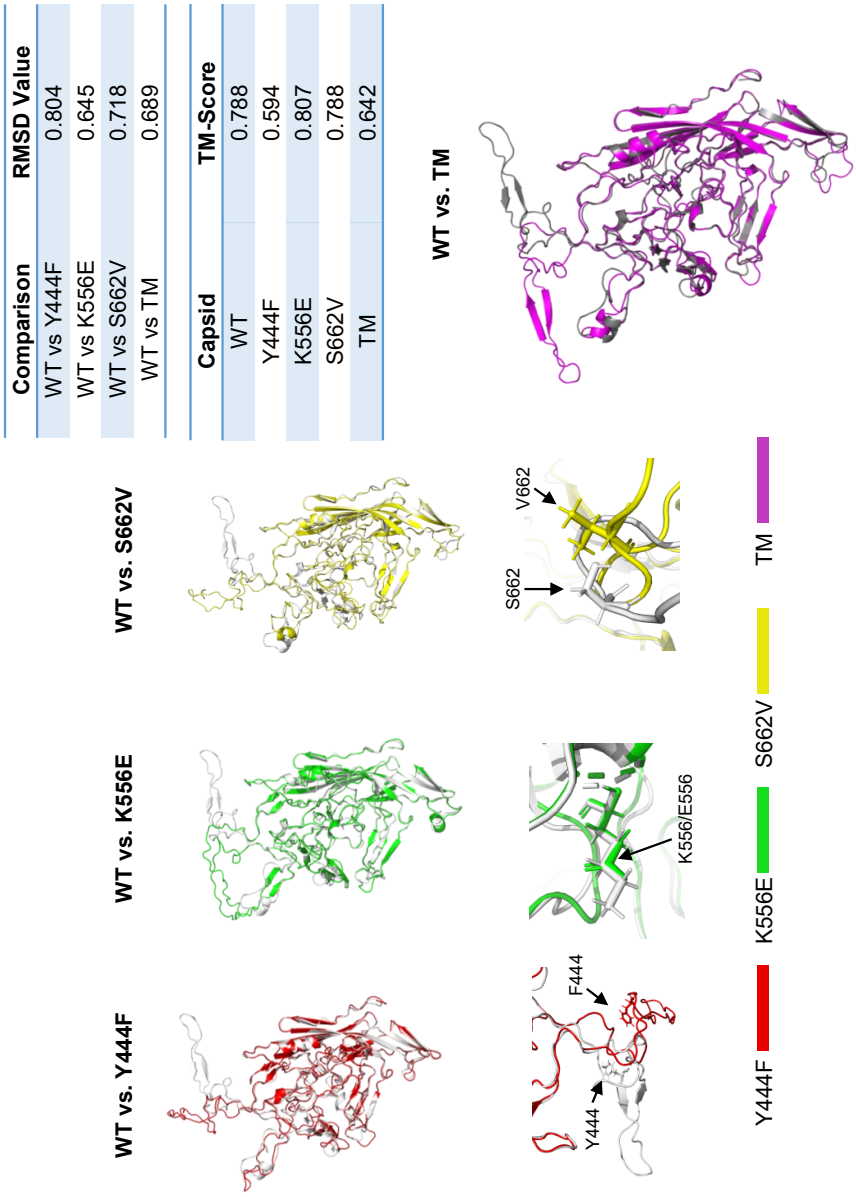

trRossetta generated predicted structures for wild-type and phosphodegron mutant capsids visualised in PyMol. High and very high TM-scores were assigned by trRossetta to its predictions, indicating a high degree of confidence with which it may have accurately calculated the protein structure. However, when the coordinate files were visualised in PyMol, gross structural changes were observed which appeared to be unrelated to the mutation. RMSD = root mean squared deviation, a measurement of the degree of structural misalignment exhibited by two protein structures.

A.2.3 Comparison of microglia and Muller glia activation after AAV2 (high titre) and AAV2 (high titre null) IVTs

Figure A.4: Comparison of microglia and Muller glia activation after AAV2 (high titre) and AAV2 (high titre null) IVTs

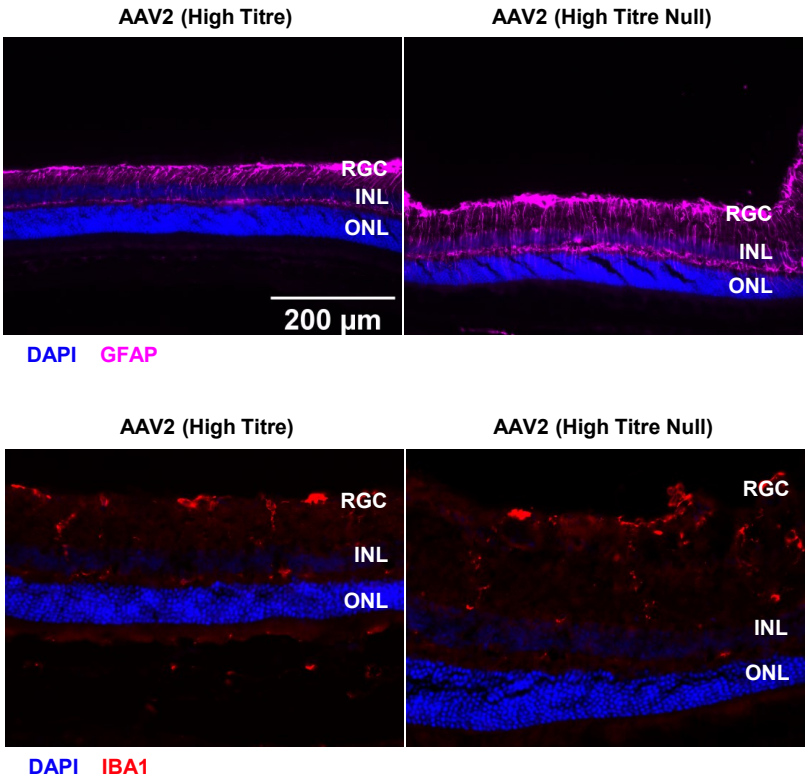

Mice received IVTs of AAV2.CAG.GFP or AAV2.CAG.Null (2E10 GC/eye). Eyes were enucleated after 3wk and tissue sections were stained for IBA1 and GFAP expression, which are markers of microglia and Muller glia activation respectively. These representative images showed that no apparent differences in innate immune activation between the two groups tested, suggesting that the immune activation observed in this study was likely due to the capsids and not the expression of GFP reporters.

A.3 Perioperative prednisolone administration attenuates immune activation following intravitreal injection of AAV2, but fails to enable repeated gene transfer to the inner retina

A.3.1 Capsid shuffling strategy fails to circumvent anti-AAV2 NAb response and enable repeated gene transfer to the murine retina

Figure A.5: Capsid shuffling strategy fails to circumvent anti-AAV2 NAb response and enable repeated gene transfer to the murine retina

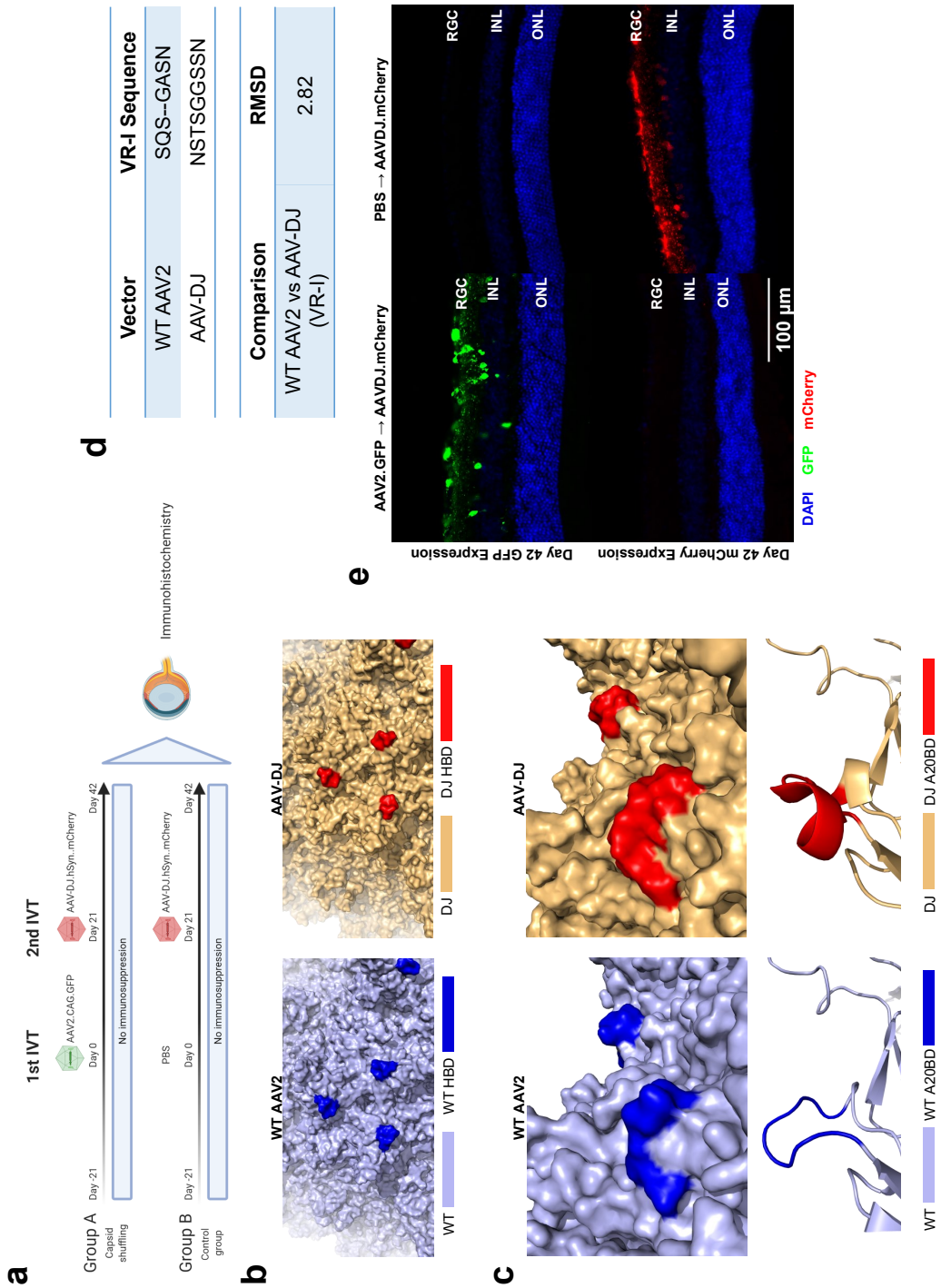

Appendix Figure A.2.1 – Capsid shuffling strategy fails to circumvent anti-AAV2 NAb response and enable repeated gene transfer to the murine retina.

(a) Overview of study plan. Group A received a 1E10 GC/eye IVT of AAV2.CAG.GFP followed by 1E10 GC/eye AAV-DJ.hSyn.mCherry. Group B received a PBS injection followed by a 1E10 GC/eye AAV-DJ.hSyn.mCherry IVT. Eyes were enucleated at day 42 for analysis.

(b) PyMol rendering of 6ih9 (a 2.8Å resolution cryoelectron microscopy (cryoEM)-derived wild-type AAV2 structure) and 7kfr (a 1.56Å resolution cryoEM-derived AAV-DJ structure) with heparin binding domains (HBD) highlighted. This shows the HBD of AAV-DJ is conserved from the parental capsid, wild-type AAV2.

(c) PyMol rendering of variable region I (VR-I) in AAV2 and AAV-DJ shows differences in the A20 binding domain (A20BD), a known anti-AAV2 NAb.

Comparison of VR-I sequences at residues 262-268/270 (AAV2 VP3 numbering), and root mean square deviation (RMSD; a measure of structural divergence between two proteins) values comparing AAV2 and AAV-DJ VR-I regions.

(d) GFP and mCherry expression following repeated bilateral IVTs of AAV2 and AAV-DJ. Eyes were enucleated on day 42, processed into 13µm cryosections, and stained for GFP and mCherry. RGC, retinal ganglion cell layer; INL, inner nuclear layer; ONL, outer nuclear layer.